Dissertation zur Erlangung des Doktorgrades der Fakultät

für Chemie und Pharmazie der

Ludwig-Maximilians-Universität München

Recombinant Spider Silk Protein Particles for a Modern Vaccination Approach

Matthias Andreas Lucke

aus Ulm, Deutschland

2017

Erklärung

Diese Dissertation wurde im Sinne von § 7 der Promotionsordnung vom 28. November 2011 von Frau PD Dr. habil. Julia Engert betreut.

Eidesstattliche Versicherung

Diese Dissertation wurde eigenständig und ohne unerlaubte Hilfe erarbeitet.

München, den 27.02.2017

_____

Matthias Andreas Lucke

Dissertation eingereicht am:	27.02.2017
1. Gutachter:	PD Dr. habil. Julia Engert
2. Gutachter:	Prof. Dr. Gerhard Winter
Mündliche Prüfung am:	17.03.2017

For my family

Acknowledgements

Embarking on a doctoral thesis is a challenging task for any scientist. Fortunately, a number of people helped me throughout the three and a half years and made this thesis a success.

First and foremost, I want to thank my first supervisor PD Dr. habil. Julia Engert for her continuous guidance and encouragement throughout the years. I really appreciate her efforts introducing me in the field of particulate drug delivery systems and her ideas in the vast area of vaccination. The whole concept of the spider silk hybrid proteins would not have been so successful without her personal support. Thank you for your patience during proof reading of my publications and this thesis and your enthusiasm in my work.

This work was further supervised by Prof. Dr. Gerhard Winter. Thank you for accepting me in this great research group. In particular, I would like to thank him for his outstanding and reliable scientific guidance and his generously shared expertise in the field of pharmaceutical technology. Under his supervision, I did not only improve as a scientist but also gained a lot for my personal development.

Prof. Dr. Wolfgang Frieß is kindly acknowledged for his dedicated interest in my research topic, for his many new ideas and advice over the last years and for his support on organizing the students course 'Biopharmacy'.

The work in this thesis was covered by a grant of the German Federal Ministry of Education and Research (BMBF). For this reason, the BMBF is acknowledged for the financial support.

I would like to express my thankfulness to Prof. Dr. Thomas Scheibel to support me and my work and the opportunity to visit his 'fiberlab' at the University of Bayreuth. In this context, I also want to thank Martina Schierling, Heike Herold, Stefanie Wohlrab and all other members of the fiberlab group to share their knowledge about spider silk proteins and chemical coupling with me.

With regard to the research on spider silk and hybrid spider silk proteins, I would like thank the entire team at AMSilk GmbH (Martinsried, Germany) and especially Dr. Ute Slotta, Dr. Lin Roemer and Dr. Stephan Reschauer for not only providing me with all the different spider silk proteins, but also for the motivating discussions and their outstanding scientific expertise.

This thesis would not have been possible without the support of many enthusiastic people at the LMU Munich. Prof. Dr. Stefan Zahler is thanked for his introduction and guidance regarding confocal microscopy. Christian Minke is kindly acknowledged for helping me with SEM measurements. Special thanks go also to the students Christina Wetzel and Mirjam Schwarz, who

supported this work during their internships.

I would like to especially thank Markus Hofer, who introduced me into the world of spider silk particles during my first months at the LMU. His terrific work was the basis for this thesis. It was a pleasure for me to have you around helping with words and deeds.

Further, I really want to thank all my colleagues and friends from the research groups of Prof. Winter and Prof. Frieß. The numerous social activities, like the skiing trips, the hiking trips, the initiation of the LMU Shakers, rafting and all the evening activities (particularly the rooftop BBQs) made the time during the PhD thesis an unforgettable one. I have not only worked together with you, but found friends for life.

My deepest gratitude goes to my whole family for all the support they gave me over all the years. Thank you for always being there for me. Especially, I want to thank my wife Tanja for her constant encouragement and, above all, her patience and her good empathy.

TABLE OF CONTENTS

I. General Introduction 5
1. Introduction 5
2. Silk Proteins 6
2.1. Silkworm silk 7
2.2. Spider silk 7
3. Silk based drug delivery systems 9
3.1. Implants and Scaffolds 9
3.2. Films 10
3.3. Coatings of drug delivery systems 10
3.4. Nano- and microfibers 11
3.5. Nano- and microparticles 11
3.6. Functionalization of silk based drug delivery systems 16
4. Particulate Delivery Systems for Vaccination 17
4.1. Nano- and microparticles based on lipids and lipid–saponin mixtures 18
4.2. Nano- and microparticles based on polymers and minerals 20
4.3. Vaccine administration 22
5. Objectives of the Thesis 23
6. References 25
II. Endotoxin depletion of eADF4(C16) protein and preparation of particles with low endotoxin values 37
1. Introduction 37
2. Materials and methods 39
2.1. Materials 39
2.2. Methods 39
2.3. Analytical methods 44
3. Results and Discussion 47
4. Conclusion 55
5. References 56
III. The effect of steam sterilization on recombinant spider silk particles 61
1. Abstract 62
2. Introduction 62
3. Materials and methods 64
3.1. Materials 64
3.2. Particle preparation 64
3.3. Particle sterilization 66
3.4. Characterization of eADF4(C16) particles 66

3.5. In vitro cytotoxicity assay 67
3.6. Statistical analysis 68
4. Results and Discussion 68
4.1. Particle Preparation in the Micron- and Submicron-Range 68
4.2. Sterilization of the eADF4(C16) Particles by Autoclave Treatment 70
5. Conclusion 77
6. Acknowledgements 77
7. References 77
IV. Chemical Coupling of SIINFEKL to eADF4(C16) Protein Particles 81
1. Introduction 81
2. Materials and methods 82
2.1. Materials 82
2.2. Methods 83
2.3. Analytical methods 87
3. Results and Discussion 88
4. Conclusion 96
5. References 97
V. Hybrid eADF4(C16) Protein Particles Designed for a Modern Vaccination Approach (First Generation) 101
1. Introduction 101
2. Materials and methods 103
2.1. Materials 103
2.2. Methods 104
2.3. Analytical methods 107
3. Results and Discussion 108
4. Conclusion 122
5. References 123
VI. Hybrid eADF4(C16) Protein Particles Containing a Cleavable Linker Sequence for Vaccination (Second Generation) 127
1. Introduction 127
2. Materials and methods 129
2.1. Materials 129
2.2. Methods 130
2.3. Analytical Methods 133
3. Results and Discussion 134
4. Conclusion 152
5. References 152

VII. Nebulization of eADF4(C16) Protein Particles 157
1. Introduction 157
2. Materials and methods 159
2.1. Materials 159
2.2. Methods 159
2.3. Analytical methods 162
3. Results and Discussion 163
4. Conclusion 169
5. References 170
VIII. Polycationic Spider Silk Protein Particles for Drug Delivery 173
1. Introduction 173
2. Materials and methods 176
2.1. Materials 176
2.2. Methods 178
3. Results and Discussion 180
4. Conclusion 190
5. References 190
IX. Final Summary And Conclusion 195
1. References 199
X. Appendix 201
1. List of Presentations and Publications 201
2. Curriculum Vitae 202

I. GENERAL INTRODUCTION

1. Introduction

Since the first biotechnology drug insulin was approved by the FDA in 1982, the need for suitable drug delivery systems for these sensitive, biological molecules have arisen [1]. The pharmacological effect of biological molecules is determined by the three-dimensional structure, which is again defined by a proteins primary, secondary, tertiary and quaternary structure [2]. However, this three-dimensional structure is prone to several chemical and physical alterations, which may lead to a loss of action or even toxicity [3, 4]. In addition, the short half-life of circulating proteins makes it difficult to administer biotechnological drugs [5]. Therefore, research focuses on strategies to overcome these drawbacks. Several techniques have been developed, including stabilization by the addition of excipients like sugars or salts to a protein formulation, stabilization of the protein using freeze-drying or modification of the protein molecule by polyethylene glycol (PEG) to prolong the plasma circulation time [3].

Over the last decades, polymer drug delivery systems, especially those having biocompatible and biodegradable properties, have become interesting new alternatives for protein delivery [6]. Polymer drug delivery systems can be utilized for controlled delivery of protein drugs in order to achieve a reduction of the application frequency [7]. In order to achieve sustained or controlled delivery of proteins, several delivery systems including implants, micro- and nanoparticles and injectable solutions have been investigated [8]. Currently, research is performed on poly-lactid acid (PLA), poly-lactic-co-glycolic acid (PLGA), cellulose, starch, chitosan, alginate, dextran, hyaluronic acid, collagen, albumin, gelatin, lipid-based carriers (micelles/liposomes) and silk fibroin [9, 10]. In the past, research was focused mainly on the PLGA based drug delivery systems, as the US Food and Drug Administration (FDA) has approved the biocompatible PLGA for use in humans [11]. Consequently, it is hardly surprising, that PLGA based sustained delivery systems for the peptides leuprorelin, octreotide and triptorelin have been approved. Moreover, the only marketed delivery system for a protein (Nutropin Depot®, recombinant human growth hormone) was also based on PLGA [12].

In search for an ideal polymer for particulate biomedical applications, silk protein appears to be a promising alternative. Due to its biodegradable and biocompatible properties as well as the unique mechanical characteristics, silk is an ideal candidate for pharmaceutical applications [13, 14]. Silk

proteins from the silkworm fibroin of *Bombyx mori* as well as spider silk proteins have been processed into different forms including gels, films and particles [15]. The possibility to utilize an all-aqueous preparation method made silk protein an interesting research object in the field of drug delivery for protein molecules [16].

2. Silk Proteins

Silk fibroin from silkworm has been used because of its impressive mechanical properties for biomedical use, for example as suture material [17]. Silk is produced by different animals like insects or spiders. Insects like the silkworm *Bombyx mori* use silk for their development in cocoons, whereas spiders use it for hunting their prey via the spider webs or as safety lines to prevent dropping from their nets [18].

Compared to currently used biodegradable polymers like collagen or PLGA, use of silk as a drug delivery system would be beneficial due to its biocompatibility, stability and weak immunogenic properties [19, 20]. Natural silk protein has an extraordinary high thermal stability up to temperatures of 140°C [21]. Both, thermal stability and biodegradation rate are affected by the crystalline β-sheet content and can therefore be modified by post-treatment with alcohols and kosmotropic salts [18]. The degradation of the most commonly used polymer PLGA causes a decrease in pH value by the generation of acidic cleavage products [22]. These acidic moieties lead to an immune response and acidic catalyzed drug degradation, whereas silk protein is degraded to non-toxic amino acids [23]. On the downside, crystalline silk fibroin is poorly water soluble. Highly concentrated salt solutions of guanidinium thiocyanate, lithium thiocyanate, calcium thiocyanate, lithium bromide or calcium chloride are used for dissolving silk fibroin in water [24–26]. Such chaotropic agents act by disrupting β-sheet stabilizing bonds and increase the hydrophilic properties of the protein [27]. Disadvantageous is therefore the additional step required to remove these electrolytes, for example by dialysis against water or aqueous buffers. Hexafluoroisopropranol, hexafluoroacetone or formic acid may also be used as solvents for silk proteins, however, their use is contra-productive for the preparation of drug delivery systems, as an all-aqueous preparation process is a major plus for silk as drug delivery polymer for sensitive proteins [25, 28]. The short physico-chemical stability of dissolved aqueous silk solutions is another issue, because silk protein is spontaneously precipitating into the water insoluble β-sheet state [29].

Although silk proteins from spiders and silkworms possess several similarities [30], the following two sections will focus on the characteristics of the individual proteins.

2.1. Silkworm silk

Besides the use as suture material, silkworm silk has been used in textile production for many years, because silkworms are easy to cultivate [31]. Most of the silkworm silk is collected from the cocoon of the silkworm *Bombyx mori*. Silkworm silk consists of two different structural proteins, a fibroin heavy and light chain, which are held together by sericin proteins [18]. The sericin coating has been identified as a potential allergen which causes a Type I allergic reaction [17]. To overcome this issue, sericin is removed by boiling the silkworm silk cocoons in aqueous sodium carbonate solutions for 30-60 minutes [32–34]. Nonetheless, silk fibroin from silkworm is a natural product. This means, for example, that the quality of the silk protein may vary between one silkworm species like *Bombyx mori* to other species like *Antheraea mylitta* and also within individuals of one species [35]. The sericin removal process and the variable quality is problematic with regards to quality control and approval by authorities [21].

Although the majority of the silk fibroins are obtained from the natural cocoons of the silkworms, synthesis of recombinant silk-elastin-like polymers (SELPs) is performed in *E. coli*, in yeast or by transgenic *B. mori* silkworms [36–38]. The design of SELPs is a repeated amino acid sequence of the silk-like block (Gly–Ala–Gly–Ala–Gly–Ser) and the elastin-like block (Gly–Val–Gly–Val–Pro) [39]. The ratio of these two building blocks can be varied to achieve the desired properties of the SELP protein. The degradation rate, the resorption and solubility of SELPs are highly affected by the ratio of silk-like to elastin-like blocks [40, 41].

2.2. Spider silk

Due to the cannibalistic nature of spiders, industrial farming of spiders is restricted and the collection of natural spider silk is very limited [42]. Natural spider silk consists of two major proteins, namely MaSp1 and MaSp2 from *N. clavipes* as well as ADF-3 and ADF-4 from *Araneus diadematus* [14]. Natural spider silk is produced in the major ampullate gland of the spiders. The amazing mechanical properties result from a mixture of hydrophobic blocks with crystalline features (rich in β-sheets) and hydrophilic elements with an amorphous structure [43]. As reported by Gosline et al., some natural silk fibers exhibit a higher toughness than Kevlar fibers [44]. Recombinant spider silk proteins are derived from the above-mentioned proteins of *N. clavipes* and *A. diadematus*. However, the recombinant synthesis of spider silk proteins has been difficult, because the natural spider silk sequence contains several repetitive and guanine and cytosine rich structures [42]. Consequently, publications on spider silk proteins were rare until the mid-end

1990ies (see Figure I-1). The progress in protein engineering (Figure I-1) finally enabled the production of spider silk proteins in a cost-effective manner and to achieve larger amounts than in previous years [45].

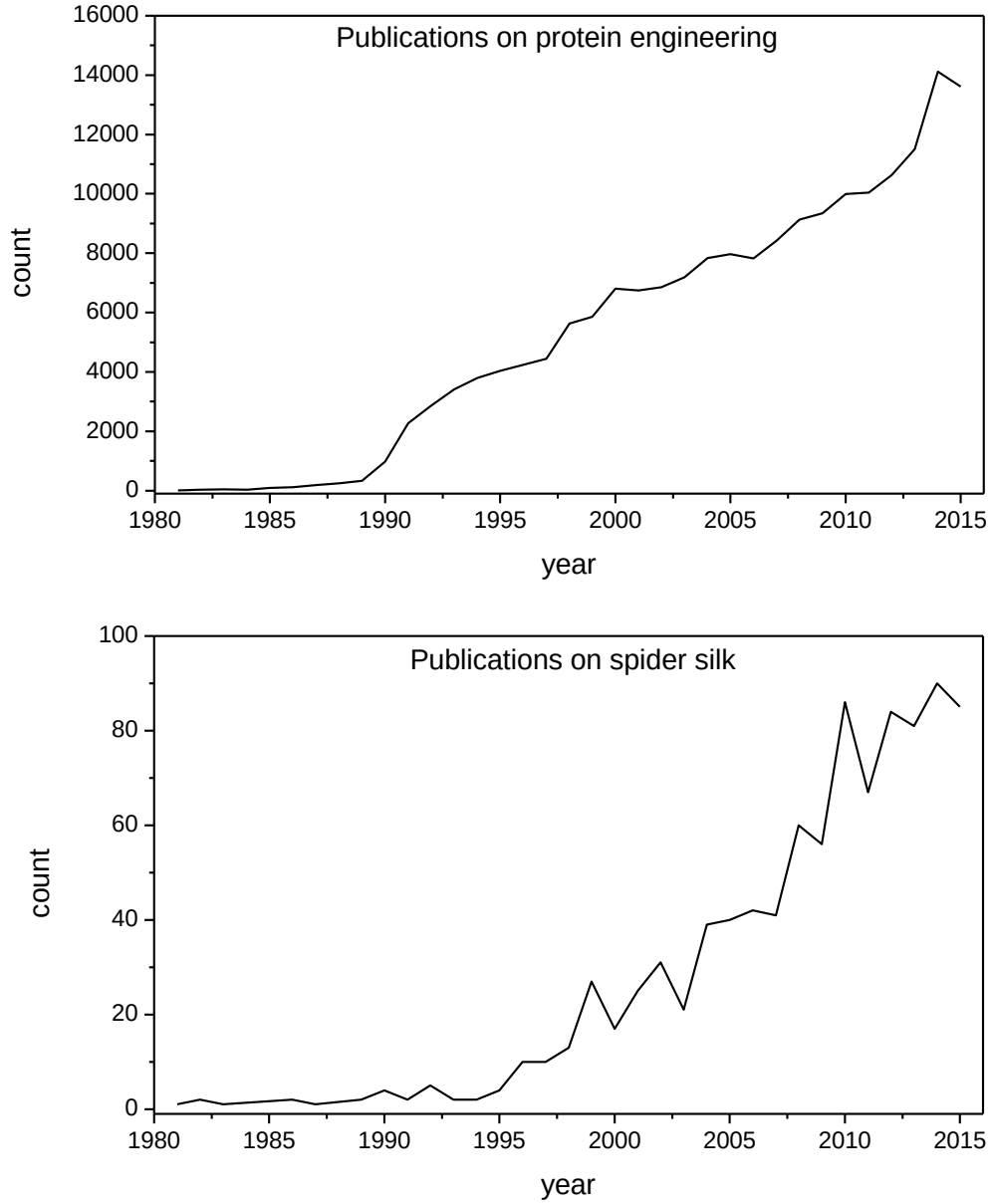

Figure I-1: Number of publications addressing the topics "protein engineering" and "spider silk" as a result of the Pubmed tool "Results by year" performed on April, 24th 2016 [46].

Protein engineering made it possible to design recombinant spider silk proteins with almost native silk properties. For this purpose, repetitive sequences were combined with non-repetitive sequences, which were then recombinantly produced in *E. coli* [45].

Most of the recombinant spider silk proteins are produced in *E. coli* bacteria [42]. Additionally, expression in yeast with a yield of 300-1,000 mg/l silk protein is also possible [18]. Other organisms

like plants, insects, animal cells and even whole transgenic animals have been used for recombinant spider silk protein production [27].

The protein engineering approach was further utilized to add functional ligands to the spider silk sequence, thereby creating hybrid spider silk proteins. In literature, several ligands like the cell binding RGB domain [47], tumor-homing peptides [48], cell-penetrating peptides for targeted drug delivery [49] or a His-Tag at the *N-terminus* of the protein to simplify the purification procedure [50] have already been reported to enhance the native spider silk properties.

3. Silk based drug delivery systems

Silk proteins offer the possibility to be processed into a variety of drug delivery systems, including implants, scaffolds, films, coatings, nano- and microparticles, hydrogels or fibers [21]. Drug incorporation into these systems has been studied, starting from small molecules like paracetamol [51] up to proteins like lysozyme [52] and different growth factors [53, 54].

3.1. Implants and Scaffolds

Mechanical properties are a major issue in scaffold production. Compared to other commonly used polymers such as collagen, chitosan and PLGA, silk fibroin possesses great strength and elasticity without the need for further crosslinking [55]. Silk-based scaffolds and implants have been used in research for tissue regeneration or controlled local drug delivery. For bone regeneration, bone morphogenetic protein-2 (BMP-2) was incorporated into 3D silk fibroin scaffolds and studied *in vitro* and *in vivo* [54]. Silk scaffolds offer the possibility to mimic the porous structures of natural bones and have the ability to deliver growth factors over an extended time to the tissue. It is not surprising that a lot of studies have been carried out using bone morphogenetic protein *in vitro* and *in vivo* [54, 56, 57].

Adenosine loaded silk-based implants have been used for sustained release studies and controlled release over a period of 2 weeks has been reported. Controlled degradation and release of the API from the silk-based implants offered the use in refractory epilepsy treatments [58].

Other model drugs, which have been tested using silk implants and scaffolds, are horseradish peroxidase (HRP) [59], nerve growth factor (NGF) [60], bovine serum albumin (BSA) [61], and insulin-like growth factor I (IGF-I) [53].

3.2. Films

Film casting can be performed in an all-aqueous process or by usage of hexafluoro-2-propanol or formic acid [62]. The dissolved silk protein is processed into films by casting on plates [51] or in molds [34].

Silk films have been used in two different ways of which the first is the application as drug carrier. Sensitive drugs, for example glucose oxidase, lipase and horseradish peroxidase, have been incorporated into silk films for protection against degradation [63]. The authors were able to show that the model proteins were not affected in the film after storage for ten months at 37°C. While the incorporated drugs were released after degradation of the silk film, the physically adsorbed proteins showed a high burst release at the beginning [63]. The phenomenon of high burst release from physically adsorbed drugs or proteins is a common issue. Agostini et al. addressed this topic and systematically evaluated several possibilities to slow down the release from silk films [51]. The authors found that a multilayer approach, where the drug containing film is covered by two non-loaded films, significantly slows down release of incorporated drugs. Due to the extra step in the production of such multilayer films, the authors also used 2-pyrrolidone as plasticizer for the film matrix of monolayer films. The 2-pyrrolidone treated films showed excellent mechanical properties and a sustained release of the incorporated protein over several months [51].

Covalent decoration of silk films with functional peptides is the other field of application. RGD-modified silk films, where the RGD motif was either chemically coupled or attached via genetic modification and recombinant production, increased the fibroblast adhesion and proliferation in an *in vitro* approach [64]. The integrin recognition sequence (RGD) was used in combination with a parathyroid hormone by Sofia et al. for new bone formation [65]. The RGD-modified silk films showed a superior osteoblast-based mineralization compared to a control parathyroid hormone and plastic implants [65]. Both studies highlight the high potential of modified silk films for tissue engineering in the future.

3.3. Coatings of drug delivery systems

The possibility of drug incorporation in or between coating layers as well as the possibility to coat a large variety of systems is advantageous in modern drug delivery [21]. Silk protein was used for layer-by-layer coating of quartz crystals or glass surfaces. The first experiments were used to evaluate the properties of the silk layer after coating. The silk based coatings can vary between 10 nm per layer up to a layer thickness 1 µm or even 10 µm [66, 67]. The secondary structure of the silk protein is of high importance for coatings, turning the silk layer into an aqueous insoluble conformation and controlling the degradation rate [67].

Drug incorporated, multilayered silk coatings have been developed using heparin, paclitaxel or clopidogrel on metallic stents [68]. Wang et el. demonstrated in their study, that silk coated stents loaded with heparin, paclitaxel or clopidogrel reduced the attachment and proliferation of cells on the stent in an *in vitro* study [68]. Furthermore, the authors were able to show a prevention of restenosis and the stability of the silk coating in an *in vivo* pig study.

Silk coatings can also be used without drug incorporation. Zeplin et al. used the recombinant spider silk protein eADF4(C16) for coating of silicone implants [69]. A common drawback of breast implants is the recognition of the implant by the immune system with subsequent attraction of inflammatory cells resulting in fibrosis. The formed fibrotic capsule around the implant can lead to painful complications after surgery. However, silk coated implants were able to successfully reduce the cell proliferation on the implant surface resulting in less fibrosis by masking the silicone [69]. The easy modification by dip coating makes silk coatings an attractive improvement of the current silicone implants.

3.4. Nano- and microfibers

In contrast to silk implants, fibers can mimic the extracellular matrix due to their nanoscale size. Fibers are commonly prepared by electrospinning, where an electrical field is used to form small-scale fibers from a silk solution in a syringe [70]. Silk fibers containing BMP-2 and hydroxyapatite showed efficient drug delivery for *in vitro* bone formation in human mesenchymal stem cells [71]. Due to their small-scale dimensions and variability by adjustment of solution and preparation properties, electrospun fibers had become popular in tissue engineering [72]. For example, silk nanofibers with incorporated silver nanoparticles were characterized for their use as antimicrobial wound dressings [73]. The silver particles were added by easy dip coating and subsequent photo reduction on the surface of the electrospun silk nanofibers.

3.5. Nano- and microparticles

The significant potential of particulate delivery forms has been used for the delivery of therapeutic molecules. Nanoparticles as well as microparticles have been prepared for different applications in the field of severe diseases like cancer, AIDS or tuberculosis [74–76]. Size, surface charge and surface decoration have been identified as important parameters for interaction with the cell membrane and penetration into body tissue [10]. In some cases, protein based nano- and microparticles have been prepared under all-aqueous conditions to overcome the shortcomings of commonly used preparation methods like emulsification and coacervation [35, 77, 78].

Silk particles have been produced in various dimensions, ranging from microparticles with

diameters up to 440 µm [9] to nanoparticles with diameters small as 70 nm [79] using several different preparation techniques. Some of them shall be presented below.

3.5.1. Preparation of silk particles

Nanoparticles from silkworm *B. mori* and tropical silkworm *A. mylitta* have been prepared by a desolvation technique using dimethyl sulfoxide as desolvating agent [35]. Particle diameters of both silk types were comparable in the size range of 155-180 nm. These particles exhibited good stability, no toxicity and a negative surface charge. The loaded growth factor showed sustained release over three weeks in the cytosol of murine squamous carcinoma cells [35].

Recombinant spider silk protein was processed into micro- and nanoparticles. Different particle fabrication techniques, including dialysis, mixing with a pipette and micromixing in a syringe pump were compared [16]. Essentially, particle formation was driven by a salting out effect in a potassium phosphate solution [32]. Using a 500 mM solution (pH 8) resulted in the formation of clusters of aggregates whereas the silk protein formed stable spherical particles after treatment with a 1 M potassium phosphate solution [16]. When using dialysis of silk solution against potassium phosphate, particles were in the range of micrometers with a broad size distribution. However, simple mixing of the solutions with a pipette yielded in stable nanoparticles with average diameters between 350 nm and 510 nm. Syringe pump mixing generated particles with sizes of 290-370 nm applying a flow rate of 2 ml/min and 250-320 nm for turbulent flow conditions at a flow rate of 50 ml/min [16]. Increasing the silk protein concentration during particle preparation always resulted in larger particles.

Micrometer sized silkworm silk particles were prepared by spray-drying [26]. The stability of the particles and the water insolubility was increased by a post treatment step using either water vapor or methanol [26, 80]. The post treatment led to an increase of the proteins β-sheet content. However, the high inlet temperatures during spray-drying, which may lead to a damage of the encapsulated drug, and potential post treatment procedures to induce water insolubility, are disadvantages of spray drying as fabrication method.

Silkworm silk microspheres have been prepared by Wenk et al. using a laminar jet break-up technology [9]. This technique has been used for alginate beads preparation before [81]. An aqueous silk solution was sprayed into a bath of liquid nitrogen, using a vibration unit for droplet generation [9]. Subsequently, the shock frozen particles were freeze dried at -25°C for 12 h. Particle shrinkage has been observed after methanol or water vapor treatment to average diameters of 260 µm and 200 µm, respectively. Moreover, a diluted silk solution resulted in

smaller particles [9].

A traditional water-in-oil preparation method was used for microcapsule fabrication. Due to its amphiphilic nature, silk protein assembled at the toluene/water interface generating a film and encapsulated an aqueous core. By varying the stirring speed of the solution, the authors were able to control the size of the resulting particles [82].

Wen et al. used a novel ultra-fine particle processing system [6]. This system was built to continuously produce particles in the micron size. Main elements of this new system are a feeding nozzle for the silk solution, which is placed in center of a rotating disc. To control and dry the droplets after leaving the rotating disc, three different airflow systems are integrated into the system. A collecting vessel with carrier gas ensures the complete dryness of the particles and moves them forward to a sample collector. Particles prepared with this system show mean diameters of 63, 42 and 30 µm for disc speeds of 6,000, 9,000 and 12,000 rpm with a narrow size distribution. As shown before, higher concentrated silk solutions generated larger particles. SEM micrographs showed a spherical shape with a lot of dents. Uniform drug distribution was achieved by a simple encapsulation process [6].

Most of the currently performed preparation methods for silk particles require a post treatment step to induce water insolubility of the particles. Frequently used post treatment methods are using methanol, salt solutions or water vapor [83]. All these treatments are used to transform a random coil or helical conformation of the proteins into a β-sheet rich structure, which is necessary to achieve water insolubility [84]. Using methanol for this purpose has the disadvantage of introducing an organic solvent into the preparation process. Furthermore, previous studies have shown a loss of activity for lysozyme after treating silk fibroin films with methanol [85]. Nevertheless, silk particle preparation is also possible in an all-aqueous preparation process resulting in water insoluble particles, offering the possibility for encapsulation of sensitive drugs [52].

3.5.2. Drug loading of silk particles

Essentially, there are three options of drug loading, with i) remote loading after preparation of the drug carrier, ii) covalent coupling of the drug to the delivery system and iii) direct encapsulation of the drug during the preparation process [21].

Remote loading as a post-fabrication method allows the preparation of the delivery system in advance and an addition of the drug after the preparation procedure. The drug is protected against harsh processing conditions during the preparation process. On the contrary, there are also

limitations for post-fabrication loading. If the desired drug is larger than the pores in the delivery system, no core diffusion will occur and simple adsorption on the surface is the only loading principle. Surface adsorbed drug is easily removed from the delivery system, in particular, if adsorption is only driven by electrostatic interactions, and therefore ensuring controlled release of a drug could be an issue. Moreover, loading is limited to the adsorption capabilities of drug and carrier material. With regards to the isoelectric points of 3.48 for spider silk [86] or 4.2 for silkworm silk [87], positively charged drugs preferably interact with spider silk systems at neutral pH values.

Lammel et al. compared in their study the loading behavior of 12 small molecule drugs on spider silk particles [88]. The authors observed that small molecule drugs diffuse into the core of spider silk particles by comparing the loading behavior between spider silk particles and dense glass beads. In addition, they verified the strong electrostatic dependence between drug and silk delivery systems. Basic drugs with a positive charge showed good loading efficiencies whereas negatively charged drugs were poorly incorporated or no loading was possible [88].

Loading of macromolecular drugs on spider silk particles was demonstrated by Hofer et al. [52]. Using lysozyme as a model protein, successful loading of up to 30% [w/w] lysozyme by simple co-incubation of spider silk particles and lysozyme in phosphate buffer was possible. Electrostatic interactions between lysozyme and spider silk particles were demonstrated by comparing loading at different ionic strengths. During lysozyme loading, neither the zeta-potential decreased nor the particle size increased. This observation support the authors' argument that lysozyme diffuses into the particle matrix [52].

The second and most straightforward possibility of drug incorporation is direct encapsulation during processing. The main challenge is to ensure that the drug is not damaged during the preparation procedure and the drug's activity is preserved. In addition, the drug should not influence the preparation process itself.

Wenk et al. prepared microspheres with directly encapsulated drugs [9]. The authors used a liquid nitrogen bath to collect the manufactured microspheres from an encapsulator with an oscillation nozzle. Salicylic acid, propranolol and insulin-like growth factor I (IGF-I) were dissolved prior to spraying the solution to the liquid nitrogen bath. Although all model drugs were incorporated in the particle matrix during fabrication, a high burst release was observed for salicylic acid and propranolol hydrochloride, while the IGF-I protein showed a sustained release profile. [9]. Wang et al. prepared the silk microspheres after addition of lipid templates, using dextran and horseradish peroxidase as model drugs [80]. Similar to Wenk et al., liquid nitrogen was utilized in the particle preparation process. Additionally, three freeze-thaw steps were included to obtain

smaller particles with a homogeneous size distribution. Without further post treatment in NaCl solution, a high burst release was observed likewise [80]. So, the disadvantage of these preparation methods is the necessity of a post treatment after preparation process, which is required to generate water insoluble particles.

Hermanson et al. prepared microcapsules with a water-in-oil emulsification method. Recombinant spider silk protein quickly adsorbed at the water/oil interface and encapsulated the water-soluble model substance dextran. The majority of the fluorescently labeled dextran with a molecular weight of 40 kDa was retained inside the microcapsule, while only a small fraction diffused trough the microcapsule. The release rate was highly affected by the enzymatic degradation of the silk microcapsule. Cross-linking the silk membrane to prevent enzymatic degradation increased the stability of the silk microcapsules. In contrast to non-crosslinked microcapsules, which released the encapsulated dextran immediately after proteinase K addition, cross-linked microcapsules were stable for one hour of proteinase K incubation at 37°C [89].

A direct comparison between the remote loading and direct encapsulation process was conducted by Blüm et al. [90]. The authors used recombinant spider silk and the small molecule rhodamine B to prepare loaded spider silk particles. The direct encapsulation led to an improved loading efficiency of the particles compared to the remote loading. Additionally, further crosslinking of the spider silk protein particles using ammonium persulfate (APS) and Tris(2,2'-bipyridyl)dichlororuthenium(II) (Rubpy) led to a slower drug release from the particles [90].

The last drug loading possibility is covalent coupling of the drug to the matrix of the delivery system. In this case, the drug has a permanent connection to the delivery system with a reduced risk of leaching. This advantage comes in a price with the negative consequence of an additional processing step and risk of toxic residues in the delivery system.

Covalent coupling of insulin to silkworm silk nanoparticles has been shown by Yan et al. [79]. The authors covalently coupled insulin to the silk nanoparticles using a 0.7% glutaraldehyde solution. Higher concentrations of glutaraldehyde and a longer incubation time led to increased insulin denaturation. *In vitro* stability studies indicated an improved stability of cross-linked insulin with silk fibroin nanoparticles as well as an increased activity compared to unbound insulin [79].

Similarly, Florczak et al. used carbodiimide (EDC) and N-hydroxysulfosuccinimide (Sulfo-NHS) chemistry to covalently conjugate peptides and an anti-Her2 antibody to spider silk protein spheres [74]. The conjugated spheres were used for a targeted drug delivery of the toxic cancer chemotherapeutic doxorubicin [74].

Covalent coupling has been also applied for PEGylation of silk nanoparticles. Wongpinyochit et al. decorated the nanoparticle surface with polyethylene glycol (PEG) via covalent conjugation [91]. The PEGylated silk nanoparticles showed less plasma membrane binding and a modulated cellular uptake compared to non- PEGylated nanoparticles [91].

3.6. Functionalization of silk based drug delivery systems

Functionalization of silk based drug delivery systems can be either performed via covalent linkage or by using genetic modification. Sofia et al. introduced different target peptides to their silk films, including the integrin recognition sequence RGD via carbodiimide chemistry [65]. Analysis of the osteoblast like cell response demonstrated a higher affinity of the cells to the RGD decorated films when compared to non-decorated silk films [65].

A different strategy was assessed by Wang et al. to introduce specific molecules under mild conditions [92]. The authors decorated silk gels and microspheres covalently with NeutrAvidin™, a genetically modified version of avidin with a high affinity to biotin. Introducing NeutrAvidin™ had no effect on the self-assembly properties of the silk molecules or morphology of silk particles. Biotinylated horseradish peroxidase (HRP) was used for binding studies on the film, demonstrating a high specific binding rate of 90% to NeutrAvidin™ decorated silk gels. However, unspecific binding of biotinylated HRP led to a binding rate of 70% to non-decorated gels. The mild conditions of this method offer the possibility to link biotinylated molecules to several material surfaces under neutral pH and room temperature [92].

A great benefit of recombinant spider silk proteins is the possibility to introduce various motifs directly into the primary structure via genetic modification. The cell adhesion motif RGD was used by Wohlrab et al. to create a genetic modified hybrid protein [64]. The authors processed the new hybrid protein and a chemically coupled version into silk films. While the RGD motif had no influence on the silk properties, the hybrid protein films showed a slightly better performance compared to the conjugated films *in vitro* [64].

Gomes et al. used genetic modification to design antimicrobial spider silk proteins [93]. Three human antimicrobial peptides (HNP-2, HNP-4 and hepcidin) were fused to the native spider silk protein without changing the properties during film processing. *In vitro* antimicrobial studies against Gram- and Gram+ bacteria showed that the antimicrobial activity of the peptides maintained their activity after processing into films. Due to the low cytotoxicity of the hybrid protein films, the antimicrobial spider silk proteins can be a potential approach against bacterial infections for example in wound healing.

In a similar approach, Currie et al. fused a silver binding peptide to a spider silk protein [94]. The recombinant silver binding silk proteins were processed into films. The silver binding peptides in the film matrix were able to nucleate silver ions from an added silver nitrate solution. Like the human antimicrobial peptide hybrid proteins before, the silver-binding silk films inhibited the microbial growth of gram negative and gram positive microorganisms *in vitro*.

A hybrid spider silk protein for the targeted cancer therapy was engineered by Florczak et al. [74]. A variant of the recombinant spider silk protein MS1 (adapted from the major ampullate silk protein of *N. clavipes*) comprised the Her2 binding peptides (H2.1 or H2.2) in order to address cells overexpressing the Her2 receptor. While the self-assembling properties of the silk protein were unchanged, the authors were able to show that the N-terminal addition of the Her2 binding peptides was superior to the C-terminal attachment. Both variants showed effective binding to Her2 overexpressing cells, demonstrating the potential for a targeted drug delivery.

4. Particulate Delivery Systems for Vaccination

Vaccines are used in healthy persons to prevent infectious diseases. For this purpose, vaccines are highly effective, as can be seen by the eradication of smallpox and the control of diseases like measles, mumps, rubella and many more [95]. Due to the fact that healthy persons are treated, vaccines of all kinds (live attenuated, inactivated or subunit vaccines, with or without adjuvant) need to be particularly safe during and after application [96].

Conventional vaccines have been prepared by using native pathogens, which were inactivated or attenuated during the development. These vaccines were highly immunogenic and able to produce both humoral and cellular immunity. On the contrary, there are serious safety concerns as pathogens may revert back to their virulent form or when such vaccines are administered to immunodeficient individuals [97]. Consequently, recent research has focused on more controllable formulations using DNA or subunit vaccines. DNA vaccines consist of genes encoding a specific antigen, but have solely been used for veterinary applications so far [98]. Subunit vaccines contain only a well-defined part of the original pathogen. Besides an increased safety profile of these vaccines, every antigen can be produced by recombinant preparation method, even if it is impossible to grow the original pathogen in culture. When DNA or subunit vaccines are used, the addition of an immunostimulatory adjuvant is usually needed, as the antigen alone is only weakly immunogenic [99].

Adjuvants (from Latin, "*adjuvare*": to support, to help) are molecules which assist the active pharmaceutical ingredient to achieve its effect [100]. Usually, this term is used in relation to

vaccines. The traditional definition of a vaccine adjuvant is a molecule, which enhances the effect of antigens to elicit an immune reaction [101]. Traditional approved adjuvants like aluminum salts or MF59 (an oil-in-water emulsion) act directly as immunostimulatory agents, which activate the immune system to react on the administered antigen [102]. However, particulate delivery systems may also serve as adjuvants by targeting specific immune cells [97]. Antigen loaded particles can mimic the natural size of pathogens, so that the immune system can recognize the antigen easier and the uptake by antigen presenting cells (APCs) is enhanced [103]. After entering the body, circulating APCs present the epitope in the local lymph nodes to immune cells in order to induce an immune response [104]. By that, a cell-mediated immune response is triggered via cross-presentation the antigen by both MHC-I and MHC-II pathway [105]. Another attractive feature of particulate antigen delivery systems is the possibility of a sustained antigen release via an antigen depot [106]. With respect to antigen stability, antigen entrapped in particles is protected against degradation by proteolytic enzymes, especially as some antigens are destabilized by traditional adjuvants like aluminum salts [107]. Additionally, particles can help to deliver the antigen together with an immunostimulatory adjuvant to the same group of APCs and affect the type of immune response [108]. Moreover, toxic side effects of immunostimulatory adjuvants could be eliminated by encapsulation. The simultaneous release of the antigen and adjuvant after uptake by APCs can reduce systemic bioavailability and increase the immune response at the same time [96].

The strict safety regulations for the approval of new adjuvants are challenging, as many adjuvants have shown potent immune stimulation, but are too toxic for routine use [101]. Due to the simple reason that healthy individuals, including infants or elderly people, are treated with vaccines, only adjuvants with minimal adverse effects are suitable for regular use in vaccination [96].

4.1. Nano- and microparticles based on lipids and lipid–saponin mixtures

4.1.1. Liposomes

Liposomes are spherical bilayer vesicles composed of phospholipids with an aqueous core. They can be easily prepared in the large scale and their sizes can range from 50 nm up to some micrometers. Liposomes have been widely studied for drug delivery. These studies led to the development of Doxil® (liposomal doxorubicin) and Ambisome® (liposomal amphotericin B), two approved liposomal drug formulations, which are used regularly in the clinical routine [109]. However, the use of liposomes has also some drawbacks. Conventional liposomes have only a low encapsulation efficacy, short circulation time, show limited stability and a high aggregation tendency in liquids [110]. Antigens can be incorporated either in the aqueous core or in the lipid

shell of the liposomes, all of which can protect the antigen from degradation [95]. Modifying the liposome surface with viral envelope proteins led to so called virosomes [103]. With enhanced immunostimulatory features, virosomes have the possibility to fuse with the endosomal membrane of the target cells and release the antigen to the cytosol [111]. The administration of virosomes can elicit both, a humoral and cellular immune response [100]. Besides being just a delivery system for the antigen, positively charged liposomes efficiently induced a cell mediated immune response [112]. Liposomal formulations were found to be safe and easy to administer, which led to the approval of the liposomal vaccines Epaxal® and Inflexal® V [113]. A virosome based influenza vaccine, however, showed serious adverse events after intranasal administration and resulted in the withdrawal of the formulation from the market [114].

4.1.2. Viral-vectors

Vectored vaccines use a non-replicating pathogen to deliver the DNA encoding for an antigen of the pathogen to which immunity is desired. As such vaccines contain the envelope of normal pathogens, they elicit a strong immune response and show potential for mucosal immunization via nasal application [95]. Many different viral or bacterial vectors are possible candidates, but those which have been most used are adenoviruses, poxviruses or Bacillus Calmette-Guérin [115]. These vectors combine good safety profiles with an easy production method. Their potential to stimulate a cellular T-cell response was studied using HIV vaccines [116]. A prime-boost regimen was established to increase the immune response, where the first immunization was carried out using a viral-vectored vaccine, followed by a booster dose of the same protein in a soluble form or in another type of vector [117]. This procedure was used successfully in vaccination studies against malaria [117].

4.1.3. Immunostimulating complexes

Immunostimulating complexes (ISCOMs) are spherical, cage-like colloidal structures composed of an antigen, cholesterol, phospholipid and Quil A saponin [118, 119]. The saponin is derived from the bark of the South American *Quillaja saponaria Molina* tree. The hydrophobic antigen can be loaded directly into the lipid matrix, whereas hydrophilic antigens need a modification step prior to that [103]. ISCOMs have shown a strong immune response with both cellular and humoral immunity. Compared to a standard flu vaccine, an ISCOM based vaccine elicited a higher immune response rate with a good safety and toxicity profile in humans [120]. Despite their good performance, ISCOM vaccines are still not used in human vaccines due to safety concerns with regards to saponin toxicity at higher concentrations [95]. However, ISCOM based vaccines are

approved in veterinary applications [103].

Using the same structure as ISCOMs but excluding the antigen led to the development of ISCOMATRIX®. This formulation provides a more general use, because the antigen can be added later during the formulation step. Indicating a safe and immunogenic immune response both in humans and in animals, ISCOMATRIX® could be used as new adjuvant in vaccine formulations [121, 122].

ISCOMs have also been converted into their positively-charged counterparts, so-called PLUSCOMs. Due to their positive charge, it was possible to load the negatively charged model antigen ovalbumin by electrostatic interactions [123].

4.2. Nano- and microparticles based on polymers and minerals

4.2.1. Calcium phosphate particles

Calcium phosphate particles can be fabricated by stirring a combined solution of calcium chloride, sodium phosphate and sodium citrate resulting in final particle sizes of less than 1.2 µm [124]. As calcium phosphate is naturally present in human body, safety issues are of minor importance. The calcium phosphate particles adsorb antigens similar like the commonly used alum salts, although to a smaller extent [125]. The intramuscular administration of calcium phosphate nanoparticles was well tolerated by guinea pigs in an *in vivo* study [126]. Further studies indicated that calcium phosphate nanoparticles were superior when compared to soluble antigen alone *in vitro* [127] and *in vivo* in mice [128]. The ability to induce a mucosal immunity was shown in studies against an HSV-2 antigen [125]. Furthermore, co-delivery of an immunostimulatory adjuvant together with an antigen is possible with calcium phosphate nanoparticles [127].

4.2.2. Poly lactic-co-glycolic acid (PLGA) particles

The most commonly studied polymers for use as drug delivery vehicles are poly-lactic acid (PLA) and poly-lactic-co-glycolic acid (PLGA) [11]. These polymers have also been used for particulate antigen delivery in the field of vaccination. Already in 1999, PLGA nanoparticles loaded with a *Helicobacter pylori* lysate was found to effectively induce a systemic and mucosal immune response after oral administration in mice [129]. The fabrication process of PLGA particles can already be used to encapsulate antigens into the polymer matrix. However, simple surface adsorption is also possible for pre-fabricated PLGA particles [130]. The biocompatible and biodegradable properties make PLGA highly attractive for a systemic administration. The degradation rate of the PLGA particles can be tailored to the desired release kinetics of the

antigen, where the particles serve as an antigen depot [131]. Joshi et al. reported in their study about release times up to 350 hours [132]. Nevertheless, a high burst release after administration is commonly observed when PLGA particles are used [133]. In addition, the polymer degradation via acidic hydrolysis can lead to a damage of the entrapped antigen due to a shift to acidic pH values [134].

4.2.3. Chitosan particles

Chitosan is a natural polymer, which is obtained by alkaline deacetylation of chitin [135]. Due to the biodegradable, biocompatible and nontoxic properties, chitosan is commonly used for different drug delivery systems [136]. Chitosan based particles are used for protein, peptide and DNA vaccination [137–139]. An advantage of chitosan is the stabilization of entrapped DNA, which is then protected against degradation by nuclease [140]. Due to the bioadhesive properties, chitosan particles are efficiently taken up by enterocytes [141]. The bioadhesive properties of chitosan nanoparticles were often demonstrated after oral, nasal and pulmonary antigen delivery [142]. However, the oral route is often avoided, because chitosan particles are degraded in an acidic environment [143]. If oral vaccination by chitosan particles is desired, alginate is used to cover the chitosan particles. The alginate cover is sensitive to a basic pH in the intestine, releasing the antigen loaded chitosan particles [139]. Other studies demonstrated that chitosan particles were also successful inducing an immune response after intradermal [144] or parenteral administration [145].

4.2.4. Gelatin particles

Like chitosan, gelatin is a natural polymer. Two types of gelatin are commercially available, which are obtained by acidic or alkaline hydrolysis of collagen [146]. Due to its pharmaceutical use since decades, gelatin is considered as GRAS (generally regarded as safe) material by the FDA [147]. Although gelatin nanoparticles (GNPs) are studied for use in several pharmaceutical applications, they have been poorly studied for vaccination. Coester et al. showed the experimental uptake of GNPs loaded with fluorescent dextran into bone marrow derived dendritic cells (BMDCs) [148]. A comparison of tetanus toxoid loaded GNPs with traditional aluminum salts showed a slightly better performance of the GNPs after subcutaneous administration in mice [149]. In addition, cationized GNPs showed excellent uptake by dendritic cells and an enhanced immunostimulatory activity of the loaded CpG oligodeoxynucleotides [150]. The protein based structure of the gelatin is an additional feature, which could be used for the simultaneous delivery of an antigen and an immunostimulatory adjuvant. The release of the loaded antigen is mainly driven by the

degradation of the gelatin matrix by lysosomal enzymes [151]. However, the need of crosslinking with the potential risk of toxic crosslinking residues is one main disadvantage of the GNPs for their use in vaccination [152]. In addition, the influence of the crosslinker on the loaded antigen has to be considered carefully.

4.2.5. Gold particles

In addition to the several biodegradable particles, which are studied for their use as vaccine adjuvants, gold nanoparticles have also been evaluated with respect to their applicability as particulate delivery systems. Gold nanoparticles are easy to fabricate and shapeable into different systems like spheres or rods [153]. The solid structure of gold nanoparticles allows the adsorption of antigens on the particle surface as the only loading mechanism [154]. The surface, however, can be modified by a sugar coating, which allows further binding of probes or peptides and an interaction with other carbohydrates [155]. Gold nanoparticles have been used as a carrier for DNA vaccines [156], proteins [157] and peptides [158]. Especially DNA delivery is of high interest. The low potency of commonly studied DNA vaccines was obviously enhanced when using electroporation [159]. Electroporation is using an electrical field to increase the permeability of cells and therefore the uptake of foreign material into the cell. However, electroporation is not an option for human use, as the high voltage pulses will cause drastic cell mortality [160]. The use of gold nanoparticles without the assistance of electroporation, however, led to a relatively low transfection rate of DNA loaded gold nanoparticles [161]. Due to the non-biodegradable nature of the gold nanoparticles, the particles will remain for a relatively long time at the site of injection, which may result in an antigen depot showing sustained antigen release. The studies on gold nanoparticles revealed that both humoral and cellular immunity is induced following their administration [142].

4.3. Vaccine administration

Vaccines are traditionally administered either via subcutaneous (s.c.) or intramuscular (i.m.) injection. With the exception of one influenza vaccine, the s.c. and i.m. injections are practiced using syringes and needles. This procedure has the drawbacks of requiring trained personnel, can lead to needle stick injuries followed by transmission of diseases or end up in the rejection of vaccination based on a fear of needles [162]. Some of these drawbacks are bypassed by the PharmaJet Stratis®. This jet injector device is approved by the FDA for a needle-free i.m. influenza vaccination [163]. However, the site of administration still did not change until the approval of FluMist® in 2003 [164]. FluMist® is an influenza vaccine administered intranasally. The intranasal

application has the big advantage of mimicking the natural pulmonary, nasal and oral pathway of many pathogens. Because of that, the body has a huge mucosal immune system [165]. Using the mucosal vaccination route can activate secretory immunoglobulin A (IgA) antibodies [166]. IgA can elicit a strong immune response, because the presentation to local lymph nodes is very effective, and was shown to be more cross-protective against different strains of a pathogen [167]. Furthermore, activated lymphocytes can migrate via local lymph nodes to the bloodstream and other mucosal tissues and elicit a strong immune response [168]. However, the nasal application has the drawback of just using a small mucosal area, eliciting a more local immunity and a high variation of response [169]. In contrast, the lung has a very large surface area for interaction with inhaled pathogens or vaccines [170]. In addition, various types of dendritic cells and macrophages are located in the lung parenchyma for efficient pathogen internalization and subsequent T cell presentation [171]. Because of that, pulmonary vaccination can activate both a humoral and cellular immune response [172]. Several studies have shown that pulmonary vaccination is safe and effective. For example, de Swart et al. compared an aerosol measles vaccination with a traditional parenteral injection in an *in vivo* monkey study [173]. The authors demonstrated, that the aerosol vaccination had no detrimental or toxic side effects and was as effective as the liquid injection. While de Swart et al. used no adjuvant for their study, particulate adjuvants can enhance the immune response. Copland et al. used free antigen, antigen in non-modified liposomes and antigen in mannosylated liposomes. The mannosylated liposomes in the size range of 260 nm activated T cells more efficiently than the non-modified liposomes or the free antigens [174]. However, the main safety concern is the efficiency of pulmonary vaccines on people with respiratory diseases and a potential exacerbation of the diseases after vaccination [175].

5. Objectives of the Thesis

The overall aim of this thesis was to fabricate recombinant spider silk particles for a modern vaccination approach. The need for new vaccines is more relevant than ever. Traditional vaccine formulations reach their limits with regard to initiating an immune response towards a cell mediated immunity or activation for a therapeutic vaccination for indications such as allergy, cancer and chronic viral infections.

First of all, the relevant prerequisites that should be met for studies in the field of vaccination and immunization had to be evaluated. Due to the recombinant production of the eADF4(C16) spider silk protein, a suitable purification process to remove endotoxins had to be established. These fragments of bacterial cell walls may negatively affect *in vitro* and *in vivo* studies, as they act as

strong immunostimulatory agents. Due to the very stable character of endotoxins, resisting extreme temperatures and pH values, removal of endotoxins from proteins is challenging. Therefore, a simple and scalable endotoxin purification process of the eADF4(C16) spider silk protein had to be established.

Additionally, the pharmacopeias request sterility as an indispensable prerequisite for parenterally administered formulations [176]. On the basis of the extraordinary properties of the spider silk protein, an easy and simple method for the sterilization of final eADF4(C16) protein particles had to be found.

Following the establishment of a suitable endotoxin depletion and sterilization procedure, two different possibilities to attach a model vaccine antigen to the spider silk particles were assessed: chemical linkage and inclusion of the antigen in the recombinant production process to result in spider silk hybrid particles.

Chemical linkage of the antigen to the eADF4(C16) protein was evaluated, in order to have a benchmark to the current state-of-the-art method. Therefore, two different cleavable linkers were selected for the attachment of the model antigen. The influence of different linkers and preparation methods had to be evaluated with respect to coupling efficiency, particle size and particle surface charge.

The main focus of the thesis was, however, the design of an eADF4(C16)-antigen hybrid protein, where the antigen is directly incorporated into the primary structure of the spider silk protein. This strategy may allow a preparation of antigen containing particulate delivery systems in a one-step fabrication process. Different hybrid proteins with and without cleavable linkers were processed into spider silk submicroparticles. The properties the eADF4(C16)-antigen hybrid protein particles had to be studied in comparison to non-modified eADF4(C16) protein particles to detect possible alterations by the addition of the antigen. Parameters like particle size and surface charge, protein secondary structure, thermal behavior, cellular uptake and antigen release were selected for this comparison.

The toxicity of both non-modified spider silk particles and spider silk hybrid particles was assessed *in vitro* using a MTT assay. The *in vitro* results were an essential milestone to show the low toxicity of the particles and enabled to move the system forward to *in vivo* studies.

The final aim of this thesis was the preparation of eADF4(C16) protein particles for *in vivo* investigation to determine the vaccination efficiency of the newly designed eADF4(C16)-antigen protein particles following subcutaneous administration.

In addition to a traditional subcutaneous administration of the vaccine, the possibility to administer the eADF4(C16) protein particle also via lung deposition was shown using nebulization experiments. The possibility to use mucosal immunization via pulmonary delivery is a promising route for future vaccination, because it mimics the natural route of most infections. Two different nebulization techniques were selected for the ability to aerosolize differently sized eADF4(C16) protein particles.

The introduction showed, that loading is a challenging task for most particulate delivery systems. Remote loading is a simple and cost effective method, but requires interaction between the delivery system and the target molecule. In case of the eADF4(C16) protein, surface charge is negative at neutral pH and loading is only possible with positively charged molecules. The characterization of a newly designed spider silk protein with an altered surface charge was finally the last objective of this thesis. The new spider silk protein was genetically modified and negatively charged amino acids were replaced by positively charged ones to result in a positive surface charge at neutral pH. The stability and suitability of the positively charged spider silk particles serving as potential drug delivery carrier for negatively charged protein drugs was addressed in the last chapter.

6. References

[1] L. R. Judge, “Biotechnology: Highlights of the Science and Law Shaping the Industry,” in *Santa Clara Computer & High Technology Law Journal*, vol. 20, 2003, pp. 79–93.

[2] W. Wang, “Instability, stabilization, and formulation of liquid protein pharmaceuticals,” *Int. J. Pharm.*, vol. 185, no. 2, pp. 129–188, 1999.

[3] S. Frokjaer and D. E. Otzen, “Protein drug stability: a formulation challenge,” *Nat. Rev. Drug Discov.*, vol. 4, no. 4, pp. 298–306, 2005.

[4] M. C. Manning, K. Patel, and R. T. Borchardt, “Stability of Protein Pharmaceuticals,” *Pharm. Res.*, vol. 6, no. 11, pp. 903–918, 1989.

[5] M. C. Manning, D. K. Chou, B. M. Murphy, R. W. Payne, and D. S. Katayama, “Stability of protein pharmaceuticals: an update,” *Pharm. Res.*, vol. 27, no. 4, pp. 544–575, 2010.

[6] X. Wen, X. Peng, H. Fu, Y. Dong, K. Han, J. Su, Z. Wang, R. Wang, X. Pan, L. Huang, and C. Wu, “Preparation and in vitro evaluation of silk fibroin microspheres produced by a novel ultra-fine particle processing system,” *Int. J. Pharm.*, vol. 416, no. 1, pp. 195–201, 2011.

[7] K. S. Soppimath, T. M. Aminabhavi, A. R. Kulkarni, and W. E. Rudzinski, “Biodegradable polymeric nanoparticles as drug delivery devices,” *J. Control. Release*, vol. 70, no. 1–2, pp. 1–20, 2001.

[8] J. L. Cleland, A. Daugherty, and R. Mrsny, “Emerging protein delivery methods,” *Curr. Opin. Biotechnol.*, vol. 12, no. 2, pp. 212–219, 2001.

[9] E. Wenk, A. J. Wandrey, H. P. Merkle, and L. Meinel, “Silk fibroin spheres as a platform for controlled drug delivery,” *J. Control. Release*, vol. 132, no. 1, pp. 26–34, 2008.

[10] A. Kumari, S. K. Yadav, and S. C. Yadav, "Biodegradable polymeric nanoparticles based drug delivery systems," *Colloids Surfaces B Biointerfaces*, vol. 75, no. 1, pp. 1–18, 2010.

[11] D. S. Pisal, M. P. Kosloski, and S. V Balu-Iyer, "Delivery of therapeutic proteins," *J. Pharm. Sci.*, vol. 99, no. 6, pp. 2557–275, 2010.

[12] Y. Shi and L. C. Li, "Current advances in sustained-release systems for parenteral drug delivery," *Expert Opin. Drug Deliv.*, vol. 2, no. 6, pp. 1039–1058, 2005.

[13] G. Luckachan and C. Pillai, "Biodegradable Polymers-A Review on Recent Trends and Emerging Perspectives," *J. Polym. Environ.*, vol. 19, no. 3, pp. 637–676, 2011.

[14] T. Scheibel, "Spider silks: recombinant synthesis, assembly, spinning, and engineering of synthetic proteins," *Microb. Cell Fact.*, vol. 3, no. 1, pp. 1–10, 2004.

[15] V. Werner and L. Meinel, "From silk spinning in insects and spiders to advanced silk fibroin drug delivery systems," *Eur. J. Pharm. Biopharm.*, vol. 97, no. Pt B, pp. 392–399, 2015.

[16] A. Lammel, M. Schwab, U. Slotta, G. Winter, and T. Scheibel, "Processing conditions for the formation of spider silk microspheres," *ChemSusChem*, vol. 1, no. 5, pp. 413–416, 2008.

[17] G. H. Altman, F. Diaz, C. Jakuba, T. Calabro, R. L. Horan, J. Chen, H. Lu, J. Richmond, and D. L. Kaplan, "Silk-based biomaterials," *Biomaterials*, vol. 24, no. 3, pp. 401–416, 2003.

[18] K. Numata and D. L. Kaplan, "Silk-based delivery systems of bioactive molecules," *Adv. Drug Deliv. Rev.*, vol. 62, no. 15, pp. 1497–1508, 2010.

[19] Y. Wang, D. D. Rudym, A. Walsh, L. Abrahamsen, H.-J. Kim, H. S. Kim, C. Kirker-Head, and D. L. Kaplan, "In vivo degradation of three-dimensional silk fibroin scaffolds," *Biomaterials*, vol. 29, no. 24–25, pp. 3415–3428, 2008.

[20] C. Fredriksson, M. Hedhammar, R. Feinstein, K. Nordling, G. Kratz, J. Johansson, F. Huss, and A. Rising, "Tissue Response to Subcutaneously Implanted Recombinant Spider Silk: An in Vivo Study," *Materials (Basel).*, vol. 2, no. 4, pp. 1908–1922, 2009.

[21] E. Wenk, H. P. Merkle, and L. Meinel, "Silk fibroin as a vehicle for drug delivery applications," *J. Control. Release*, vol. 150, no. 2, pp. 128–141, 2011.

[22] T. Estey, J. Kang, S. P. Schwendeman, and J. F. Carpenter, "BSA degradation under acidic conditions: a model for protein instability during release from PLGA delivery systems," *J. Pharm. Sci.*, vol. 95, no. 7, pp. 1626–1639, 2006.

[23] R. L. Horan, K. Antle, A. L. Collette, Y. Wang, J. Huang, J. E. Moreau, V. Volloch, D. L. Kaplan, and G. H. Altman, "In vitro degradation of silk fibroin," *Biomaterials*, vol. 26, no. 17, pp. 3385–3393, Jun. 2005.

[24] A. N. Mitropoulos, G. Perotto, S. Kim, B. Marelli, D. L. Kaplan, and F. G. Omenetto, "Synthesis of silk fibroin micro- and submicron spheres using a co-flow capillary device," *Adv. Mater.*, vol. 26, no. 7, pp. 1105–1110, 2014.

[25] C. B. Borkner, M. B. Elsner, and T. Scheibel, "Coatings and films made of silk proteins," *ACS Appl. Mater. Interfaces*, vol. 6, no. 18, pp. 15611–15625, 2014.

[26] T. Hino, M. Tanimoto, and S. Shimabayashi, "Change in secondary structure of silk fibroin during preparation of its microspheres by spray-drying and exposure to humid atmosphere," *J. Colloid Interface Sci.*, vol. 266, no. 1, pp. 68–73, 2003.

[27] M. Heim, D. Keerl, and T. Scheibel, "Spider Silk: From Soluble Protein to Extraordinary Fiber," *Angew. Chemie Int. Ed.*, vol. 48, no. 20, pp. 3584–3596, 2009.

[28] U.-J. Kim, J. Park, H. J. Kim, M. Wada, and D. L. Kaplan, "Three-dimensional aqueous-derived biomaterial scaffolds from silk fibroin," *Biomaterials*, vol. 26, no. 15, pp. 2775–2785, 2005.

[29] I. C. Um, H. Kweon, Y. H. Park, and S. Hudson, "Structural characteristics and properties of the regenerated silk fibroin prepared from formic acid," *Int. J. Biol. Macromol.*, vol. 29, no. 2, pp. 91–97, 2001.

[30] O. Hakimi, D. P. Knight, F. Vollrath, and P. Vadgama, “Spider and mulberry silkworm silks as compatible biomaterials,” *Compos. Part B Eng.*, vol. 38, no. 3, pp. 324–337, 2007.

[31] H. Dams-Kozlowska, A. Majer, P. Tomasiewicz, J. Lozinska, D. L. Kaplan, and A. Mackiewicz, “Purification and cytotoxicity of tag-free bioengineered spider silk proteins,” *J Biomed Mater Res A*, vol. 101, no. 2, pp. 456–464, 2012.

[32] A. S. Lammel, X. Hu, S.-H. Park, D. L. Kaplan, and T. R. Scheibel, “Controlling silk fibroin particle features for drug delivery,” *Biomaterials*, vol. 31, no. 16, pp. 4583–4591, 2010.

[33] L. Meinel, S. Hofmann, V. Karageorgiou, L. Zichner, R. Langer, D. Kaplan, and G. Vunjak-Novakovic, “Engineering cartilage-like tissue using human mesenchymal stem cells and silk protein scaffolds,” *Biotechnol. Bioeng.*, vol. 88, no. 3, pp. 379–391, 2004.

[34] B. D. Lawrence, F. Omenetto, K. Chui, and D. L. Kaplan, “Processing methods to control silk fibroin film biomaterial features,” *J. Mater. Sci.*, vol. 43, no. 21, pp. 6967–6985, 2008.

[35] J. Kundu, Y.-I. Chung, Y. H. Kim, G. Tae, and S. C. Kundu, “Silk fibroin nanoparticles for cellular uptake and control release,” *Int. J. Pharm.*, vol. 388, no. 1–2, pp. 242–250, 2010.

[36] R. Hino, M. Tomita, and K. Yoshizato, “The generation of germline transgenic silkworms for the production of biologically active recombinant fusion proteins of fibroin and human basic fibroblast growth factor,” *Biomaterials*, vol. 27, no. 33, pp. 5715–5724, 2006.

[37] R. Price, A. Poursaid, J. Cappello, and H. Ghandehari, “In vivo evaluation of matrix metalloproteinase responsive silk-elastinlike protein polymers for cancer gene therapy,” *J. Control. Release*, vol. 213, pp. 96–102, 2015.

[38] J. Huang, C. Wong Po Foo, and D. L. Kaplan, “Biosynthesis and Applications of Silk-like and Collagen-like Proteins,” *Polym. Rev.*, vol. 47, no. 1, pp. 29–62, 2007.

[39] J. Cappello, J. W. Crissman, M. Crissman, F. A. Ferrari, G. Textor, O. Wallis, J. R. Whitledge, X. Zhou, D. Burman, L. Aukerman, and E. R. Stedronsky, “In-situ self-assembling protein polymer gel systems for administration, delivery, and release of drugs,” *J. Control. Release*, vol. 53, no. 1–3, pp. 105–117, 1998.

[40] J. Cappello, J. Crissman, M. Dorman, M. Mikolajczak, G. Textor, M. Marquet, and F. Ferrari, “Genetic engineering of structural protein polymers,” *Biotechnol. Prog.*, vol. 6, no. 3, pp. 198–202, 1990.

[41] Z. Megeed, J. Cappello, and H. Ghandehari, “Genetically engineered silk-elastinlike protein polymers for controlled drug delivery,” *Adv. Drug Deliv. Rev.*, vol. 54, no. 8, pp. 1075–1091, 2002.

[42] T. Scheibel, “Spider silks: recombinant synthesis, assembly, spinning, and engineering of synthetic proteins,” *Microb. Cell Fact.*, vol. 3, no. 1, 2004.

[43] J. G. Hardy, L. M. Römer, and T. R. Scheibel, “Polymeric materials based on silk proteins,” *Polymer (Guildf).*, vol. 49, no. 20, pp. 4309–4327, 2008.

[44] J. Gosline, P. Guerette, C. Ortlepp, and K. Savage, “The mechanical design of spider silks: from fibroin sequence to mechanical function,” *J. Exp. Biol.*, vol. 202, no. 23, pp. 3295–3303, 1999.

[45] D. Huemmerich, C. W. Helsen, S. Quedzuweit, J. Oschmann, R. Rudolph, and T. Scheibel, “Primary Structure Elements of Spider Dragline Silks and Their Contribution to Protein Solubility,” *Biochemistry*, vol. 43, no. 42, pp. 13604–13612, 2004.

[46] US National Library of Medicine National Institutes of Health, “Results by year from MEDLINE/PubMed.” [Online]. Available: http://www.ncbi.nlm.nih.gov/pubmed/?term=spider+silk. [Accessed: 02-May-2016].

[47] E. Bini, C. W. P. Foo, J. Huang, V. Karageorgiou, B. Kitchel, and D. L. Kaplan, “RGD-functionalized bioengineered spider dragline silk biomaterial,” *Biomacromolecules*, vol. 7, no. 11, pp. 3139–3145, 2006.

[48] K. Numata, M. R. Reagan, R. H. Goldstein, M. Rosenblatt, and D. L. Kaplan, “Spider Silk-Based Gene Carriers for Tumor Cell-Specific Delivery,” *Bioconjug. Chem.*, vol. 22, no. 8, pp. 1605–1610, 2011.

[49] S. Yigit, O. Tokareva, A. Varone, I. Georgakoudi, and D. L. Kaplan, “Bioengineered silk gene delivery system for nuclear targeting,” *Macromol. Biosci.*, vol. 14, no. 9, pp. 1291–1298, 2014.

[50] M. Stark, S. Grip, A. Rising, M. Hedhammar, W. Engström, G. Hjälm, and J. Johansson, "Macroscopic Fibers Self-Assembled from Recombinant Miniature Spider Silk Proteins," *Biomacromolecules*, vol. 8, no. 5, pp. 1695–1701, 2007.

[51] E. Agostini, G. Winter, and J. Engert, "Water-based preparation of spider silk films as drug delivery matrices," *J. Control. Release*, vol. 213, pp. 134–141, 2015.

[52] M. Hofer, G. Winter, and J. Myschik, "Recombinant spider silk particles for controlled delivery of protein drugs," *Biomaterials*, vol. 33, no. 5, pp. 1554–1562, 2012.

[53] L. Uebersax, H. P. Merkle, and L. Meinel, "Insulin-like growth factor I releasing silk fibroin scaffolds induce chondrogenic differentiation of human mesenchymal stem cells," *J. Control. Release*, vol. 127, no. 1, pp. 12–21, 2008.

[54] V. Karageorgiou, M. Tomkins, R. Fajardo, L. Meinel, B. Snyder, K. Wade, J. Chen, G. Vunjak-Novakovic, and D. L. Kaplan, "Porous silk fibroin 3-D scaffolds for delivery of bone morphogenetic protein-2 in vitro and in vivo," *J. Biomed. Mater. Res. Part A*, vol. 78A, no. 2, pp. 324–334, 2006.

[55] M. Xu and R. V. Lewis, "Structure of a protein superfiber: spider dragline silk," *Proc. Natl. Acad. Sci.*, vol. 87, no. 18, pp. 7120–7124, 1990.

[56] Y. Zhang, L. Nothdurft, C. Wu, Y. Zhou, R. Crawford, Y. Xiao, and Wei Fan, "In vitro and in vivo evaluation of adenovirus combined silk fibroin scaffolds for BMP-7 gene delivery," *Tissue Eng. Part C Methods*, vol. 17, no. 8, pp. 789–797, 2011.

[57] S. Hofmann, H. Hagenmüller, A. M. Koch, R. Müller, G. Vunjak-Novakovic, D. L. Kaplan, H. P. Merkle, and L. Meinel, "Control of in vitro tissue-engineered bone-like structures using human mesenchymal stem cells and porous silk scaffolds," *Biomaterials*, vol. 28, no. 6, pp. 1152–1162, 2007.

[58] A. Wilz, E. M. Pritchard, T. Li, J.-Q. Lan, D. L. Kaplan, and D. Boison, "Silk polymer-based adenosine release: therapeutic potential for epilepsy," *Biomaterials*, vol. 29, no. 26, pp. 3609–3616, 2008.

[59] C. P. Vepari and D. L. Kaplan, "Covalently immobilized enzyme gradients within three-dimensional porous scaffolds," *Biotechnol. Bioeng.*, vol. 93, no. 6, pp. 1130–1137, 2006.

[60] L. Uebersax, M. Mattotti, M. Papaloïzos, H. P. Merkle, B. Gander, and L. Meinel, "Silk fibroin matrices for the controlled release of nerve growth factor (NGF)," *Biomaterials*, vol. 28, no. 30, pp. 4449–4460, 2007.

[61] B. B. Mandal and S. C. Kundu, "Calcium alginate beads embedded in silk fibroin as 3D dual drug releasing scaffolds," *Biomaterials*, vol. 30, no. 28, pp. 5170–5177, 2009.

[62] K. Spiess, R. Ene, C. D. Keenan, J. Senker, F. Kremer, and T. Scheibel, "Impact of initial solvent on thermal stability and mechanical properties of recombinant spider silk films," *J. Mater. Chem.*, vol. 21, no. 35, pp. 13594–13604, 2011.

[63] Q. Lu, X. Wang, X. Hu, P. Cebe, F. Omenetto, and D. L. Kaplan, "Stabilization and Release of Enzymes from Silk Films," *Macromol. Biosci.*, vol. 10, no. 4, pp. 359–368, 2010.

[64] S. Wohlrab, S. Müller, A. Schmidt, S. Neubauer, H. Kessler, A. Leal-Egana, and T. Scheibel, "Cell adhesion and proliferation on RGD-modified recombinant spider silk proteins," *Biomaterials*, vol. 33, no. 28, pp. 6650–6659, 2012.

[65] S. Sofia, M. B. McCarthy, G. Gronowicz, and D. L. Kaplan, "Functionalized silk-based biomaterials for bone formation," *J. Biomed. Mater. Res.*, vol. 54, no. 1, pp. 139–148, 2001.

[66] X. Wang, H. J. Kim, P. Xu, A. Matsumoto, and D. L. Kaplan, "Biomaterial coatings by stepwise deposition of silk fibroin," *Langmuir*, vol. 21, no. 24, pp. 11335–11341, 2005.

[67] X. Wang, E. Wenk, X. Hu, G. R. Castro, L. Meinel, X. Wang, C. Li, H. Merkle, and D. L. Kaplan, "Silk coatings on PLGA and alginate microspheres for protein delivery," *Biomaterials*, vol. 28, no. 28, pp. 4161–4169, 2007.

[68] X. Wang, X. Zhang, J. Castellot, I. Herman, M. Iafrati, and D. L. Kaplan, "Controlled release from multilayer silk biomaterial coatings to modulate vascular cell responses," *Biomaterials*, vol. 29, no. 7, pp. 894–903, 2008.

[69] P. H. Zeplin, N. C. Maksimovikj, M. C. Jordan, J. Nickel, G. Lang, A. H. Leimer, L. Römer, and T. Scheibel, "Spider Silk Coatings as a Bioshield to Reduce Periprosthetic Fibrous Capsule Formation," *Adv. Funct. Mater.*, vol. 24, no. 18, pp. 2658–2666, 2014.

[70] B.-M. Min, G. Lee, S. H. Kim, Y. S. Nam, T. S. Lee, and W. H. Park, "Electrospinning of silk fibroin nanofibers and its effect on the adhesion and spreading of normal human keratinocytes and fibroblasts in vitro," *Biomaterials*, vol. 25, no. 7–8, pp. 1289–1297, 2004.

[71] C. Li, C. Vepari, H.-J. Jin, H. J. Kim, and D. L. Kaplan, "Electrospun silk-BMP-2 scaffolds for bone tissue engineering," *Biomaterials*, vol. 27, no. 16, pp. 3115–3124, 2006.

[72] X. Zhang, M. R. Reagan, and D. L. Kaplan, "Electrospun silk biomaterial scaffolds for regenerative medicine.," *Adv. Drug Deliv. Rev.*, vol. 61, no. 12, pp. 988–1006, 2009.

[73] M. Kang, R. Jung, H.-S. Kim, J. H. Youk, and H.-J. Jin, "Silver Nanoparticles Incorporated Electrospun Silk Fibers," *J. Nanosci. Nanotechnol.*, vol. 7, no. 11, pp. 3888–3891, 2007.

[74] A. Florczak, A. Mackiewicz, and H. Dams-Kozlowska, "Functionalized Spider Silk Spheres As Drug Carriers for Targeted Cancer Therapy," *Biomacromolecules*, vol. 15, no. 8, pp. 2971–2981, Aug. 2014.

[75] S. K. Jain, Y. Gupta, A. Jain, A. R. Saxena, P. Khare, and A. Jain, "Mannosylated gelatin nanoparticles bearing an anti-HIV drug didanosine for site-specific delivery," *Nanomedicine Nanotechnology, Biol. Med.*, vol. 4, no. 1, pp. 41–48, 2008.

[76] J.-H. Park, H.-E. Jin, D.-D. Kim, S.-J. Chung, W.-S. Shim, and C.-K. Shim, "Chitosan microspheres as an alveolar macrophage delivery system of ofloxacin via pulmonary inhalation," *Int. J. Pharm.*, vol. 441, no. 1–2, pp. 562–569, Jan. 2013.

[77] A. Lammel, M. Schwab, M. Hofer, G. Winter, and T. Scheibel, "Recombinant spider silk particles as drug delivery vehicles," *Biomaterials*, vol. 32, no. 8, pp. 2233–2240, 2011.

[78] Y.-Z. Zhao, X. Li, C.-T. Lu, Y.-Y. Xu, H.-F. Lv, D.-D. Dai, L. Zhang, C.-Z. Sun, W. Yang, X.-K. Li, Y.-P. Zhao, H.-X. Fu, L. Cai, M. Lin, L.-J. Chen, and M. Zhang, "Experiment on the feasibility of using modified gelatin nanoparticles as insulin pulmonary administration system for diabetes therapy," *Acta Diabetol.*, vol. 49, no. 4, pp. 315–325, 2012.

[79] H.-B. Yan, Y.-Q. Zhang, Y.-L. Ma, and L.-X. Zhou, "Biosynthesis of insulin-silk fibroin nanoparticles conjugates and in vitro evaluation of a drug delivery system," *J. Nanoparticle Res.*, vol. 11, no. 8, pp. 1937–1946, 2009.

[80] X. Wang, E. Wenk, A. Matsumoto, L. Meinel, C. Li, and D. L. Kaplan, "Silk microspheres for encapsulation and controlled release," *J. Control. Release*, vol. 117, no. 3, pp. 360–370, 2007.

[81] H. Brandenberger and F. Widmer, "A new multinozzle encapsulation/immobilisation system to produce uniform beads of alginate," *J. Biotechnol.*, vol. 63, no. 1, pp. 73–80, 1998.

[82] K. D. Hermanson, D. Huemmerich, T. Scheibel, and A. R. Bausch, "Engineered Microcapsules Fabricated from Reconstituted Spider Silk," *Adv. Mater.*, vol. 19, no. 14, pp. 1810–1815, 2007.

[83] T. Yucel, M. L. Lovett, and D. L. Kaplan, "Silk-based biomaterials for sustained drug delivery.," *J. Control. Release*, vol. 190, pp. 381–97, Sep. 2014.

[84] K. Spiess, A. Lammel, and T. Scheibel, "Recombinant Spider Silk Proteins for Applications in Biomaterials," *Macromol. Biosci.*, vol. 10, no. 9, pp. 998–1007, 2010.

[85] S. Hofmann, C. T. Wong Po Foo, F. Rossetti, M. Textor, G. Vunjak-Novakovic, D. L. Kaplan, H. P. Merkle, and L. Meinel, "Silk fibroin as an organic polymer for controlled drug delivery," *J. Control. Release*, vol. 111, no. 1–2, pp. 219–227, 2006.

[86] M. B. Elsner, H. M. Herold, S. Müller-Herrmann, H. Bargel, and T. Scheibel, "Enhanced cellular uptake of engineered spider silk particles," *Biomater. Sci.*, vol. 3, no. 3, pp. 543–551, 2015.

[87] A. E. Terry, D. P. Knight, D. Porter, and F. Vollrath, "pH Induced Changes in the Rheology of Silk Fibroin Solution from the Middle Division of Bombyx m ori Silkworm," *Biomacromolecules*, vol. 5, no. 3, pp. 768–772, 2004.

[88] A. Lammel, G. Winter, J. Myschik, M. Schwab, T. Scheibel, and M. Hofer, "Patent: Spider silk particles for controlled and sustained delivery of compounds," 2011.

[89] K. D. Hermanson, D. Huemmerich, T. Scheibel, and A. R. Bausch, "Engineered Microcapsules Fabricated from Reconstituted Spider Silk," *Adv. Mater.*, vol. 19, no. 14, pp. 1810–1815, 2007.

[90] C. Blüm and T. Scheibel, "Control of Drug Loading and Release Properties of Spider Silk Sub-Microparticles," *Bionanoscience*, vol. 2, no. 2, pp. 67–74, 2012.

[91] T. Wongpinyochit, P. Uhlmann, A. J. Urquhart, and F. P. Seib, "PEGylated Silk Nanoparticles for Anticancer Drug Delivery," *Biomacromolecules*, vol. 16, no. 11, pp. 3712–3722, 2015.

[92] X. Wang and D. L. Kaplan, "Functionalization of Silk Fibroin with NeutrAvidin and Biotin," *Macromol. Biosci.*, vol. 11, no. 1, pp. 100–110, 2011.

[93] S. C. Gomes, I. B. Leonor, J. F. Mano, R. L. Reis, and D. L. Kaplan, "Antimicrobial functionalized genetically engineered spider silk," *Biomaterials*, vol. 32, no. 18, pp. 4255–4266, 2011.

[94] H. A. Currie, O. Deschaume, R. R. Naik, C. C. Perry, and D. L. Kaplan, "Genetically Engineered Chimeric Silk-Silver Binding Proteins," *Adv. Funct. Mater.*, vol. 21, no. 15, pp. 2889–2895, 2011.

[95] L. J. Peek, C. R. Middaugh, and C. Berkland, "Nanotechnology in vaccine delivery," *Adv. Drug Deliv. Rev.*, vol. 60, no. 8, pp. 915–928, 2008.

[96] M. Singh, A. Chakrapani, and D. O'Hagan, "Nanoparticles and microparticles as vaccine-delivery systems," *Expert Rev. Vaccines*, vol. 6, no. 5, pp. 797–808, 2007.

[97] D. T. O'Hagan and M. Singh, "Microparticles as vaccine adjuvants and delivery systems," *Expert Rev. Vaccines*, vol. 2, no. 2, pp. 269–283, 2003.

[98] K. Dhama, M. Mahendran, P. K. Gupta, and A. Rai, "DNA vaccines and their applications in veterinary practice: current perspectives," *Vet. Res. Commun.*, vol. 32, no. 5, pp. 341–356, 2008.

[99] P. M. Moyle and I. Toth, "Modern Subunit Vaccines: Development, Components, and Research Opportunities," *ChemMedChem*, vol. 8, no. 3, pp. 360–376, 2013.

[100] T. Mohan, P. Verma, and D. N. Rao, "Novel adjuvants & delivery vehicles for vaccines development: a road ahead," *Indian J. Med. Res.*, vol. 138, no. 5, pp. 779–795, 2013.

[101] E. De Gregorio, E. Caproni, and J. B. Ulmer, "Vaccine Adjuvants: Mode of Action," *Front. Immunol.*, vol. 4, p. 214, 2013.

[102] R. Arnon and T. Ben-Yedidia, "Old and new vaccine approaches," *Int. Immunopharmacol.*, vol. 3, no. 8, pp. 1195–1204, 2003.

[103] M.-L. De Temmerman, J. Rejman, J. Demeester, D. J. Irvine, B. Gander, and S. C. De Smedt, "Particulate vaccines: on the quest for optimal delivery and immune response," *Drug Discov. Today*, vol. 16, no. 13–14, pp. 569–582, 2011.

[104] M. Black, A. Trent, M. Tirrell, and C. Olive, "Advances in the design and delivery of peptide subunit vaccines with a focus on Toll-like receptor agonists," *Expert Rev. Vaccines*, vol. 9, no. 2, pp. 157–173, 2010.

[105] M. O. Oyewumi, A. Kumar, and Z. Cui, "Nano-microparticles as immune adjuvants: correlating particle sizes and the resultant immune responses," *Expert Rev. Vaccines*, vol. 9, no. 9, pp. 1095–1107, 2010.

[106] A. C. Rice-Ficht, A. M. Arenas-Gamboa, M. M. Kahl-McDonagh, and T. A. Ficht, "Polymeric particles in vaccine delivery," *Curr. Opin. Microbiol.*, vol. 13, no. 1, pp. 106–112, 2010.

[107] L. S. Jones, L. J. Peek, J. Power, A. Markham, B. Yazzie, and C. R. Middaugh, "Effects of Adsorption to Aluminum Salt Adjuvants on the Structure and Stability of Model Protein Antigens," *J. Biol. Chem.*, vol. 280, no. 14, pp. 13406–13414, 2005.

[108] E. Schlosser, M. Mueller, S. Fischer, S. Basta, D. H. Busch, B. Gander, and M. Groettrup, "TLR ligands and antigen need to be coencapsulated into the same biodegradable microsphere for the generation of potent cytotoxic T lymphocyte responses," *Vaccine*, vol. 26, no. 13, pp. 1626–1637, 2008.

[109] J. Szebeni, P. Bedőcs, Z. Rozsnyay, Z. Weiszhár, R. Urbanics, L. Rosivall, R. Cohen, O. Garbuzenko, G. Báthori, M. Tóth, R. Bünger, and Y. Barenholz, "Liposome-induced complement activation and related cardiopulmonary distress in pigs: factors promoting reactogenicity of Doxil and AmBisome," *Nanomedicine Nanotechnology, Biol. Med.*, vol. 8, no. 2, pp. 176–184, 2012.

[110] H. Wang, P. Zhao, X. Liang, T. Song, X. Gong, R. Niu, and J. Chang, "Construction of a novel cationic polymeric liposomes formed from PEGylated octadecyl-quaternized lysine modified chitosan/cholesterol for enhancing storage stability and cellular uptake efficiency," *Biotechnol. Bioeng.*, vol. 106, no. 6, pp. 952–962, 2010.

[111] C. Moser, M. Amacker, A. R. Kammer, S. Rasi, N. Westerfeld, and R. Zurbriggen, "Influenza virosomes as a combined vaccine carrier and adjuvant system for prophylactic and therapeutic immunizations," *Expert Rev. Vaccines*, vol. 6, no. 5, pp. 711–721, 2007.

[112] T. Nakanishi, J. Kunisawa, A. Hayashi, Y. Tsutsumi, K. Kubo, S. Nakagawa, M. Nakanishi, K. Tanaka, and T. Mayumi, "Positively charged liposome functions as an efficient immunoadjuvant in inducing cell-mediated immune response to soluble proteins," *J. Control. Release*, vol. 61, no. 1–2, pp. 233–240, 1999.

[113] Y. Fan and Q. Zhang, "Development of liposomal formulations: From concept to clinical investigations," *Asian J. Pharm. Sci.*, vol. 8, no. 2, pp. 81–87, 2013.

[114] A. Huckriede, L. Bungener, T. Stegmann, T. Daemen, J. Medema, A. M. Palache, and J. Wilschut, "The virosome concept for influenza vaccines," *Vaccine*, vol. 23, pp. S26–S38, 2005.

[115] S. A. Plotkin, "Vaccines: past, present and future," *Nat. Med.*, vol. 10, no. 4s, pp. S5–S11, 2005.

[116] W. Jaoko, E. Karita, K. Kayitenkore, G. Omosa-Manyonyi, S. Allen, S. Than, E. M. Adams, B. S. Graham, R. A. Koup, R. T. Bailer, C. Smith, L. Dally, B. Farah, O. Anzala, C. M. Muvunyi, J. Bizimana, T. Tarragona-Fiol, P. J. Bergin, P. Hayes, M. Ho, K. Loughran, W. Komaroff, G. Stevens, H. Thomson, M. J. Boaz, J. H. Cox, C. Schmidt, J. Gilmour, G. J. Nabel, P. Fast, and J. Bwayo, "Safety and Immunogenicity Study of Multiclade HIV-1 Adenoviral Vector Vaccine Alone or as Boost following a Multiclade HIV-1 DNA Vaccine in Africa," *PLoS One*, vol. 5, no. 9, p. e12873, 2010.

[117] A. V. S. Hill, A. Reyes-Sandoval, G. O'Hara, K. Ewer, A. Lawrie, A. Goodman, A. Nicosia, A. Folgori, S. Colloca, R. Cortese, S. C. Gilbert, and S. Draper, "Prime-boost vectored malaria vaccines: Progress and prospects," *Hum. Vaccin.*, vol. 6, no. 1, pp. 78–83, 2010.

[118] B. Morein, B. Sundquist, S. Hoglund, K. Dalsgaard, and A. Osterhaus, "Iscom, a novel structure for antigenic presentation of membrane proteins from enveloped viruses," *Nature*, vol. 308, no. 5958, pp. 457–460, 1984.

[119] M. T. Sanders, L. E. Brown, G. Deliyannis, and M. J. Pearse, "ISCOMTM-based vaccines: The second decade," *Immunol. Cell Biol.*, vol. 83, no. 2, pp. 119–128, 2005.

[120] F. A. Ennis, J. Cruz, J. Jameson, M. Klein, D. Burt, and J. Thipphawong, "Augmentation of Human Influenza A Virus-Specific Cytotoxic T Lymphocyte Memory by Influenza Vaccine and Adjuvanted Carriers (ISCOMS)," *Virology*, vol. 259, no. 2, pp. 256–261, 1999.

[121] M. PEARSE and D. DRANE, "ISCOMATRIX adjuvant for antigen delivery," *Adv. Drug Deliv. Rev.*, vol. 57, no. 3, pp. 465–474, 2005.

[122] M. Schnurr, M. Orban, N. C. Robson, A. Shin, H. Braley, D. Airey, J. Cebon, E. Maraskovsky, and S. Endres, "ISCOMATRIX Adjuvant Induces Efficient Cross-Presentation of Tumor Antigen by Dendritic Cells via Rapid Cytosolic Antigen Delivery and Processing via Tripeptidyl Peptidase II," *J. Immunol.*, vol. 182, no. 3, pp. 1253–1259, 2009.

[123] W. T. McBurney, D. G. Lendemans, J. Myschik, T. Hennessy, T. Rades, and S. Hook, "In vivo activity of cationic immune stimulating complexes (PLUSCOMs)," *Vaccine*, vol. 26, no. 35, pp. 4549–4556, 2008.

[124] Q. He, A. R. Mitchell, S. L. Johnson, C. Wagner-Bartak, T. Morcol, and S. J. D. Bell, "Calcium Phosphate Nanoparticle Adjuvant," *Clin. Vaccine Immunol.*, vol. 7, no. 6, pp. 899–903, Nov. 2000.

[125] Q. He, A. Mitchell, T. Morcol, and S. J. D. Bell, "Calcium Phosphate Nanoparticles Induce Mucosal Immunity and Protection against Herpes Simplex Virus Type 2," *Clin. Vaccine Immunol.*, vol. 9, no. 5, pp. 1021–1024, 2002.

[126] D. H. Joyappa, C. Ashok Kumar, N. Banumathi, G. R. Reddy, and V. V. S. Suryanarayana, “Calcium phosphate nanoparticle prepared with foot and mouth disease virus P1-3CD gene construct protects mice and guinea pigs against the challenge virus,” *Vet. Microbiol.*, vol. 139, no. 1–2, pp. 58–66, 2009.

[127] V. Sokolova, T. Knuschke, A. Kovtun, J. Buer, M. Epple, and A. M. Westendorf, “The use of calcium phosphate nanoparticles encapsulating Toll-like receptor ligands and the antigen hemagglutinin to induce dendritic cell maturation and T cell activation,” *Biomaterials*, vol. 31, no. 21, pp. 5627–5633, 2010.

[128] X. Liu, H. Lin, Q. Tang, C. Li, S. Yang, Z. Wang, C. Wang, Q. He, B. Cao, Z. Feng, X. Guan, and J. Zhu, “Characterization of a Human Antibody Fragment Fab and Its Calcium Phosphate Nanoparticles that Inhibit Rabies Virus Infection with Vaccine,” *PLoS One*, vol. 6, no. 5, p. e19848, 2011.

[129] S.-Y. Kim, H.-J. Doh, M.-H. Jang, Y.-J. Ha, S.-I. Chung, and H.-J. Park, “Oral Immunization with Helicobacter pylori-Loaded Poly(d, l-Lactide-Co-Glycolide) Nanoparticles,” *Helicobacter*, vol. 4, no. 1, pp. 33–39, 1999.

[130] J. Wendorf, M. Singh, J. Chesko, J. Kazzaz, E. Soewanan, M. Ugozzoli, and D. O’Hagan, “A Practical Approach to the use of Nanoparticles for Vaccine Delivery,” *J. Pharm. Sci.*, vol. 95, no. 12, pp. 2738–2750, 2006.

[131] J. Panyam and V. Labhasetwar, “Biodegradable nanoparticles for drug and gene delivery to cells and tissue,” *Adv. Drug Deliv. Rev.*, vol. 55, no. 3, pp. 329–347, 2003.

[132] V. B. Joshi, S. M. Geary, and A. K. Salem, “Biodegradable Particles as Vaccine Delivery Systems: Size Matters,” *AAPS J.*, vol. 15, no. 1, pp. 85–94, 2013.

[133] S. D. Allison, “Effect Of Structural Relaxation On The Preparation And Drug Release Behavior Of Poly(lactic-co-glycolic)acid Microparticle Drug Delivery Systems,” *J. Pharm. Sci.*, vol. 97, no. 6, pp. 2022–2035, 2008.

[134] A. C. R. Grayson, M. J. Cima, and R. Langer, “Size and temperature effects on poly(lactic-co-glycolic acid) degradation and microreservoir device performance,” *Biomaterials*, vol. 26, no. 14, pp. 2137–2145, 2005.

[135] W. Gao, J. C. K. Lai, and S. W. Leung, “Functional enhancement of chitosan and nanoparticles in cell culture, tissue engineering, and pharmaceutical applications,” *Front. Physiol.*, vol. 3, p. 321, 2012.

[136] S. Şenel and S. J. McClure, “Potential applications of chitosan in veterinary medicine,” *Adv. Drug Deliv. Rev.*, vol. 56, no. 10, pp. 1467–1480, 2004.

[137] G. Feng, Q. Jiang, M. Xia, Y. Lu, W. Qiu, D. Zhao, L. Lu, G. Peng, and Y. Wang, “Enhanced Immune Response and Protective Effects of Nano-chitosan-based DNA Vaccine Encoding T Cell Epitopes of Esat-6 and FL against Mycobacterium Tuberculosis Infection,” *PLoS One*, vol. 8, no. 4, p. e61135, 2013.

[138] K. Zhao, G. Chen, X.-M. Shi, T.-T. Gao, W. Li, Y. Zhao, F.-Q. Zhang, J. Wu, X. Cui, and Y.-F. Wang, “Preparation and Efficacy of a Live Newcastle Disease Virus Vaccine Encapsulated in Chitosan Nanoparticles,” *PLoS One*, vol. 7, no. 12, p. e53314, 2012.

[139] O. Borges, A. Cordeiro-da-Silva, J. Tavares, N. Santarém, A. de Sousa, G. Borchard, and H. E. Junginger, “Immune response by nasal delivery of hepatitis B surface antigen and codelivery of a CpG ODN in alginate coated chitosan nanoparticles,” *Eur. J. Pharm. Biopharm.*, vol. 69, no. 2, pp. 405–416, 2008.

[140] A. Bolhassani, S. Javanzad, T. Saleh, M. Hashemi, M. R. Aghasadeghi, and S. M. Sadat, “Polymeric nanoparticles,” *Hum. Vaccin. Immunother.*, vol. 10, no. 2, pp. 321–332, 2014.

[141] A. des Rieux, V. Fievez, M. Garinot, Y.-J. Schneider, and V. Préat, “Nanoparticles as potential oral delivery systems of proteins and vaccines: A mechanistic approach,” *J. Control. Release*, vol. 116, no. 1, pp. 1–27, 2006.

[142] A. Hajizade, F. Ebrahimi, A.-H. Salmanian, A. Arpanae, and J. Amani, “Nanoparticles in Vaccine Development,” *J. Appl. Biotechnol. Reports*, vol. 1, no. 4, pp. 125–134, 2015.

[143] B. Malik, A. K. Goyal, T. S. Markandeywar, G. Rath, F. Zakir, and S. P. Vyas, “Microfold-cell targeted surface engineered polymeric nanoparticles for oral immunization,” *J. Drug Target.*, vol. 20, no. 1, pp. 76–84, 2012.

[144] S. M. Bal, B. Slütter, E. van Riet, A. C. Kruithof, Z. Ding, G. F. A. Kersten, W. Jiskoot, and J. A. Bouwstra, "Efficient induction of immune responses through intradermal vaccination with N-trimethyl chitosan containing antigen formulations," *J. Control. Release*, vol. 142, no. 3, pp. 374–383, 2010.

[145] S. Boyoglu, K. Vig, S. Pillai, V. Rangari, V. A. Dennis, F. Khazi, and S. R. Singh, "Enhanced delivery and expression of a nanoencapsulated DNA vaccine vector for respiratory syncytial virus," *Nanomedicine Nanotechnology, Biol. Med.*, vol. 5, no. 4, pp. 463–472, 2009.

[146] P. H. von Hippel, "The Macromolecular Chemistry of Gelatin," *J. Am. Chem. Soc.*, vol. 87, no. 8, pp. 1824–1824, 1965.

[147] A. O. Elzoghby, W. M. Samy, and N. A. Elgindy, "Protein-based nanocarriers as promising drug and gene delivery systems," *J. Control. Release*, vol. 161, no. 1, pp. 38–49, 2012.

[148] C. Coester, P. Nayyar, and J. Samuel, "In vitro uptake of gelatin nanoparticles by murine dendritic cells and their intracellular localisation.," *Eur. J. Pharm. Biopharm.*, vol. 62, no. 3, pp. 306–14, 2006.

[149] M. S. Sudheesh, S. P. Vyas, and D. V Kohli, "Nanoparticle-based immunopotentiation via tetanus toxoid-loaded gelatin and aminated gelatin nanoparticles," *Drug Deliv.*, vol. 18, no. 5, pp. 320–330, 2011.

[150] K. Zwiorek, C. Bourquin, J. Battiany, G. Winter, S. Endres, G. Hartmann, and C. Coester, "Delivery by Cationic Gelatin Nanoparticles Strongly Increases the Immunostimulatory Effects of CpG Oligonucleotides," *Pharm. Res.*, vol. 25, no. 3, pp. 551–562, 2008.

[151] A. O. Elzoghby, "Gelatin-based nanoparticles as drug and gene delivery systems: Reviewing three decades of research," *J. Control. Release*, vol. 172, no. 3, pp. 1075–1091, 2013.

[152] C. Pinto Reis, R. J. Neufeld, A. J. Ribeiro, and F. Veiga, "Nanoencapsulation I. Methods for preparation of drug-loaded polymeric nanoparticles," *Nanomedicine Nanotechnology, Biol. Med.*, vol. 2, no. 1, pp. 8–21, 2006.

[153] K. Niikura, T. Matsunaga, T. Suzuki, S. Kobayashi, H. Yamaguchi, Y. Orba, A. Kawaguchi, H. Hasegawa, K. Kajino, T. Ninomiya, K. Ijiro, and H. Sawa, "Gold Nanoparticles as a Vaccine Platform: Influence of Size and Shape on Immunological Responses in Vitro and in Vivo," *ACS Nano*, vol. 7, no. 5, pp. 3926–3938, 2013.

[154] N. L. Rosi, D. A. Giljohann, C. S. Thaxton, A. K. R. Lytton-Jean, M. S. Han, and C. A. Mirkin, "Oligonucleotide-modified gold nanoparticles for intracellular gene regulation.," *Science*, vol. 312, no. 5776, pp. 1027–1030, 2006.

[155] M. Marradi, F. Chiodo, I. García, and S. Penadés, "Glyconanoparticles as multifunctional and multimodal carbohydrate systems," *Chem. Soc. Rev.*, vol. 42, no. 11, p. 4728, 2013.

[156] X. Zhou, X. Zhang, X. Yu, X. Zha, Q. Fu, B. Liu, X. Wang, Y. Chen, Y. Chen, Y. Shan, Y. Jin, Y. Wu, J. Liu, W. Kong, and J. Shen, "The effect of conjugation to gold nanoparticles on the ability of low molecular weight chitosan to transfer DNA vaccine," *Biomaterials*, vol. 29, no. 1, pp. 111–117, 2008.

[157] A. E. Gregory, E. D. Williamson, J. L. Prior, W. A. Butcher, I. J. Thompson, A. M. Shaw, and R. W. Titball, "Conjugation of Y. pestis F1-antigen to gold nanoparticles improves immunogenicity," *Vaccine*, vol. 30, no. 48, pp. 6777–6782, 2012.

[158] Y.-S. Chen, Y.-C. Hung, W.-H. Lin, and G. S. Huang, "Assessment of gold nanoparticles as a size-dependent vaccine carrier for enhancing the antibody response against synthetic foot-and-mouth disease virus peptide.," *Nanotechnology*, vol. 21, no. 19, p. 195101, 2010.

[159] L. Zhang, G. Widera, S. Bleecher, D. A. Zaharoff, B. Mossop, and D. Rabussay, "Accelerated Immune Response to DNA Vaccines," *DNA Cell Biol.*, vol. 22, no. 12, pp. 815–822, 2003.

[160] D. J. Wells, "Gene Therapy Progress and Prospects: Electroporation and other physical methods," *Gene Ther.*, vol. 11, no. 18, pp. 1363–1369, 2004.

[161] A. L. Rakhmilevich, M. Imboden, Z. Hao, M. D. Macklin, T. Roberts, K. M. Wright, M. R. Albertini, N.-S. Yang, and P. M. Sondel, "Effective Particle-mediated Vaccination against Mouse Melanoma by Coadministration of Plasmid DNA Encoding Gp100 and Granulocyte-Macrophage Colony-Stimulating Factor," *Clin. Cancer Res.*, vol. 7, no. 4, pp. 952–961, 2001.

[162] H. J. Dean, D. Fuller, and J. E. Osorio, “Powder and particle-mediated approaches for delivery of DNA and protein vaccines into the epidermis,” *Comp. Immunol. Microbiol. Infect. Dis.*, vol. 26, no. 5, pp. 373–388, 2003.

[163] L. Engelke, G. Winter, S. Hook, and J. Engert, “Recent insights into cutaneous immunization: How to vaccinate via the skin,” *Vaccine*, vol. 33, no. 37, pp. 4663–4674, 2015.

[164] S. B. Mossad, “Demystifying FluMist, a new intranasal, live influenza vaccine.,” *Cleve. Clin. J. Med.*, vol. 70, no. 9, pp. 801–806, 2003.

[165] J. R. McGhee, J. Mestecky, M. T. Dertzbaugh, J. H. Eldridge, M. Hirasawa, and H. Kiyono, “The mucosal immune system: from fundamental concepts to vaccine development,” *Vaccine*, vol. 10, no. 2, pp. 75–88, 1992.

[166] J. R. McGhee, J. Mestecky, C. O. Elson, and H. Kiyono, “Regulation of IgA synthesis and immune response by T cells and interleukins,” *J. Clin. Immunol.*, vol. 9, no. 3, pp. 175–199, 1989.

[167] Y. Asahi-Ozaki, T. Yoshikawa, Y. Iwakura, Y. Suzuki, S. Tamura, T. Kurata, and T. Sata, “Secretory IgA antibodies provide cross-protection against infection with different strains of influenza B virus,” *J. Med. Virol.*, vol. 74, no. 2, pp. 328–335, 2004.

[168] D. Lu and A. J. Hickey, “Pulmonary vaccine delivery,” *Expert Rev. Vaccines*, vol. 6, no. 2, pp. 213–226, 2007.

[169] F. T. Cutts, C. J. Clements, and J. V. Bennett, “Altenative Routes of Measles Immunization: a Review,” *Biologicals*, vol. 25, no. 3, pp. 323–338, 1997.

[170] D. A. Groneberg, H. Paul, and T. Welte, “Novel strategies of aerosolic pharmacotherapy,” *Exp. Toxicol. Pathol.*, vol. 57, pp. 49–53, 2006.

[171] B. N. Lambrecht, J.-;B. Prins, and H. C. Hoogsteden, “Lung dendritic cells and host immunity to infection,” *Eur. Respir. J.*, vol. 18, no. 4, pp. 692–704, 2001.

[172] J. Holmgren, C. Czerkinsky, N. Lycke, and A.-M. Svennerholm, “Mucosal Immunity: Implications for Vaccine Development,” *Immunobiology*, vol. 184, no. 2, pp. 157–179, 1992.

[173] R. L. de Swart, T. Kuiken, J. Fernandez-de Castro, M. J. Papania, J. V. Bennett, J. L. Valdespino, P. Minor, C. L. Witham, S. Yüksel, H. Vos, G. van Amerongen, and A. D. M. E. Osterhaus, “Aerosol measles vaccination in macaques: Preclinical studies of immune responses and safety,” *Vaccine*, vol. 24, no. 40, pp. 6424–6436, 2006.

[174] M. J. Copland, M. A. Baird, T. Rades, J. L. McKenzie, B. Becker, F. Reck, P. C. Tyler, and N. M. Davies, “Liposomal delivery of antigen to human dendritic cells,” *Vaccine*, vol. 21, no. 9, pp. 883–890, 2003.

[175] J.-P. Amorij, W. L. Hinrichs, H. W. Frijlink, J. C. Wilschut, and A. Huckriede, “Needle-free influenza vaccination,” *Lancet Infect. Dis.*, vol. 10, no. 10, pp. 699–711, 2010.

[176] Council of Europe, *European Pharmacopoeia, 8th edition incl. Supplement 8.7*. 2014.

II. ENDOTOXIN DEPLETION OF EADF4(C16) PROTEIN AND PREPARATION OF PARTICLES WITH LOW ENDOTOXIN VALUES

1. Introduction

Within the new field of pharmaceutical biopolymers, spider silk proteins have gained more and more interest in the course of the last years. Several reviews describe the possible applications for spider silk materials, which can be coatings for medical devices, matrices for wound healing [1] or sustained drug delivery systems [2]. All these applications have in common, that they have to be administered parenterally. Spider silk proteins cannot be obtained from natural harvesting like silk fibroin from the silkworm [3] because spiders cannot be held in captivity in groups [4]. The commonly used spider silk protein variants are all produced recombinantly in cell culture, where a homogeneous batch to batch quality can be obtained [1, 5].

A challenge of a cell based manufacturing process is the protein purification step. As recombinant spider silk proteins are often produced in gram-negative bacteria, it is important to analyze protein batches for the presence of bacterial endotoxins. Endotoxins, also called lipopolysaccharides (LPS), are fragments of the outer cell membrane of gram-negative bacteria. These lipopolysaccharides consist of a non-polar lipid component (lipid A), a core oligosaccharide and a surface antigen (O-antigen) [6]. This structure results in a molecular weight of 10-20 kDa for the monomer [7]. Endotoxins are highly heat stable requiring a minimum of 100-180°C for deactivation [7, 8]. The phosphate groups of the lipid A component lead to a negative surface charge of the endotoxins while the hydrophobic part leads to binding to hydrophobic materials [6]. If endotoxins are administered to a patient or animal, they can lead to fever, septic shock and disseminated intravascular coagulation [9]. Due to the risks arising from endotoxins administered to humans, both the US Food and Drug Administration (FDA) and the European Medicines Agency (EMA) demand the analysis of endotoxins in their guidelines for parenteral drugs. The commonly used endotoxin analysis method is based on the coagulation of the lysate of the horseshoe crab, which is called limulus amebocyte lysate test (LAL test). This analysis method replaced the formerly used rabbit pyrogen assay, because the LAL test is a more specific and a highly sensitive method for the detection of bacterial endotoxins from gram-negative bacteria [10]. However, the detection and removal of endotoxins, especially from biopharmaceutical samples, is still challenging [6]. Even if FDA approved reagents are used, the type of glass- or plastic material used in laboratories can

affect the detection of endotoxins [11]. For example, frequently used polypropylene tubes may bind a seriously large amount of endotoxins [12]. Furthermore, the removal of endotoxins is a challenging task itself. A variety of different methods have been evaluated for a successful endotoxin deactivation, which include ultrafiltration, affinity chromatography, adsorption, hydrolysis and the application of heat [13]. However, some of the methods are not applicable to protein based pharmaceuticals. The application of heat or use of acidic or basic hydrolysis would lead to a damage of the protein [14]. Furthermore, every technique has defined limits for operation. Ultrafiltration, for example, is only suitable for very small proteins, whereas anionic-exchange chromatography is not feasible for negatively charged proteins [15]. Additionally, every protein has unique characteristics making it necessary to investigate a suitable endotoxin removal process.

Hedhammar et al. already examined a possible route for endotoxin depletion of a recombinantly produced spider silk protein [16]. However, this process requires implicitly the need for a special cell wash procedure during protein purification. The preparation process for the eADF4(C16) spider silk protein used here was already defined, making it impossible to change the overall protein fabrication process. For this reason, we focused on methods that are applicable to the final spider silk protein after the recombinant production in *E. coli*. The endotoxin depletion methods were evaluated with regards to their possible influence on the spider silk protein particle forming behavior, secondary structure and thermal stability. To assess the endotoxin level of the investigated eADF4(C16) protein, we used a FDA approved chromogenic LAL test and analyzed cells after incubation with a traditional 3-(4,5-dimethylthiazol-2-yl)-2,5-diphenyltetrazoliumbromide (MTT) assay in order to estimate the influence of the endotoxin level on living cells.

2. Materials and methods

2.1. Materials

2.1.1. Recombinantly produced spider silk protein eADF4(C16)

The spray dried eADF4(C16) protein was provided by AMSilk GmbH (Martinsried, Germany). This bioengineered spider silk protein is based on the natural amino acid sequence of the ADF4 spidroin from *A. diadematus*. The design resulted in a molecular mass of 47.7 kDa, which is a result of one T7 Tag and sixteen repeats of the amino acid sequence GSSAAAAAAAASGPGGYGPENQGPSGPGGYGPGGP. The theoretical isoelectric point of the eADF4(C16) protein is 3.48, resulting in a net negative charge at a physiological pH of 7.4.

2.1.2. Chemicals and reagents

Highly purified water (HPW) used in this study was generated using a purelab® device (ELGA LabWater, Celle, Germany). Sodium hydroxide solution (1 mol/L, EMPROVE® bio), di-potassium hydrogen phosphate (EMPROVE bio, European Pharmacopoeia (Ph. Eur.), British Pharmacopoeia (BP)), potassium dihydrogen phosphate (EMPROVE bio, Ph. Eur., BP, United States National Formulary (NF)) and fuming hydrochloric acid 37% (EMPROVE bio, Ph. Eur, BP, Japanese Pharmacopoeia (JP)) were purchased from Merck KGaA, Darmstadt, Germany. Ethanol 96% (v/v) and sodium chloride (NaCl, AnalaR NORMAPUR) were obtained from VWR Chemicals, Darmstadt, Germany. Tris(hydroxymethyl)aminomethane (Tris, Trizma® base, purity ≥99.9%) was purchased from Sigma Aldrich GmbH, Steinheim, Germany. Guanidinium thiocyanate (for molecular biology) was purchased from AppliChem GmbH, Darmstadt, Germany. Luer Lock syringes (HSW NORM-JECT® 10ml) were purchased from Henke-Sass Wolf GmbH, Tuttlingen, Germany. Needles (Sterican® 20G, 40 mm length) were obtained from B. Braun Melsungen, Melsungen, Germany. The Endotoxin cartridges (Endosafe-PTS® Cartridges PTS20005F, Sensitivity 0.005 EU/ml) were purchased from Charles River, Lyon, France.

2.2. Methods

2.2.1. Endotoxin removal from eADF4(C16) protein

Endotoxin removal from eADF4(C16) protein was performed by three different approaches. The first approach was filtration by syringe filters appropriate to remove endotoxins from protein solutions. In this case, the eADF4(C16) protein was dissolved for endotoxin removal. The second

approach used dry and moist heat for endotoxin destruction. For that purpose, dry heat at 180°C and steam at 121°C were chosen. In the third approach, strong alkali was used. Therefore, the eADF4(C16) protein was suspended in a 1 M sodium hydroxide (NaOH) solution to destroy endotoxins. For the two latter approaches, the eADF4(C16) protein was used as powder. The dissolution and analysis was performed afterwards with endotoxin free lab equipment and endotoxin free solutions.

2.2.1.1. Endotoxin removal by filtration

Filtration is a well-established method for sterilization of liquids. Major benefits of filtration are the ease of handling and the possibility to perform filtration at any step of a process. Therefore, filtration was used as one of the methods for endotoxin removal. We selected four filters for the endotoxin filtration approach which have not been used for the endotoxin removal from eADF4(C16) proteins before. The filtration step was performed right before particle preparation. Previous tests with the eADF4(C16) protein already used immobilized metal ion affinity chromatography and EndoTrap® affinity chromatography (Hyglos GmbH, Bernried am Starnberger See, Germany) for endotoxin removal. In this study, a Sartobind Q IEX pico (Sartorius Stedim Biotech GmbH, Goettingen, Germany), a Millex®-FG 0.2 µm (Merck Millipore, Darmstadt, Germany), an Acrodisc® Unit with Mustang® E Membrane and an Acrodisc® Unit with Mustang® Q XT capsule (Pall GmbH, Dreieich, Germany) were tested for their endotoxin removal capacity of eADF4(C16) protein.

The eADF4(C16) spray dried protein powder was dissolved in a 6 M guanidinium thiocyanate solution and dialyzed against a 10 mM TRIS/HCl solution pH 8.0 for 24 hours. After dialysis, the eADF4(C16) protein solution was filtered with a 0.2 µm cellulose acetate filter (VWR International, Radnor, USA) and adjusted to a concentration of 2 mg/ml with 10 mM TRIS/HCl buffer pH 8.0. This solution was used for the filtration experiments. A volume of 5 ml was filled into syringes (HSW NORM-JECT® 10ml Luer Lock, Henke-Sass Wolf GmbH, Tuttlingen, Germany) and connected to the respective syringe filters. The syringes were placed in a self-constructed perfusor (University of Munich, Munich, Germany) to ensure a uniform filtration speed.

Each filter needed special pre-treatment prior to filtration.

The Sartobind Q IEX pico was first flushed with 1 M NaOH at a flowrate of 0.5 ml/min for 40 minutes followed by 20 ml highly purified water (HPW) and 10 ml of a 10 mM TRIS/HCl buffer pH 8 at flowrates of 2.0 ml/min. Finally, the filter was flushed with additional 5 ml of the 10 mM TRIS/HCl buffer pH 8 from the outlet to the inlet.

The Millex®-FG 0.2 µm was wetted with 10 ml ethanol at a flowrate of 1.0 ml/min followed by 5 ml HPW and 10 ml of the 10 mM TRIS/HCl buffer pH 8 at flowrates of 2.0 ml/min.

The Acrodisc® Unit with Mustang® E Membrane was flushed with 10 ml of the 10 mM TRIS/HCl buffer pH 8 at a flowrate of 2.0 ml/min.

The Acrodisc® Unit with Mustang® Q XT capsule was preconditioned with 5 ml of a 1 M NaOH followed by 5 ml of a 1 M sodium chloride (NaCl) solution at flowrates of 1.0 ml/min. Finally, the filter was flushed with 10 ml of the 10 mM TRIS/HCl buffer pH 8 at a flowrate of 2 ml/min.

After completion of the filter pre-treatment, the eADF4(C16) solution was pumped at a flowrate of 2 ml/min through the filters. The first 500 µl of each batch were discarded to avoid dilution effects from residual buffer in the filters. Then, 2 ml of the filtered solutions were collected and analyzed. The protein recovery was calculated by determining the protein concentration after filtration photometrically at 276 nm (Agilent 8453 UV-Vis spectrophotometer, Agilent, Waldbronn, Germany). Endotoxin concentration was determined using a limulus amoebocyte lysate (LAL) chromogenic endpoint assay (Endosafe®-PTS™, Charles River, Lyon, France) after a 100-fold dilution with HPW (except for the solution prior to filtration). A dilution of 1:1,000,000 with HPW for endotoxin analysis was necessary for the unfiltered eADF4(C16) solution prior to filtration.

2.2.1.2. Endotoxin removal by heat

As a further approach, endotoxin removal by heat was tested. Here, the eADF4(C16) protein was used as powder. The dry heat approach used the lowest known temperature for endotoxin destruction at 180°C for 3 hours [17]. About 150 mg of the eADF4(C16) protein were weighed into glass vials (DIN 10R) and the vials were closed with aluminum foil. The closed glass vials were placed into an oven (Binder FED 53, Binder GmbH, Tuttlingen, Germany), which was programmed to heat up to 180°C and keep this temperature constant for 3 hours. After cooling down, a 6 M guanidinium thiocyanate solution was added for protein dissolution.

The second heat approach used moist heat by steam sterilization. About 150 mg of the eADF4(C16) protein was weighed into glass vials (DIN 10R) and was suspended with 7.5 ml HPW. The vials were closed with rubber stoppers and crimped with aluminum caps. Steam sterilization was performed for 15 minutes at 121°C in a GTA 50 autoclave (Fritz Gössner, Hamburg, Germany). After cooling down, the eADF4(C16) suspension was centrifuged at 10,000 rpm (SIGMA 4K15, Sigma Laborzentrifugen, Osterode am Harz, Germany) for 30 minutes and the supernatant was discarded. The centrifuged eADF4(C16) protein was dissolved in a 6 M guanidinium thiocyanate

solution.

The eADF4(C16) protein solutions were subsequently dialyzed against an endotoxin free 10 mM TRIS/HCl solution pH 8.0 for 24 hours. After dialysis, the eADF4(C16) protein solutions were centrifuged at 14,000 rpm (SIGMA 4K15, Sigma Laborzentrifugen, Osterode am Harz, Germany) for 30 minutes to remove precipitated protein. The protein concentration was determined photometrically at 276 nm (Agilent 8453 UV-Vis spectrophotometer, Agilent, Waldbronn, Germany). The protein concentration was adjusted to 2 mg/ml with an endotoxin free 10 mM TRIS/HCl solution pH 8.0. The endotoxin values were tested using the Endosafe®-PTS reader. The dry heat solution was diluted 2,500-fold with HPW, whereas the autoclaved solution was diluted 1:20,000 with HPW.

2.2.1.3. Endotoxin removal by alkali

As a further approach, incubation of eADF4(C16) protein in a 1 M sodium hydroxide (NaOH) solution was investigated. About 150 mg of the eADF4(C16) protein was weighed into glass vials (DIN 10R). After adding a volume of 7.5 ml of the 1 M NaOH solution to the eADF4(C16) protein, the vials were closed with rubber stoppers and crimped with aluminum caps. After incubation for 2 hours, the eADF4(C16) protein was fully dissolved in the 1 M NaOH solution. Therefore, this solution was directly dialyzed against an endotoxin free 10 mM TRIS/HCl solution pH 8.0 for 24 hours without the intermediate step of adding a 6 M guanidinium thiocyanate solution for protein dissolution. After dialysis, the eADF4(C16) protein solution was centrifuged at 14,000 rpm (SIGMA 4K15, Sigma Laborzentrifugen, Osterode am Harz, Germany) for 30 minutes to remove precipitated protein. The protein concentration was determined photometrically at 276 nm (Agilent 8453 UV-Vis spectrophotometer, Agilent, Waldbronn, Germany). The protein concentration was adjusted to 2 mg/ml with an endotoxin free 10 mM TRIS/HCl solution pH 8.0. The endotoxin value was tested using the Endosafe®-PTS reader after dilution 1:2,000 with HPW.

2.2.1.4. Endotoxin removal by combination of filtration and autoclave treatment

A combination of two endotoxin depleting methods was also evaluated. To do so, we combined autoclave treatment and subsequent filtration to a two-step endotoxin depletion process. In a first step, about 150 mg of the eADF4(C16) protein were weighed into glass vials (DIN 10R). The eADF4(C16) protein was subsequently suspended with 7.5 ml HPW. The vials were closed with rubber stoppers and crimped with aluminum caps. Steam sterilization was performed for 15 minutes at 121°C in a GTA 50 autoclave (Fritz Gössner, Hamburg, Germany). After cooling down, the eADF4(C16) suspension was centrifuged at 10,000 rpm (SIGMA 4K15, Sigma

Laborzentrifugen, Osterode am Harz, Germany) for 30 minutes and the supernatant was discarded. The centrifuged eADF4(C16) protein was dissolved in a 6 M guanidinium thiocyanate solution and dialyzed against an endotoxin free 10 mM TRIS/HCl solution pH 8.0 for 24 hours. After dialysis, the eADF4(C16) protein solution was filtered through a 0.2 µm polyethersulfone (PES) filter (VWR International, Radnor, USA) and adjusted to a concentration of 2 mg/ml with an endotoxin free 10 mM TRIS/HCl buffer pH 8.0. In a second step, the Acrodisc® Unit with Mustang® E Membrane was pre-flushed with 10 ml of endotoxin free 10 mM TRIS/HCl buffer pH 8. Subsequently, the eADF4(C16) solution was filtered with the prepared Mustang® E filter. About 500 µl of each batch were discarded at the beginning. The protein concentration of the filtered eADF4(C16) solution was calculated photometrically at 276 nm (Agilent 8453 UV-Vis spectrophotometer, Agilent, Waldbronn, Germany). The endotoxin values were tested using the Endosafe®-PTS reader after dilution 1:20 or 1:40 with HPW.

2.2.2. Particle preparation after endotoxin removal

After endotoxin removal, the eADF4(C16) protein solutions were adjusted to 1 mg/ml with endotoxin free 10 mM TRIS/HCl buffer pH 8.0 for particle preparation. Particle preparation was carried out by micromixing using a high pressure syringe pump system. The syringe pump cylinders were depyrogenized by 70% (v/v) ethanol over 48 hours. Subsequently, the cylinders were washed three times with HPW to remove any organic solvent. After depyrogenation, both cylinders of the syringe pump system (Model 100 DX and Series D pump controller, Teledyne Isco, Lincoln, USA) were filled with pre-tempered eADF4(C16) solution and pre-tempered endotoxin free 2 M potassium phosphate buffer pH 8.0 of 60°C. The solutions were pumped at a high flow rate of 50 ml/min to a T-shape mixing element (inner diameter 0.5 mm, P-727 PEEK tee, Upchurch Scientific, Oak Harbor, USA) leading to an outlet tubing (inner diameter 0.5 mm, 1532 PEEK Tubing, Upchurch Scientific, Oak Harbor, USA) for suspension collection. The eADF4(C16) particle suspensions were subsequently centrifuged at 14,000 rpm (SIGMA 4K15, Sigma Laborzentrifugen, Osterode am Harz, Germany) and washed with HPW three times. A two minute ultrasonication (Sonopuls HD 3200, Bandelin electronic, Berlin, Germany) step completed the particle preparation procedure. The particle concentrations in mg/ml were determined gravimetrically after drying the particles under vacuum (13 mbar) overnight.

2.2.3. Endotoxin adsorption to polypropylene labware

To assess the reported adsorption of endotoxins to polypropylene, we evaluated the used lab tubes (15 ml tube, Sarstedt AG & Co., Nümbrecht, Germany) with control endotoxin. Control

endotoxin (E. coli 055:B5, Charles River, Lyon, France) was dissolved in HPW and diluted to an endotoxin value below 100 EU/ml. Volumes of 2 ml were filled into the lab tubes and the solutions were subsequently incubated for 8 hours at room temperature. The solutions were analyzed at t=0 hours, t=4 hours and t=8 hours with the Endosafe®-PTS reader.

2.3. Analytical methods

2.3.1. Endotoxin testing

The endotoxin values of eADF4(C16) protein solutions, particles and all other used salt solutions were determined using the Endosafe®-PTS reader (Charles River, Lyon, France). The Endosafe®-PTS reader is capable of using Endosafe®-PTS cartridges for endotoxin measurement. In our studies, we used cartridges which used the chromogenic endpoint assay based on the limulus amoebocyte lysate (LAL) test. The assay is based on the reaction of bacterial endotoxins which initiate a cascading series of serine proteases in the LAL from the American Horseshoe Crabs. In case of the chromogenic endpoint assay, a modified substrate undergoes cleavage of p-nitroaniline (the chromophore) in presence of bacterial endotoxins. The p-nitroaniline can be photometrically measured at 395 nm by the Endosafe®-PTS reader. The here used FDA-licensed cartridges had sensitivities of 0.005 - 0.5 EU/ml and four channels for endotoxin testing. Two of the four channels were defined for sample testing whereas the other two channels contained a defined control endotoxin spike and served as positive controls for the assay. Each sample was diluted with HPW (tested endotoxin value <0.005 EU/ml) 20 to 200-fold before measurement. Only glassware (depyrogenation at 220°C for 1 hour [18]) was used for the dilution and storage of samples intended for endotoxin analysis. The exact dilution is given in the respective section. A volume of 25 µl of the samples was pipetted to the four channels and the test was started. Within 20 minutes, the endotoxin values were displayed by the Endosafe®-PTS reader. Within 20 minutes, the endotoxin values were read from the Endosafe®-PTS reader.

2.3.2. Dynamic light scattering (DLS)

Particle size and size distribution of submicroparticles were measured in triplicate by dynamic light scattering (DLS) using a Zetasizer Nano ZS (Malvern Instruments, Worcestershire, UK). Particle size is given as the Z-average value, and the particle size distribution is displayed by the polydispersity index (PDI). Directly before each measurement, samples were diluted to a final concentration of 0.01 mg/ml with HPW. All measurements were conducted at 25°C.

2.3.3. Zeta potential

The zeta potential of eADF(C16) particles was measured using a disposable capillary cell (DTS1061, Malvern Instruments, Worcestershire, United Kingdom) in a Zetasizer Nano ZS (Malvern Instruments, Worcestershire, United Kingdom). The eADF4(C16) particle samples were diluted with a freshly prepared 20 mM NaCl solution to a final NaCl concentration of 19 mM. The NaCl solution was filtered with a 0.2 µm PES membrane filter (VWR International, Radnor, USA) before used. The final eADF4(C16) particle concentration after dilution with NaCl solution was 0.05 mg/ml. All measurements were conducted in triplicate at 25°C.

2.3.4. Scanning electron microscopy (SEM)

Small droplets of eADF4(C16) particle suspensions were placed onto Thermanox® plastic cover slips (Nunc, Rochester, USA), which adhered to Leit-Tabs (Plano GmbH, Wetzlar, Germany). A conductive copper band (Plano GmbH, Wetzlar, Germany) connected the plastic cover slips with the sample holder. The eADF4(C16) particle suspensions were dried and carbon sputtered under vacuum at room temperature. Analysis was performed using a Joel JSM-6500F field emission scanning electron microscope (Joel Inc., Peabody, USA).

2.3.5. Differential Scanning Calorimetry (DSC)

DSC measurements were performed after drying eADF4(C16) suspensions under vacuum and transferring the samples (3-5 mg) to aluminum pans. The sealed pans were perforated with a hole in the lid and measured under constant nitrogen gas flow on a Netzsch DSC 204 (Netzsch Gerätebau, Selb, Germany) using a scanning rate of 10°C/min. The samples were heated to 110°C to remove residual water from the samples. After a 10 minute equilibration step, samples were cooled down to -40°C and the actual measurement was started by heating up to 400°C [19].

2.3.6. Protein secondary structure

Protein secondary structures of submicroparticles produced from untreated (control) and differently endotoxin depleted eADF4(C16) proteins were determined by Fourier transform infrared spectroscopy (FTIR) using a Bruker Tensor 27 FTIR spectrometer (Billerica, USA). Particle suspensions (c=20 mg/ml) were analyzed by adding 20 µl into a BioATRCell II (Harrick Scientific, Pleasantville, USA). The measurement temperature was controlled at 25°C using a water bath. Each spectrum comprises the average of 120 scans at the resolution of 4 cm^{-1}. All measurements were performed in triplicate in the range of 850 and 4000 cm^{-1}.

2.3.7. In vitro cytotoxicity assay

Cytotoxicity of eADF4(C16) submicroparticles was assessed via the cell viability of human dermal fibroblasts. Submicroparticles produced from endotoxin depleted eADF4(C16) protein (combination of steam sterilization and endotoxin filtration) were compared to submicroparticles produced from untreated eADF4(C16) protein using the 3-(4,5-dimethylthiazol-2-yl)-2,5-diphenyltetrazoliumbromide (MTT) assay [20]. Briefly, fibroblasts were seeded at 3.5×10^4 cells/well in a 24-well plate in Dulbecco's Modified Eagles Medium containing 10% (v/v) heat-inactivated fetal bovine serum, penicillin 100 I.U./ml and streptomycin 100 µg/ml (DMEM growth medium) as described previously [21]. After 24 hour incubation (37°C, 5% CO2), medium was changed to Dulbecco's Modified Eagles Medium without fetal bovine serum (DMEM basal medium). The eADF4(C16) particle suspensions were centrifuged and the supernatant discarded. The eADF4(C16) particles were diluted in DMEM basal medium. According to a pipetting scheme, differently concentrated eADF4(C16) particle suspensions were added to the wells (final volume = 500 µl). As a positive control, DMEM basal medium was added. A 10% Triton-X in DMEM basal medium solution was used as a negative control. After addition of eADF4(C16) submicroparticles, the cells were further incubated for 72 hours (37°C, 5% CO2). Then, 40 µl of a 5 mg/ml MTT solution was added to each well under exclusion of light. After 4 hour incubation, the medium was removed carefully and the precipitated blue formazan product was extracted in 250 µl DMSO and centrifuged at 14,000 rpm for 30 minutes to avoid light scattering effects from the eADF4(C16) particles. 150 µl of the supernatant was transferred to a 96-well plate and the absorbance was measured at λ = 540 nm using a 96-well micro plate reader (FLUOstar Omega, BMG Labtech, Ortenberg, Germany). The assay was performed three times with human dermal fibroblasts from three different donors. Within one approach, the controls were conducted in triplicate, while each of the differently concentrated eADF4(C16) particle suspensions were incubated in duplicate.

2.3.8. Statistical analysis

One-way analysis of variance (ANOVA) was used to analyze statistical differences between the negative control and tested samples in the cytotoxicity experiment. In case of significance, post hoc pair wise tests were performed using Tukey multiple comparison procedures with SigmaPlot 12.5 software (Systat Software, San Jose, USA). Differences were considered significant with p values < 0.05.

3. Results and Discussion

The first objective of this study was the evaluation of endotoxin binding to the plastic tubes used in the lab routine. Relevant remarks about endotoxin adsorption to different kinds of plastics have already been published in 1986 [12]. In order to prevent false negative endotoxin results by endotoxin binding to the plastic labware, we evaluated the polypropylene tubes used in the lab if they are suitable for endotoxin measurements. Control endotoxin was diluted into endotoxin free highly purified water (HPW) to a final concentration of 56.7 EU/mL as determined by the limulus amebocyte lysate (LAL) test. This endotoxin solution was filled in polypropylene tubes and analyzed after 4 hours and 8 hours. The analysis after 4 hours exhibited a drop in the endotoxin concentration to 48.9 EU/mL, which further decreased to 46.4 EU/mL after incubation for 8 hours (Figure II-1)

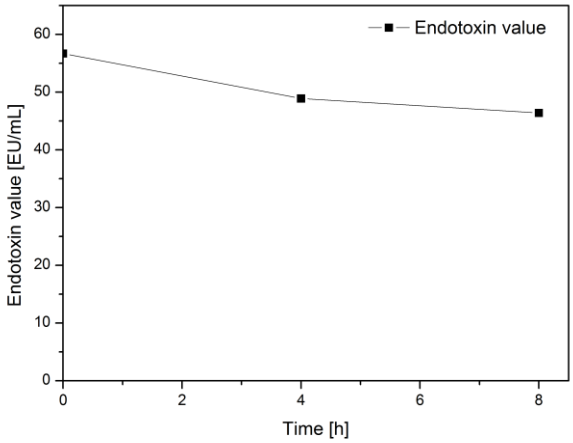

Figure II-1: Measured endotoxin values of HPW spiked with control endotoxin stored in polypropylene tubes over a time period of 8 hours.

Although the total decrease of the endotoxin value is not as dramatic as in studies reported before [12], we observed a relevant loss of endotoxin of more than 5 EU/mL within the first 4 hours. As we expected endotoxin values below 1 EU/mL in our studies, we decided to avoid any polypropylene tubes for storage of our products or dilution for endotoxin testing. Instead of using plastic tubes, we favored glassware for sample handling, which can be depyrogenized by dry heat before [18].

The second objective was endotoxin depletion of the eADF4(C16) protein. As some methods have already been tested for endotoxin removal from eADF4(C16) protein like immobilized metal ion affinity chromatography and EndoTrap® affinity chromatography from Hyglos, we searched for alternative methods and selected different approaches. In total, three different methods for

endotoxin removal were chosen which included filtration, heat treatment and alkali treatment. For the filtration approach of eADF4(C16) protein in solution, we selected endotoxin filters from different manufacturers. As endotoxins are hydrophobic molecules [17], they adsorb well to the hydrophobic eADF4(C16) protein [22]. This is of course a great challenge for endotoxin filtration, as a high protein recovery after filtration is necessary for further eADF4(C16) particle processing. In total, we selected four different filters from three different companies, which were a Sartorius Sartobind Q IEX pico, a Millex®-FG 0.2 µm from Millipore, a Pall Acrodisc® Unit with Mustang® E Membrane and a Pall Acrodisc® Unit with Mustang® Q XT. After standardized filtration of 2 ml eADF4(C16) protein solution, endotoxin values of the filtrate and the protein recovery were measured (see Table II-1).

Table II-1: Properties of the native eADF4(C16) protein and of the filters used for endootxin removal from the eADF4(C16) solution.

	Native eADF4(C16) protein	**PALL Acrodisc Unit with Mustang E Membrane**	**PALL XT Acrodisc Unit with Mustang Q Membrane**	**Millipore MILLEX-FG 0,2 µm Filter Unit**	**Sartorius Sartobind Q IEX pico**
Endotoxin value of eADF4(C16) solution [EU/mg]	47,505	<0.529	<0.500	>50	1.421
Protein recovery of filtered eADF4(C16) solution	-	60%	<1 %	88%	25%
Principles of endotoxin removal	-	Hydrophobic and electrostatic interactions	electrostatic interactions (ion exchange)	Hydrophobic interactions	Electrostatic interactions
Maximum amount of endotoxin depletion	-	500,000 EU/unit	no information provided	no information provided	1,200,000 EU/unit

We chose a small volume of just 2 ml filtration solution in order to avoid endotoxin overload of the tested filters. As shown in Table II-1, the initial eADF4(C16) solution had an endotoxin level of 47,505 EU/mg protein. Three of the tested filters were able to effectively reduce the final endotoxin concentration to less than 50 EU/mg protein. The Millex-FG filter was incapable of

removing endotoxins from an eADF4(C16) protein solution. On the other hand, two of the three effective endotoxin filters also removed a large amount of the eADF4(C16) protein from the solution. The protein recovery, measured by UV-Vis spectrometry, was even below 1% after filtration with a Pall Acrodisc® Unit with Mustang® Q XT. Slightly better results were obtained for a Sartobind Q IEX pico filter with 25% protein recovery, which is still not acceptable for routine filtration. The Acrodisc® Unit with Mustang® E Membrane was able to lower the endotoxin level of the eADF4(C16) protein solution below 0.529 EU/mg protein and 60% of the filtered protein were recovered. This was a good starting point for optimization of the endotoxin removal process for the eADF4(CF16) protein. The endotoxin filter is a good way to guarantee an eADF4(C16) solution with a very low endotoxin level for particle preparation, because the endotoxin filtration can be performed right before the particle fabrication process. However, the maximum endotoxin removal capacity per filter is limited (e.g. 500,000 EU/unit for the Acrodisc® Unit with Mustang® E Membrane and 1,200,00 EU/unit for the Sartobind IEX pico). Taking the endotoxin level of 47,505 EU/mg eADF4(C16) protein as a basis, only 10 mg (Acrodisc® Unit with Mustang® E Membrane) or 25 mg (Sartobind IEX pico) of the untreated eADF4(C16) protein can be processed with one of the filter units. Therefore, endotoxin removal by heat and alkali treatment was further tested for the eADF4(C16) protein. For the evaluation of the heat treatment, two different methods were tested. The first one was the already published endotoxin removal procedure by dry heat at 180°C for three hours [15]. The eADF4(C16) powder was heated in a dry state prior to further processing into particles (optical evaluation shown in Figure II-2 A). For the second method, we used steam sterilization in a wet state. Usually, this method is not applicable for endotoxin inactivation [17], but was also tested for the eADF4(C16) protein in this study. The eADF4(C16) protein powder was suspended in HPW and placed in an autoclave for treatment at 121°C for 15 minutes. After treatment, the eADF4(C16) suspension was inspected visually (Figure II-2 B).

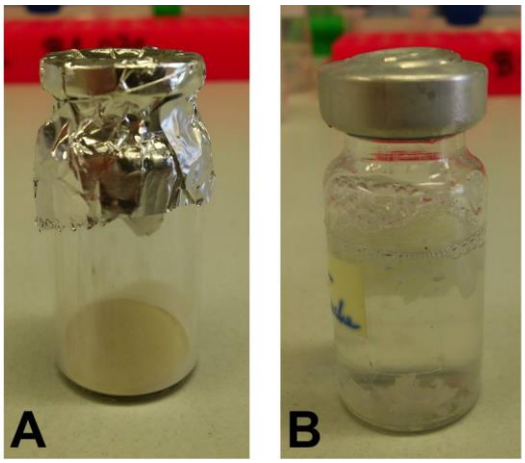

Figure II-2: Optical evaluation of thermally treated eADF4(C16) protein powder.
A) eADF4(C16) powder after dry heat treatment at 180°C.
B) Suspended eADF4(C16) powder in HPW after autoclave treatment at 121°C.

During optical evaluation, a color change of the initial white eADF4(C16) powder to a yellow brownish powder was observed after heating to 180°C (Figure II-2 A). This was a strong hint that heating the protein to 180°C is changing the eADF4(C16) protein irreversibly. On the other hand, the autoclaved eADF4(C16) suspension did not change optically before and after autoclave treatment (Figure II-2 B). As last option for endotoxin depletion, treatment by alkali was described in literature [15, 17] and was examined for endotoxin removal of the eADF4(C16) protein. The minimum effective concentration was reported at 0.1 M [15]. In order to have some safety margin during the alkali treatment, we chose to use a 1 M sodium hydroxide (NaOH) solution for depyrogenation. The eADF4(C16) powder was suspended in the NaOH solution and incubated for 2 hours.

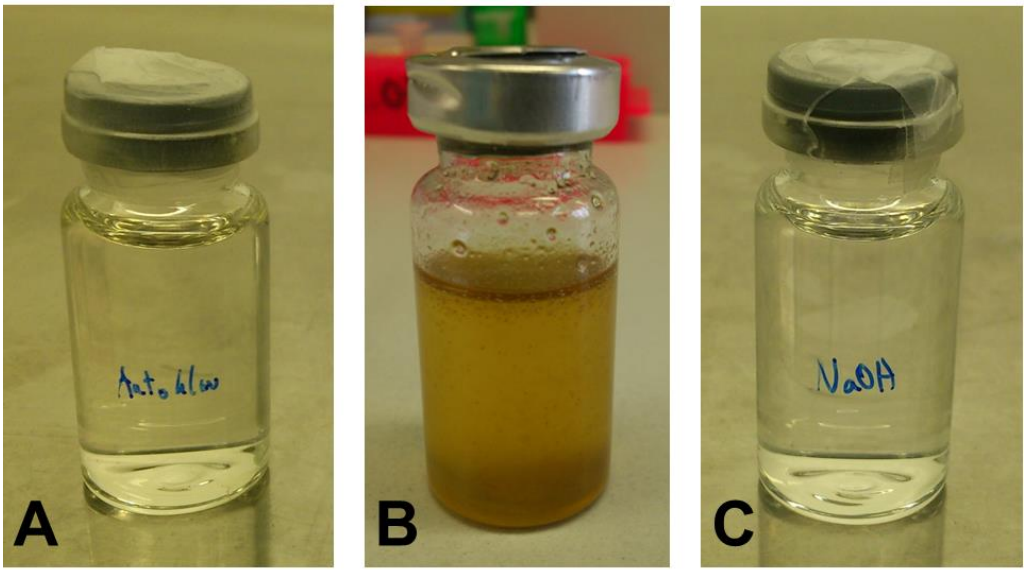

Figure II-3: Optical evaluation of eADF4(C16) solutions after dissolution.
A) eADF4(C16) protein powder after autoclave treatment and dissolution in 6 M GdmSCN.
B) eADF4(C16) protein after dry heat treatment and dispersion in 6 M GdmSCN.
C) eADF4(C16) protein after alkali treatment using 1 M NaOH. The protein dissolved during the treatment time of 2 hours in 1 M NaOH.

NaOH has not been described as dissolution medium of eADF4(C16) protein [23], so we did not expect the powder to dissolve. Surprisingly, the eADF4(C16) powder completely dissolved in the NaOH solution after incubation and did not need further processing for solubilization. The two heat treated eADF4(C16) powders were mixed with a 6 M guanidinium thiocyanate solution as done routinely for eADF4(C16) dissolution [24, 25]. At this point, the eADF4(C16) powder treated by dry heat did not dissolve as expected. As shown in Figure II-3 B, the protein is dispersed in the guanidinium thiocyanate solution resulting in a yellow to brown colored suspension.

The color change of the powder after heating and the fact that the protein did not dissolve by the standard procedure caused the exclusion of the dry heat treatment for further analysis. The dissolved eADF4(C16) material of the autoclave and the NaOH treatment were dialyzed against a 10 mM Tris solution (Figure II-3 A and C) and then analyzed for their endotoxin content. Both methods reduced the endotoxin load of the native eADF4(C16) protein, surprisingly the autoclave treatment more effectively to values of 0.293 - 1.03 EU/mg protein (Table II-2).

Table II-2: Measured endotoxin values of eADF4(C16) solutions after treatment by different endotoxin depletion methods and subsequent processing by the standard method for the native eADF4(C16) protein. Alkali Treatment was performed using 1 M NaOH for 2 hours. Autoclave treatment was performed using 121°C for 15 minutes. Filtration was performed using the PALL Acrodisc Unit with Mustang E Membrane. The autoclave treatment and filtration approach were combined to evaluate an additive effect of both methods (Combined). Untreated eADF4(C16) protein with an endotoxin level of 47,505 EU/mg protein was used. Data is showing the range of two independent experiments.

	Alkali	Autoclave	Filtration	Combined
Endotoxin value [EU/mg]	4,741 - 6,977	0.293 - 1.03	<0.265 - 0.492	<0.1 - 0.506

The vast endotoxin depletion by the autoclave method was surprising, especially because other protein polymers do not withstand a steam sterilization treatment [26]. In addition, previous studies [17, 27] did not advise autoclaving for depyrogenation. As a result of this fact, we analyzed the supernatant of the autoclaved samples, but were not able to detect high concentrations of endotoxin (values below 12.5 EU/ml). Therefore, we excluded our first theory of simple desorption of the endotoxins from the eADF4(C16) protein by autoclaving. In contrast to the common opinion that autoclaving is not able to inactivate endotoxins, some publications report about successful endotoxin depletion by steam sterilization [13, 28]. Tim Sandle summarized general depyrogenation methods in his review from 2011 [13]. Although he stated that autoclaving is not the method of choice, he refers to reports of successful depyrogenation by prolonged steam sterilization or steam sterilization at lower pH. Autoclaving as a method for depyrogenation has also been reported by da Silva et al [28]. The authors investigated dry and moist heat (autoclaving) for endotoxin inactivation on surgical equipment. After intended endotoxin contamination of the endodontic files, both methods were equally effective for endotoxin removal.

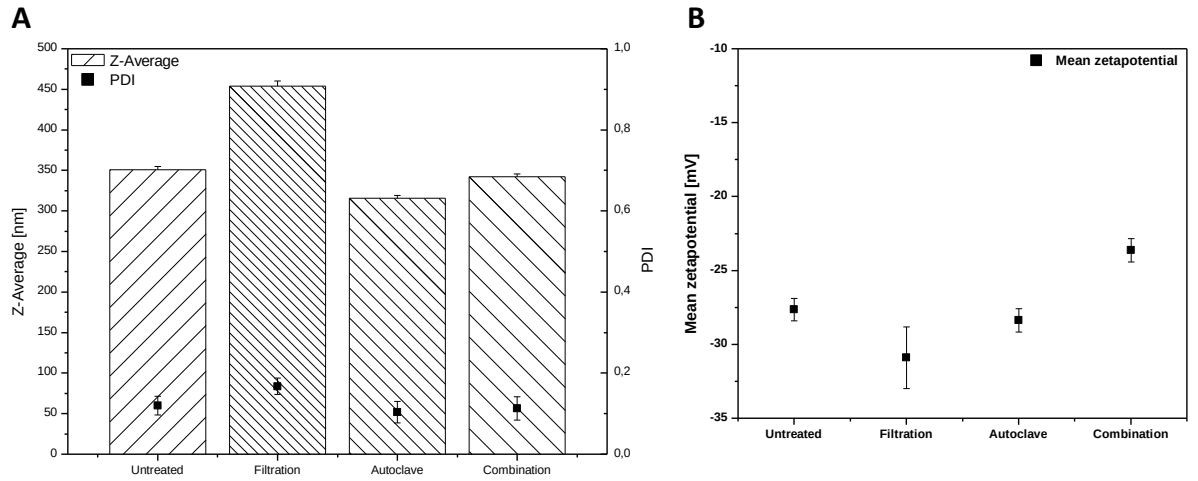

Figure II-4: eADF4(C16) particle properties. A) Particle size given as the Z-average value and the PDI of untreated and endotoxin depleted eADF4(C16) protein particles, treated with different endotoxin depletion methods. B) Zeta potential of untreated and endotoxin depleted eADF4(C16) protein particles.

Our own results and the reported cases of effective endotoxin depletion by steam sterilization encouraged us to further investigate autoclaving as a method for the endotoxin removal from eADF4(C16) protein. The autoclaving of the eADF4(C16) protein powder as first step followed by filtration by the Acrodisc Unit with Mustang E Membrane was chosen as endotoxin removal procedure. Each step as well as the combination of both steps was analyzed with respect to endotoxin value, particle size, protein secondary structure and thermal stability.

As displayed in Table II-2, the combination of both endotoxin depletion methods was as effective as the filtration method in removing endotoxins. The advantage of the combined method over the filtration only approach is the fact, that autoclave treatment as first step of the combined method already reduces the endotoxin load to low levels. Due to the endotoxin load reduction, the maximum endotoxin removal capacity of the filters is no longer of importance and filtration can be used as second step in the combined method. The combined method guaranteed the lowest possible endotoxin level, because the autoclave process was up-scaleable for larger batches and the remaining level was further reduced by the endotoxin filtration.

The size analysis of the fabricated eADF4(C16) particles supports the combination of both endotoxin depletion methods. (Figure II-4 A) While filtration alone resulted in larger particles compared to untreated reference particles, the single autoclave process generated smaller particles. Both methods did have an influence on the final particle size, which was not observed after a combination of both methods (Combined). It is already known from former publications that the eADF4(C16) protein tends to aggregate after change of pH, ionic strength or temperature [22, 29]. Maybe, this aggregation behavior was changed during endotoxin removal treatment and

further particle processing. However, the zeta potential was slightly less negative after combination of both endotoxin depletion methods. (Figure II-4 B). As this level still guaranteed a stable particle suspension, this change was not considered as critical; especially since both FTIR and DSC measurements indicated stable particles with high β-sheet content.

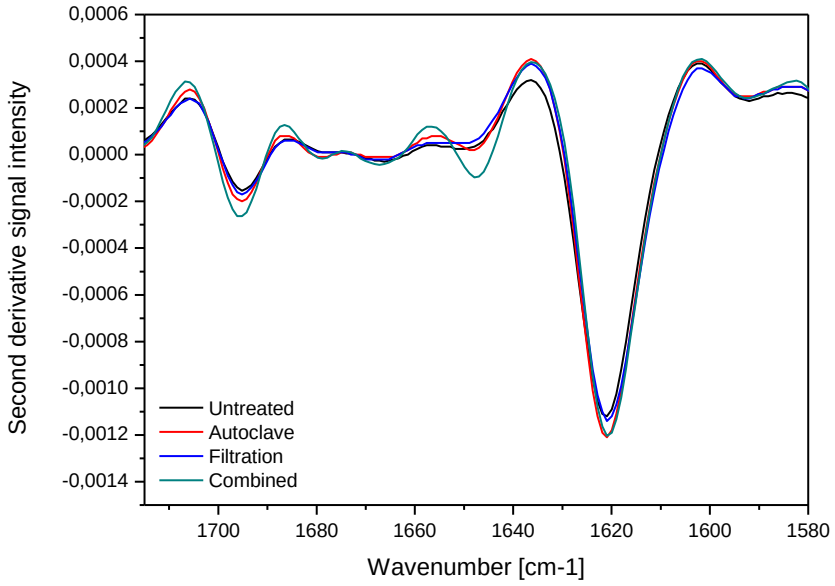

Figure II-5: Second derivative of the averaged FTIR spectra in the amide I region of eADF4(C16) protein particles after endotoxin depletion by different methods compared to untreated eADF4(C16) particles as control. Data is showing the mean of two particle batches. Data was analyzed with the Bruker OPUS software (version 6.5).

Figure II-5 shows the spectra of the amide I band between 1600 and 1700 cm^{-1} in the second derivative of the FTIR measurements. The two minima at 1620 and 1695 cm^{-1} in the spectra indicate high β-sheet and β-turn structures for the eADF4(C16) protein as reported before [30]. As there are no shifts of the minima and maxima in the spectra, all endotoxin depletion methods resulted in stable particles with regard to protein secondary structure. This statement is further supported by DSC measurements presented in Figure II-6. All analyzed particles have a high degradation temperature around 320°C. After further analysis, differences between the applied methods were detectable. While the particles after autoclave treatment or filtration did have a degradation temperature of 318°C, the untreated reference particles and the particles after the combined endotoxin depletion method displayed a degradation point of 323°C.

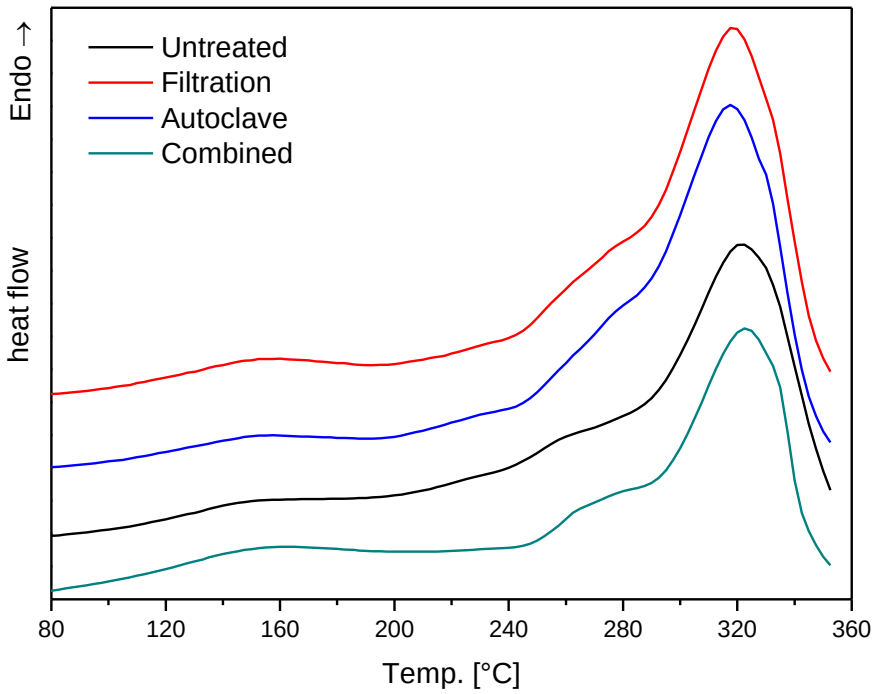

Figure II-6: DSC thermograms of endotoxin depleted eADF4(C16) protein particles compared to untreated eADF4(C16) particles as control. The graph shows the second heating ramp after the removal of residual water from the particles. Data is showing the mean of two particle batches.

Taking all these results together, a combination of autoclave treatment and filtration is an excellent way of preparing endotoxin depleted eADF4(C16) particles. To determine whether the endotoxin depletion process had an effect on cytotoxicity, we applied an 3-(4,5-dimethylthiazol-2-yl)-2,5-diphenyltetrazoliumbromide (MTT) test with human dermal fibroblasts [20]. Within this cell based assay, endotoxin depleted eADF4(C16) submicroparticles (combined endotoxin depletion method) were directly compared to untreated eADF4(C16) submicroparticles at different particle concentrations. After incubation for 72 hours, the endotoxin depleted eADF4(C16) submicroparticles were tolerated well by the fibroblasts and showed almost no cytotoxic potential at any of the tested concentrations up to 5 mg/ml (Figure II-7). However, when using particles without prior endotoxin depletion, the cell viability after 72 hours decreased concentration dependently. While no differences between untreated and endotoxin depleted particles were visible at low concentrations, a significant drop of the cell viability was detectable at 1 mg/ml and 5 mg/ml. While the cells still tolerated the endotoxin depleted eADF4(C16) submicroparticles at 1 mg/ml, the cell viability significantly decreased to around 80% at the highest tested particle concentration of 5 mg/ml. However, the cell viability of 80% for the endotoxin depleted particles was still much higher compared to the cell viability of below 60% for the untreated eADF4(C16) particles. Because the untreated and endotoxin depleted eADF4(C16)

submicroparticles were composed of the same raw material, the observed difference in cytotoxicity was most likely due to the presence of endotoxins.

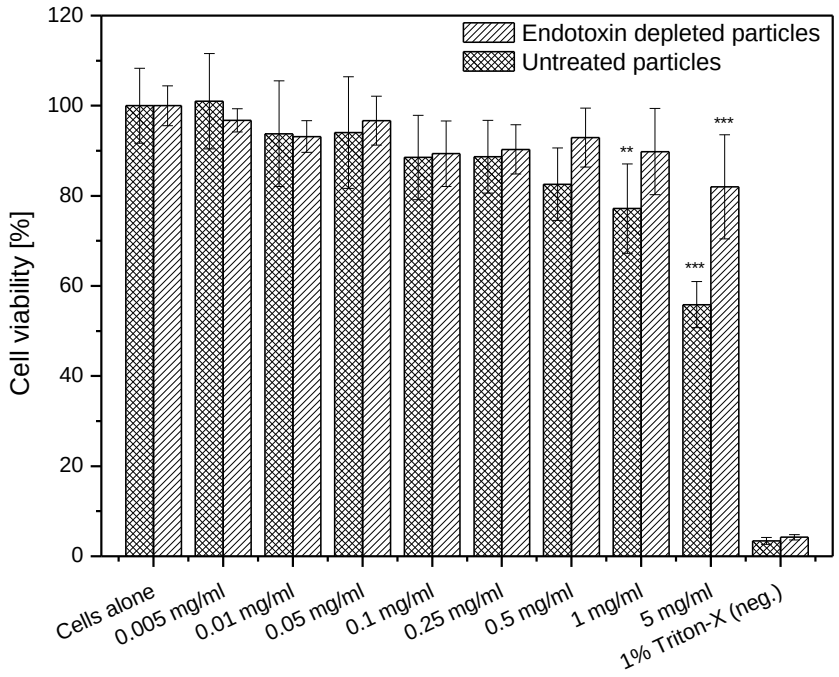

Figure II-7: Cell viability assessed by the MTT assay following 72 hour exposure of endotoxin depleted and untreated eADF4(C16) particles on human dermal fibroblasts. Data are shown as % viability compared to the positive control and are presented as mean ± SD of three separate experiments (fibroblasts from three different donors). ** Values are significantly different, p < 0.01; * values are significantly different, p < 0.001.**

Previous studies had already shown the cytotoxic effect of endotoxins on macrophages after incubation over 72h [31]. Yamamoto et el. also observed a drop in cell viability below 60% for LPS incubated macrophages and a much better viability for cells incubated with detoxified LPS [31]. The MTT results finally encouraged us to use the combined endotoxin depletion method by autoclaving and filtration for all further eADF4(C16) studies, where particles with a very low endotoxin level were needed.

4. Conclusion

The results presented in this chapter demonstrate the possibility to produce eADF4(C16) particles with low endotoxin values. Various methods have been tested to determine an optimal way of endotoxin inactivation without changing the final eADF4(C16) particle properties. We were able to show that the eADF4(C16) protein can withstand one autoclave cycle at 121°C, but not dry heat of 180°C. In contrast to many previously reported studies, the autoclave treatment was effective

for endotoxin depletion of eADF4(C16) protein. Additionally, we screened several filters for endotoxin removal from an eADF4(C16) protein solution and found one system that effectively removes endotoxins with high protein recovery. However, all these methods influenced the final particle properties when applied. Only when autoclave treatment of the eADF4(C16) protein powder and subsequent filtration of the dissolved eADF4(C16) protein were combined, the final particle size was comparable to those of untreated eADF4(C16) particles.

The comparison of untreated and endotoxin depleted eADF4(C16) particles by a cell based MTT test highlighted the necessity of endotoxin removal prior to high concentration *in vitro* studies. While eADF4(C16) particles without endotoxin depletion may be applied in settings up to a maximum concentration of 0.5 mg/ml, higher concentrations of untreated particles lead to a concentration dependent cytotoxicity and may distort the final outcome of future studies. The endotoxin depleted eADF4(C16) particles also showed a concentration dependent cytotoxicity, however the cell viability levels were much higher compared to the untreated particles. This demonstrates the need for endotoxin removal of eADF4(C16) particles prior to *in vitro/ in vivo* based experiments.

In summary, all results showed that the combined endotoxin depletion method was an effective and secure way to produce eADF4(C16) particles for *in vitro* and *in vivo* studies, which can be integrated easily into the whole eADF4(C16) particle preparation process.

5. References

[1] K. Schacht and T. Scheibel, “Processing of recombinant spider silk proteins into tailor-made materials for biomaterials applications,” *Curr. Opin. Biotechnol.*, vol. 29, pp. 62–69, 2014.

[2] T. Yucel, M. L. Lovett, and D. L. Kaplan, “Silk-based biomaterials for sustained drug delivery,” *J. Control. Release*, vol. 190, pp. 381–397, 2014.

[3] F. G. Omenetto and D. L. Kaplan, “New Opportunities for an Ancient Material,” *Science (80-.).*, vol. 329, no. 5991, pp. 528–531, 2010.

[4] J. G. Hardy, L. M. Römer, and T. R. Scheibel, “Polymeric materials based on silk proteins,” *Polymer (Guildf).*, vol. 49, no. 20, pp. 4309–4327, 2008.

[5] M. Widhe, J. Johansson, M. Hedhammar, and A. Rising, “Invited review current progress and limitations of spider silk for biomedical applications,” *Biopolymers*, vol. 97, no. 6, pp. 468–478, 2012.

[6] D. Petsch, “Endotoxin removal from protein solutions,” *J. Biotechnol.*, vol. 76, no. 2–3, pp. 97–119, 2000.

[7] J. Hurley, “Endotoxemia: methods of detection and clinical correlates,” *Clin. Microbiol. Rev.*, vol. 8, no. 2, pp. 268–292, 1995.

[8] U. K. Slotta, S. Rammensee, S. Gorb, and T. Scheibel, “An Engineered Spider Silk Protein Forms Microspheres,” *Angew. Chemie Int. Ed.*, vol. 47, no. 24, pp. 4592–4594, 2008.

[9] D. C. Morrison and J. L. Ryan, “Endotoxins and Disease Mechanisms,” *Annu. Rev. Med.*, vol. 38, no. 1, pp. 417–432, 1987.

[10] M. J. Devleeschouwer, M. F. Cornil, and J. Dony, “Studies on the sensitivity and specificity of the Limulus amebocyte lysate test and rabbit pyrogen assays,” *Appl. Environ. Microbiol.*, vol. 50, no. 6, pp. 1509–1511, 1985.

[11] K. Z. McCullough, “Variability in the LAL Test,” *PDA J. Pharm. Sci. Technol.*, vol. 44, no. 1, pp. 19–21, 1990.

[12] T. J. Novitsky, J. Schmidt-Gengenbach, and J. F. Remillard, “Factors Affecting Recovery of Endotoxin Adsorbed to Container Surfaces,” *PDA J. Pharm. Sci. Technol.*, vol. 40, no. 6, pp. 284–286, 1986.

[13] T. Sandle, “A Practical Approach to Depyrogenation Studies Using Bacterial Endotoxin,” *J. GXP Compliance*, vol. 15, no. 4, pp. 90–96, 2011.

[14] C. Tanford, “Protein denaturation,” *Adv. Protein Chem.*, vol. 23, pp. 121–282, 1968.

[15] P. de O. M. D. Batista, A. M. Lopes, P. G. Mazzola, C. de O. R. Yagui, T. C. V. Penna, and A. Pessoa Júnior, “Methods of Endotoxin Removal from Biological Preparations: a Review,” *J. Pharm. Pharm. Sci.*, vol. 10, no. 3, pp. 388–404, 2007.

[16] M. Hedhammar, H. Bramfeldt, T. Baris, M. Widhe, G. Askarieh, K. Nordling, S. von Aulock, and J. Johansson, “Sterilized Recombinant Spider Silk Fibers of Low Pyrogenicity,” *Biomacromolecules*, vol. 11, no. 4, pp. 953–959, 2010.

[17] M. B. Gorbet and M. V Sefton, “Endotoxin: The uninvited guest,” *Biomaterials*, vol. 26, no. 34, pp. 6811–6817, 2005.

[18] Deutsche Gesellschaft für Krankenhaushygiene e.V., “Empfehlung für die Validierung und Routineüberwachung von Sterilisationsprozessen mit trockener Hitze für Medizinprodukte,” Berlin, 2009.

[19] K. Spiess, R. Ene, C. D. Keenan, J. Senker, F. Kremer, and T. Scheibel, “Impact of initial solvent on thermal stability and mechanical properties of recombinant spider silk films,” *J. Mater. Chem.*, vol. 21, no. 35, pp. 13594–13604, 2011.

[20] T. Mosmann, “Rapid colorimetric assay for cellular growth and survival: application to proliferation and cytotoxicity assays,” *J. Immunol. Methods*, vol. 65, no. 1–2, pp. 55–63, 1983.

[21] N. B. Wolf, S. Küchler, M. R. Radowski, T. Blaschke, K. D. Kramer, G. Weindl, B. Kleuser, R. Haag, and M. Schäfer-Korting, “Influences of opioids and nanoparticles on in vitro wound healing models,” *Eur. J. Pharm. Biopharm.*, vol. 73, no. 1, pp. 34–42, 2009.

[22] D. Huemmerich, C. W. Helsen, S. Quedzuweit, J. Oschmann, R. Rudolph, and T. Scheibel, “Primary Structure Elements of Spider Dragline Silks and Their Contribution to Protein Solubility,” *Biochemistry*, vol. 43, no. 42, pp. 13604–13612, 2004.

[23] C. B. Borkner, M. B. Elsner, and T. Scheibel, “Coatings and films made of silk proteins,” *ACS Appl. Mater. Interfaces*, vol. 6, no. 18, pp. 15611–15625, 2014.

[24] A. Lammel, M. Schwab, M. Hofer, G. Winter, and T. Scheibel, “Recombinant spider silk particles as drug delivery vehicles,” *Biomaterials*, vol. 32, no. 8, pp. 2233–2240, 2011.

[25] M. Hofer, G. Winter, and J. Myschik, “Recombinant spider silk particles for controlled delivery of protein drugs,” *Biomaterials*, vol. 33, no. 5, pp. 1554–1562, 2012.

[26] K. W. Wissemann and B. S. Jacobson, “Pure gelatin microcarriers: Synthesis and use in cell attachment and growth of fibroblast and endothelial cells,” *Vitr. Cell. Dev. Biol.*, vol. 21, no. 7, pp. 391–401, 1985.

[27] J. C. Hurley, “Endotoxemia: methods of detection and clinical correlates,” *Clin. Microbiol. Rev.*, vol. 8, no. 2, pp. 268–292, 1995.

[28] R. A. B. da Silva, M. R. Leonardo, L. H. Faccioli, A. I. Medeiros, and P. Nelson-Filho, “Effect of different methods of sterilization on the inactivation of bacterial endotoxin (LPS) in endodontic files,” *Brazilian J. Microbiol.*, vol. 38, no. 2, pp. 270–272, 2007.

[29] A. Lammel, M. Schwab, U. Slotta, G. Winter, and T. Scheibel, “Processing conditions for the formation of spider silk microspheres,” *ChemSusChem*, vol. 1, no. 5, pp. 413–416, 2008.

[30] U. Slotta, S. Hess, K. Spieß, T. Stromer, L. Serpell, and T. Scheibel, “Spider Silk and Amyloid Fibrils: A Structural Comparison,” *Macromol. Biosci.*, vol. 7, no. 2, pp. 183–188, 2007.

[31] Y. Yamamoto, P. He, T. W. Klein, and H. Friedman, “Endotoxin induced cytotoxicity of macrophages is due to apoptosis caused by nitric oxide production,” *Innate Immun.*, vol. 1, no. 3, pp. 181–187, 1994.

III. THE EFFECT OF STEAM STERILIZATION ON RECOMBINANT SPIDER SILK PARTICLES

This chapter was published in the International Journal of Pharmaceutics:

M. Lucke, G. Winter, and J. Engert †, "The effect of steam sterilization on recombinant spider silk particles," Int. J. Pharm., vol. 481, no. 1–2, pp. 125–131, Jan. 2015.

† Corresponding author

The experiments described in this chapter have been performed by Matthias Lucke. The paper has been written by Matthias Lucke. The following chapter would have not been possible without the scientific guidance of both my supervisors Gerhard Winter and Julia Engert and my colleague from the LMU Kay Strüver. Julia Engert provided guidance regarding the spider silk particle preparation and characterization. Kay Strüver provided his knowledge regarding the cytotoxicity assay. Gerhard Winter and Julia Engert helped a lot to interpret the collected data and critically discussed the results of the experiments. Julia Engert finally submitted the manuscript to the journal.

In the following, the text of the manuscript as submitted is reprinted

1. Abstract

In this work, the recombinant spider silk protein eADF4(C16) was used to fabricate particles in the submicron range using a micromixing method. Furthermore, particles in the micrometer range were produced using an ultrasonic atomizer system. Both particle species were manufactured by an all-aqueous process. The submicroparticles were 332 nm in average diameter, whereas 6.70 µm was the median size of the microparticles. Both particle groups showed a spherical shape and exhibited high β-sheet content in secondary structure. Submicro- and microparticles were subsequently steam sterilized and investigated with respect to particle size, secondary structure and thermal stability. Sterilization temperature and time were increased to assess the thermal stability of eADF4(C16) particles. Actually, particles remained stable and their properties did not change even after autoclaving at 134°C. Both, the untreated and the autoclaved submicroparticles showed no overt cytotoxicity on human dermal fibroblasts after incubation for 72 hours. The eADF4(C16) particles were already loaded with proteins and small molecules in previous studies. With that, we can provide a highly promising parenteral drug delivery system based on a defined polypeptide carrier, manufactured with an all-aqueous process and being fully sterilizable.

2. Introduction

Biocompatible and biodegradable polymers have gained increasing interest for drug delivery applications in recent years [1]. Such biomaterials should have appropriate properties for use in medicine and surgery such as adequate initial strength and controlled degradation rate in addition to the possibility to be processed into different morphologies [1]. According to the requirements of the pharmacopeias, sterility is an indispensable prerequisite for parenterally administered compounds [2]. The European Agency for the Evaluation of Medicinal Products and the Evaluation of Medicines for Human Use provides a decision tree for the selection of an optimal sterilization method [3]. In case of aqueous based formulations, sterilization by moist heat at 121°C for 15 minutes is the method of choice. Commonly used biodegradable polymers like poly(lactic-co-glycolic) acid (PLGA) are often not able to withstand these harsh environments. Steam sterilization of PLGA composites leads to a degradation and hydrolysis of the polymer [4, 5]. In addition, PLGA degradation leads to an acidic microenvironment inside the composite and as a consequence an elevated degradation of the loaded protein [6]. Other biodegradable materials have already been tested for their ability to be autoclaved. For instance, gelatin beads showed degradation after autoclave treatment [7], and heating collagen above the shrinkage temperature changed the

protein chemistry and physical properties of the material [8, 9]. Ahmed et al. studied the effect of steam sterilization on polyurethane materials [10]. While the non-degradable polymer withstood the autoclave treatment, the biodegradable poly(caprolactone-urea)urethane polymer degraded during steam sterilization, resulting in the loss of structural integrity. Therefore, aseptic processing was assumed to be the only method to fabricate biopolymers until other sterilization techniques were evaluated for sensitive biomaterials in the past [8, 11]. Physical sterilization methods like gamma irradiation or chemical methods like gas sterilization with ethylene oxide have been tested. Nonetheless, even these techniques are not applicable to many biopolymers. For instance, a general problem of chemical sterilization with ethylene oxide is the risk of toxic residues in the final product [8]. Ahmed et al. showed that polyurethane nanocomposite biomaterials sterilized with gamma irradiation had cytotoxic effects in cell culture [10]. In addition, changes in the physical properties of tested PLGA microparticles were observed [12]. On that account, other biopolymers, which can easily be sterilized by autoclave treatment, needed to be considered. Chitosan nanoparticles have been successfully steam sterilized without an effect on particle size or morphology [13]. As chitosan can be processed in an all-aqueous environment, it is often used as drug carrier for sensitive drugs like proteins [14]. One disadvantage is that crosslinking agents are often necessary to control the release kinetics of chitosan based systems [15].

Silk proteins represent a promising alternative to the aforementioned biopolymers. It is possible to transform the silk protein into different morphologies such as films, hydrogels, scaffolds, micro- and nanoparticles [16, 17]. Moreover, Hedhammar et al. have already shown that spider silk fibers can be steam sterilized [18]. They proved that a simple steam sterilization process did not affect the fibers morphology and had no influence on the secondary structure of the protein.

In our study, we used the engineered spider silk protein eADF4(C16). This protein is a recombinant part of the natural spider silk protein ADF4 from the European garden spider *Araneus diadematus*. Lammel et al. already proved the ability of eADF4(C16) particles to be used as a drug delivery system [19], which can be easily fabricated in the submicron scale by an all-aqueous micromixing process [20]. We fabricated eADF4(C16) submicroparticles using this micromixing system and introduce the ultrasonic atomizer system as an additional method for the preparation of eADF4(C16) microparticles. Furthermore, we systematically investigated the effects of different steam sterilization conditions on both eADF4(C16) micro- and submicroparticles. Starting with the standard autoclave conditions of 121°C for 15 minutes [3], we subsequently increased the thermal load of eADF4(C16) micro- and submicroparticles. We focused on characterization of particle size, secondary structure and thermal stability related to the selected steam sterilization conditions.

Cytotoxic effects of steam sterilized eADF4(C16) submicroparticles were evaluated and compared to unsterilized particles.

3. Materials and methods

3.1. Materials

3.1.1. Recombinantly produced spider silk protein eADF4(C16)

The spray dried eADF4(C16) protein was provided by AMSilk GmbH (Martinsried, Germany). This spider silk protein is a recombinant part of the natural amino acid sequence of ADF4 from *A. diadematus*. A molecular mass of 47.7 kDa is resulting by 16 repeats of the sequence GSSAAAAAAAASGPGGYGPENQGPSGPGGYGPGGP. Due to this amino acid sequence, eADF4(C16) has a theoretical isoelectric point of 3.48 and a net negative charge at a physiological pH of 7.4.

3.1.2. Chemicals

Trizma base (Tris(hydroxymethyl) aminomethane, primary standard and buffer grade, ≥99.9%) and Dulbecco's Modified Eagles Medium were purchased from Sigma Aldrich (St. Louis, USA). Triton X-100 (analytical grade), di-potassium hydrogen phosphate (EMPROVE bio, European Pharmacopoeia (Ph. Eur.), British Pharmacopoeia (BP)) and potassium dihydrogen phosphate (EMPROVE bio, Ph. Eur., BP, United States National Formulary (NF)) were obtained from Merck KGaA (Darmstadt, Germany). Guanidinium thiocyanate (molecular biology grade) was purchased from AppliChem (Darmstadt, Germany). 3-(4,5-dimethylthiazol-2-yl)-2,5-diphenyltetrazoliumbromide (MTT) was provided from Calbiochem (Darmstadt, Germany). Fetal bovine serum (FKS), L-Glutamine, Trypsin/EDTA solution (0.05%/0.02% (w/v)) and Phosphate buffered saline (PBS) were purchased from Biochrom (Berlin, Germany). Penicillin/Streptomycin solution (100x) was obtained from PAA Laboratories (Pasching, Austria).

3.2. Particle preparation

The eADF4(C16) protein solution for particle preparation was prepared as described earlier [20]. Briefly, eADF4(C16) protein powder was dissolved in a 6 M guanidinium thiocyanate solution and subsequently dialyzed against a 10 mM Tris(hydroxymethyl)aminomethane(Tris)/HCl solution at 2-8°C. A dialysis membrane with a molecular weight cut-off of 8,000 Da (Spectrum Laboratories, Rancho Dominguez, USA) was used. After dialysis, the solution was centrifuged and filtered

through a 0.2 µm PES filter (VWR International, Radnor, USA). The concentration of eADF4(C16) protein in solution was determined by an Agilent 8453 UV-Vis spectrophotometer (Agilent, Waldbronn, Germany) using a molar extinction coefficient of eADF4(C16) at 276 nm (ε = 46,400 $M^{-1}*cm^{-1}$). This solution was further adjusted to the desired concentrations for particle preparation with a filtered 10 mM Tris solution.

Particle preparation using a micromixing system: Processing of the spider silk solution into submicroparticle dispersions was carried out by micromixing using a high pressure syringe pump system as described earlier [20]. Briefly, two cylinders of the syringe pump system (Model 100 DX and Series D pump controller, Teledyne Isco, Lincoln, USA) were filled with pre-tempered eADF4(C16) solution (c=1.0 mg/ml) or pre-tempered 2 M potassium phosphate solution (pH 8) at 60°C. The pumps were connected via a T-shape mixing element (inner diameter 0.5 mm, P-727 PEEK tee, Upchurch Scientific, Oak Harbor, USA) into which the solutions were pumped at a flow rate of 50 ml/min.

Particle preparation using an ultrasonic nozzle: An ultrasonic atomizer system was used for the preparation of microparticles. The ultrasonic nozzle (Sono-Tek, 120-00456, Milton, USA) was powered by a broadband ultrasonic generator (Sono-tek, 06-05108) to generate small atomized droplets. A 2 M potassium phosphate solution was fed into the ultrasonic nozzle using a peristaltic pump (Ismatec ISM932, Glattbrugg, Switzerland) at a constant flow rate of 3.0 ml/min. The potassium phosphate solution was atomized at 0.9 W into a stirred eADF4(C16) protein solution (c=10.0 mg/ml) reservoir (V=3.0 ml). To ensure a constant flow of the potassium phosphate solution into the nozzle, tubes were completely filled with the potassium phosphate solution prior to the atomization of the potassium phosphate solution. After one minute, the peristaltic pump was stopped and the resulting particle suspension was stirred for an additional minute.

Particle suspensions from both preparation methods were subsequently centrifuged at 14,000 rpm (SIGMA 4K15, Sigma Laborzentrifugen, Osterode am Harz, Germany) and washed with highly purified water (HPW) three times. A two minute ultrasonication (Sonopuls HD 3200, Bandelin electronic, Berlin, Germany) step completed the particle preparation procedure. Particles prepared by micromixing were subsequently filtered through a 1.2 µm filter (Acrodisc 32 mm syringe filter, Pall Life Sciences, Ann Arbor, USA) to remove any residual agglomerates. No crosslinking step was applied. The final particle concentration in mg/ml was determined gravimetrically after drying the particles under vacuum (13 mbar) overnight.

3.3. Particle sterilization

Suspensions of eADF4(C16) particles were sterilized by autoclave treatment in a GTA 50 autoclave (Fritz Gössner, Hamburg, Germany). All eADF4(C16) particles were suspended in highly purified water, and the concentration was adjusted to 1 mg/ml. Sterilization was performed in glass vials (DIN 10R, closed with stoppers and crimped with aluminum caps) for 15, 30 and 60 minutes at 121°C; 3 minutes at 134°C or repeated sterilization cycles for 1 x 15 minutes, 2 x 15 minutes and 3 x 15 minutes at 121°C. A control sample (Ref sample) was stored at 2-8°C and was analyzed along with the treated samples.

3.4. Characterization of eADF4(C16) particles

3.4.1. Dynamic light scattering (DLS)

Particle size and size distribution of submicroparticles were measured in triplicate by dynamic light scattering (DLS) using a Zetasizer Nano ZS (Malvern Instruments, Worcestershire, UK). Particle size is shown as the Z-average value, and the particle size distribution is displayed by the polydispersity index (PDI). Directly before each measurement, samples were diluted to a final concentration of 0.01 mg/ml with highly purified water. All measurements were conducted at 25°C.

3.4.2. Laser Diffraction Spectrometry (LDS)

Particle size and size distribution measurements of microparticles were performed using a Partica LA-950 (Horiba, Kyoto, Japan). Particle size is shown as the median particle size of laser diffraction analysis using refractive indices of 1.33 for water and 1.60 for protein. Particle distribution is given as the span value. The particle size and particle size distribution are the results of a volume based distribution. Samples were diluted into water directly before each measurement to obtain transmittance values of 75-90%. All measurements were performed in triplicate.

3.4.3. Scanning electron microscopy (SEM)

Small droplets of eADF4(C16) particle suspensions were placed onto Thermanox® plastic cover slips (Nunc, Rochester, USA), which adhered to Leit-Tabs (Plano GmbH, Wetzlar, Germany). A conductive copper band (Plano GmbH, Wetzlar, Germany) connected the plastic cover slips with the sample holder. The eADF4(C16) particle suspensions were dried and carbon sputtered under vacuum at room temperature. Analysis was performed using a Joel JSM-6500F field emission scanning electron microscope (Joel Inc., Peabody, USA).

3.4.4. Differential Scanning Calorimetry (DSC)

DSC measurements were performed after drying eADF4(C16) suspensions under vacuum and transferring the samples (3-5 mg) to aluminum pans. The sealed pans were perforated with a hole in the lid and measured under constant nitrogen gas flow on a Netzsch DSC 204 (Netzsch Gerätebau, Selb, Germany) using a scanning rate of 10°C/min. To prevent false results, samples were heated up to 110°C to remove residual water from the samples. After a 10 minute equilibration step, samples were cooled down to -40°C and the actual measurement was started by heating up to 400°C [21].

3.4.5. Protein secondary structure

Protein secondary structures before and after autoclaving were determined by Fourier transform infrared spectroscopy (FTIR) using the Bruker Tensor 27 FTIR spectrometer (Billerica, USA). Particle suspensions (c=20 mg/ml) were analyzed by adding 20 µl into a BioATRCell II (Harrick Scientific, Pleasantville, USA). Measurement temperature was controlled at 25°C using a water bath. Each spectrum comprises the average of 120 scans at the resolution of 4 cm^{-1}. All measurements were performed in triplicate in the range of 850-4000 cm^{-1}.

3.5. In vitro cytotoxicity assay

Cytotoxicity of eADF4(C16) submicroparticles was assessed as cell viability of human dermal fibroblasts. Steam sterilized submicroparticles (121°C, 15 minutes) were compared to untreated submicroparticles using the 3-(4,5-dimethylthiazol-2-yl)-2,5-diphenyltetrazoliumbromide (MTT) assay [22]. Briefly, fibroblasts were seeded at 3.5×10^4 cells/well in a 24-well plate in Dulbecco's Modified Eagles Medium containing 10% (v/v) heat-inactivated fetal bovine serum, penicillin 100 I.U./ml and streptomycin 100 µg/ml (DMEM growth medium) as described previously [23]. After 24 h incubation (37°C, 5% CO_2), medium was changed to Dulbecco's Modified Eagles Medium without fetal bovine serum (DMEM basal medium). eADF4(C16) particle suspensions were centrifuged and the supernatant discarded. The eADF4(C16) particles were diluted in DMEM basal medium. According to a pipetting scheme, differently concentrated eADF4(C16) particle suspensions were added to the wells (final volume = 500 µl). As a positive control, DMEM basal medium was added. A 10% Triton-X in DMEM basal medium solution was used as a negative control. After addition of eADF4(C16) submicroparticles, the cells were further incubated for 72 h (37°C, 5% CO_2). Then, 40 µl of a 5 mg/ml MTT solution was added to each well under exclusion of light. After 4 h incubation, the medium was removed carefully and the precipitated blue formazan product was extracted in 250 µl DMSO and centrifuged at 14000 rpm for 30 minutes to avoid light

scattering effects from the eADF4(C16) particles. 150 µl of the supernatant was transferred to a 96-well plate and absorbance was measured at λ = 540 nm using a 96-well micro plate reader (FLUOstar Omega, BMG Labtech, Ortenberg, Germany). The assay was performed three times with human dermal fibroblasts from three different donors. Within one approach, the positive and negative controls were conducted in triplicate, the incubation with each particle concentration in duplicate.

3.6. Statistical analysis

One-way analysis of variance (ANOVA) was used to analyze statistical differences between the negative control and tested samples in the cytotoxicity experiment. In case of significance, post hoc pair wise tests were performed using Tukey multiple comparison procedures with SigmaPlot 12.5 software (Systat Software, San Jose, USA). Differences were considered significant with p-values < 0.05.

4. Results and Discussion

4.1. Particle Preparation in the Micron- and Submicron-Range

Two types of particles were produced using the recombinant spider silk protein eADF4(C16). The submicroparticle preparation process using the micromixing system was utilized as described by Hofer *et al.* [20]. A new method for the preparation of eADF4(C16) spider silk microparticles without use of any organic solvent is presented in this study. The particle fabrication using the ultrasonic atomizer system resulted in a final eADF4(C16) particle size of 6.70 µm under the selected conditions. A span value of 1.13 is demonstrating a uniform particle distribution. No post treatment is necessary after particle preparation. The continuous fabrication process is advantageous and complements the earlier published spider silk microparticle preparation methods [24]. The ultrasonic atomizer system was previously used for the preparation of liposomes [25] or protein based nanoparticles [26] by spray-freeze-drying. In our case, eADF4(C16) based particles were sufficiently stable to be purified by repeated centrifugation and washing steps without the need of freeze drying. According to the scanning electron microscopy (SEM) graphs, the submicroparticles (Figure III-1) as well as the microparticles (Figure III-2) display a spherical shape with a smooth and dense surface.

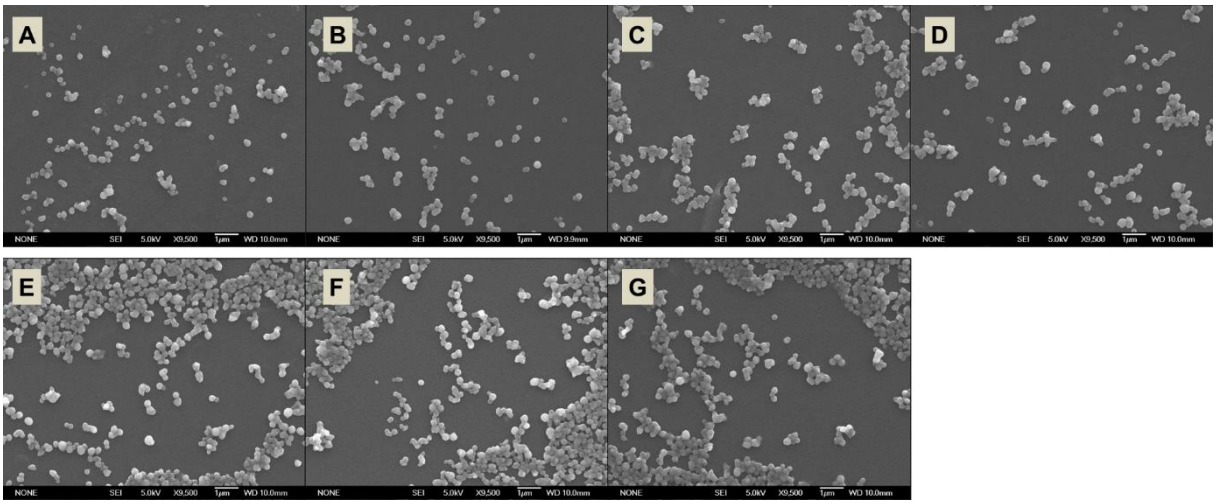

Figure III-1: SEM micrographs (magnification: 9500×) of different eADF4(C16) submicroparticles. (A) Ref particles, (B) 1 × 15 min, (C) 2 × 15 min, (D) 3 × 15 min, (E) 1 × 30 min, (F) 1 × 60 min, (G) 134 °C.

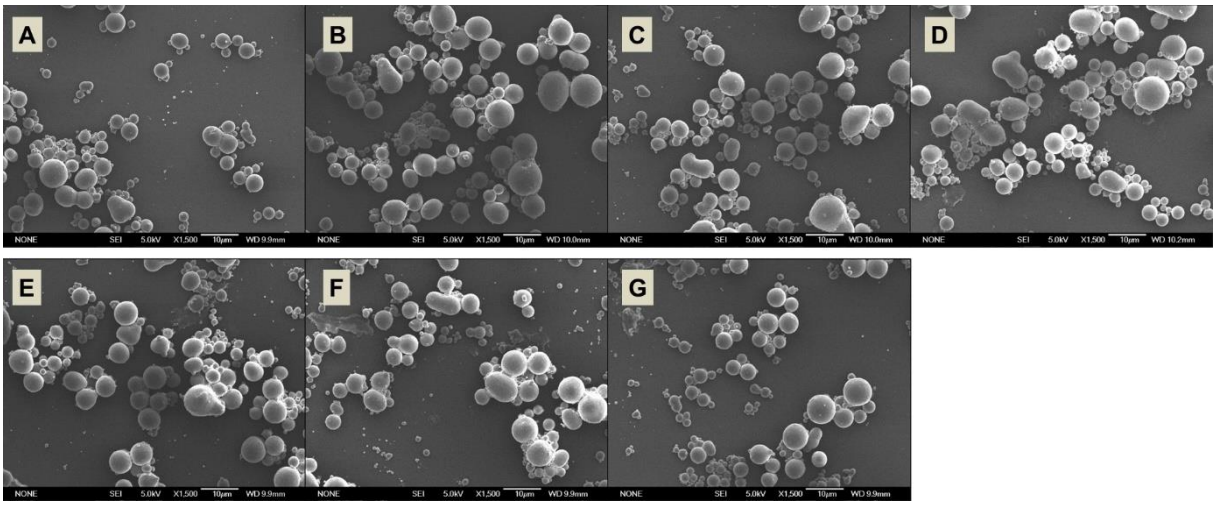

Figure III-2: SEM micrographs (magnification: 1500×) of different eADF4(C16) microparticles. (A) Ref particles, (B) 1 × 15 min, (C) 2 × 15 min, (D) 3 × 15 min, (E) 1 × 30 min, (F) 1 × 60 min, (G) 134 °C.

Both fabrication methods are transforming the spider silk protein into a β-sheet rich secondary structure. (Ref in Figure III-3) Temperature, flow rate and protein concentrations were different for the two fabrication methods. The common element in both fabrication methods was the potassium phosphate solution. The salting out process by a highly molar potassium phosphate solution was already discussed earlier [27]. Therefore, eADF4(C16) particle size can be adjusted by temperature, flow rate, protein concentration or change of the fabrication method, while preserving the high β-sheet content by the use of a concentrated potassium phosphate solution.

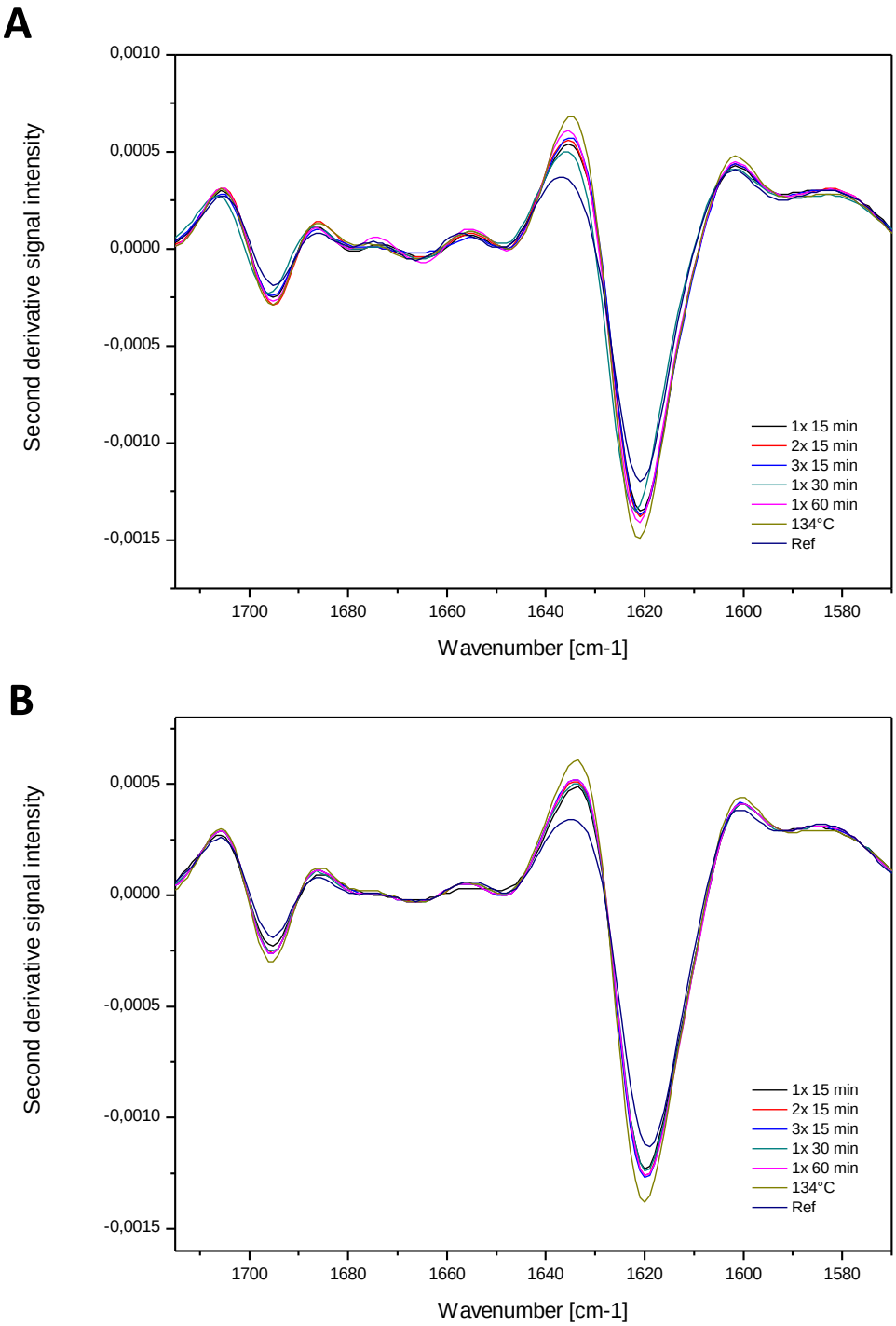

Figure III-3: Second derivative of the averaged FTIR spectra in the amide I region of (A) eADF4(C16) submicroparticles and (B) eADF4(C16) microparticles after extended sterilization conditions and stored at 2–8 °C as reference. Data was analyzed with the Bruker OPUS software (version 6.5).

4.2. Sterilization of the eADF4(C16) Particles by Autoclave Treatment

We tested two particle species (submicro- and microparticles) in terms of their thermal resistance during different steam sterilization processes. The particle size and particle size distribution was analyzed before and after the treatment. Particle size measurements (Figure III-4) showed that

the particle size remained the same for all applied sterilization conditions. In Figure III-4 A the submicroparticle sample which was autoclaved at 134°C showed the highest particle distribution index (PDI) as well as the highest standard deviation on measured particle size. Besides the high temperature of 134°C, samples were also exposed to a higher pressure of 3 bars. Similarly, the microparticle sample in Figure III-4 B which was autoclaved three times at 121°C for 15 minutes displayed higher standard deviations for particle size and a span value close to 1.2. A visual confirmation of particle size by scanning electron microscopy (Figure III-1 and Figure III-2) showed that all particles retained their smooth surface and round shape even after autoclave treatment. No collapse of the particles or surface defects were visible in the SEM micrographs.

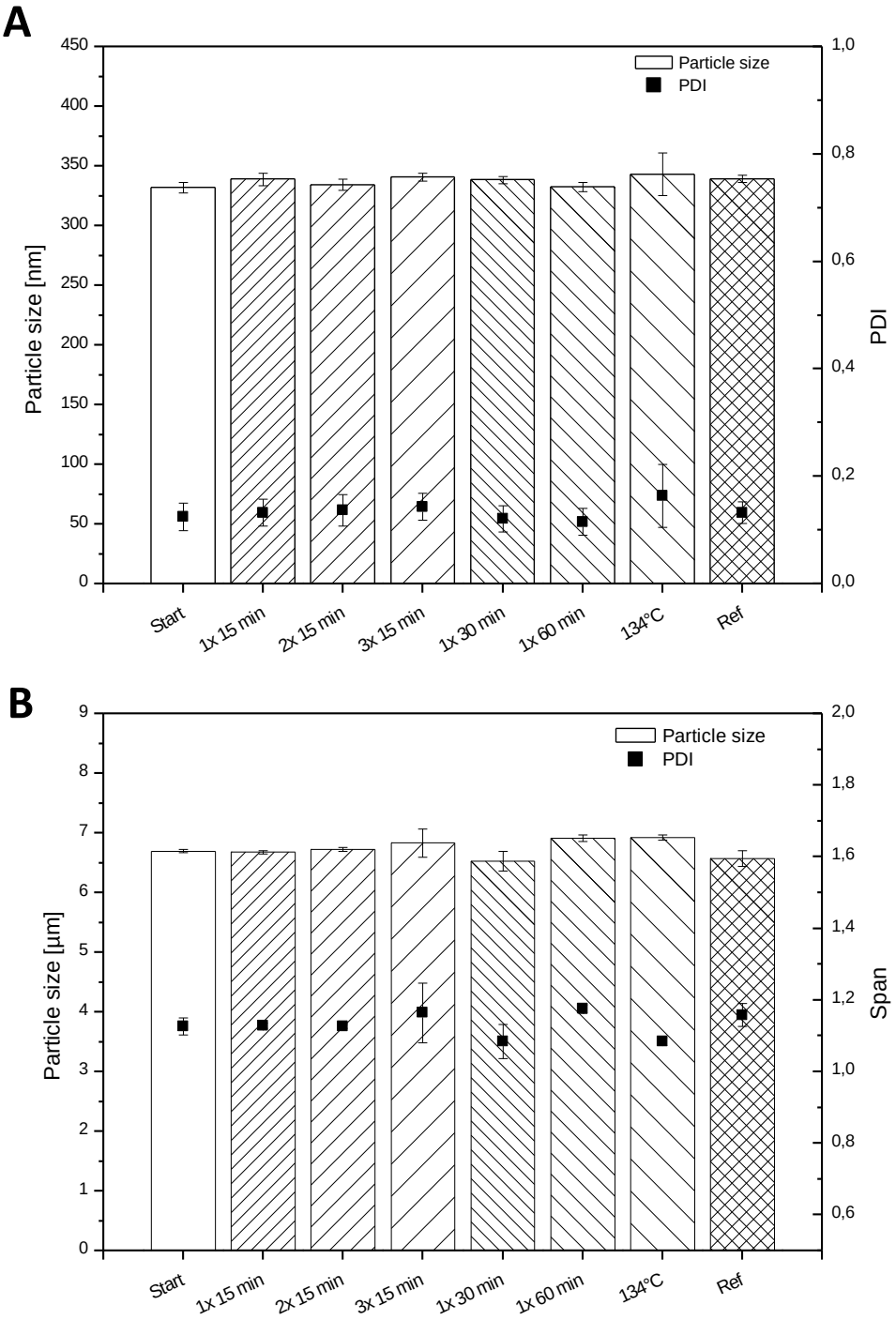

Figure III-4: (A) Particle size and polydispersity index of eADF4(C16) submicroparticles prior to sterilization, after different sterilization conditions and stored at 2–8 °C as reference.
(B) Particle size and span value of eADF4(C16) microparticles prior to sterilization, after different sterilization conditions and stored at 2–8 °C as reference.

If particle size is relevant for a desired application, the fabrication of spider silk particles in the submicron or micron range can easily be executed in a non-sterile environment, followed by a steam sterilization step. Compared to other protein based biomaterials (e.g. collagen), which

thermally denatures during a steam sterilization process [28], it is remarkable that eADF4(C16) is extremely durable even though it is a protein based biopolymer.

To determine the effect of steam sterilization on the secondary structure of the eADF4(C16) particles, FTIR measurements of all samples were performed. Figure III-3 shows the spectra of the amine I band between 1600 and 1700 cm^{-1} in the second derivative. The two minima at 1620 and 1695 cm^{-1} in the FTIR spectra indicate high β-sheet content in both micro- and submicroparticles. Slight intensity differences between the reference and autoclaved particles were visible in the spectra, but above all, no shift of the local minima was observed after the autoclave treatment. The high β-sheet content of the untreated reference particles was consistent after steam sterilization. In conclusion, the combination of high temperature, humidity and pressure resulted in no observable change in secondary structure of eADF4(C16) particles.

We additionally studied the robustness of spider silk particles under elevated temperatures. All particle batches were analyzed by differential scanning calorimetry (DSC). DSC thermograms of submicroparticles (Figure III-5 A) showed a distinct shoulder at around 260-280°C, which is not that pronounced in the thermogram of microparticles (Figure III-5 B). Additionally, the shoulder is also missing for the submicroparticles autoclaved at 134°C. Spiess *et al.* reported that this shoulder is due to a bimodal degradation of eADF4(C16) material [21]. Taking these findings together, the rather harsh conditions during the autoclave process at 134°C may already force particles to a partial degradation. This first degradation point is then missing in the thermogram of submicroparticles treated at 134°C. Overall, final degradation of submicroparticle samples before and after autoclave treatment takes place at the same degradation point at 326-327°C (Figure III-5 A). On the contrary, thermograms of the microparticles show differences between the untreated particles (Ref) and all other steam sterilized particles (Figure III-5 B). The degradation point of the untreated microparticles was notably lower (320°C) and shifted after the steam sterilization process. The degradation point of steam sterilized microparticles was at the level of the submicroparticles. No increase upon extended steam sterilization conditions was observed and the degradation point remained at 326-329°C for all samples. This result leads to the hypothesis, that the fabrication using the ultrasonic atomizer system at room temperature forms particles with yet a high β-sheet content. However, the β-sheet content is not as high as in the submicroparticles which were prepared using the micromixing system at 60°C. The steam sterilization process in that case serves as a post treatment for the microparticles, comparable to the published water vapor treatment for other silk particles [29]. The hypothesis of increasing β-sheet content after steam sterilization is additionally supported by the recently published results

of Gil *et al.* [30]. The authors reported a change in enzymatic degradation and an increase of the thermal stability of their silk porous 3D scaffolds after steam sterilization. Comparable to our FTIR results, they did not observe wavelength shifts in the FTIR spectra. Hofmann *et al.* reported changes in the mechanical properties after sterilization of 3D silk scaffolds [31]. As 3D scaffolds are often used for tissue regeneration, cell diffusion rate into the porous scaffolds may be altered after sterilization. On the contrary, particles are mostly used as drug delivery systems. For that purpose, the physical stability of the system is a crucial parameter. After sterilization by autoclave treatment no changes in size or secondary structure were observed. Additional DSC scans demonstrated a degradation point far above the used steam sterilization temperatures. We can therefore support the statement of Hedhammar *et al.*, who recommended autoclaving as good sterilization method for spider silk systems [18]. In addition, we showed that eADF4(C16) particles are able to withstand a steam sterilization temperature of 134°C for 3 minutes. These conditions are required for prion inactivation when spider silk particles may be used as medical device [32].

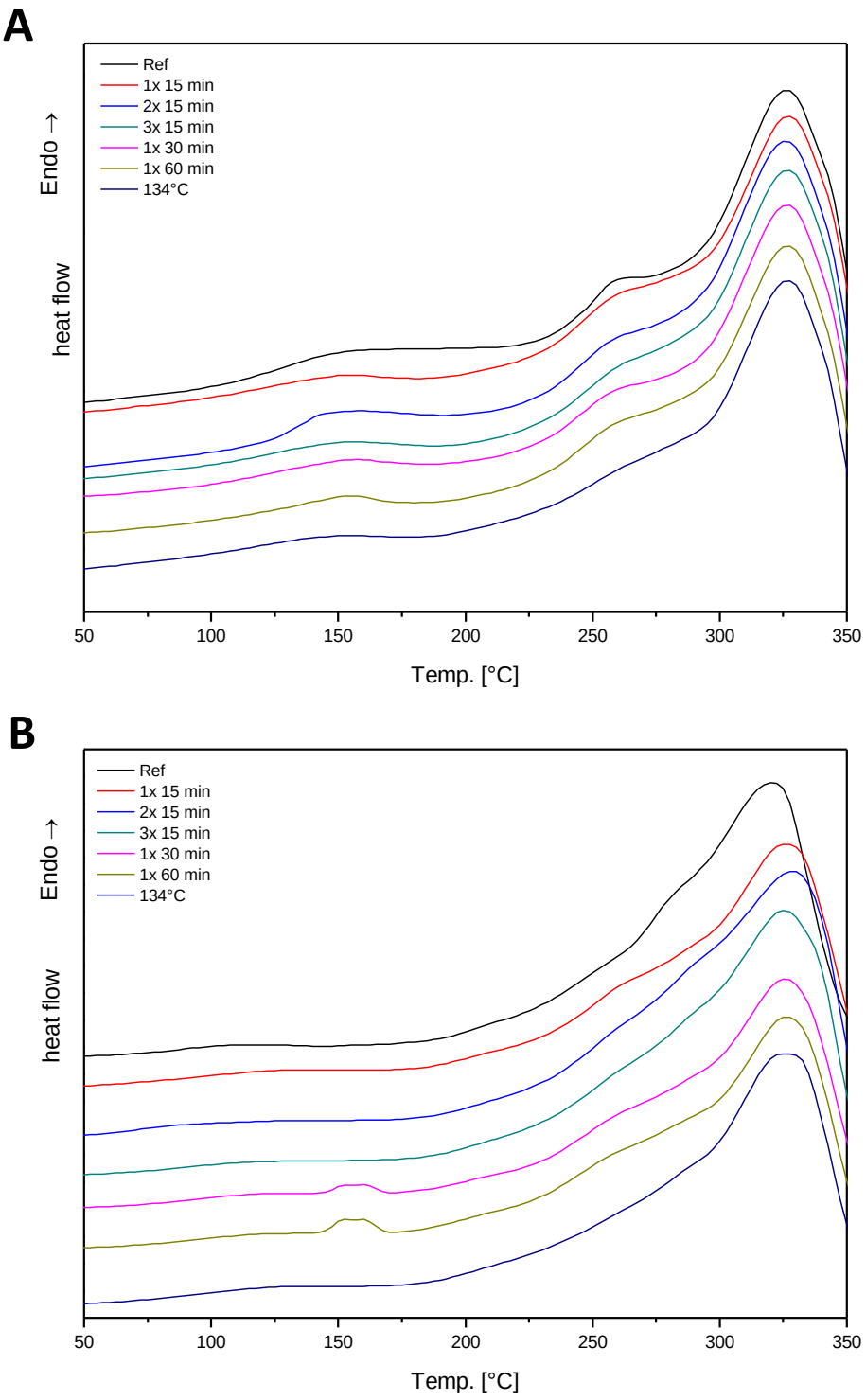

Figure III-5: DSC thermograms of (A) eADF4(C16) submicroparticles and (B) eADF4(C16) microparticles after extended sterilization conditions and stored at 2–8 °C as reference.

The effect of sterilized and untreated spider silk submicroparticles on human dermal fibroblasts was analyzed in an *in vitro* assay [33]. We used the 3-(4,5-dimethylthiazol-2-yl)-2,5-diphenyltetrazoliumbromide (MTT) assay, which is based on the reduction of MTT to a blue colored formazan [22]. Evidently, there are no differences in cell viability between the untreated and steam sterilized submicroparticles (Figure III-6).

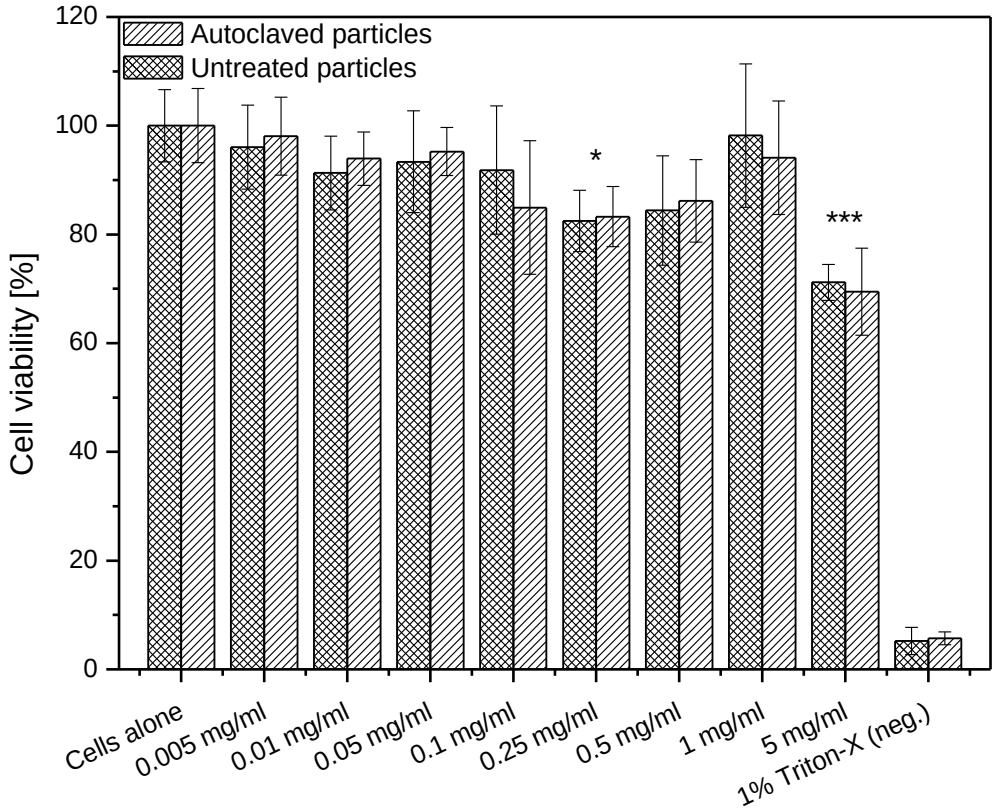

Figure III-6: Cell viability assessed by the MTT assay following 72 h exposure of eADF4(C16) submicroparticles on human dermal fibroblasts. Data are shown as % viability compared to the positive control and are presented as mean ± SD of three separate experiments (fibroblasts from three different donors). * Values are significantly different, $p < 0.05$; * values are significantly different, $p < 0.001$.**

The good overall cell viability after 72 h of incubation shows the good compatibility of spider silk particles on human dermal fibroblasts. As expected, the negative controls incubated with 1% Triton-X showed a significant decrease of cell viability to a level of 5-6%. Up to a final particle concentration of 1 mg/ml, the cell viability remains between 80-100% compared to the positive control. A drop in cell survival to around 70% at the 5 mg/ml groups indicates a concentration dependent increase in cytotoxicity of both, untreated and steam sterilized spider silk submicroparticles. The first statistically significant difference to the control groups appears at the particle concentration of 0.25 mg/ml and is even more pronounced at the concentration of 5 mg/ml. Unfortunately, this trend is not supported by the data for the 0.5 and 1.0 mg/ml groups, where no significant difference was observed. One reason could obviously be the large standard deviation observed in these two groups. Nonetheless, our results are in good agreement with previously reported results related to PLGA particles [34, 35]. Although the authors tested their PLGA particles using different cell types, they received comparable cell viability levels. Kundu *et al.* studied the influence of silk protein particles gained from the silkworm *Antheraea mylitta* on fibroblasts [36]. They observed a drop of cell viability to around 70% at a particle concentration of 0.2 mg/ml after incubation for 24 h. The *in vitro* cell cytotoxicity of recombinant spider silk

proteins was examined by Dams-Kozlowska *et al.* [37]. They compared two different recombinant spider silk proteins with different concentrations for 24 and 48 h. At their highest protein concentration of 1 mg/ml the cell viability was significantly reduced to levels between 64% and 4%. Based on the comparison to these other silk proteins, it can be concluded that eADF4(C16) submicroparticles are not cytotoxic.

5. Conclusion

In this study, we prepared eADF4(C16) spider silk protein particles in the submicron and micron range. While the preparation of submicroparticles is already well established, the ultrasonic atomizer system presents an additional method for the fabrication of eADF4(C16) microparticles. Both particle manufacturing methods are all-aqueous processes avoiding the risk of residual organic solvents.

After preparation of eADF4(C16) particles in a non-sterile environment, we performed a systematic analysis of the particles after extended steam sterilization conditions. Sterilization of spider silk particles (both in the submicron and micron range) had no detrimental effect on particle size, secondary structure and thermal stability. In case of the microparticles, thermal stability was actually increased after autoclave treatment. No cytotoxic effects of eADF4(C16) particles on human dermal fibroblasts were observed up to a final concentration of 5 mg/ml. While the sterilization in the present study was performed with unloaded particles, the effect of steam sterilization on drug loaded particles needs to be determined separately for every drug.

6. Acknowledgements

The authors would like to thank AMSilk GmbH (Martinsried, Germany) for kindly providing the spider silk protein. Kay Strüver (LMU Munich) is thanked for his assistance with the cytotoxicity assay. Christina Wetzel and Mirjam Schwarz are thanked for their contributions to this project during their elective. This work was supported by a grant from the Federal Ministry of Education and Research, Germany (grant number: 13N11341).

7. References

[1] G. Luckachan and C. Pillai, “Biodegradable Polymers-A Review on Recent Trends and Emerging Perspectives,” *J. Polym. Environ.*, vol. 19, no. 3, pp. 637–676, 2011.

[2] Council of Europe, *European Pharmacopoeia. 7th edition incl. supplement 7.8*. Strasbourg, 2011.

[3] EMEA, "Decision trees for the selection of sterilisation methods (CPMP/QWP/054/98)," London, 2000.

[4] K. Athanasiou, G. Niederauer, and C. Agrawal, "Sterilization, toxicity, biocompatibility and clinical applications of polylactic acid/ polyglycolic acid copolymers," *Biomaterials*, vol. 17, no. 2, pp. 93–102, 1996.

[5] J. M. Anderson and M. S. Shive, "Biodegradation and biocompatibility of PLA and PLGA microspheres," *Adv. Drug Deliv. Rev.*, vol. 28, no. 1, pp. 5–24, 1997.

[6] T. Estey, J. Kang, S. P. Schwendeman, and J. F. Carpenter, "BSA degradation under acidic conditions: a model for protein instability during release from PLGA delivery systems," *J. Pharm. Sci.*, vol. 95, no. 7, pp. 1626–1639, 2006.

[7] K. W. Wissemann and B. S. Jacobson, "Pure gelatin microcarriers: Synthesis and use in cell attachment and growth of fibroblast and endothelial cells," *Vitr. Cell. Dev. Biol.*, vol. 21, no. 7, pp. 391–401, 1985.

[8] C. Wiegand, M. Abel, P. Ruth, T. Wilhelms, D. Schulze, J. Norgauer, and U.-C. Hipler, "Effect of the sterilization method on the performance of collagen type I on chronic wound parameters in vitro," *J. Biomed. Mater. Res. Part B Appl. Biomater.*, vol. 90B, no. 2, pp. 710–719, 2009.

[9] L. C. Bonar and M. J. Glimcher, "Thermal denaturation of mineralized and demineralized bone collagens," *J. Ultrastruct. Res.*, vol. 32, no. 5–6, pp. 545–557, Sep. 1970.

[10] M. Ahmed, G. Punshon, A. Darbyshire, and A. M. Seifalian, "Effects of sterilization treatments on bulk and surface properties of nanocomposite biomaterials," *J. Biomed. Mater. Res. B. Appl. Biomater.*, 2013.

[11] A. Yaman, "Alternative methods of terminal sterilization for biologically active macromolecules," *Curr Opin Drug Discov Devel*, vol. 4, no. 6, pp. 760–763, 2001.

[12] W. Friess and M. Schlapp, "Sterilization of gentamicin containing collagen/PLGA microparticle composites," *Eur. J. Pharm. Biopharm.*, vol. 63, no. 2, pp. 176–187, 2006.

[13] L. Qi, Z. Xu, X. Jiang, C. Hu, and X. Zou, "Preparation and antibacterial activity of chitosan nanoparticles," *Carbohydr. Res.*, vol. 339, no. 16, pp. 2693–2700, 2004.

[14] Y. Xu and Y. Du, "Effect of molecular structure of chitosan on protein delivery properties of chitosan nanoparticles," *Int. J. Pharm.*, vol. 250, no. 1, pp. 215–226, 2003.

[15] J. Berger, M. Reist, J. M. Mayer, O. Felt, N. A. Peppas, and R. Gurny, "Structure and interactions in covalently and ionically crosslinked chitosan hydrogels for biomedical applications," *Eur. J. Pharm. Biopharm.*, vol. 57, no. 1, pp. 19–34, 2004.

[16] K. Spiess, A. Lammel, and T. Scheibel, "Recombinant Spider Silk Proteins for Applications in Biomaterials," *Macromol. Biosci.*, vol. 10, no. 9, pp. 998–1007, 2010.

[17] Y. Wang, D. D. Rudym, A. Walsh, L. Abrahamsen, H.-J. Kim, H. S. Kim, C. Kirker-Head, and D. L. Kaplan, "In vivo degradation of three-dimensional silk fibroin scaffolds," *Biomaterials*, vol. 29, no. 24–25, pp. 3415–3428, 2008.

[18] M. Hedhammar, H. Bramfeldt, T. Baris, M. Widhe, G. Askarieh, K. Nordling, S. von Aulock, and J. Johansson, "Sterilized Recombinant Spider Silk Fibers of Low Pyrogenicity," *Biomacromolecules*, vol. 11, no. 4, pp. 953–959, 2010.

[19] A. Lammel, M. Schwab, M. Hofer, G. Winter, and T. Scheibel, "Recombinant spider silk particles as drug delivery vehicles," *Biomaterials*, vol. 32, no. 8, pp. 2233–2240, 2011.

[20] M. Hofer, G. Winter, and J. Myschik, "Recombinant spider silk particles for controlled delivery of protein drugs," *Biomaterials*, vol. 33, no. 5, pp. 1554–1562, 2012.

[21] K. Spiess, R. Ene, C. D. Keenan, J. Senker, F. Kremer, and T. Scheibel, "Impact of initial solvent on thermal stability and mechanical properties of recombinant spider silk films," *J. Mater. Chem.*, vol. 21, no. 35, pp. 13594–13604, 2011.

[22] T. Mosmann, "Rapid colorimetric assay for cellular growth and survival: application to proliferation and cytotoxicity assays," *J. Immunol. Methods*, vol. 65, no. 1–2, pp. 55–63, 1983.

[23] N. B. Wolf, S. Küchler, M. R. Radowski, T. Blaschke, K. D. Kramer, G. Weindl, B. Kleuser, R. Haag, and M. Schäfer-Korting, "Influences of opioids and nanoparticles on in vitro wound healing models," *Eur. J. Pharm. Biopharm.*, vol. 73, no. 1, pp. 34–42, 2009.

[24] A. Lammel, M. Schwab, U. Slotta, G. Winter, and T. Scheibel, "Processing conditions for the formation of spider silk microspheres," *ChemSusChem*, vol. 1, no. 5, pp. 413–416, 2008.

[25] X. Zhang, S. Guo, Y. Gan, and F. Yin, "Preparation of redispersible liposomal dry powder using an ultrasonic spray freeze-drying technique for transdermal delivery of human epithelial growth factor," *Int. J. Nanomedicine*, vol. 9, pp. 1665–1676, 2014.

[26] H. Schiffter, J. Condliffe, and S. Vonhoff, "Spray-freeze-drying of nanosuspensions: the manufacture of insulin particles for needle-free ballistic powder delivery," *J. R. Soc. Interface*, vol. 7, pp. S483–S500, 2010.

[27] U. K. Slotta, S. Rammensee, S. Gorb, and T. Scheibel, "An Engineered Spider Silk Protein Forms Microspheres," *Angew. Chemie Int. Ed.*, vol. 47, no. 24, pp. 4592–4594, 2008.

[28] W. Friess, "Collagen – biomaterial for drug delivery," *Eur. J. Pharm. Biopharm.*, vol. 45, no. 2, pp. 113–136, 1998.

[29] E. Wenk, A. J. Wandrey, H. P. Merkle, and L. Meinel, "Silk fibroin spheres as a platform for controlled drug delivery," *J. Control. Release*, vol. 132, no. 1, pp. 26–34, 2008.

[30] E. S. Gil, S.-H. Park, X. Hu, P. Cebe, and D. L. Kaplan, "Impact of Sterilization on the Enzymatic Degradation and Mechanical Properties of Silk Biomaterials," *Macromol. Biosci.*, vol. 14, no. 2, pp. 257–269, 2013.

[31] S. Hofmann, K. S. Stok, T. Kohler, A. J. Meinel, and R. Muller, "Effect of sterilization on structural and material properties of 3-D silk fibroin scaffolds," *Acta Biomater*, vol. 10, no. 1, pp. 308–317, 2014.

[32] W. A. Rutala and D. J. Weber, "Disinfection and sterilization in health care facilities: what clinicians need to know," *Clin. Infect. Dis.*, vol. 39, no. 5, pp. 702–709, 2004.

[33] J. Weyermann, D. Lochmann, and A. Zimmer, "A practical note on the use of cytotoxicity assays," *Int J Pharm*, vol. 288, no. 2, pp. 369–376, 2005.

[34] J. M. Chan, L. Zhang, K. P. Yuet, G. Liao, J.-W. Rhee, R. Langer, and O. C. Farokhzad, "PLGA-lecithin-PEG core-shell nanoparticles for controlled drug delivery," *Biomaterials*, vol. 30, no. 8, pp. 1627–1634, 2009.

[35] C. Thomas, V. Gupta, and F. Ahsan, "Influence of surface charge of PLGA particles of recombinant hepatitis B surface antigen in enhancing systemic and mucosal immune responses," *Int. J. Pharm.*, vol. 379, no. 1, pp. 41–50, 2009.

[36] J. Kundu, Y.-I. Chung, Y. H. Kim, G. Tae, and S. C. Kundu, "Silk fibroin nanoparticles for cellular uptake and control release," *Int. J. Pharm.*, vol. 388, no. 1–2, pp. 242–250, 2010.

[37] H. Dams-Kozlowska, A. Majer, P. Tomasiewicz, J. Lozinska, D. L. Kaplan, and A. Mackiewicz, "Purification and cytotoxicity of tag-free bioengineered spider silk proteins," *J Biomed Mater Res A*, vol. 101, no. 2, pp. 456–464, 2012.

IV. Chemical Coupling of SIINFEKL to eADF4(C16) Protein Particles

1. Introduction

The aim of the present study was to evaluate the possibility of connecting a peptide based antigen (SIINFEKL) with eADF4(C16) protein particles as carrier to produce a modern vaccine platform. In chapter 5 and chapter 6, the genetically modified eADF4(C16) hybrid protein particles are described as vaccine delivery platform. These hybrid proteins comprise the native eADF4(C16) structure and the peptide based antigen (SIINFEKL). While SIINFEKL was introduced genetically for the hybrid proteins in chapter 5 and chapter 6, we focused on chemical coupling in the present chapter. Because of the importance of peptide cleavage after cellular uptake, which was shown in chapter 6, SIINFEKL and the native eADF4(C16) protein were chemically coupled using cleavable linkers. With that, an alternative to the eADF4(C16) hybrid proteins was established, which does not require intensive genetical engineering but simple bioconjugation.

Different linkers have been used for the structure analysis of proteins [1, 2], investigation of protein-protein interactions [3, 4], immobilization of proteins for the solid phase synthesis [5–7], PEGylation of proteins [8, 9], preparation of immunotoxins by coupling a protein with a toxin [10, 11], preparation of links between nucleic acids and proteins [12, 13], and for the formation of protein-protein, protein-drug and antibody-drug conjugates [14–19]. In case of prodrugs like protein-protein, protein-drug or antibody-drug conjugates, the use of a linker which is cleavable under mild chemical conditions is mandatory [20]. In addition, the linkage has to be stable under physiological conditions (including pH and temperature) and degradation by endogenous proteases during blood circulation has to be excluded [21]. Three types of linkers fulfill these criteria, but they differ by the type of release of the active molecule from the conjugate [22]. A first group of linkers covers the enzymatically cleavable linkers, which are cleaved by special enzymes like cathepsins after uptake into lysosomes. This type of linker is used in the antibody-drug conjugate Brentuximab vedotin (trade name Adcetris®) [23] or in the second generation eADF4(C16) hybrid proteins described in chapter 6. Disulfide linkage is used for the second group of cleavable linkers. The heterobifunctional linker N-Succinimidyl 3-(2-pyridyldithio)propionate (SPDP) is probably one of the most commonly used cross-linkers in science and was originally developed by Carlson et al. [24]. The disulfide bond is cleavable by reduction, for example by

endogenous glutathione [25]. The third group covers pH sensitive linkers, which are cleaved under acidic conditions. This group of linkers uses the fact that the lysosomal pH changes from about pH 6 to pH 4.5 to enhance the intracellular degradation rate of foreign matters [26, 27]. The objective of all three linker groups is the reversible binding of two molecules. The advantages of cleavable over non-cleavable linkers were also identified for modern vaccine designs [28]. Various reports in literature led to the development of pH sensitive liposomes [29, 30] and in recent years also to more stable acid-degradable particles for vaccination [31, 32]. Newly developed acid-degradable particles by Standley et al. were superior to non-degradable particles due to better release of the antigen after cellular uptake [33]. The authors used an acid labile linker to cross-link the particle matrix in order to improve the particle stability.

This short feasibility study used a reductive-cleavable and an acid-cleavable linker, which should both be cleavable after cellular uptake. We evaluated the influence of the activation, modification and peptide linkage on the eADF4(C16) protein with regards to particle size and zeta potential. In addition, we determined the coupling efficiency of the two linking strategies and sent samples of eADF4(C16)-SIINFEKL linked protein particles after coupling with both linkers to our cooperation partner for further *in vitro* studies and comparison to the eADF4(C16) hybrid protein particles of chapter 6.

2. Materials and methods

2.1. Materials

2.1.1. Recombinantly produced spider silk protein eADF4(C16)

The spray dried eADF4(C16) protein was provided by AMSilk GmbH (Martinsried, Germany). This bioengineered spider silk protein is based on the natural amino acid sequence of the ADF4 spidroin from *A. diadematus*. The design resulted in a molecular mass of 47.7 kDa, which is a result of one T7 Tag and sixteen repeats of the amino acid sequence GSSAAAAAAAASGPGGYGPENQGPSGPGGYGPGGP. The theoretical isoelectric point of the eADF4(C16) protein is 3.48, resulting in a net negative charge at a physiological pH of 7.4.

2.1.2. Chemicals and reagents

Highly purified water (HPW) used for this study was generated by a purelab® device (ELGA LabWater, Celle, Germany). Sodium hydroxide solution (1 mol/L, EMPROVE® bio), di-potassium hydrogen phosphate (EMPROVE bio, European Pharmacopoeia (Ph. Eur.), British Pharmacopoeia

(BP)), potassium dihydrogen phosphate (EMPROVE bio, Ph. Eur., BP, United States National Formulary (NF)) and the fuming hydrochloric acid 37% (EMPROVE bio, Ph. Eur, BP, Japanese Pharmacopoeia (JP)) were purchased from Merck KGaA, Darmstadt, Germany. Ethanol 96% (v/v) and sodium chloride (NaCl, AnalaR NORMAPUR) were obtained from VWR Chemicals, Darmstadt, Germany. Tris(hydroxymethyl)aminomethane (Tris, Trizma® base, purity ≥99.9%), DL-Dithiothreitol (DTT, purity ≥98%), Trifluoroacetic acid (ReagentPlus®, 99%) and fluorescein isothiocyanate (suitable for protein labeling) were purchased from Sigma Aldrich GmbH, Steinheim, Germany. Guanidinium thiocyanate (for molecular biology) and 4-(2-Hydroxyethyl)-1-piperazine-1-ethanesulfonic acid (HEPES, for molecular biology) were purchased from AppliChem GmbH, Darmstadt, Germany. N-Succinimidyl-p-Formylbenzoate (SFB, Purity ≥98%) and 3-(2-Pyridyldithio)propionic Acid N-Succinimidyl Ester (SPDP, Purity ≥97%) were obtained from Santa Cruz Biotechnology, Dallas, TX, USA. The peptide with the sequence SIINFEKL ($Ova_{257-264}$, purity ≥95%) was purchased from AnaSpec, Fremont, CA, USA. The chemically modified peptides SIINFEKL-hydrazide (Charge# 2811M05, Purity 97.7%) and (3-nitro-2-pyridylthio)-cysteine-SIINFEKL ((Npys)-CSIINFEKL) (Charge# 2811M04, Purity 98.6%) were purchased from peptides&elephants GmbH, Potsdam, Germany. Acetonitrile (HPLC Grade) was obtained from Fisher Scientific, Waltham, MA USA. Dimethyl sulfoxide (DMSO, purity ≥99%) was purchased from Grüssing GmbH Analytika, Filsum, Germany. Ammonium sulfate (purity ≥99%) was obtained from Bernd Kraft GmbH, Duisburg, Germany. The Endotoxin cartridges (Endosafe-PTS® Cartridges PTS20005F, Sensitivity 0.005 EU/ml) were purchased from Charles River, Lyon, France.

2.2. Methods

2.2.1. Coupling of SIINFEKL to eADF4(C16) protein

Two different possibilities of coupling the SIINFEKL peptide to the eADF4(C16) protein were evaluated. The first one was coupling the peptide in solution prior to particle preparation and the second one was coupling after particle preparation to the fabricated eADF4(C16) protein particles.

2.2.2. Coupling of SIINFEKL to eADF4(C16) protein in solution

eADF4(C16) protein was dissolved in a 6 M guanidinium thiocyanate solution and dialyzed against a 50 mM HEPES solution pH 7.5 for 24 hours. The protein solution was adjusted to a concentration of 10 mg/ml for modification and activation of the eADF4(C16) protein. A 10-fold molar excess of either a 100 mM N-Succinimidyl-p-Formylbenzoate (SFB) in dimethyl sulfoxide (DMSO) solution or a 100 mM 3-(2-Pyridyldithio)propionic Acid N-Succinimidyl Ester (SPDP) in DMSO solution was

added to eADF4(C16) under mild agitation (Polymax 1040, Heidolph Instruments GmbH, Schwabach, Germany). After 6 hours reaction at room temperature, the resulting modified eADF4(C16) protein was purified by dialysis. The SFB modified eADF4(C16) protein was dialyzed against a 50 mM HEPES buffer pH 6.0. After dialysis, the eADF4(C16)-SFB protein was coupled with the SIINFEKL-hydrazide peptide in a molar ratio of 1:2. The SIINFEKL-hydrazide peptide was dissolved in a 20% DMSO in HPW solution and added dropwise to the activated eADF4(C16)-SFB protein. Coupling of SIINFEKL-hydrazide to eADF4(C16)-SFB was allowed to proceed for 13 hours under mild agitation. The solution was used for particle preparation of eADF4(C16)-hydrazone-SIINFEKL conjugate particles without further purification.

The SPDP modified eADF4(C16) protein was dialyzed against a 50 mM HEPES buffer pH 8.0. The purified eADF4(C16)-SPDP protein was reduced by the addition of a 50-fold excess of DL-Dithiothreitol (DTT) for 15 minutes. Remaining DTT was removed by an additional dialysis step against a 50 mM HEPES buffer pH 8.0 for 24 hours. The resulting eADF4(C16)-SH protein was coupled with the (Npys)-CSIINFEKL peptide in a molar ratio of 1:2. The (Npys)-CSIINFEKL peptide was dissolved in a 20% DMSO in HPW solution and added dropwise to the activated eADF4(C16)-SH protein. Coupling of (Npys)-CSIINFEKL to eADF4(C16)-SH was allowed to proceed for 13 hours under mild agitation. The solution was used for particle preparation of eADF4(C16)-Disulfide-SIINFEKL conjugate particles without further purification.

2.2.3. Particle preparation

Either a 2 M potassium phosphate solution pH 8.0 or a 4 M ammonium sulfate solution were used as precipitating salt solutions. The syringe pump system and both the protein solution and the precipitating salt solution were pre-tempered at 80°C. The pumps were connected via a T-shape mixing element and flowrate was set to 50 ml/min. Resulting particles were centrifuged and washed with HPW three times. The concentration of the final eADF4(C16) particle suspension was determined gravimetrically.

2.2.4. Coupling of SIINFEKL to eADF4(C16) protein particles

eADF4(C16) protein was dissolved in a 6 M guanidinium thiocyanate solution and dialyzed against a 10 mM TRIS/HCl solution pH 8.0 for 24 hours. The protein solution was adjusted to a concentration of 1 mg/ml. Either a 2M potassium phosphate solution pH 8.0 or a 4 M ammonium sulfate solution were used as precipitating salt solutions. The syringe pump system and both protein solution and precipitating salt solution were pre-tempered at 80°C. The pumps were connected via a T-shape mixing element and the flowrate was set to 50 ml/min. Resulting particles

were centrifuged and washed with HPW three times. The concentration of the final eADF4(C16) particle suspension was determined gravimetrically and adjusted to a concentration of 10 mg/ml with a 50 mM HEPES buffer pH 7.5 for modification of the eADF4(C16) protein particles. A 10-fold molar excess of either a 100 mM SFB in DMSO solution or a 100 mM SPDP in DMSO solution was added to the eADF4(C16) particles under mild agitation (Polymax 1040, Heidolph Instruments GmbH, Schwabach, Germany). After 6 hours reaction at room temperature, the resulting modified eADF4(C16) protein particles were centrifuged and washed with 50 mM HEPES buffer for three times.

In case of the SFB modified eADF4(C16) particles, the pH value of the HEPES buffer was 6.0. After purification by centrifugation, the eADF4(C16)-SFB particles were coupled with the SIINFEKL-hydrazide peptide in a molar ratio of 1:2. The SIINFEKL-hydrazide peptide was dissolved in a 20% DMSO in HPW solution and added dropwise to the activated eADF4(C16)-SFB particles. Coupling of SIINFEKL-hydrazide to the eADF4(C16)-SFB particles was allowed to proceed for 13 hours under mild agitation. Finally, uncoupled peptide was removed from the eADF4(C16)-hydrazone-SIINFEKL particles by centrifugation and washing with HPW.

The SPDP modified eADF4(C16) particles were washed with a HEPES buffer at pH 8.0. The eADF4(C16)-SPDP particles were reduced by the addition of a 50-fold excess DTT for 15 minutes. Residual DTT was removed by an additional centrifugation and washing step with 50 mM HEPES buffer pH 8.0. The resulting eADF4(C16)-SH particles were coupled with the (Npys)-CSIINFEKL peptide in a molar ratio of 1:2. The (Npys)-CSIINFEKL peptide was dissolved in a 20% DMSO in HPW solution and added dropwise to the activated eADF4(C16)-SH particle suspension. Coupling of (Npys)-CSIINFEKL to eADF4(C16)-SH was allowed to proceed for 13 hours under mild agitation. The resulting eADF4(C16)-Disulfide-SIINFEKL particles were centrifuged and washed with HPW to remove uncoupled (Npys)-CSIINFEKL peptide. The concentrations of the final eADF4(C16)-SIINFEKL particle suspensions were determined gravimetrically.

Additionally, particle intermediates after modification by SFB or SPDP without further SIINFEKL coupling were centrifuged and washed with HPW to analyze the impact of the modification on the eADF4(C16) particle size.

2.2.5. Particle preparation of chemically coupled SIINFEKL for *in vitro* studies

After evaluation of the two different coupling schemes, a procedure for particle preparation of chemically coupled SIINFEKL particles for *in vitro* studies was established. The coupling in solution was chosen for the particle preparation of eADF4(C16)-hydrazone-SIINFEKL particles, whereas the

coupling at final particles was selected for eADF4(C16)-Disulfide-SIINFEKL particles. Both preparation methods were also modified to result in endotoxin free particles. In general, the eADF4(C16) protein powder was autoclaved as described before. After steam sterilization, the autoclaved eADF4(C16) powder was dissolved in a 6 M guanidinium thiocyanate solution.

For coupling in solution, the eADF4(C16) protein solution was dialyzed against a 50 mM HEPES solution pH 7.5 for 24 hours. The protein solution was adjusted to a concentration of 10 mg/ml for modification and activation of the eADF4(C16) protein. A 10-fold molar excess of a 100 mM SFB in DMSO solution was added to the eADF4(C16) protein under mild agitation (Polymax 1040, Heidolph Instruments GmbH, Schwabach, Germany). After 6 hours reaction at room temperature, the resulting modified eADF4(C16) protein was purified by dialysis. The SFB modified eADF4(C16) protein was dialyzed against a 50 mM HEPES buffer pH 6.0. After dialysis, the eADF4(C16)-SFB protein was coupled with the SIINFEKL-hydrazide peptide in a molar ratio of 1:2. The SIINFEKL-hydrazide peptide was dissolved in a 20% DMSO in HPW solution and added dropwise to the activated eADF4(C16)-SFB protein. Coupling of SIINFEKL-hydrazide to eADF4(C16)-SFB was allowed to proceed for 13 hours under mild agitation. After incubation, the eADF4(C16)-hydrazone-SIINFEKL protein solution was filtered first with a 0.2 µm polyethersulfone (PES) filter (VWR International, Radnor, USA) and subsequently filtered with a pre-flushed Mustang® E filter for endotoxin depletion. The endotoxin values were tested using the Endosafe®-PTS reader after dilution 1:40 with HPW. This eADF4(C16)-hydrazone-SIINFEKL protein solution was further adjusted to a concentration of 1.0 mg/ml for particle preparation with an endotoxin free 50 mM HEPES buffer pH 6.0. A 2 M potassium phosphate solution pH 8.0 was used for particle preparation in the syringe pump system at 80°C. The flow rate was set to 50 ml/min. Both cylinders of the syringe pump system and the Sonopuls HD 3200 sonotrode were depyrogenized by 70% (v/v) ethanol over 48 hours prior to particle preparation. The particle suspensions were centrifuged and washed with HPW three times after fabrication.

For coupling the particles, dissolved eADF4(C16) protein was dialyzed against an endotoxin free 20 mM HEPES solution pH 8.0 at 2-8°C for 24 hours. After dialysis, centrifugation and filtration, the solution was adjusted to a concentration of 2.0 mg/ml with endotoxin free 10 mM TRIS/HCl solution pH 8.0. The dialyzed eADF4(C16) protein solution was first filtered with a 0.2 µm PES filter and subsequently filtered with a pre-flushed Mustang® E filter. The eADF4(C16) protein solution was adjusted to a protein concentration of 1 mg/ml for particle preparation by the syringe pump system at 80°C using a flow rate of 50 ml/min and a 4 M ammonium sulfate solution. Both cylinders of the syringe pump system and the Sonopuls HD 3200 sonotrode were depyrogenized

by 70% (v/v) ethanol over 48 hours prior to particle preparation. The particle suspensions were centrifuged at 14,000 rpm and washed with HPW three times after fabrication. The concentration of the final eADF4(C16) particle suspension was determined gravimetrically and adjusted to a concentration of 10 mg/ml with a 50 mM HEPES buffer pH 7.5 for modification of the eADF4(C16) protein particles. A 10-fold molar excess of a 100 mM SPDP in DMSO solution was added to the eADF4(C16) particles under mild agitation. After 6 hours reaction at room temperature, the resulting eADF4(C16)-SPDP protein particles were centrifuged and washed with 50 mM HEPES buffer pH 8.0 for three times. The eADF4(C16)-SPDP particles were reduced by the addition of a 50-fold excess of DTT for 15 minutes. Residual DTT was removed by an additional centrifugation and washing step with 50 mM HEPES buffer pH 8.0. The resulting eADF4(C16)-SH particles were coupled with the (Npys)-CSIINFEKL peptide in a molar ratio of 1:2. The (Npys)-CSIINFEKL peptide was dissolved in a 20% DMSO in HPW solution and added dropwise to the activated eADF4(C16)-SH particle suspension. Coupling of (Npys)-CSIINFEKL to eADF4(C16)-SH was allowed to proceed for 13 hours under mild agitation. The resulting eADF4(C16)-Disulfide-SIINFEKL particles were centrifuged and washed with HPW to remove uncoupled (Npys)-CSIINFEKL peptide. The concentrations of the final eADF4(C16)-SIINFEKL particle suspensions were determined gravimetrically.

2.3. Analytical methods

2.3.1. Dynamic light scattering (DLS)

Particle size and size distribution of submicroparticles were measured as described in chapter 2.

2.3.2. Zeta potential

The zeta potential of eADF(C16) particles was measured as described in chapter 2.

2.3.3. Scanning electron microscopy (SEM)

SEM measurements of eADF4(C16) particle suspensions were conducted as described in chapter 2.

2.3.4. RP-HPLC Analysis - Coupling Efficiency

The conjugated particles were analyzed to determine the coupling efficiency of SIINFEKL. The SFB coupled particles were diluted with HPW to a defined particle concentration. Hydrochloric acid was added to a final concentration of 0.5 M for the release of SFB coupled SIINFEKL. The SPDP

coupled particles were diluted with HPW to a defined particle concentration. A 1 M DTT stock solution was added to the particles to a final concentration of 10 mM DTT. Both particle suspensions were incubated in a Thermomixer comfort (Eppendorf, Hamburg, Germany) for 30 minutes and 500 rpm at room temperature. Particle suspensions were centrifuged two times at 14,000 rpm (SIGMA 4K15, Sigma Laborzentrifugen, Osterode am Harz, Germany) to obtain the supernatant with the released SIINFEKL peptides.

The supernatant was analyzed by RP-HPLC separation. After centrifugation, 50 µl of the corresponding supernatant were separated at 30°C by a reversed phase YMC-Triart C18 column (YMC Europe GmbH, Dinslaken, Germany) using a Waters 2695 separations module (Waters Corporation, Milford, MA, USA). A gradient with two mobile phases was applied, using water + 0.1% [m/m] TFA (solvent A) and 100% acetonitrile + 0.1% [m/m] TFA (solvent B). Each run started with two minutes of 95% solvent A, and was followed by a linear increase of solvent B from 5% to 100% over 28 minutes. A five minute washing step with 100% solvent B was used to wash residual peptide/protein from the column. The separation run stopped with a five minute equilibration of the column at 95% solvent A. The detection was carried out on a Waters UV-Vis detector 2487 (Waters Corporation, Milford, MA, USA) at wavelengths of 220nm and 280nm. A calibration curve of native SIINFEKL, SIINFEKL-hydrazide and (Npys)-CSIINFEKL at concentrations of 12.5, 25, 50 and 100 µg/ml dissolved in 50% DMSO / 50% water was injected and analyzed. The area of each of the peptides in the chromatogram was integrated and used for calculation of calibration curves. To avoid false results due to a decrease of the power of the UV-Vis lamp over time, another calibration curve was used with concentrations of 10, 20, 30, 50 and 100 µg/ml dissolved in 50% DMSO / 50% water for later analysis. The calibration curves were used to calculate the concentration of SIINFEKL in the supernatant after integration of the SIINFEKL peaks with corresponding retention time. Data analysis was performed with Chromeleon® 6.80 software (Dionex GmbH, Germering, Germany).

3. Results and Discussion

The native eADF4(C16) protein was used as drug delivery platform for the octapeptide $OVA_{257-264}$ (SIINFEKL), which is the CD8 epitope of ovalbumin. To realize the idea of a cleavable linker between the eADF4(C16) protein particles as drug delivery platform and the SIINFEKL peptide as vaccine antigen, a two-step modification and coupling process was necessary. A comparison between the introduction of a reductive cleavable disulfide bond and an acid-labile hydrazone bond between

the eADF4(C16) protein and the SIINFEKL peptide is outlined in Figure IV-1. The first step of this two-step coupling process was a modification and activation of the eADF4(C16) protein by either 3-(2-Pyridyldithio)propionic Acid N-Succinimidyl Ester (SPDP) or N-Succinimidyl-p-Formylbenzoate (SFB). The subsequent coupling as the second step of the process was performed with chemically modified SIINFEKL peptides containing either a Cys(Npys) or a hydrazide group.

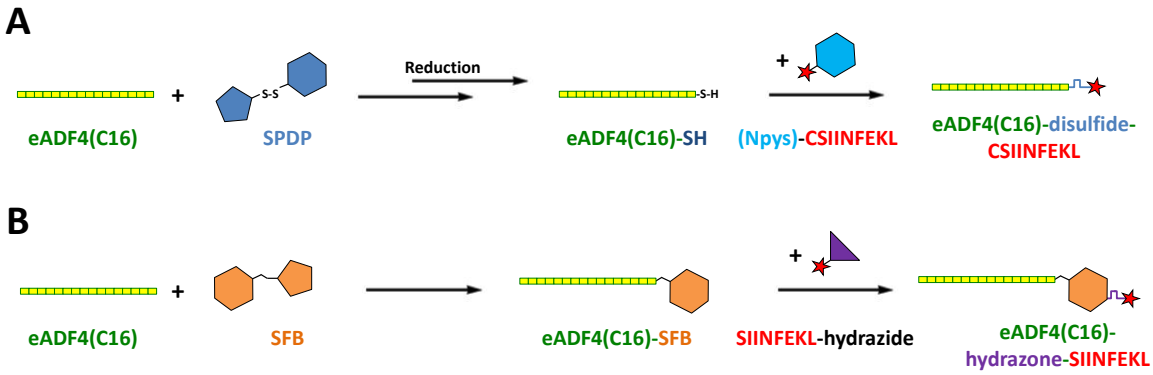

Figure IV-1: Schematic illustration of the eADF4(C16) protein modification and SIINFEKL coupling. A) Synthesis of a eADF4(C16)-SIINFEKL conjugate with a reductive cleavable disulfide bond. B) Synthesis of a eADF4(C16)-SIINFEKL conjugate with an acid-labile hydrazone bond.

As the complete eADF4(C16) modification and coupling process can be conducted either with the eADF4(C16) protein dissolved in solution or with in advance prepared eADF4(C16) protein particles suspended in highly purified water (HPW), these two options were compared with respect to final particle size and zeta potential.

First, the impact of the eADF4(C16) protein modification and activation by either SPDP or SFB on the particle size and zeta potential has been studied. The eADF4(C16) protein was dialyzed against a 50 mM HEPES buffer pH 7.5 for the modification of the eADF4(C16) protein in solution. Another portion of the eADF4(C16) protein was taken to fabricate eADF4(C16) protein particles with the micromixing approach [34] using a 2 M potassium phosphate solution. The prepared eADF4(C16) protein particles were suspended in a 50 mM HEPES buffer pH 7.5 for the modification by SPDP or SFB. A 10-fold molar excess of SPDP or SFB dissolved in DMSO was used for the modification of the eADF4(C16) protein in solution and the modification of the eADF4(C16) protein particles. After 6 hours at room temperature, the eADF4(C16) protein in solution was diluted with a 50 mM HEPES buffer for the particle preparation process, while the modified eADF4(C16) protein particles were centrifuged and washed with HPW to remove the residual SPDP or SFB. After particle preparation and purification, the particle size and zeta potential were determined.

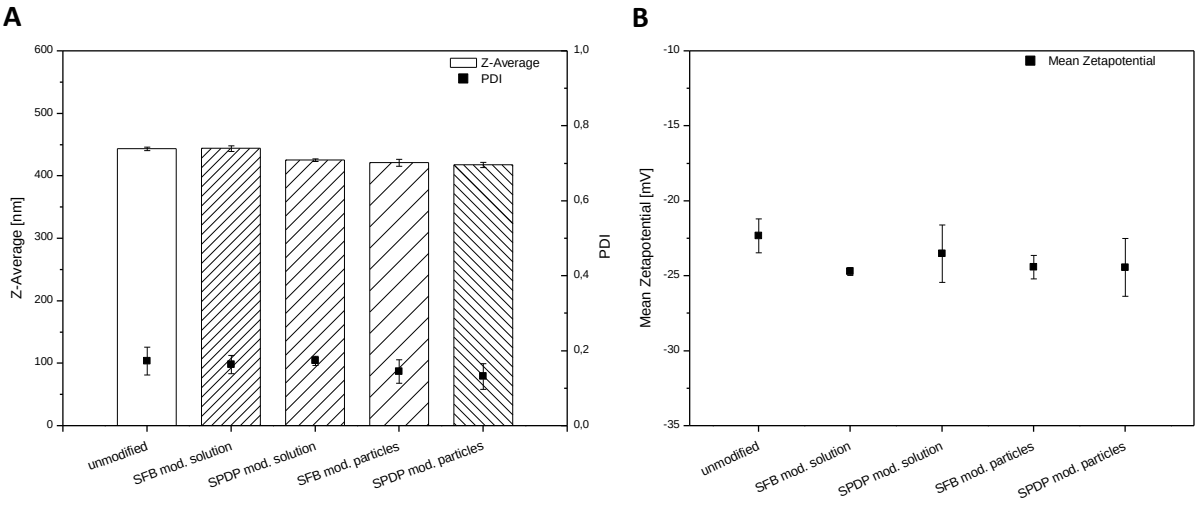

Figure IV-2: Comparison of the SPDP or SFB modified eADF4(C16) protein particles compared to native, unmodified eADF4(C16) protein particles. Modification was either performed in solution or with final eADF4(C16) protein particles.
A) Particle size given as the Z-average and the particle dispersity index (PDI) of eADF4(C16) particles prepared at 80°C and at protein concentration of 1.0 mg/ml.
B) Zeta potential of particles described in A).

The illustrated results in Figure IV-2 show that both the particle size and zeta potential of all modified eADF4(C16) particles do not differ from the unmodified eADF4(C16) particles. The results show that the modification step of the eADF4(C16) protein by SPDP or SFB has no effect on the resulting particle size. In addition, the modification process of the eADF4(C16) protein either dissolved in solution or suspended as particles in HPW shows no differences regarding the particle size and zeta potential. While no change of particle size was reported before, Blüm et el. reported a significant difference of the zeta potential between non-crosslinked and crosslinked eADF4(C16) protein particles [35]. While the zeta potential differed between 6-9 mV between the non-crosslinked and crosslinked eADF4(C16) protein particles, the cross-linking process had no effect on the particle size and surface morphology [35].

Secondly, the impact of the coupling between the modified and activated eADF4(C16) protein and the chemically modified SIINFEKL peptide was studied. We compared again the impact of the coupling process conducted in solution with the coupling to modified eADF4(C16) protein particles in suspension. Figure IV-3 shows the final particle size and zeta potential of the spider silk particles after the coupling procedure has been performed in solution. The eADF4(C16) protein particles were prepared by the micromixing device at a protein concentration of 1 mg/ml and a temperature of 80°C. The coupled eADF4(C16)-SIINFEKL proteins were precipitated either with a 2 M potassium phosphate solution or a 4 M ammonium sulfate solution, resulting in different particle sizes.

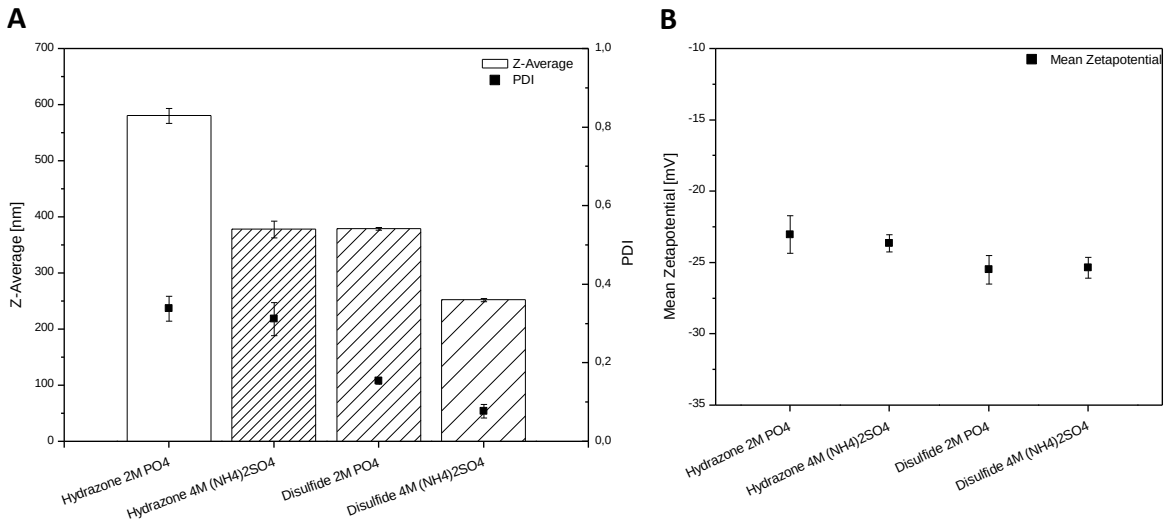

Figure IV-3: Properties of eADF4(C16)-SIINFEKL protein particles after coupling in solution and subsequent particle preparation. Preparation was either performed with a 2 M potassium phosphate or a 4 M ammonium sulfate solution.
A) Particle size given as the Z-average and the particle dispersity index (PDI) of eADF4(C16)-SIINFEKL particles coupled in solution.
B) Zeta potential of particles described in A.

We had already shown that the use of the 4 M ammonium sulfate solution results in smaller particles compared to the particles fabricated with a 2 M potassium phosphate solution. More important is the fact, that the eADF4(C16)-SIINFEKL particles with the pH-sensitive hydrazone bond are remarkably larger than the disulfide linked particles. The particle size of the hydrazone linked particles prepared with the 2 M potassium phosphate solution was 581 nm compared to 379 nm of the disulfide linked particles. The same situation is also apparent for the particles prepared with the 4 M ammonium sulfate solution, where the hydrazone linked particles display a particle size of 378 nm compared to the disulfide linked particles at a size of 252 nm. These results demonstrate the influence of the final coupling step of the SIINFEKL peptide to the modified eADF4(C16) protein in solution. Like for the modification studies before, we also performed the SIINFEKL coupling to pre-fabricated eADF4(C16) protein particles in suspension to understand the coupling process in more detail. At this time, we used differently sized particles for the preparation of the hydrazone linked and the disulfide linked particles. In order to evaluate the influence of the coupling process on the final particle size, the original particle size of the respective unmodified particles was added to the graphs in Figure IV-4.

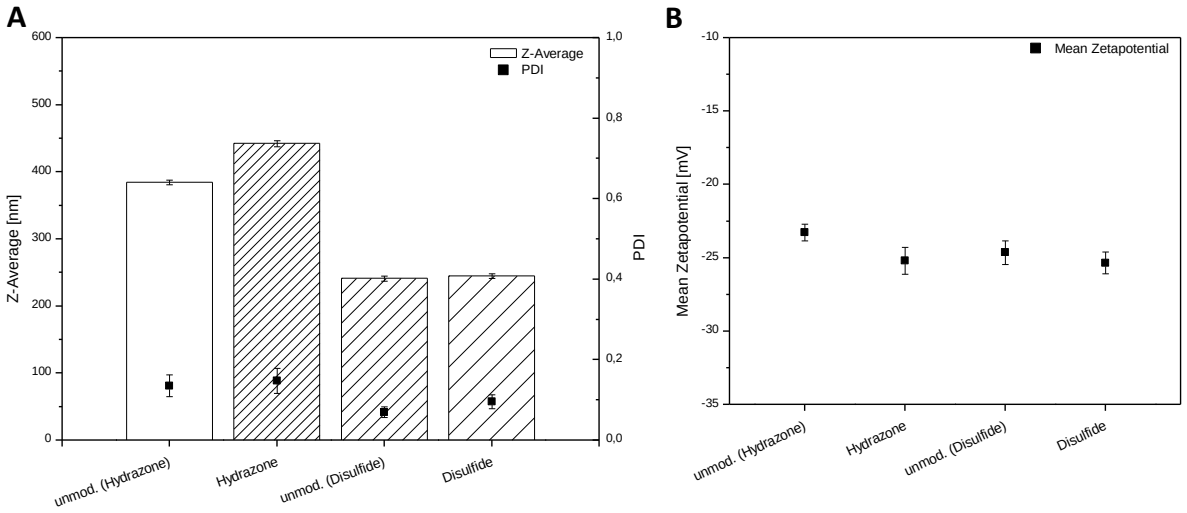

Figure IV-4: Properties of eADF4(C16)-SIINFEKL protein particles after coupling the peptide to pre-fabricated eADF4(C16) protein particles. The eADF4(C16)-SIINFEKL protein particles after coupling are compared to the respective unmodified particles.
A) Particle size given as the Z-average and the particle dispersity index (PDI) of eADF4(C16)-SIINFEKL particles.
B) Zeta potential of particles described in A).

While the particle size of the disulfide linked eADF4(C16)-SIINFEKL particles is identical to the unmodified particles used for the SPDP coupling, the particle size of the hydrazone linked particles increased again after coupling from 384 nm to 442 nm. On the contrary, the zeta potential was again in the same range for both SIINFEKL coupled and both unmodified eADF4(C16) protein particles.

The success of the chemical linkage of the SIINFEKL molecules to the spider silk carrier was evaluated as coupling efficiency (the fraction of SIINFEKL molecules that reacted with the activated spider silk protein in %). Coupling efficiency (CE) was determined by cleavage of the coupled SIINFEKL peptide from the eADF4(C16) protein particles. Hydrochloric acid was added to a final concentration of 0.5 M for SIINFEKL release from the acid-sensitive hydrazone linked eADF4(C16) particles. The disulfide linkage between the eADF4(C16) protein and the SIINFEKL peptide was cleaved by the addition of a DTT stock solution added to a final concentration of 10 mM DTT. After incubation for 30 minutes, the supernatants were analyzed by RP-HPLC for the amount of released SIINFEKL peptide. Table IV-1 shows the results of the coupling efficiency determination after RP-HPLC analysis.

Table IV-1: Coupling efficiencies of the eADF4(C16)-SIINFEKL particles after cleavage of the SIINFEKL peptide from the eADF4(C16) protein particle and analysis by RP-HPLC.

Coupling conditions	Coupling efficiency (CE)	
	Hydrazone linkage	**Disulfide linkage**
Coupling in solution	42.0 - 80.3%	17.9 - 24.9%
Coupling to particles	15.3%*	78.9 - 98.9%

** Due to the low CE, coupling to particles using the hydrazone linker was performed n=1.*

According to the data in Table IV-1, coupling of SIINFEKL peptide to the eADF4(C16) protein via the hydrazone linkage is more effective if the coupling process is conducted in solution. The coupling process in solution is favorable in the context of an endotoxin free particle preparation process, as the final eADF4(C16) protein solution can be filtered with an endotoxin depletion filter directly before the particle preparation. However, the CE of the disulfide coupling in solution is three times less effective than the coupling of the SIINFEKL peptide via disulfide linkage to pre-produced eADF4(C16) protein particles. Although the coupling in solution was favored due to above mentioned reasons, disulfide linkage to pre-produced eADF4(C16) protein particles was chosen for further activities due to the better CE.

Because chemically linked eADF4(C16)-SIINFEKL particles are a possible alternative for the eADF4(C16) hybrid protein particles containing a cathepsin cleavable linker sequence (see chapter 6), chemically linked eADF4(C16)-SIINFEKL particles were prepared for *in vitro* studies. The *in vitro* studies were planned to show the performance of the chemically linked eADF4(C16)-SIINFEKL particles compared to the eADF4(C16) hybrid protein particles in terms of cytotoxicity, immunogenicity and T cell activation. Figure IV-5 shows the particle size, the zeta potential and SEM micrographs of chemically linked eADF4(C16)-SIINFEKL particles used for *in vitro* studies.

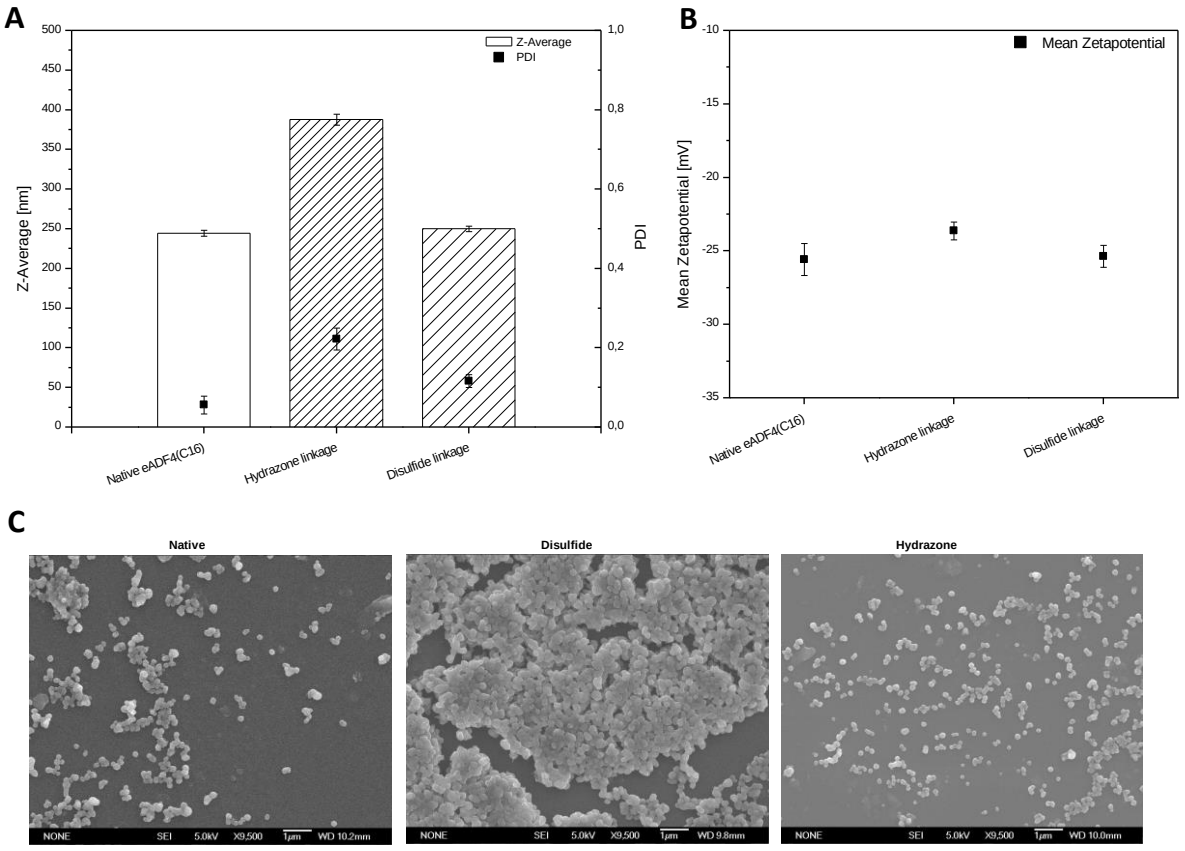

Figure IV-5: Properties of the eADF4(C16)-SIINFEKL protein particles prepared for *in vitro* studies.
A) Particle size given as the Z-average and the particle dispersity index (PDI) of eADF4(C16)-SIINFEKL particles prepared by hydrazone linkage or disulfide linkage. Native eADF4(C16) protein particles serve as control.
B) Zeta potential of particles described in A).
C) SEM micrographs of particles described in A) at a magnification of 9,500x. The particles were dried under vacuum and carbon sputtered before measurement.

Hydrazone linked eADF4(C16)-SIINFEKL particles were prepared by coupling in solution, resulting in a final particle size of 387.8 nm. A particle size of 249.8 nm resulted from the coupling of pre-produced particles by disulfide linkage, which is close to the particle size of 244.5 nm of the native eADF4(C16) protein control particles (Figure IV-5 A). The zeta potential of the three particle types was in the same range (Figure IV-5 B). The hydrazone linked and the disulfide linked particles are shown in direct comparison to native eADF4(C16) protein control particles in the SEM micrographs in Figure IV-5 C. Except for the different particle size, there are no differences observable between the linked and unmodified control particles.

The particle batches shown in Figure IV-5 were sent to our cooperation partner Prof. Dr. Carole Bourquin at the University of Fribourg, Switzerland for further *in vitro* and *in vivo* tests. Inès Mottas performed *in vitro* pre-tests comparing the chemically linked eADF4(C16)-SIINFEKL particles with the eADF4(C16) hybrid protein particles containing the cathepsin S and cathepsin B cleavable linker sequences during October 2014 to November 2014. I did not participate in the investigation

of the following experiments. All *in vitro* results and graphs (Figure IV-6 and Figure IV-7) were compiled by Inès Mottas. She shared the data for discussion and conclusion of the current chapter.

Due to the fact that the hydrazone linked particles are not producible in the same size range like the other eADF4(C16) protein particles using the endotoxin free, all-aqueous preparation process, these particles were not used in further studies (see chapter 6 for *in vivo* experiments using particles with cathepsin cleavable linker). Additionally, the hydrazone linked eADF4(C16)-SIINFEKL particles showed an intrinsic immunogenicity, which was not seen for the eADF4(C16) hybrid protein particles (Figure IV-6).

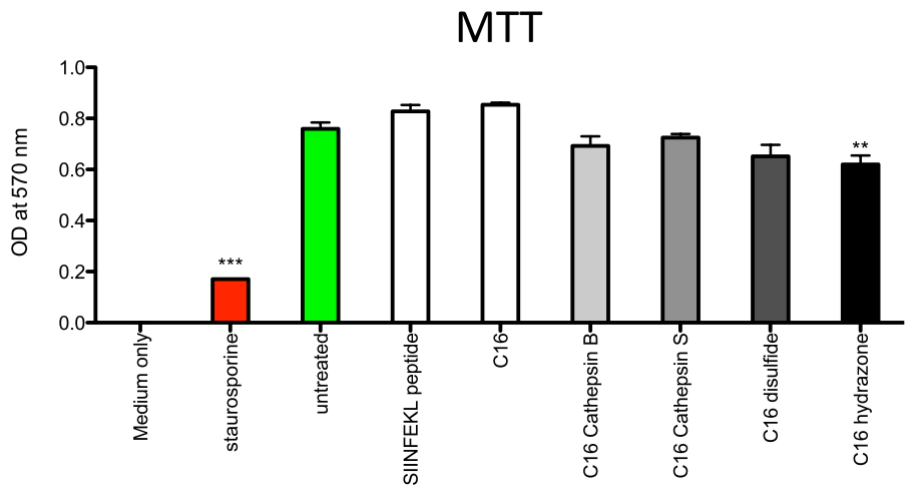

Figure IV-6: Cell viability assessed by the MTT assay following 24 hours exposure of different eADF4(C16) particles on J774 macrophages. Data are shown as % viability compared to the positive control and are presented as mean ± SD of three separate experiments. Asterisks (, P<0.01; ***, P<0.001) indicate significant differences between treated groups using two-way ANOVA followed by Tukey's multiple comparison test.**

Moreover, the hydrazone linked eADF4(C16)-SIINFEKL particles showed no antigen presentation on the major histocompatibility complex I (MHC-I) on dendritic cells (data not shown).

On the contrary, disulfide linked eADF4(C16)-SIINFEKL particles showed better results in the MTT test (Figure IV-6). However, the disulfide linked eADF4(C16)-SIINFEKL particles were unable to prime a T cell proliferation after 96 hours of incubation (Figure IV-7).

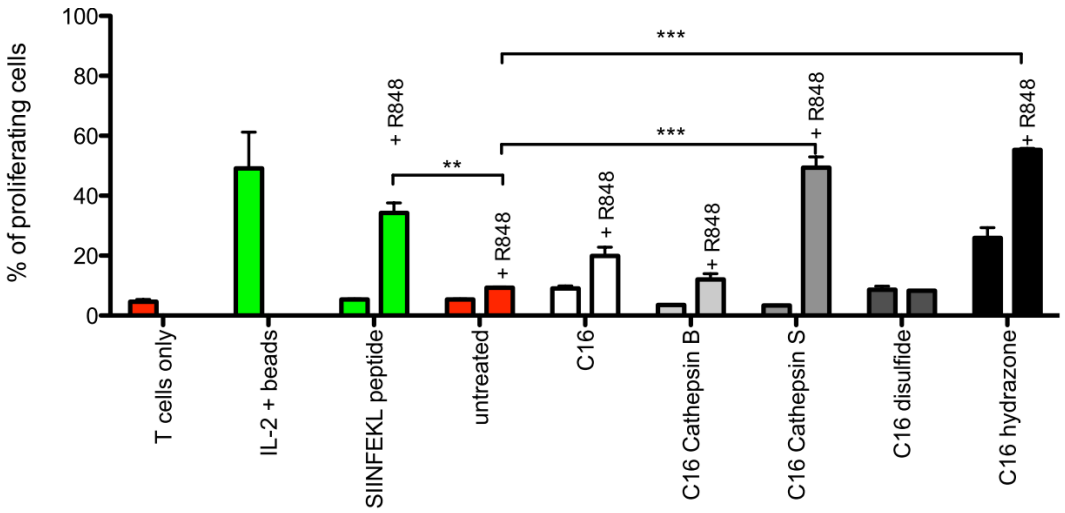

Figure IV-7: The disulfide linked eADF4(C16)-SIINFEKL particles are not effective to induce SIINFEKL-dependent *in vitro* T-cell proliferation. BMDC (5x10^4 ells /well) were cultured with spider silk particles at 50 µg NP/mL. R848 (0.25ug/mL) was used as adjuvant for BMDC activation. After 24 hours of incubation, CFSE-labelled CD3+CD8+ OT-I cells (10^5 cells /well) were added. After 3 days of co-culture, the cells were analyzed by flow cytometry. Percentage of proliferating cells within the T cell population (CD3+CD8+). Each bar represents mean ± SEM of 2 independent experiments performed in quadruplicate. Asterisks (, P<0.01; ***, P<0.001) indicate significant differences between R848-treated groups using two-way ANOVA followed by Tukey's multiple comparison test.**

4. Conclusion

The possibility to load the SIINFEKL antigen on eADF4(C16) protein particles using two different cleavable linkers was demonstrated in this study. It was shown, that the modification of the eADF4(C16) protein had no effect on the resulting particle size or zeta potential. However, the subsequent coupling of the chemically modified SIINFEKL-hydrazide peptide had an impact on the resulting particle size. Although coupling was evaluated with both the dissolved eADF4(C16) protein in solution and the pre-produced eADF4(C16) protein particles in suspension, the resulting particle size of the hydrazone linked particles was larger than the control particles. At the same time, the comparison of dissolved eADF4(C16) protein in solution and pre-produced eADF4(C16) protein particles in suspension revealed differences in the CE.

While the hydrazone linked eADF4(C16)-SIINFEKL particles displayed a higher CE in the dissolved state, the disulfide linkage had to be conducted to pre-produced eADF4(C16) protein particles in order to achieve an acceptable CE. Further studies might be able to optimize the coupling in solution with respect to different parameters like the conjugation buffer, temperature or time [36].

The *in vitro* results shared by Inès Mottas showed a poor performance of the chemically linked eADF4(C16)-SIINFEKL particles compared to the eADF4(C16) hybrid protein particles. Therefore,

we can support the statement of Wohlrab et al. to preferably use the genetically modified eADF4(C16) protein for further tests [37]. However, if the pH-sensitive or reductive cleavable character of a linker is of special interest, chemical coupling can be performed with the eADF4(C16) protein and the model peptide SIINFEKL.

5. References

[1] M. Q. Müller, F. Dreiocker, C. H. Ihling, M. Schäfer, and A. Sinz, "Cleavable Cross-Linker for Protein Structure Analysis: Reliable Identification of Cross-Linking Products by Tandem MS," *Anal. Chem.*, vol. 82, no. 16, pp. 6958–6968, 2010.

[2] D. Paramelle, G. Miralles, G. Subra, and J. Martinez, "Chemical cross-linkers for protein structure studies by mass spectrometry," *Proteomics*, vol. 13, no. 3–4, pp. 438–456, 2013.

[3] S. Fields and O. Song, "A novel genetic system to detect protein-protein interactions," *Nature*, vol. 340, no. 6230, pp. 245–246, 1989.

[4] A. Sinz, "Chemical cross-linking and mass spectrometry to map three-dimensional protein structures and protein–protein interactions," *Mass Spectrom. Rev.*, vol. 25, no. 4, pp. 663–682, 2006.

[5] F. Guillier, D. Orain, and M. Bradley, "Linkers and Cleavage Strategies in Solid-Phase Organic Synthesis and Combinatorial Chemistry," *Chem. Rev.*, vol. 100, no. 6, pp. 2091–2158, 2000.

[6] S. Bräse, "The Virtue of the Multifunctional Triazene Linkers in the Efficient Solid-Phase Synthesis of Heterocycle Libraries," *Acc. Chem. Res.*, vol. 37, no. 10, pp. 805–816, 2004.

[7] T. P. Sullivan and W. T. S. Huck, "Reactions on Monolayers: Organic Synthesis in Two Dimensions," *European J. Org. Chem.*, vol. 2003, no. 1, pp. 17–29, 2003.

[8] D. Filpula and H. Zhao, "Releasable PEGylation of proteins with customized linkers," *Adv. Drug Deliv. Rev.*, vol. 60, no. 1, pp. 29–49, 2008.

[9] F. M. Veronese and G. Pasut, "PEGylation, successful approach to drug delivery," *Drug Discov. Today*, vol. 10, no. 21, pp. 1451–1458, 2005.

[10] J. Neville, DM, K. Srinivasachar, R. Stone, and J. Scharff, "Enhancement of immunotoxin efficacy by acid-cleavable cross-linking agents utilizing diphtheria toxin and toxin mutants," *J. Biol. Chem.*, vol. 264, no. 25, pp. 14653–14661, 1989.

[11] J. A. McKenzie, R. L. Raison, and D. E. Rivett, "Development of a bifunctional crosslinking agent with potential for the preparation of immunotoxins," *J. Protein Chem.*, vol. 7, no. 5, pp. 581–592, 1988.

[12] E. Hébert, "Improvement of exogenous DNA nuclear importation by nuclear localization signal-bearing vectors: a promising way for non-viral gene therapy?," *Biol. Cell*, vol. 95, no. 2, pp. 59–68, 2003.

[13] K. M. Meisenheimer and T. H. Koch, "Photocross-Linking of Nucleic Acids to Associated Proteins," *Crit. Rev. Biochem. Mol. Biol.*, vol. 32, no. 2, pp. 101–140, 1997.

[14] E. S. Rector, R. J. Schwenk, K. S. Tse, and A. H. Sehon, "A method for the preparation of protein-protein conjugates of predetermined composition," *J. Immunol. Methods*, vol. 24, no. 3–4, pp. 321–336, 1978.

[15] S. J. McKenzie and J. F. Halsey, "Cholera toxin B subunit as a carrier protein to stimulate a mucosal immune response," *J. Immunol.*, vol. 133, no. 4, pp. 1818–1824, 1984.

[16] V. P. Torchilin and A. N. Lukyanov, "Peptide and protein drug delivery to and into tumors: challenges and solutions," *Drug Discov. Today*, vol. 8, no. 6, pp. 259–266, 2003.

[17] Y. Morimoto and S. Fujimoto, "Albumin microspheres as drug carriers," *Crit. Rev. Ther. Drug Carrier Syst.*, vol. 2, no. 1, pp. 19–63, 1985.

[18] R. S. Zolot, S. Basu, and R. P. Million, “Antibody–drug conjugates,” *Nat. Rev. Drug Discov.*, vol. 12, no. 4, pp. 259–260, 2013.

[19] K. J. Hamblett, “Effects of Drug Loading on the Antitumor Activity of a Monoclonal Antibody Drug Conjugate,” *Clin. Cancer Res.*, vol. 10, no. 20, pp. 7063–7070, 2004.

[20] B. Testa, “Prodrugs: bridging pharmacodynamic/pharmacokinetic gaps,” *Curr. Opin. Chem. Biol.*, vol. 13, no. 3, pp. 338–344, 2009.

[21] C. M. Dawidczyk, C. Kim, J. H. Park, L. M. Russell, K. H. Lee, M. G. Pomper, and P. C. Searson, “State-of-the-art in design rules for drug delivery platforms: Lessons learned from FDA-approved nanomedicines,” *J. Control. Release*, vol. 187, pp. 133–144, 2014.

[22] G. Leriche, L. Chisholm, and A. Wagner, “Cleavable linkers in chemical biology,” *Bioorg. Med. Chem.*, vol. 20, no. 2, pp. 571–582, 2012.

[23] J. Katz, J. E. Janik, and A. Younes, “Brentuximab Vedotin (SGN-35),” *Clin. Cancer Res.*, vol. 17, no. 20, pp. 6428–6436, 2011.

[24] J. Carlsson, H. Drevin, and R. Axén, “Protein thiolation and reversible protein-protein conjugation. N - Succinimidyl 3-(2-pyridyldithio)propionate, a new heterobifunctional reagent,” *Biochem. J.*, vol. 173, no. 3, pp. 723–737, 1978.

[25] B. J. Mills and C. A. Lang, “Differential distribution of free and bound glutathione and cyst(e)ine in human blood,” *Biochem. Pharmacol.*, vol. 52, no. 3, pp. 401–406, 1996.

[26] J. L. Mego, “Role of thiols, pH and cathepsin D in the lysosomal catabolism of serum albumin,” *Biochem. J.*, vol. 218, no. 3, pp. 775–783, 1984.

[27] K. Honey and A. Y. Rudensky, “Lysosomal cysteine proteases regulate antigen presentation,” *Nat. Rev. Immunol.*, vol. 3, no. 6, pp. 472–482, 2003.

[28] J. M. Timmerman, “Carrier protein conjugate vaccines: The ‘missing link’ to improved antibody and CTL responses?,” *Hum. Vaccin.*, vol. 5, no. 3, pp. 181–183, 2009.

[29] E. Roux, C. Passirani, S. Scheffold, J.-P. Benoit, and J.-C. Leroux, “Serum-stable and long-circulating, PEGylated, pH-sensitive liposomes,” *J. Control. Release*, vol. 94, no. 2–3, pp. 447–451, 2004.

[30] C. Fonseca, J. N. Moreira, C. J. Ciudad, M. C. Pedroso de Lima, and S. Simões, “Targeting of sterically stabilised pH-sensitive liposomes to human T-leukaemia cells,” *Eur. J. Pharm. Biopharm.*, vol. 59, no. 2, pp. 359–66, 2005.

[31] Y. J. Kwon, S. M. Standley, S. L. Goh, and J. M. J. Fréchet, “Enhanced antigen presentation and immunostimulation of dendritic cells using acid-degradable cationic nanoparticles,” *J. Control. Release*, vol. 105, no. 3, pp. 199–212, 2005.

[32] A. Potineni, D. M. Lynn, R. Langer, and M. M. Amiji, “Poly(ethylene oxide)-modified poly(β-amino ester) nanoparticles as a pH-sensitive biodegradable system for paclitaxel delivery,” *J. Control. Release*, vol. 86, no. 2–3, pp. 223–234, 2003.

[33] S. M. Standley, Y. J. Kwon, N. Murthy, J. Kunisawa, N. Shastri, S. J. Guillaudeu, L. Lau, and J. M. J. Fréchet, “Acid-Degradable Particles for Protein-Based Vaccines: Enhanced Survival Rate for Tumor-Challenged Mice Using Ovalbumin Model,” *Bioconjug. Chem.*, vol. 15, no. 6, pp. 1281–1288, 2004.

[34] M. Hofer, G. Winter, and J. Myschik, “Recombinant spider silk particles for controlled delivery of protein drugs,” *Biomaterials*, vol. 33, no. 5, pp. 1554–1562, 2012.

[35] C. Blüm and T. Scheibel, “Control of Drug Loading and Release Properties of Spider Silk Sub-Microparticles,” *Bionanoscience*, vol. 2, no. 2, pp. 67–74, 2012.

[36] J. Nicolas, S. Mura, D. Brambilla, N. Mackiewicz, and P. Couvreur, “Design, functionalization strategies and biomedical applications of targeted biodegradable/biocompatible polymer-based nanocarriers for drug delivery,” *Chem. Soc. Rev.*, vol. 42, no. 3, pp. 1147–1235, 2013.

[37] S. Wohlrab, S. Müller, A. Schmidt, S. Neubauer, H. Kessler, A. Leal-Egana, and T. Scheibel, “Cell adhesion and proliferation on RGD-modified recombinant spider silk proteins,” *Biomaterials*, vol. 33, no. 28, pp. 6650–6659, 2012.

V. Hybrid eADF4(C16) Protein Particles Designed for a Modern Vaccination Approach (First Generation)

1. Introduction

More than 90 years ago, Ramon discovered the immunostimulatory mode of action of several compounds on the antitoxin level of diphtheria and tetanus [1]. Since then, aluminum salts (alum) have been often used as immunostimulatory adjuvants in vaccine formulations [2]. Adjuvants are commonly required in several vaccine formulations to stimulate a sufficient immune response [3]. The need to artificially boost the innate immune system became more important with the introduction of the highly purified subunit vaccines [3]. These novel vaccines contain only parts of the whole microorganisms and display an increased safety profile, coming along with the lack of immunogenicity [4]. Alum has been the only approved immunostimulatory adjuvant on the market for a long time [5]. Meanwhile, only few adjuvants have been approved either in Europe and/or in the United States of America, which include MF59, AS03 and AF03 (all oil-in-water emulsions), virosomes and AS04 (monophosphoryl lipid A (MPL) in combination with alum) [6]. Due to the high safety requirements for adjuvants used for human administration, several potential adjuvants failed to show the required lack of toxicity for approval [7]. Additionally, alum is not suitable for use in frozen vaccine formulations and does not induce a cytotoxic T cell response, which is required for the immunization against intracellular pathogens [7]. In addition to the previously mentioned immunostimulatory adjuvants, another type of adjuvant has been described in literature. O'Hagan et al. differentiated adjuvants with only immunostimulatory effects (like MPL or CpG) to those acting as particulate delivery systems for antigens [8]. The class of particulate delivery systems includes micro- and nanoparticles, emulsions, immunostimulatory complexes (ISCOMs), virosomes and liposomes [9]. Using particulate delivery systems has advantages such as an improved antigen stabilization [10] or targeting specific immune cells, thereby enhancing the immune response [11]. MF59 (a squalene oil-in-water emulsion) was approved in Europe in 1997 and is one representative for particulate delivery systems [8]. The efficacy of particulate delivery systems has been reported in several publications and reviews [12–14]. Various polymers have already been used as carriers for antigens in several studies, demonstrating the ability to produce a safe and effective delivery system applicable for vaccination. In this manner, non-biodegradable particles consisting of gold [15] and

polystyrene [16] as well as biodegradable polymer particles consisting of alginate [17], chitosan [18], gelatin [19] and PLGA [20] have been used. The latter one offer the advantage of degradation over time within the body, thereby causing no problems in terms of regulatory aspects for the administration to humans [9]. The benefit of all particulate delivery systems is the possibility to be designed and adjusted for various tasks. The size and surface charge of polymer particles can be modified to achieve a targeted antigen delivery to APCs [10]. This approach also allows an activation of proliferating T cells which can be used for an anti-tumoral therapy [10]. Furthermore, nano- and microparticles can be loaded with antigen and immunostimulatory adjuvant for a co-administration to the same immune cells [9]. Besides simple mixing of the antigen with an adjuvant system, Oyewumi et al. described three methods for an antigen loading [21]. Adsorption of the antigen to the surface of the adjuvant is a relatively simple technique [21]. Aluminum based formulations adsorb antigens in a reversible manner, allowing the adjuvant to diffuse away after administration [3]. Encapsulation or entrapment into the polymer matrix during manufacturing is a second procedure for antigen loading [21]. Although this method can lead to antigen depots for a sustained release [22], the antigen is exposed to the harsh conditions commonly applied during particle preparation [9]. Moreover, the release of the antigen is dependent of the polymer matrix degradation [23]. In case of the PLGA based delivery systems, the acidic hydrolysis products can lead to a damage of the entrapped antigen [24]. The third described antigen loading method is chemical conjugation to the polymer [21]. For example, chemical linkage can be designed to obtain a desired, pH dependent release profile with an intracellular removal of the antigen [25]. Although the chemical conjugation is a feasible tool for the preparation of tunable vaccines, the risk of losing certain epitopes of the antigen during conjugation is high [21]. Furthermore, all mentioned loading methods require an additional step during or after particle preparation. We present in this study an alternative approach of an antigen loaded particle delivery system based on the recombinant spider silk protein eADF4(C16). The possibility to further modify recombinantly produced spider silk proteins has already been shown by several authors. Wohlrab et al. added the integrin recognition sequence RGD genetically to the eADF4(C16) spider silk protein to form a new hybrid protein [26]. The proliferation rate of attached fibroblasts was significantly improved by the addition of the RGD motif. Also, Gomes et al. formed a chimeric spider silk protein by the addition of an antimicrobial peptide sequence [27]. The antimicrobial activity of the added peptide sequences was demonstrated as well as the preservation of the spider silk's secondary structure, which is important for the material performance and the stability.

The aim of this study was to characterize the properties of an eADF4(C16)-antigen hybrid protein. We used the CD8 epitope of ovalbumin (OVA), $OVA_{257-264}$ (SIINFEKL), for future applicability of the system for vaccination. The peptide sequence of the used epitope was attached either on the C-terminal, the N-terminal or at the C- and N-terminal part of the native eADF4(C16) protein, resulting in three eADF4(C16) hybrid spider silk proteins. The influence of the added epitope on the particle forming behavior, the secondary structure and the thermal stability was assessed in this study. Additionally, cellular uptake studies were conducted with eADF4(C16) hybrid spider silk protein particles of low endotoxin level to examine their *in vitro* behavior. Some formulations containing eADF4(C16) hybrid protein particles of low endotoxin level were shipped to the group of Prof. Dr. Carole Bourquin at the University of Fribourg, Switzerland for further *in vitro* experiments, addressing the antigen presentation of dendritic cells.

2. Materials and methods

2.1. Materials

2.1.1. Recombinantly produced spider silk protein eADF4(C16) and engineered eADF4(C16) hybrid protein

The spray dried eADF4(C16) protein was provided by AMSilk GmbH (Martinsried, Germany). The properties of the native eADF4(C16) protein have been described earlier. The engineered eADF4(C16) hybrid proteins maintain the same basic framework of the module C protein like the native eADF4(C16) protein. In cooperation with the group of Prof. Dr. Carole Bourquin and the group of Prof. Dr. Thomas Scheibel, a model antigen from the egg white protein ovalbumin was selected. The CD8 epitope of OVA, $OVA_{257-264}$ (SIINFEKL), was fused to the eADF4(C16) protein framework for the vaccination studies. SIINFEKL has a molecular weight of 963 Da and is commonly used in vaccination studies [28, 29]. The SIINFEKL sequence was fused to the eADF4(C16) framework on the N-terminal, at the C-terminal and both at the N- and C-terminal (bi-terminal) end of the eADF4(C16) protein. The molecular weight did not change dramatically, as no T7-TAG was used for these hybrid proteins (first generation). The N-terminal hybrid protein has a molecular weight of 47,390 Da and the C-terminal hybrid protein has a molecular weight of 47,464 Da. Both proteins have a theoretical isoelectric point (pI) of 3.45. The bi-terminal hybrid protein displays a molecular weight of 48,898 and a pI of 3.62. The genetic modification of the spider silk proteins was realized at the group of Prof. Dr. Thomas Scheibel at the University of

Bayreuth. The production in *E. coli* and downstream processing was performed at AMSilk GmbH. The final protein was spray dried at the laboratories of AMSilk to a fairly free-flowing powder with a white color. An extinction coefficient of 46,400 $M^{-1}*cm^{-1}$ at 276 nm was used for the concentration determination by UV-Vis-spectroscopy.

2.1.2. Chemicals and reagents

Highly purified water (HPW) used for this study was generated by a purelab® device (ELGA LabWater, Celle, Germany). Sodium hydroxide solution (1 mol/L, EMPROVE® bio), di-potassium hydrogen phosphate (EMPROVE bio, European Pharmacopoeia (Ph. Eur.), British Pharmacopoeia (BP)), potassium dihydrogen phosphate (EMPROVE bio, Ph. Eur., BP, United States National Formulary (NF)) and fuming hydrochloric acid 37% (EMPROVE bio, Ph. Eur, BP, Japanese Pharmacopoeia (JP)) were purchased from Merck KGaA, Darmstadt, Germany. Ethanol 96% (v/v) and sodium chloride (NaCl, AnalaR NORMAPUR) were obtained from VWR Chemicals, Darmstadt, Germany. Tris(hydroxymethyl)aminomethane (Tris, Trizma® base, purity ≥99.9%), Trizma® base (cell culture tested, ≥99.9%), Hoechst 33258 solution, fluorescein isothiocyanate (suitable for protein labeling) and 4% paraformaldehyde solution were purchased from Sigma Aldrich GmbH, Steinheim, Germany. Guanidinium thiocyanate (for molecular biology) and 4-(2-Hydroxyethyl)-1-piperazine-1-ethanesulfonic acid (HEPES, for molecular biology) were purchased from AppliChem GmbH, Darmstadt, Germany. Fetal bovine serum (FKS), L-Glutamine and Phosphate buffered saline (PBS) were purchased from Biochrom (Berlin, Germany). Penicillin/Streptomycin solution (100x) was obtained from PAA Laboratories (Pasching, Austria). Endotoxin cartridges (Endosafe-PTS® Cartridges PTS20005F, Sensitivity 0.005 EU/ml) were purchased from Charles River, Lyon, France.

2.2. Methods

2.2.1. Preparation of eADF4(C16) hybrid protein particles

The preparation of eADF4(C16) hybrid protein particles was performed using a preparation technique by a micromixing system established for the native eADF4(C16) described previously [30]. The eADF4(C16) hybrid protein powders were dissolved in a 6 M guanidinium thiocyanate solution and subsequently dialyzed against a 10 mM Tris/HCl solution at 2-8°C for 24 hours. A dialysis membrane with a molecular weight cut-off of 8000 Da (Spectrum Laboratories, Rancho Dominguez, USA) was used. After dialysis, the solution was centrifuged and filtered through a 0.2 µm polyethersulfone (PES) filter (VWR International, Radnor, USA). Concentrations of the

eADF4(C16) hybrid proteins in solution were determined by an Agilent 8453 UV-Vis spectrophotometer (Agilent, Waldbronn, Germany) using a molar extinction coefficient of eADF4(C16) hybrid protein at 276 nm (ε = 46,400 $M^{-1}*cm^{-1}$). This solution was further adjusted to concentrations between 0.5-1.0 mg/ml for particle preparation with a filtered 10 mM Tris/HCl solution. Both cylinders of the syringe pump system (Model 100 DX and Series D pump controller, Teledyne Isco, Lincoln, USA) were filled with pre-tempered eADF4(C16) solution and pre-tempered 2 M potassium phosphate solution of 60 - 80°C. The syringe pump cylinders were jacketed by a bath circulator SC100-A10 (Thermo Scientific, Karlsruhe, Germany) which was tempered at 60 - 80°C. The solutions were pumped at a high flow rate of 50 ml/min to a T-shape mixing element (inner diameter 0.5 mm, P-727 PEEK tee, Upchurch Scientific, Oak Harbor, USA) leading to an outlet tubing (inner diameter 0.5 mm, 1532 PEEK Tubing, Upchurch Scientific, Oak Harbor, USA) for suspension collection. The eADF4(C16) hybrid protein particle suspensions were subsequently centrifuged at 14,000 rpm (SIGMA 4K15, Sigma Laborzentrifugen, Osterode am Harz, Germany) and washed with HPW three times. A two minute ultrasonication (Sonopuls HD 3200, Bandelin electronic, Berlin, Germany) step completed the particle preparation procedure. Particle concentrations in mg/ml were determined gravimetrically after drying the particles under vacuum (13 mbar) overnight.

2.2.2. Preparation of endotoxin depleted eADF4(C16) hybrid protein particles for *in vitro* studies

The particle preparation process described before was slightly adjusted for endotoxin depleted particles. Endotoxin depletion aimed for final endotoxin values below the detection limit of the assay, which was 0.1-0.2 EU/mg, depending on the necessary dilution steps. The eADF4(C16) hybrid protein powder was suspended with HPW in a glass vial (DIN 10R), closed with a rubber stopper and crimped with an aluminum cap. Steam sterilization was performed for 15 minutes at 121°C in a GTA 50 autoclave (Fritz Gössner, Hamburg, Germany). After cooling down, the eADF4(C16) hybrid protein suspension was centrifuged at 10,000 rpm (SIGMA 4K15, Sigma Laborzentrifugen, Osterode am Harz, Germany) for 30 minutes and the supernatant discarded. The centrifuged eADF4(C16) hybrid protein was dissolved in a 6 M guanidinium thiocyanate solution and dialyzed against an endotoxin free 10 mM TRIS/HCl solution pH 8.0 for 24 hours. After dialysis, the eADF4(C16) hybrid protein solution was filtered with a 0.2 µm PES filter (VWR International, Radnor, USA) and adjusted to a concentration of 2 mg/ml with an endotoxin free 10 mM TRIS/HCl buffer pH 8.0. Concentrations of the eADF4(C16) hybrid proteins in solution were determined by an Agilent 8453 UV-Vis spectrophotometer (Agilent, Waldbronn, Germany) using

a molar extinction coefficient of eADF4(C16) hybrid protein at 276 nm (ε = 46,400 $M^{-1}*cm^{-1}$). Subsequently, the eADF4(C16) hybrid protein solution was filtered with a pre-flushed Mustang® E filter (Pall GmbH, Dreieich, Germany). About 500 µl of each batch were discarded at the beginning. The protein concentration of the filtered eADF4(C16) solution was calculated photometrically at 276 nm (Agilent 8453 UV-Vis spectrophotometer, Agilent, Waldbronn, Germany). Endotoxin values were tested using the Endosafe®-PTS reader after a 20- to 40-fold dilution with HPW. This eADF4(C16) hybrid protein solution was further adjusted to a concentration of 1.0 mg/ml for particle preparation with an endotoxin free 10 mM Tris/HCl solution pH 8.0. Both cylinders of the syringe pump system and the Sonopuls HD 3200 sonotrode were depyrogenized by 70% (v/v) ethanol over 48 hours prior to particle preparation. The protein concentration for the particle preparation was 1 mg/ml and preparation temperature was 80°C. All other parameters were identical with the particle preparation for regular eADF4(C16) hybrid protein particles described before.

2.2.3. Fluorescent labelling

Labelling of eADF4(C16) protein with fluorescein isothiocyanate (FITC) was performed based on the published method by Spieß et al [31] using the terminal amine group of eADF4(C16). The eADF4(C16) protein powder was autoclaved as described before. After steam sterilization, the autoclaved eADF4(C16) powder was dissolved in a 6 M guanidinium thiocyanate solution but dialyzed against an endotoxin free 20 mM HEPES solution pH 8.0 at 2-8°C for 24 hours. After dialysis, centrifugation and filtration, the solution was adjusted to a concentration of 2.0 mg/ml with endotoxin free 20 mM HEPES solution pH 8.0 for coupling in solution. A 20-fold molar excess of FITC (dissolved in DMSO) was added slowly to the eADF4(C16) solution. After addition of FITC, the solution was incubated in the dark for three hours. After incubation, the FITC coupled eADF4(C16) protein solution was filtered first with a 0.2 µm PES filter (VWR International, Radnor, USA) and subsequently filtered with a pre-flushed Mustang® E filter (Pall GmbH, Dreieich, Germany). The filtered FITC coupled eADF4(C16) protein solution was adjusted to a protein concentration of 1 mg/ml for particle preparation by the syringe pump system at a temperature of 80°C. All other parameters were identical with the previously described particle preparation process.

2.2.4. Uptake of eADF4(C16) particles into macrophages

The uptake of eADF4(C16) particles in J774.A1 macrophages was analyzed with endotoxin depleted fluorescently labeled particles. The murine macrophages cell line J774.A1 was obtained

from the German collection of Microorganisms and Cell Cultures, Heidelberg. J774.A1 macrophages were seeded out at $1.5x10^6$ cells / 75 cm² in cell culture flasks (Becton-Dickinson, Heidelberg, Germany) and cultivated for 3 days (37°C, 5% CO_2) in Dulbecco's Modified Eagle's Medium (DMEM) with 10% (v/v) heat-inactivated fetal bovine serum (FBS), penicillin 100 I.U./ml and streptomycin 100 µg/ml. Cells were harvested at $4.5x10^7$ cells / 75 cm² by addition of 3 ml TRIS/HCl buffer and gently tapping the culture flask against a table to detach cells. The cells were centrifuged (1,000 rpm, 10 minutes) and washed with DMEM three times. 280 µl of this J774.A1 macrophages cell suspension was seeded at a concentration of $6x10^5$ cells/ml in DMEM with 10% (v/v) heat-inactivated FBS, penicillin 100 I.U./ml and streptomycin 100 µg/ml. After 4 hours incubation in 8-well IBIDI µ-slides (IBIDI, Martinsried, Germany), 20 µl of a either a 1 or 2 mg/ml eADF4(C16) particle suspension was added in triplicate to the cells. The cells were incubated with the eADF4(C16) particles for 45 minutes at 37° or on ice after homogenization by pipetting up and down. A negative control using 20 µl highly purified water without eADF4(C16) particles was added in parallel to the cells. The particle/cell suspension was washed three times with phosphate buffered saline (PBS) and fixed with 4% paraformaldehyde. A cell core staining was applied using Hoechst 33258 solution (Sigma-Aldrich, Steinheim, Germany) for 15 minutes.

2.3. Analytical methods

2.3.1. Endotoxin testing

The endotoxin values of eADF4(C16) hybrid protein solutions and particles used for the *in vitro* studies were determined as described in chapter 2.

2.3.2. Dynamic light scattering (DLS)

Particle size and size distribution of submicroparticles were measured as described in chapter 2.

2.3.3. Zeta potential

The zeta potential of eADF(C16) particles was measured as described in chapter 2.

2.3.4. Scanning electron microscopy (SEM)

SEM measurements of eADF4(C16) particle suspensions were conducted as described in chapter 2.

2.3.5. Differential Scanning Calorimetry (DSC)

DSC measurements were performed as described in chapter 2.

2.3.6. Protein secondary structure

Protein secondary structure of untreated eADF4(C16) submicroparticles was determined as described in chapter 2.

2.3.7. Flow cytometry

A BD Biosciences FACS Canto II (BD Biosciences, Franklin Lakes, USA) equipped with forward scatter, side scatter and fluorescence detector was used for flow cytometry measurements. Fluorescently labeled eADF4(C16) particle uptake into J744.A1 macrophages was quantified with forward scatter (FSC) sensitivity of 174 volts and green fluorescence detector sensitivity of 385 volts. A triplicate of 10,000 events each was collected per group. Flow cytometry data was analyzed using the Diva (BD Biosciences) software using the mean fluorescence per cell.

2.3.8. Confocal Microscopy

The uptake and internalization of fluorescently labeled eADF4(C16) particles (extinction 460/ emission 500) into macrophages was examined using a Zeiss LSM 510-NLO confocal microscope (Carl Zeiss Microscope systems, Jena, Germany) with identical setting for all groups. A Carl Zeiss 63x oil immersion objective was used for acquisition. Ultraviolet laser (364 nm), Argon laser (488 nm) and HeNe laser (543 nm) were used as excitation wavelengths, corresponding the emissions of band pass (BP) 385-470 nm, BP 505-530 nm and long pass (LP) 560 nm, respectively. Images were averaged 4 times and scan speed was set to 6. Experiments were performed in triplicate.

3. Results and Discussion

The aim of this study was the development and formulation of a novel antigen delivery system for vaccination. The spider silk protein was genetically modified by including a defined antigen sequence, the CD8 epitope of OVA SIINFEKL ($OVA_{257-264}$) either on the C-terminal, the N-terminal or at the C- and N-terminal (bi-terminal) part of the native eADF4(C16) protein. The addition of the epitope to the eADF4(C16) framework resulted in three different eADF4(C16) hybrid proteins, illustrated in Figure V-1.

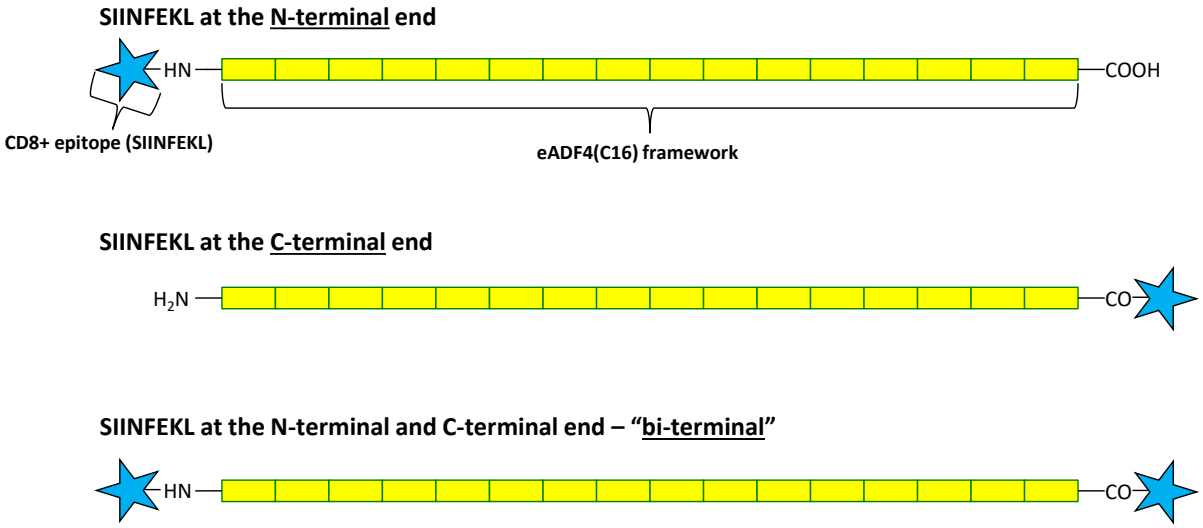

Figure V-1: Schematic illustration of the three eADF4(C16) hybrid proteins. The $OVA_{257-264}$ epitope (illustrated as blue star) was added on the C-terminal, the N-terminal or at the C- and N-terminal (bi-terminal) part of the native eADF4(C16) framework.

The addition of the SIINFEKL sequence resulted in a molecular weight of 47,390 Da for the N-terminal hybrid protein and 47,464 Da for the C-terminal hybrid protein. Both proteins have a theoretical isoelectric point (pI) of 3.45. The bi-terminal hybrid protein has a molecular weight of 48,898 and a theoretical pI of 3.62. In contrast to the native eADF4(C16) protein, no T7-TAG was used for all of the eADF4(C16) hybrid proteins.

Spider silk protein particles were prepared using the well-established micromixing device [30]. To assess the particle forming behavior after addition of the SIINFEKL sequence to the native eADF4(C16) framework, particles were prepared at two different temperatures and at two different protein concentrations. Figure V-2 shows the particle size, given as the Z-average value, and the polydispersity index (PDI) of fabricated eADF4(C16) hybrid protein particles. A clear trend towards smaller particles was visible when using elevated temperatures during particle preparation. Similarly, a decrease of protein concentration resulted in smaller particle sizes.

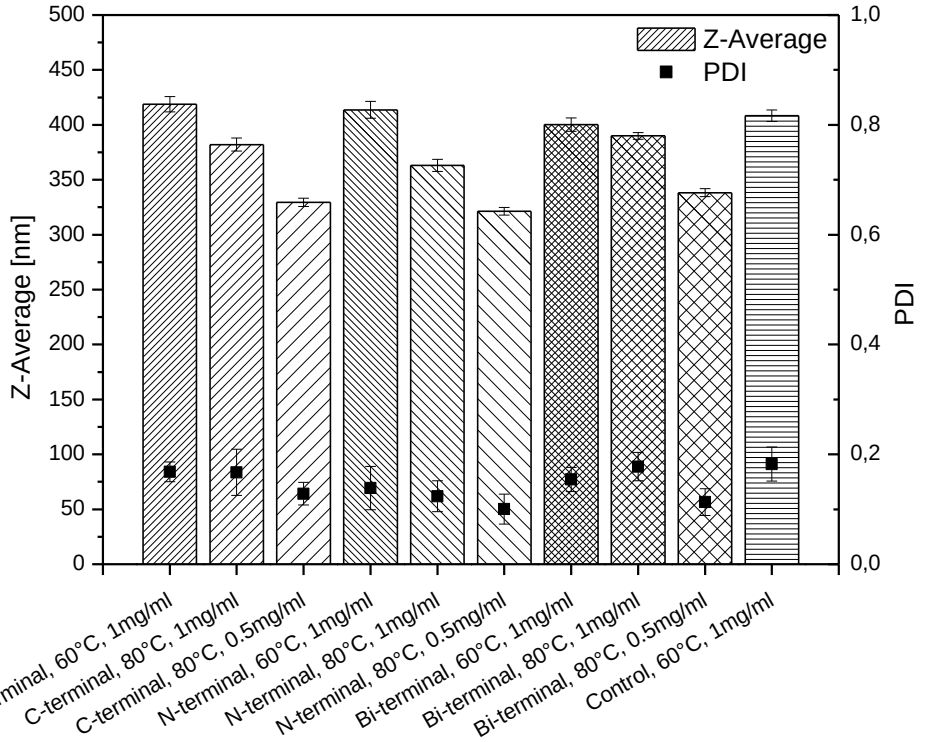

Figure V-2: Particle size of eADF4(C16) hybrid particles prepared at 60°C and 80°C and at protein concentrations of 1.0 mg/ml and 0.5 mg/ml, respectively. A clear trend towards smaller particles is visible for higher temperature and decreased eADF4(C16) protein concentration.

These results verify the outcome of previous experiments using the native eADF4(C16) protein, where an increase of the process temperature and decrease of the eADF4(C16) protein concentration led to the same trends [32]. Another important parameter for the particle stability in liquids is the zeta potential. Measurements with an artificial sodium chloride (NaCl) concentration of 19 mM resulted in values between -25 to -20 mV (Figure V-3). The results indicate good particle stabilization, as repulsion between the negatively charged particles hinders aggregation. Moreover, the results are also in good agreement with data of native eADF4(C16) protein particles prepared by Lammel et al. [33].

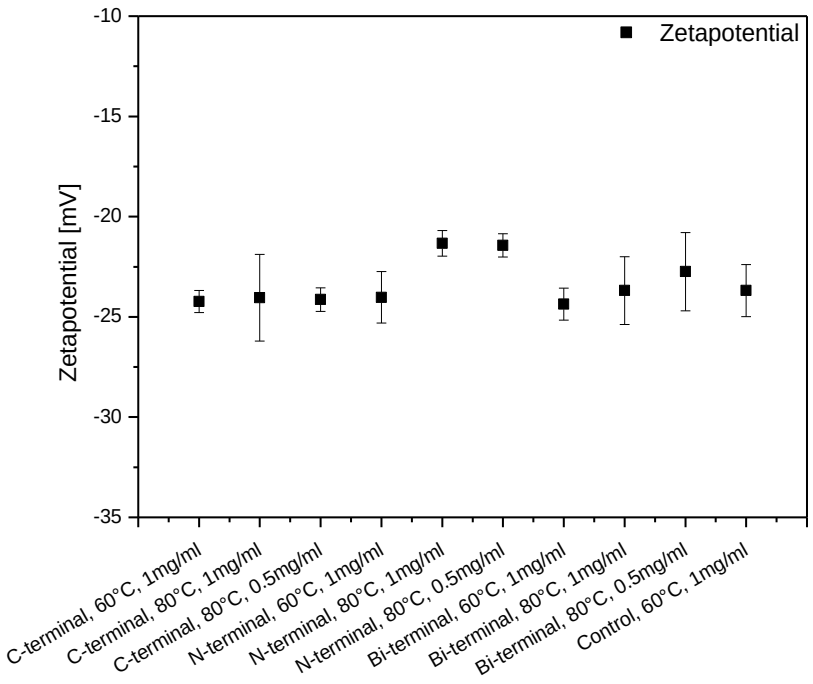

Figure V-3: Zeta potential of fabricated eADF4(C16) hybrid protein particles as a function of different processing parameters.

Taking the properties of the new eADF4(C16) hybrid protein particles together and comparing them with the native eADF4(C16) particle properties (Figure V-2 and Figure V-3), the addition of the SIINFEKL sequence did not seem to not influence the fabrication process or resulting particle properties. To determine further aspects of the antigen sequence addition, the proteins secondary structure was analyzed by FTIR measurements and the thermal stability of the fabricated particles was analyzed by DSC scans.

Figure V-4 shows the results of the FTIR measurements. The spectra of the amide I region between 1600 and 1700 cm^{-1} is displayed in the second derivative. Because the secondary structure of a protein is defined by the amino acid sequence of the primary structure, the integration of the SIINFEKL sequence could have led to an altered secondary structure. An altered secondary structure owns the risk to lead to severe dysfunctions, which was already shown for the Amyloid β-peptide years ago [34]. However, initial changes in protein secondary structure are sometimes negligible. Jastrzebska et al. investigated the influence of two different downstream purification methods on the properties of a spider silk protein [35]. Although they observed significant differences in the FTIR spectra of the soluble proteins, secondary structure after forming spider silk particles were highly similar. High secondary structure similarity was also detected for the here studied eADF4(C16) particles. The eADF4(C16) hybrid protein particles displayed the same high β-sheet rich structure as the native eADF4(C16) protein particles analyzed along as control (Figure

V-4). Neither the process parameters like temperature or protein concentration, nor the site of SIINFEKL addition to the eADF4(C16) protein had an influence on the proteins secondary structure. A high β-sheet content is important for the eADF4(C16) particle stability, as former studies with eADF4(C16) protein based films have shown that a random coil or helical conformation leads to water soluble forms [36].

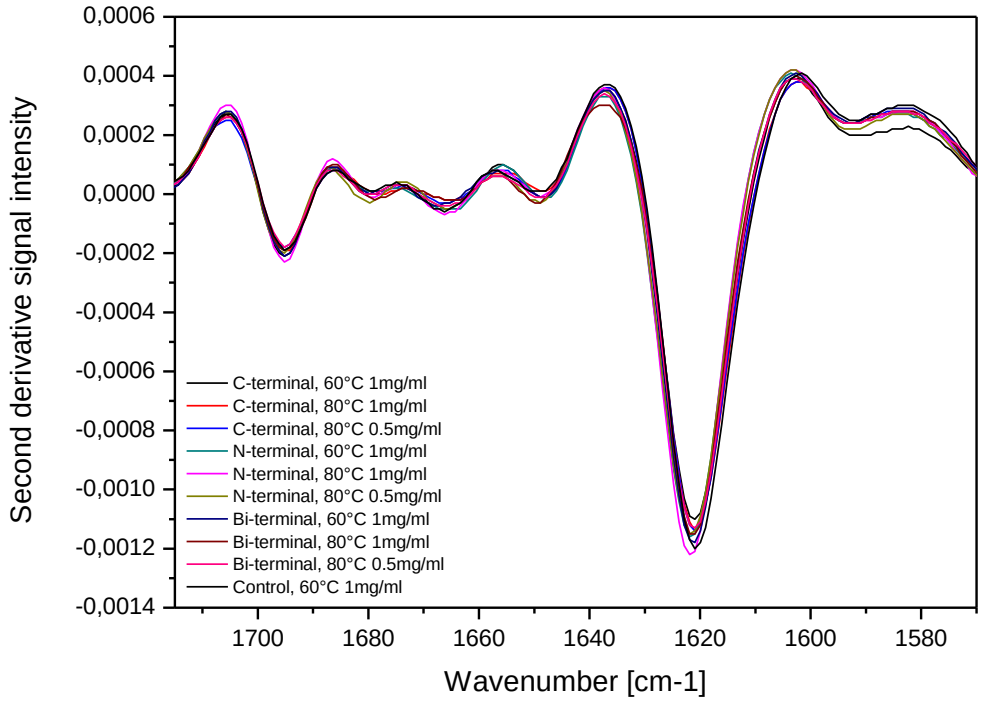

Figure V-4: Second derivative of the averaged FTIR spectra in the amide I region of eADF4(C16) hybrid protein particles prepared at 60°C and 80°C and at protein concentrations of 1.0 mg/ml and 0.5 mg/ml compared to native eADF4(C16) particles fabricated at 60°C and a protein concentration of 1 mg/ml as control. Data was analyzed with the Bruker OPUS software (version 6.5).

Figure V-5 shows the thermograms obtained by differential scanning calorimetry (DSC). The DSC measurements provided information about the stability of the eADF4(C16) hybrid protein particles at elevated temperature. A clearly definable marker in the DSC thermograms was the final degradation temperature of the eADF4(C16) particles. The analysis showed that the degradation temperature was in a narrow range between 320°C and 322.5°C for all analyzed particles. Once again, the modified eADF4(C16) hybrid protein particles did not show a distinguishable profile compared to the native eADF4(C16) protein particles used as control. Additionally, the degradation temperature of 320°C and 322.5°C is very high compared to the degradation temperature of below 300°C for films made with silk proteins from the silkworm *Bombyx mori* [37]. The previously published bimodal degradation behavior of eADF4(C16) material was also observable for the new eADF4(C16) hybrid protein particles [38]. The good temperature stability shows the unique properties of the eADF4(C16) protein. On the one hand, the proteinaceous

properties can be used for the introduction of the SIINFEKL sequence into the primary protein structure. On the other hand, the eADF4(C16) material is usable like a polymer, forming different morphologies including particles with adjustable properties and good stability.

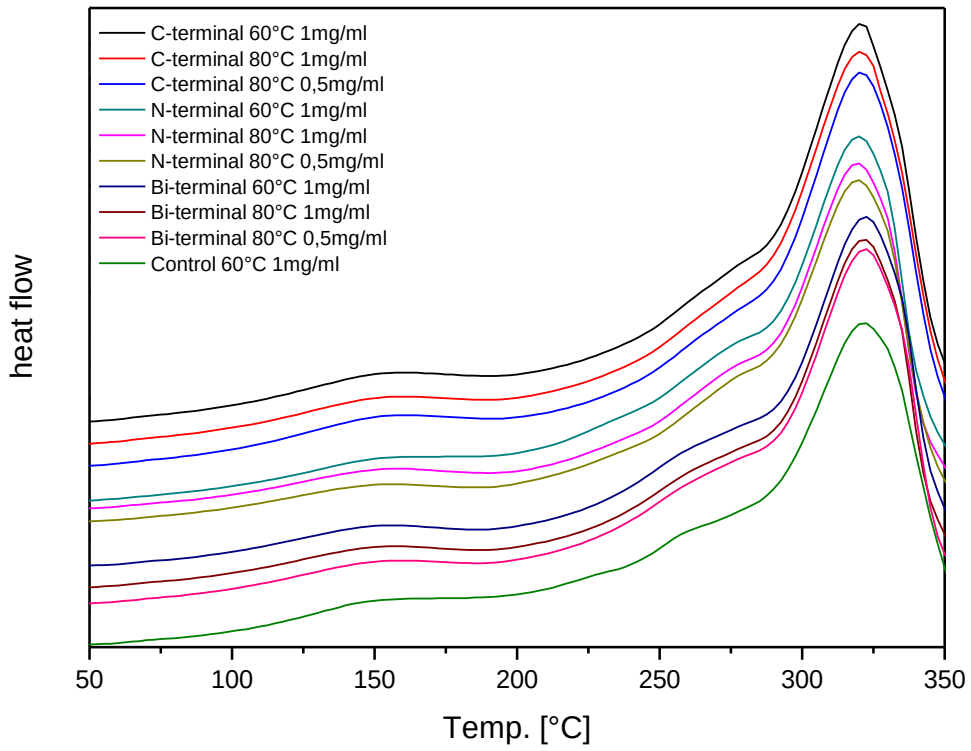

Figure V-5: DSC thermograms of eADF4(C16) hybrid protein particles prepared at 60°C and 80°C and at protein concentrations of 1.0 mg/ml and 0.5 mg/ml compared to native eADF4(C16) particles fabricated at 60°C and a protein concentration of 1 mg/ml as control. The graph shows the second heating ramp after the removal of residual water from the particles.

A visual examination of the eADF4(C16) hybrid protein particles was carried out using scanning electron microscopy (SEM). SEM micrographs of two different magnifications are shown in Figure V-6. The micrographs in Figure V-6 show round and uniform particles without visible damage. Due to the necessary drying step before the SEM measurements, the particles seemed to aggregate during the drying process. The particle size measured by DLS (Figure V-2), however, revealed separated particles in the liquid state. No differences of the shape or appearance between the different eADF4(C16) hybrid protein particles was observable in the micrographs. Additionally, the particle appearance of the eADF4(C16) hybrid protein particles was comparable to that of the native eADF4(C16) protein particles [33].

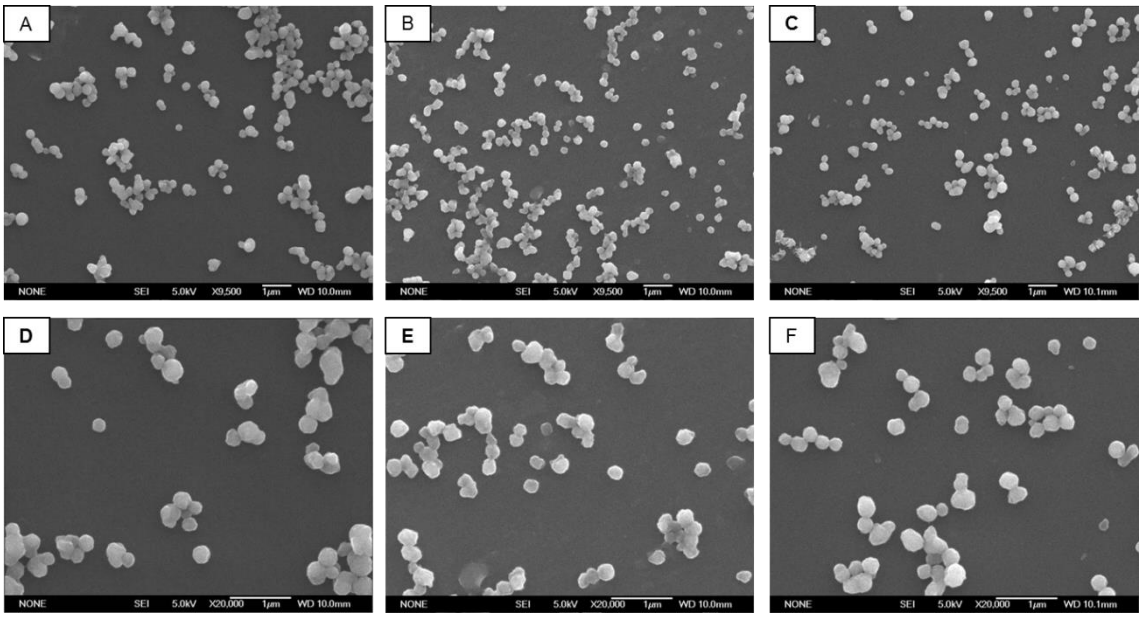

Figure V-6: SEM micrographs of eADF4(C16) hybrid particles. A-C at a magnification of 9,500x and D-E at a magnification of 20,000x. A+E: C-terminal eADF4(C16) hybrid particles. B+E: N-terminal eADF4(C16) hybrid particles. C+F: Bi-terminal eADF4(C16) hybrid particles. All particles were prepared at 80°C at a protein concentration of 1 mg/ml. The eADF4(C16) hybrid particles were dried under vacuum and carbon sputtered before measurement.

Taking these findings together, the newly designed eADF4(C16) hybrid protein particles displayed no differences to the native eADF4(C16) protein particles regarding particle size, zeta potential, protein secondary structure and thermal stability. To further evaluate the newly designed eADF4(C16) hybrid protein particles, uptake studies with J774.A1 macrophages to evaluate an active or passive internalization were carried out. Fluorescence labeling of the particles was a prerequisite for the particle detection after cellular uptake. We used an adopted coupling strategy from Spieß et al. to bind the fluorescence dye to the eADF4(C16) protein in solution [31]. Instead of the carboxy-fluorescein-succinimidylester used by Spieß et al., we labeled the eADF4(C16) proteins with fluorescein isothiocyanate (FITC). The resulting solutions were subsequently filtered with an endotoxin removal syringe filter to remove any endotoxins that may have formed during the labeling process. The fluorescein labeled proteins were formed to submicroparticles with the micromixing method and compared to non-labeled eADF4(C16) particles. The particle size, zeta potential, protein secondary structure and the endotoxin values of the eADF4(C16) native and hybrid protein particles, with and without FITC labeling, were analyzed before the start of the uptake studies. In Figure V-7, the results from the particle size and zeta potential measurements are illustrated. The results demonstrate, that the FITC labeling step prior to particle preparation had no influence on the resulting particle size and zeta potential of the native and hybrid eADF4(C16) protein particles. The addition of fluorescein to the eADF4(C16) proteins had no

influence on the overall particle charge, as the zeta potential of the labeled particles is at the same level as for the non-labeled particles. Moreover, we were able to produce four eADF4(C16) particle batches without FITC labeling and four batches eADF4(C16) particles with FITC labeling that were all in a very narrow size range (Figure V-7 A).

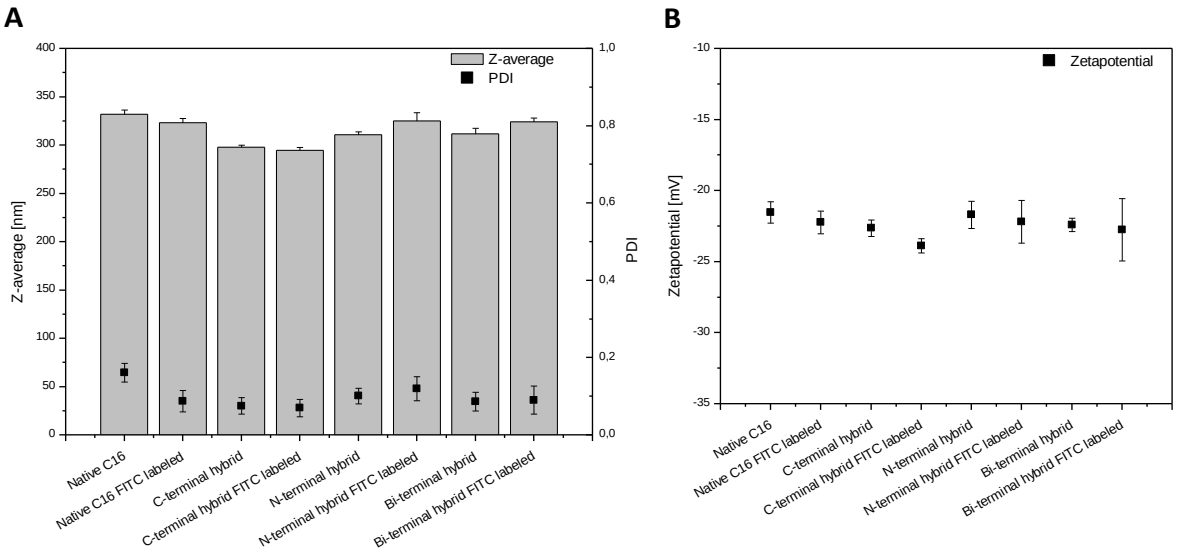

Figure V-7: eADF4(C16) particle properties. A) Particle size given as the Z-average value and the PDI of endotoxin depleted eADF4(C16) protein particles, with and without FITC labeling. B) Zetapotential of endotoxin depleted eADF4(C16) protein particles, with and without FITC labeling.

The narrow size range is a prerequisite for the comparability of the uptake studies in macrophages, because the particle size affects the extent of internalization into the cells [12]. In addition, the previously reported endotoxin depletion process, including autoclaving and endotoxin filtration, did not alter the particle size of the eADF4(C16) protein particles (see chapter 2).

Table V-1 shows the endotoxin values of the intermediate eADF4(C16) protein solutions after autoclaving and filtration. Three of the four tested eADF4(C16) solutions were below the detection limit of the assay after the necessary dilution with water. The fourth eADF4(C16) solution showed an endotoxin value of 0.665 EU/mg protein. The defined threshold of 5.0 EU/kilogram body weight by the FDA and EMA [39] would allow an application of 7.5 mg protein per kilogram body weight even with the highest endotoxin value of 0.665 EU/mg protein. The intermediate solutions were further processed to final eADF4(C16) submicroparticles by precipitation using the syringe pump system. All of the final eADF4(C16) particles displayed an endotoxin value below the detection limit of the test system, as the particle suspensions had to be diluted 200-fold with water in order to recover the spiked endotoxin in the two positive control channels. Thereafter, the final endotoxin depleted eADF4(C16) submicroparticles were characterized by FTIR analysis before starting the uptake experiments.

Table V-1:Endotoxin values of final eADF4(C16) particles and eADF4(C16) proteins in solution after applying the endotoxin depletion process.

Type	Endotoxin values of final eADF4(C16) particles	Endotoxin values of eADF4(C16) solutions after endotoxin filtration
Native eADF4(C16)	<1.00 EU/mg	<0.100 EU/mg
Native eADF4(C16) FITC labeled	<1.00 EU/mg	-
C-terminal hybrid	<1.08 EU/mg	0.665 EU/mg
C-terminal hybrid FITC labeled	<1.00 EU/mg	-
N-terminal hybrid	<1.00 EU/mg	<0.102 EU/mg
N-terminal hybrid FITC labeled	<1.00 EU/mg	-
Bi-terminal hybrid	<1.00 EU/mg	<0.102 EU/mg
Bi-terminal hybrid FITC labeled	<1.00 EU/mg	-

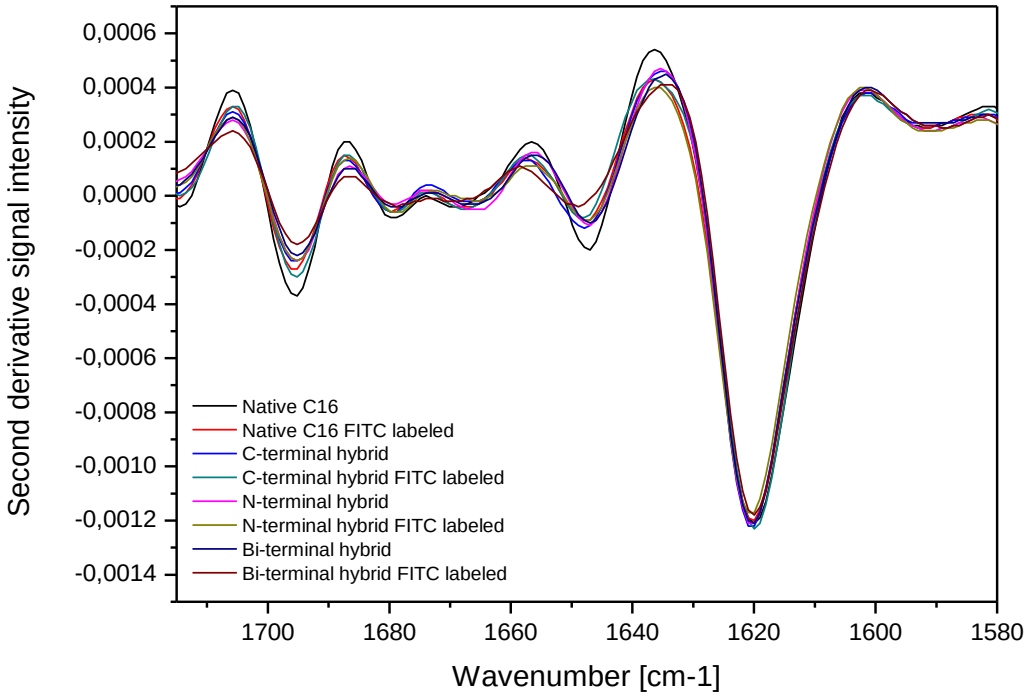

Figure V-8: Second derivative of the averaged FTIR spectra in the amide I region of native and hybrid eADF4(C16) protein particles with or without FITC labeling. Data was analyzed with the Bruker OPUS software (version 6.5).

Figure V-8 shows the spectra of native and hybrid eADF4(C16) protein particles in the amide I region between 1600 and 1700 cm^{-1} displayed in the second derivative. The FTIR analysis verifies the unchanged properties of the native and hybrid eADF4(C16) protein particles after FITC coupling. The analyzed particles prove a β-sheet rich structure, which was already observed for

the comparison of native and hybrid eADF4(C16) protein particles without endotoxin depletion and FITC coupling (Figure V-4).

The fabricated and characterized eADF4(C16) protein particles were used for uptake studies in J774.A1 macrophages. The aim of the uptake experiment was to characterize the possibility of eADF4(C16) particle uptake into macrophages and to assess the route of cellular uptake. Macrophages were chosen for this study, because they are a possible target for the eADF4(C16) hybrid protein particles designed for vaccination. The macrophages are specialized immune cells with a high phagocytosis activity [40]. Consequently, the internalization of fluorescently labeled eADF4(C16) protein particles was investigated by flow cytometry. The macrophages were incubated with fluorescently labeled eADF4(C16) protein particles at 37°C or 0°C for 45 minutes at two different particle concentrations. The incubation at 37°C reflects the regular cell metabolism environment of the cells, whereas the incubation at 0°C was chosen to neutralize any active uptake process.

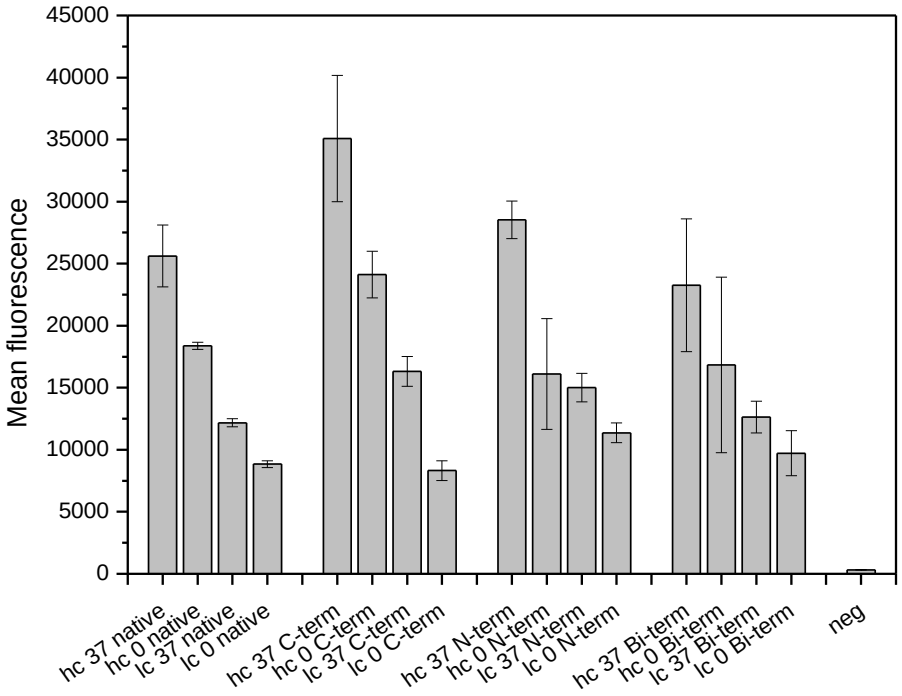

Figure V-9: Flow cytometry data of the mean fluorescence intensity of J774.A1 macrophages after incubation with eADF4(C16) particles at 37°C and 0°C. The first group of bars represent the results of incubation with native eADF4(C16) particles, the second group are C-terminal eADF4(C16) hybrid particles, the third group are N-terminal eADF4(C16) hybrid particles and the fourth group are Bi-terminal eADF4(C16) hybrid particles. All particles were tested at a high concentration (hc) of 2 mg/ml and at a low concentration (lc) of 1 mg/ml. Highly purified water served as negative control (neg).

The flow cytometry results in Figure V-9 clearly show differences between an active uptake mechanism at 37°C and a passive or non-specific uptake at 0°C. The results can only be compared

within one eADF4(C16) particle group, as the mean fluorescence intensity per particle was not determined prior to the uptake experiments. According to the data, the mean fluorescence intensity of the J774.A1 macrophages increased noticeable when the incubation took place at 37°C, although the effect is more pronounced for the higher particle concentration of 2 mg/ml. However, a significant fluorescence signal was still detectable even at the 0°C incubation groups, where no active uptake can take place. The CLSM images in Figure V-10 indicated that the particles are somehow attached to the macrophages outer cell membrane, which would explain the fluorescence signal of the 0°C incubation groups as seen in the flow cytometry results. Images E-H show the macrophages after incubation with eADF4(C16) protein particles at 0°C. The fluorescently labeled eADF4(C16) protein particles were located roundly-shaped around the cell membrane, whereas the particles were also located next to the inner cell nucleus after incubation at 37°C (images A-D). Due to the fact, that both, the outer cell membrane of the J774.A1 macrophages and the eADF4(C16) protein particles displayed a negative surface charge, the adhesion and internalization of the particles was better than expected. Previous studies have already shown that negatively charged particles are internalized in a much lower extent compared to positively charged particles in the same size range [41]. Due to the repulsive character of the two negative charges, it was unclear whether or not eADF4(C16) particles are taken up into the J774.A1 macrophages.

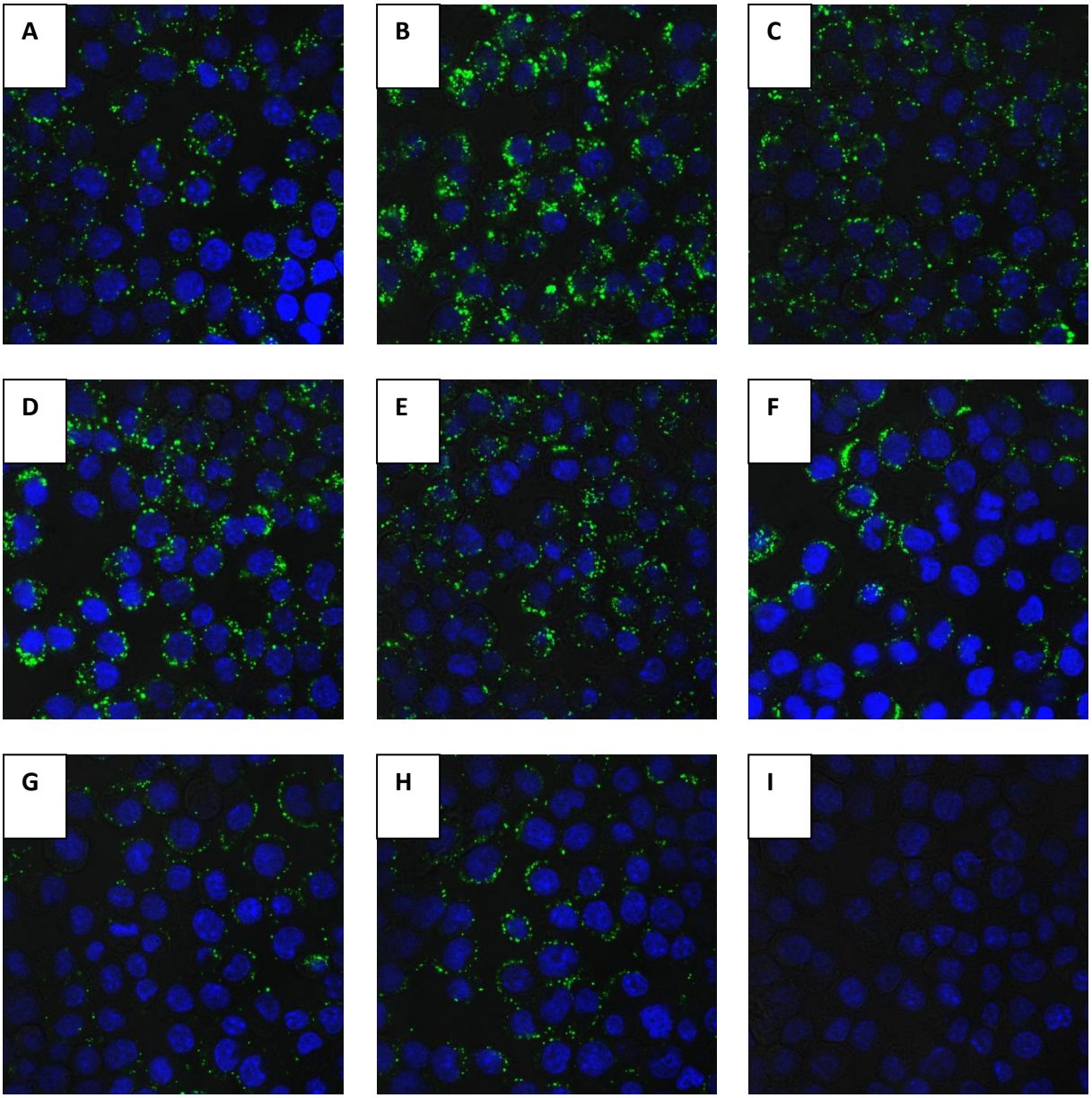

Figure V-10: Confocal laser scanning microscopy images of macrophages incubated with eADF4(C16) particles. Cell nucleus is stained with Hoechst 33258 (blue), eADF4(C16) particles are coupled with FITC (green). All images are showing the incubation of macrophages with the high particle concentration at 2 mg/ml. (A) Native eADF4(C16) particles at 37°C; (B) C-terminal hybrid particles at 37°C; (C) N-terminal hybrid particles at 37°C; (D) Bi-terminal hybrid particles at 37°C; (E) native particles on ice; (F) C-terminal hybrid particles on ice; (G) N-terminal hybrid particles on ice; (H) Bi-terminal hybrid particles on ice; (I) negative control.

The adhesive character of the eADF4(C16) particles to the outer cell membrane could raise a problem for the exact evaluation of internalized particles by flow cytometry analysis, but is favorable for the uptake itself. Gao et al. described the nanoparticle endocytosis as a two-stage process with a particle adhesion to the cell membrane followed by the internalization process into the cell [42]. As hydrophobic nanoparticles are internalized at a higher extent compared to

hydrophilic nanoparticles in the same size range [43], the driving force for the adhesion of the eADF4(C16) particles to the J774.A1 macrophages cell membrane is most likely the hydrophobicity of the eADF4(C16) material [44]. Staining of intracellular acidic organelles will prove the internalization and cellular processing of the eADF4(C16) particles.

The results presented in this chapter encouraged us to further test the *in vitro* properties of the eADF4(C16) hybrid protein particles intended for vaccination. We sent particles prepared for *in vitro* tests (properties see Figure V-7 and Figure V-8) to our cooperation partners Prof. Dr. Carole Bourquin and Dr. Tina Herbst (both at the University of Fribourg, Switzerland) for further *in vitro* tests.

All the following results and graphs were compiled by Dr. Tina Herbst during June to August 2013 using the eADF4(C16) hybrid protein particles described before. I did not participate in the investigation of the following experiments and use the shared results just for illustration and discussion of the eADF4(C16) hybrid protein particle performance.

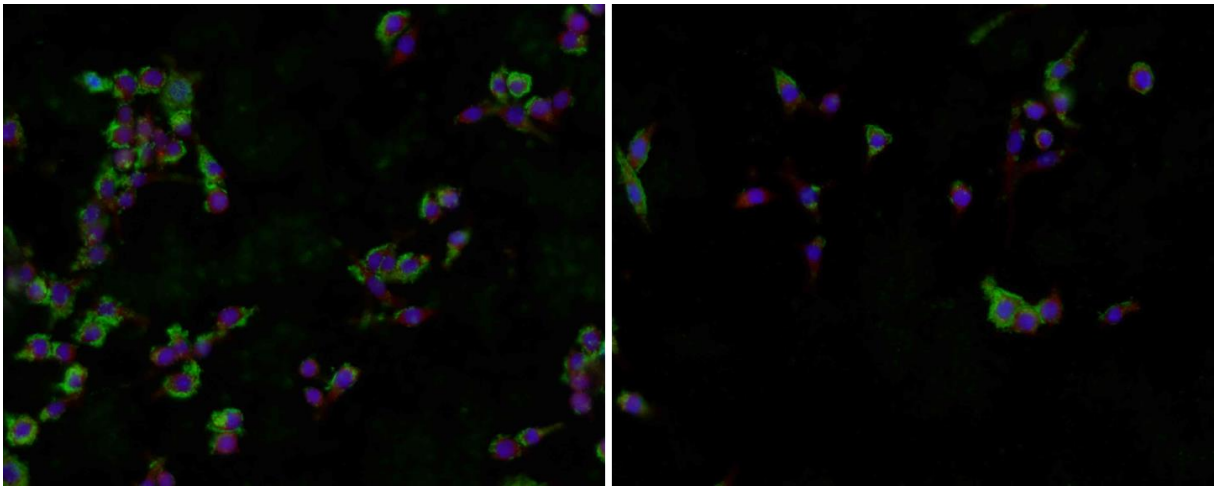

Figure V-11: Confocal laser scanning microscopy images of macrophages incubated with FITC labeled eADF4(C16) hybrid protein particles for 2 hours. Cell nucleus is stained with DAPI (blue), eADF4(C16) hybrid protein particles are coupled with FITC (green), LysoTracker® (red).

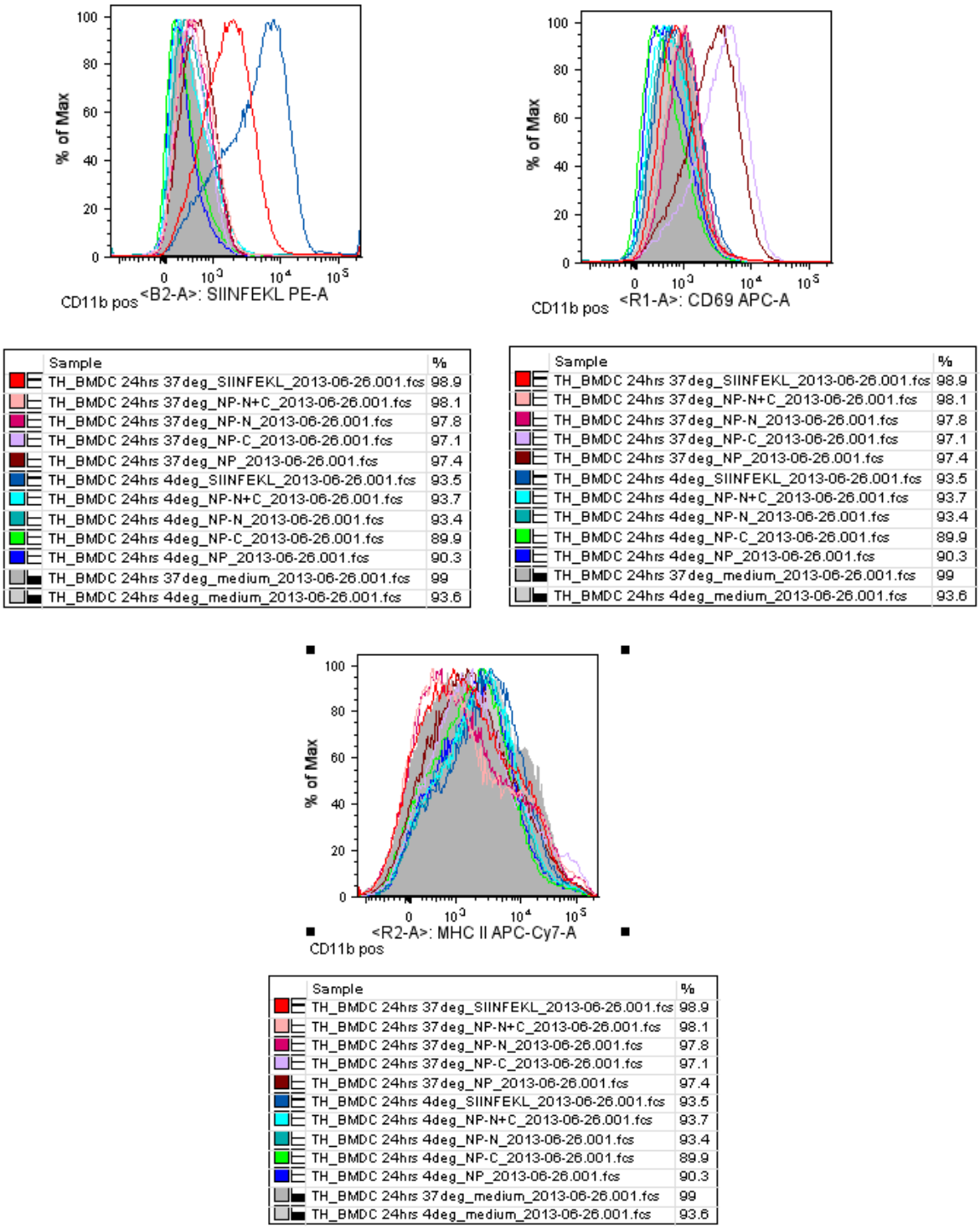

Figure V-12: Flow cytometry results of Bone Marrow-derived Dendritic Cells (BMDC) incubated for 24 hours with native and hybrid eADF4(C16) protein particles and SIINFEKL peptide as control.
(A) Histogram of the experiment with phycoerythrin-A (PE-A) labeled anti-SIINFEKL antibody for the detection of the CD8 epitope $OVA_{257-264}$ SIINFEKL.
(B) Histogram of immunogenicity detection by evaluation of the CD69 upregulation.
(C) Histogram of the experiment detecting the major histocompatibility complex class II (MHC II).

Figure V-11 again shows that eADF4(C16) hybrid protein particles were successfully taken up by macrophages. The used LysoTracker® probe gives the additional confirmation that the eADF4(C16)

particles are processed by the macrophages and end up in the acidic organelles of the cell like endosomes or lysosomes [45]. While lysosomes usually degrade cell's own as well as foreign substances in an acidic pH environment [46], lysosomal uptake can be favorable for a vaccination approach [47]. As the CD8 epitope SIINFEKL has to be cleaved from the native eADF4(C16) sequence, the uptake of the eADF4(C16) hybrid protein particles into endosomal or lysosomal compartments was a success. On the contrary, the results in Figure V-12 A clearly show that the SIINFEKL sequence was not recognized when bound to the eADF4(C16) hybrid protein particles. This fact alone would not be insufficient for the hybrid design, but Figure V-12 C clearly shows that no antigen presentation of eADF4(C16) hybrid protein particles took place. The antigen processing from the eADF4(C16) hybrid protein particles might be impaired, because the SIINFEKL sequence was not cleaved from the native eADF4(C16) sequence.

4. Conclusion

We prepared eADF4(C16) hybrid protein particles in the submicron range containing the CD8 epitope $OVA_{257-264}$ SIINFEKL. Our results demonstrate that the final particle size is adjustable by variations in temperature and protein concentration, resulting in uniform particles with high β-sheet content and a consistent degradation temperature. The newly designed eADF4(C16) hybrid protein particles were compared to the native eADF4(C16) protein particles and no changes of the investigated particle properties have been detected. The previously developed endotoxin depletion method was successfully utilized for the preparation of the eADF4(C16) hybrid protein particles. Coupling of a fluorescence dye to the eADF4(C16) protein was performed as prerequisite for the detection after cellular uptake *in vitro*. The particle preparation method using a micromixing unit was finally designed to result in four non-FITC labeled and four FITC-labeled particle batches of equal size and low endotoxin content, which were used for *in vitro* experiments. The results of the *in vitro* experiments pointed into the direction, that eADF4(C16) particles were actively internalized into macrophages and processed to endosomal or lysosomal compartments. Although the eADF4(C16) hybrid protein particles were taken up by macrophages, no antigen presentation took place. Therefore, the epitope on the eADF4(C16) hybrid protein particles was either sterically hidden inside the particle matrix or the epitope was generally recognized, but cleavage of the epitope from the eADF4(C16) sequence was impossible. Based on these findings, adjustments of the hybrid design were performed. Because eADF4(C16) particles successfully demonstrated the ability to deliver the antigen into the antigen presenting cells,

enzymatically cleavable linkers were used for the second generation eADF4(C16) hybrid proteins to facilitate the epitope cleavage from the eADF4(C16) sequence (see chapter 6).

5. References

[1] R. Edelman, "Vaccine Adjuvants," *Clin. Infect. Dis.*, vol. 2, no. 3, pp. 370–383, 1980.

[2] E. B. Lindblad, "Aluminium compounds for use in vaccines," *Immunol. Cell Biol.*, vol. 82, no. 5, pp. 497–505, 2004.

[3] E. De Gregorio, E. Caproni, and J. B. Ulmer, "Vaccine Adjuvants: Mode of Action," *Front. Immunol.*, vol. 4, p. 214, 2013.

[4] P. M. Moyle and I. Toth, "Modern Subunit Vaccines: Development, Components, and Research Opportunities," *ChemMedChem*, vol. 8, no. 3, pp. 360–376, 2013.

[5] D. T. O'Hagan, G. S. Ott, G. Van Nest, R. Rappuoli, and G. Del Giudice, "The history of MF59 ® adjuvant: a phoenix that arose from the ashes," *Expert Rev. Vaccines*, vol. 12, no. 1, pp. 13–30, 2013.

[6] S. G. Reed, M. T. Orr, and C. B. Fox, "Key roles of adjuvants in modern vaccines," *Nat. Med.*, vol. 19, no. 12, pp. 1597–1608, 2013.

[7] S. G. Reed, S. Bertholet, R. N. Coler, and M. Friede, "New horizons in adjuvants for vaccine development," *Trends Immunol.*, vol. 30, no. 1, pp. 23–32, 2009.

[8] D. T. O'Hagan and M. Singh, "Microparticles as vaccine adjuvants and delivery systems," *Expert Rev. Vaccines*, vol. 2, no. 2, pp. 269–283, 2003.

[9] M. Singh, A. Chakrapani, and D. O'Hagan, "Nanoparticles and microparticles as vaccine-delivery systems," *Expert Rev. Vaccines*, vol. 6, no. 5, pp. 797–808, 2007.

[10] Y. Fan and J. Moon, "Nanoparticle Drug Delivery Systems Designed to Improve Cancer Vaccines and Immunotherapy," *Vaccines*, vol. 3, no. 3, pp. 662–685, 2015.

[11] S. A. Agnihotri, N. N. Mallikarjuna, and T. M. Aminabhavi, "Recent advances on chitosan-based micro- and nanoparticles in drug delivery," *J. Control. Release*, vol. 100, no. 1, pp. 5–28, 2004.

[12] V. B. Joshi, S. M. Geary, and A. K. Salem, "Biodegradable Particles as Vaccine Delivery Systems: Size Matters," *AAPS J.*, vol. 15, no. 1, pp. 85–94, 2013.

[13] A. C. Rice-Ficht, A. M. Arenas-Gamboa, M. M. Kahl-McDonagh, and T. A. Ficht, "Polymeric particles in vaccine delivery," *Curr. Opin. Microbiol.*, vol. 13, no. 1, pp. 106–112, 2010.

[14] P. Sahdev, L. J. Ochyl, and J. J. Moon, "Biomaterials for Nanoparticle Vaccine Delivery Systems," *Pharm. Res.*, vol. 31, no. 10, pp. 2563–2582, 2014.

[15] K. Niikura, T. Matsunaga, T. Suzuki, S. Kobayashi, H. Yamaguchi, Y. Orba, A. Kawaguchi, H. Hasegawa, K. Kajino, T. Ninomiya, K. Ijiro, and H. Sawa, "Gold Nanoparticles as a Vaccine Platform: Influence of Size and Shape on Immunological Responses in Vitro and in Vivo," *ACS Nano*, vol. 7, no. 5, pp. 3926–3938, 2013.

[16] M. Kalkanidis, G. A. Pietersz, S. D. Xiang, P. L. Mottram, B. Crimeen-Irwin, K. Ardipradja, and M. Plebanski, "Methods for nano-particle based vaccine formulation and evaluation of their immunogenicity," *Methods*, vol. 40, no. 1, pp. 20–29, 2006.

[17] P. Li, Z. Luo, P. Liu, N. Gao, Y. Zhang, H. Pan, L. Liu, C. Wang, L. Cai, and Y. Ma, "Bioreducible alginate-poly(ethylenimine) nanogels as an antigen-delivery system robustly enhance vaccine-elicited humoral and cellular immune responses," *J. Control. Release*, vol. 168, no. 3, pp. 271–279, 2013.

[18] O. Borges, A. Cordeiro-da-Silva, J. Tavares, N. Santarém, A. de Sousa, G. Borchard, and H. E. Junginger, "Immune response by nasal delivery of hepatitis B surface antigen and codelivery of a CpG ODN in alginate coated chitosan nanoparticles," *Eur. J. Pharm. Biopharm.*, vol. 69, no. 2, pp. 405–416, 2008.

[19] K. Zwiorek, C. Bourquin, J. Battiany, G. Winter, S. Endres, G. Hartmann, and C. Coester, "Delivery by Cationic Gelatin Nanoparticles Strongly Increases the Immunostimulatory Effects of CpG Oligonucleotides," *Pharm. Res.*, vol. 25, no. 3, pp. 551–562, 2008.

[20] S. L. Demento, W. Cui, J. M. Criscione, E. Stern, J. Tulipan, S. M. Kaech, and T. M. Fahmy, "Role of sustained antigen release from nanoparticle vaccines in shaping the T cell memory phenotype," *Biomaterials*, vol. 33, no. 19, pp. 4957–4964, 2012.

[21] M. O. Oyewumi, A. Kumar, and Z. Cui, "Nano-microparticles as immune adjuvants: correlating particle sizes and the resultant immune responses," *Expert Rev. Vaccines*, vol. 9, no. 9, pp. 1095–1107, 2010.

[22] M.-L. De Temmerman, J. Rejman, J. Demeester, D. J. Irvine, B. Gander, and S. C. De Smedt, "Particulate vaccines: on the quest for optimal delivery and immune response," *Drug Discov. Today*, vol. 16, no. 13–14, pp. 569–582, 2011.

[23] L. Zhao, A. Seth, N. Wibowo, C.-X. Zhao, N. Mitter, C. Yu, and A. P. J. Middelberg, "Nanoparticle vaccines," *Vaccine*, vol. 32, no. 3, pp. 327–337, 2014.

[24] A. C. R. Grayson, M. J. Cima, and R. Langer, "Size and temperature effects on poly(lactic-co-glycolic acid) degradation and microreservoir device performance," *Biomaterials*, vol. 26, no. 14, pp. 2137–2145, 2005.

[25] G. F. Walker, C. Fella, J. Pelisek, J. Fahrmeir, S. Boeckle, M. Ogris, and E. Wagner, "Toward Synthetic Viruses: Endosomal pH-Triggered Deshielding of Targeted Polyplexes Greatly Enhances Gene Transfer in vitro and in vivo," *Mol. Ther.*, vol. 11, no. 3, pp. 418–425, 2005.

[26] S. Wohlrab, S. Müller, A. Schmidt, S. Neubauer, H. Kessler, A. Leal-Egana, and T. Scheibel, "Cell adhesion and proliferation on RGD-modified recombinant spider silk proteins," *Biomaterials*, vol. 33, no. 28, pp. 6650–6659, 2012.

[27] S. C. Gomes, I. B. Leonor, J. F. Mano, R. L. Reis, and D. L. Kaplan, "Antimicrobial functionalized genetically engineered spider silk," *Biomaterials*, vol. 32, no. 18, pp. 4255–4266, 2011.

[28] M. J. Estcourt, "Prime-boost immunization generates a high frequency, high-avidity CD8+ cytotoxic T lymphocyte population," *Int. Immunol.*, vol. 14, no. 1, pp. 31–37, 2002.

[29] M. L. Salem, S. A. EL-Naggar, A. Kadima, W. E. Gillanders, and D. J. Cole, "The adjuvant effects of the toll-like receptor 3 ligand polyinosinic-cytidylic acid poly (I:C) on antigen-specific CD8+ T cell responses are partially dependent on NK cells with the induction of a beneficial cytokine milieu," *Vaccine*, vol. 24, no. 24, pp. 5119–5132, 2006.

[30] M. Hofer, G. Winter, and J. Myschik, "Recombinant spider silk particles for controlled delivery of protein drugs," *Biomaterials*, vol. 33, no. 5, pp. 1554–1562, 2012.

[31] K. Spieß, S. Wohlrab, and T. Scheibel, "Structural characterization and functionalization of engineered spider silk films," *Soft Matter*, vol. 6, no. 17, pp. 4168–4174, 2010.

[32] M. Hofer, "Development of spider silk protein particles for pharmaceutical applications." Ludwig-Maximilians-Universität München, 04-Nov-2013.

[33] A. Lammel, M. Schwab, M. Hofer, G. Winter, and T. Scheibel, "Recombinant spider silk particles as drug delivery vehicles," *Biomaterials*, vol. 32, no. 8, pp. 2233–2240, 2011.

[34] L. Simmons, P. May, K. Tomaselli, R. Rydel, K. Fuson, E. Brigham, S. Wright, I. Lieberburg, G. Becker, and D. Brems, "Secondary structure of amyloid beta peptide correlates with neurotoxic activity in vitro," *Mol. Pharmacol.*, vol. 45, no. 3, pp. 373–379, 1994.

[35] K. Jastrzebska, E. Felcyn, M. Kozak, M. Szybowicz, T. Buchwald, Z. Pietralik, T. Jesionowski, A. Mackiewicz, and H. Dams-Kozlowska, "The method of purifying bioengineered spider silk determines the silk sphere properties," *Sci. Rep.*, vol. 6, no. 28106, 2016.

[36] K. Spiess, A. Lammel, and T. Scheibel, "Recombinant Spider Silk Proteins for Applications in Biomaterials," *Macromol. Biosci.*, vol. 10, no. 9, pp. 998–1007, 2010.

[37] A. Motta, L. Fambri, and C. Migliaresi, “Regenerated silk fibroin films: Thermal and dynamic mechanical analysis,” *Macromol. Chem. Phys.*, vol. 203, no. 10–11, pp. 1658–1665, 2002.

[38] K. Spiess, R. Ene, C. D. Keenan, J. Senker, F. Kremer, and T. Scheibel, “Impact of initial solvent on thermal stability and mechanical properties of recombinant spider silk films,” *J. Mater. Chem.*, vol. 21, no. 35, pp. 13594–13604, 2011.

[39] M. A. Vetten, C. S. Yah, T. Singh, and M. Gulumian, “Challenges facing sterilization and depyrogenation of nanoparticles: Effects on structural stability and biomedical applications,” *Nanomedicine Nanotechnology, Biol. Med.*, vol. 10, no. 7, pp. 1391–1399, 2014.

[40] A. Aderem and D. M. Underhill, “Mechanisms of phagocytosis in macrophages,” *Annu. Rev. Immunol.*, vol. 17, no. 1, pp. 593–623, 1999.

[41] L. Thiele, B. Rothen-Rutishauser, S. Jilek, H. Wunderli-Allenspach, H. P. Merkle, and E. Walter, “Evaluation of particle uptake in human blood monocyte-derived cells in vitro. Does phagocytosis activity of dendritic cells measure up with macrophages?,” *J Control Release*, vol. 76, no. 1–2, pp. 59–71, 2001.

[42] H. Gao, W. Shi, and L. B. Freund, “Mechanics of receptor-mediated endocytosis,” *Proc. Natl. Acad. Sci.*, vol. 102, no. 27, pp. 9469–9474, 2005.

[43] A. S. Zahr, C. A. Davis, and M. V Pishko, “Macrophage Uptake of Core−Shell Nanoparticles Surface Modified with Poly(ethylene glycol),” *Langmuir*, vol. 22, no. 19, pp. 8178–8185, 2006.

[44] A. S. Lammel, X. Hu, S.-H. Park, D. L. Kaplan, and T. R. Scheibel, “Controlling silk fibroin particle features for drug delivery,” *Biomaterials*, vol. 31, no. 16, pp. 4583–4591, 2010.

[45] M. Benfer and T. Kissel, “Cellular uptake mechanism and knockdown activity of siRNA-loaded biodegradable DEAPA-PVA-g-PLGA nanoparticles,” *Eur. J. Pharm. Biopharm.*, vol. 80, no. 2, pp. 247–256, 2012.

[46] H. Glaumann, I. K. Berezesky, J. L. Ericsson, and B. F. Trump, “Lysosomal degradation of cell organelles. I. Ultrastructural analysis of uptake and digestion of intravenously injected mitochondria by Kupffer cells,” *Lab. Invest.*, vol. 33, no. 3, pp. 239–51, 1975.

[47] J. PANYAM, “Rapid endo-lysosomal escape of poly(DL-lactide-co-glycolide) nanoparticles: implications for drug and gene delivery,” *FASEB J.*, vol. 16, no. 10, pp. 1217–1226, 2002.

VI. HYBRID EADF4(C16) PROTEIN PARTICLES CONTAINING A CLEAVABLE LINKER SEQUENCE FOR VACCINATION (SECOND GENERATION)

1. Introduction

The promising concept of a eADF4(C16) hybrid protein was redesigned after the *in vitro* experiments had been performed using the first generation eADF4(C16) hybrid protein particles. Although these particles were successfully taken up by antigen presenting cells (APCs) like macrophages and dendritic cells, the antigen was not cleaved from the eADF4(C16) hybrid protein particles, hence no antigen presentation took place. For that reason, the redesign of the second generation eADF4(C16) hybrid protein focused on the ability of cleavage at a certain position between the eADF4(C16) sequence and the attached antigen. The CD8 epitope $OVA_{257-264}$ (SIINFEKL), which has been used in the eADF4(C16) hybrid protein of the first generation, was again used as antigen.

The idea to introduce a cleavable linker between a polymer based carrier and a protein or peptide is not new, as several studies already used linkers for the coupling of two molecules [1]. Usually, a polymeric carrier for drug delivery is coupled to an active drug molecule [2]. The reasons to couple the active drug to a carrier system are different, but can include reduced toxicity after coupling the active drug (e.g. doxorubicin) [3] or a targeted drug delivery via coupling to an antibody [4]. During the years, several coupling strategies were developed. Soyez et al. reviewed several carrier-drug conjugates and listed several linkage options of drugs to macromolecules [5]. First, there is the possibility of sulfhydryl linkages, connecting the polymer and the drug via a disulfide bond [6]. The release of the linked drug is then achieved by reduction of the disulfide bonds in the presence of glutathione or other reductive enzymes [1]. Second, hydrolysis can be used for a pH controlled drug release from acid-labile linkages [7]. The two commonly used acid-labile linkers are cis-aconityl and hydrazone linkages, where the latter one is favored due to the higher release rate of the linked drug in a mild acidic environment around pH 5 [1]. The third type of linkers used for the attachment of drugs to polymers are enzymatically degradable linkers [5]. The intracellular variety of proteolytic enzymes allowed the development of several amino acid based linker sequences. In case of the currently approved antibody-drug conjugates, one is using a non-degradable linker (trade name Kadcyla®) and the other one uses an enzymatically degradable linker (trade name Adcetris®) [8]. All linker types are usable for the linkage of drug

molecules after fabrication of the carrier. However, only the enzymatically cleavable linkers are usable for the recombinant production of the second generation eADF4(C16) hybrid proteins, where the primary structure of the spider silk protein is already containing the sequence of the antigen. The finding that first generation eADF4(C16) hybrid protein particles are processed in the lysosome after cellular uptake directed the selection of a suitable linker towards a lysosomal cysteine protease degradable linker. Lysosomal cysteine proteases are a class of enzymes that were believed to unselectively degrade proteins intracellularly after uptake in the lysosome [9]. Nowadays, 11 human cathepsins have been identified with different unique properties [10]. Most of the cathepsins, including cathepsin S, are endopeptidases. However, cathepsin B enzyme is a carboxydipeptidase exhibiting an additional endopeptidase activity [10]. The activation and optimal activity of the cathepsins is reached after a mild acidification in the lysosome [9, 11]. In the meanwhile, most of the cathepsin enzymes are also associated to processes of the immune system and to central functions in cancer regulation [11, 12]. APCs like B cells, dendritic cells and macrophages express a various number of different cathepsins, including cathepsin S and cathepsin B [11]. Consequently, it is no surprise that previous studies already focused on the evaluation of the specific amino acid sequences that are cleaved by different cathepsins [13–15]. Gradually, with the development of faster analysis methods and the establishment of peptide libraries, the identification of more protease cleavage sites was possible [16]. The information gained from these experiments led to the design and development of cathepsin cleavable linker sequences [17]. The new cathepsin cleavable linkers were used for the design of molecules for cancer treatment [18], vaccination [19] and diagnostics [20]. From all available linker sequences, we selected two for the design of the second generation eADF4(C16) hybrid proteins. The first one is the cathepsin B cleavable linker with the one letter amino acid code GFLG, which was reported to be successfully cleaved from various molecules [3, 4, 18, 21, 22]. The second linker displays the amino acid sequence PMGLP, which was recently reported to be selectively cleaved by cathepsin S [23–25]. According to Honey et al., cathepsin S plays a crucial role in the antigen presentation *in vivo* [11].

In this study, the particle preparation process of the second generation eADF4(C16) hybrid proteins was evaluated and further optimized to result in small, uniform eADF4(C16) hybrid protein particles. The two newly designed eADF4(C16) hybrid protein particles were subsequently incubated with purified cathepsin B and S enzymes to investigate the properties of the introduced linker sequences on the release of the SIINFEKL antigen. Furthermore, eADF4(C16) hybrid protein particles with and without fluorescent labelling and low endotoxin values were prepared for *in*

vitro and *in vivo* studies and were characterized in terms of cytotoxicity, immunogenicity, uptake behavior and induction of a CD8 T cell proliferation.

2. Materials and methods

2.1. Materials

2.1.1. Recombinantly produced spider silk protein eADF4(C16) and engineered eADF4(C16) hybrid protein (second generation)

Spray dried eADF4(C16) protein was provided by AMSilk GmbH (Martinsried, Germany). The properties of the native eADF4(C16) protein have been already described in chapter 2. The engineered eADF4(C16) hybrid proteins of the first generation were further modified resulting in two eADF4(C16) hybrid proteins of the second generation. The antigen used was the $OVA_{257-264}$ epitope (SIINFEKL). The difference between the first and the second generation eADF4(C16) hybrid proteins is based on the addition of an enzyme cleavable linker between the eADF4(C16) framework and the SIINFEKL sequence. This linker was designed to be cleaved by two lysosomal cysteine proteases called cathepsin B (CatB) and cathepsin S (CatS). The cathepsin B cleavable linker contains the amino acid sequence GFLG, whereas the cathepsin S cleavable linker comprises the amino acid sequence PMGLP. Both linker sequences were fused between the C-terminal end of the eADF4(C16) framework and the epitope sequence SIINFEKL. A T7-TAG for faster purification and detection was added at the N-terminal end. The addition of the T7-TAG and the cleavable linker sequence resulted in a molecular weight of 49,415 Da (CatB hybrid) or 49,253 Da (CatS hybrid). The theoretical pI of both hybrid proteins was 3.67. Cloning the DNA to a plasmid was conducted by the group of Prof. Dr. Thomas Scheibel in Bayreuth. Again, the production in *E. coli*, downstream processing and spray-drying was handled by the AMSilk GmbH. An extinction coefficient of 46,400 $M^{-1}*cm^{-1}$ at 276 nm and the respective molecular weight of the eADF4(C16) hybrid proteins were used for the concentration determination by UV-Vis-spectroscopy.

2.1.2. Chemicals and reagents

Highly purified water (HPW) used in this study was generated by a purelab® device (ELGA LabWater, Celle, Germany). Sodium hydroxide solution (1 mol/L, EMPROVE® bio), di-potassium hydrogen phosphate (EMPROVE bio, European Pharmacopoeia (Ph. Eur.), British Pharmacopoeia (BP)), potassium dihydrogen phosphate (EMPROVE bio, Ph. Eur., BP, United States National Formulary (NF)) and hydrochloric acid 37% (EMPROVE bio, Ph. Eur, BP, Japanese Pharmacopoeia

(JP)) were purchased from Merck KGaA, Darmstadt, Germany. Ethanol 96% (v/v) and sodium chloride (NaCl, AnalaR NORMAPUR) were obtained from VWR Chemicals, Darmstadt, Germany. Tris(hydroxymethyl)aminomethane (Tris, Trizma® base, purity ≥99.9%), Trifluoroacetic acid (ReagentPlus®, 99%), DL-Dithiothreitol (DTT, purity ≥98%), Ethylenediaminetetraacetic acid (EDTA ≥98.5%) and fluorescein isothiocyanate (suitable for protein labeling) were purchased from Sigma Aldrich GmbH, Steinheim, Germany. Guanidinium thiocyanate (for molecular biology) and 4-(2-Hydroxyethyl)-1-piperazine-1-ethanesulfonic acid (HEPES, for molecular biology) were purchased from AppliChem GmbH, Darmstadt, Germany. Ammonium sulfate (purity ≥99%) was obtained from Bernd Kraft GmbH, Duisburg, Germany. Dimethyl sulfoxide (DMSO, purity ≥99%) was purchased from Grüssing GmbH Analytika, Filsum, Germany. Acetonitrile (HPLC Grade) was obtained from Fisher Scientific, Waltham, MA, USA. The peptides with the amino acid sequences SIINFEKL, IGSIINFEKLG and LPGSIINFEKLG were synthesized by GenScript USA Inc., Piscataway, NJ, USA. Cathepsin S (human spleen, purity >90%, activity 183.3 mU/mg) and cathepsin B (human liver, purity >95%, activity 274 U/mg) were purchased from Calbiochem, Merck KGaA, Darmstadt, Germany. Endotoxin cartridges (Endosafe-PTS® Cartridges PTS20005F, Sensitivity 0.005 EU/ml) were purchased from Charles River, Lyon, France.

2.2. Methods

2.2.1. Preparation of eADF4(C16) hybrid protein particles (second generation)

Preparation of eADF4(C16) hybrid protein particles was performed using the well established preparation technique using a micromixing system as described before [26]. The eADF4(C16) hybrid protein powders were dissolved in a 6 M guanidinium thiocyanate solution and subsequently dialyzed against a 10 mM Tris/HCl solution at 2-8°C for 24 hours. A dialysis membrane with a molecular weight cut-off of 8,000 Da (Spectrum Laboratories, Rancho Dominguez, USA) was used. After dialysis, the solution was centrifuged and filtered through a 0.2 µm polyethersulfone (PES) filter (VWR International, Radnor, USA). Concentrations of the eADF4(C16) hybrid proteins in solution were determined using an Agilent 8453 UV-Vis spectrophotometer (Agilent, Waldbronn, Germany). The protein solution was further adjusted to a concentration of 1.0 mg/ml for particle preparation with a filtered 10 mM Tris/HCl solution. Both cylinders of a syringe pump system (Model 100 DX and Series D pump controller, Teledyne Isco, Lincoln, USA) were filled with pre-tempered eADF4(C16) solution (c=1.0 mg/ml) and either a pre-tempered 2 M potassium phosphate solution or 4 M ammonium sulfate solution of 80°C. The syringe pump cylinders were jacketed by a bath circulator SC100-A10 (Thermo Scientific,

Karlsruhe, Germany) which was tempered at 80°C. The solutions were pumped at a high flow rate of 50 ml/min into a T-shape mixing element (inner diameter 0.5 mm, P-727 PEEK tee, Upchurch Scientific, Oak Harbor, USA) leading to an outlet tubing (inner diameter 0.5 mm, 1532 PEEK Tubing, Upchurch Scientific, Oak Harbor, USA) for suspension collection. The eADF4(C16) hybrid protein particle suspensions were subsequently centrifuged at 14,000 rpm (SIGMA 4K15, Sigma Laborzentrifugen, Osterode am Harz, Germany) and washed with HPW three times. A two minute ultrasonication (Sonopuls HD 3200, Bandelin electronic, Berlin, Germany) step completed the particle preparation procedure. The particle concentrations in mg/ml were determined gravimetrically after drying the particles at 13 mbar in a vacuum oven (Memmert, Schwabach, Germany) overnight.

2.2.2. Optimizing eADF4(C16) particle size

The micromixing particle preparation process was optimized for further reduction of the final particle size. Some parameters were changed compared to the preparation process described above. The concentration of the eADF4(C16) solution used for particle preparation was adjusted to 0.5 - 1.0 mg/ml. In addition to the regularly used 2 M potassium phosphate solution, 2 M, 3 M and 4 M ammonium sulfate solutions were used for particle precipitation. The flow rate of the salt solution was kept at 50 ml/min, whereas the flow rate of the protein solution was set to 25-50 ml/min. For these optimization studies, native eADF4(C16) protein was used. All other parameters were kept as described before and final particle size was analyzed after particle preparation.

2.2.3. Preparation of endotoxin free eADF4(C16) hybrid protein particles for *in vitro* and *in vivo* studies

The particle preparation process described before was slightly adjusted for the preparation of endotoxin free particles. The eADF4(C16) hybrid protein powder was suspended with HPW in a glass vial (DIN 10R), closed with a rubber stopper and crimped with an aluminum cap. Steam sterilization was performed for 15 minutes at 121°C in a GTA 50 autoclave (Fritz Gössner, Hamburg, Germany). After cooling, the eADF4(C16) hybrid protein suspension was centrifuged at 10,000 rpm (SIGMA 4K15, Sigma Laborzentrifugen, Osterode am Harz, Germany) for 30 minutes and the supernatant discarded. The centrifuged eADF4(C16) hybrid protein was dissolved in a 6 M guanidinium thiocyanate solution and dialyzed against an endotoxin free 10 mM TRIS/HCl solution pH 8.0 for 24 hours. After dialysis, the eADF4(C16) hybrid protein solution was filtered through a 0.2 µm PES filter (VWR International, Radnor, USA) and adjusted to a concentration of 2 mg/ml

with an endotoxin free 10 mM TRIS/HCl buffer pH 8.0. Subsequently, the eADF4(C16) hybrid protein solution was filtered with a pre-flushed Mustang® E (Pall GmbH, Dreieich, Germany) filter. About 500 µl of each batch were discarded at the beginning. The protein concentration of the filtered eADF4(C16) solution was determined photometrically at 276 nm (Agilent 8453 UV-Vis spectrophotometer, Agilent, Waldbronn, Germany). Endotoxin content was tested using an Endosafe®-PTS reader after a 20 - 40-fold dilution of the solution with HPW. This eADF4(C16) hybrid protein solution was further adjusted to a concentration of 1.0 mg/ml for particle preparation with an endotoxin free10 mM Tris/HCl solution pH 8.0. Both cylinders of the syringe pump system and the Sonopuls HD 3200 sonotrode were depyrogenized using 70% (v/v) ethanol over 48 hours prior to particle preparation. The protein concentration for particle preparation was 1 mg/ml and preparation temperature was 80°C. All other parameters were kept constant as described before.

2.2.4. Fluorescent labelling

Labelling of eADF4(C16) protein with fluorescein isothiocyanate (FITC) was performed based on the published method by Spieß et al. [27] using the terminal amine group of eADF4(C16). For the preparation of particles used for *in vivo* studies, the eADF4(C16) protein powder was autoclaved as described before. After steam sterilization, the autoclaved eADF4(C16) powder was dissolved in a 6 M guanidinium thiocyanate solution but this time dialyzed against an endotoxin free 20 mM HEPES solution pH 8.0 at 2-8°C for 24 hours. After dialysis, centrifugation and filtration, the solution was adjusted to a concentration of 2.0 mg/ml with an endotoxin free 20 mM HEPES solution pH 8.0 for coupling in solution. A 20-fold molar excess of FITC (dissolved in DMSO) was added slowly to the eADF4(C16) solution. After addition of the complete amount of dissolved FITC, the solution was incubated in the dark for three hours at room temperature. After incubation, the FITC coupled eADF4(C16) protein solution was filtered first through a 0.2 µm PES filter (VWR International, Radnor, USA) and subsequently filtered with a pre-flushed Mustang® E (Pall GmbH, Dreieich, Germany) filter. The filtered FITC coupled eADF4(C16) protein solution was adjusted to a protein concentration of 1 mg/ml for particle preparation by the syringe pump system at 80°C. All other parameters were identical with the previously described particle preparation process.

The fluorescent labelling of particles used for *in vitro* studies was carried out at pre-fabricated particles. eADF4(C16) particles were suspended at a concentration of 2.5 mg/ml in an endotoxin free 20 mM HEPES buffer pH 8.0. A 20-fold molar excess of FITC (dissolved in DMSO) was added dropwise to the particle suspension. After incubation for 72 hours in the dark, the particles were centrifuged and washed with HPW for three times. Additional ultrasonication for 2 minutes

completed the FITC labelling process of final eADF4(C16) particles.

2.2.5. *In vitro* release of SIINFEKL from hybrid eADF4(C16) particles

The release of the antigen sequence SIINFEKL from the second generation hybrid proteins was tested by the addition of cathepsin enzymes. As the second generation hybrid proteins contain cleavable linker sequences for the cathepsin S and cathepsin B enzymes, these two cathepsins were also used for the *in vitro* release studies. The eADF4(C16) hybrid protein particles were suspended to a final concentration of 2 mg/ml with a 50 mM sodium acetate buffer, pH 5.5, containing 1 mM EDTA and 2 mM DTT for incubation with the cathepsin S enzyme. Cathepsin S was diluted in the same buffer to a final concentration of 0.9 mU/ml. Slight pH modification of the buffer was necessary for the cathepsin B enzyme. The eADF4(C16) hybrid protein particles were suspended to a final concentration of 2 mg/ml with a 50 mM sodium acetate buffer, pH 5.0, containing 1 mM EDTA and 2 mM DTT for incubation with the cathepsin B enzyme. Cathepsin B was diluted in the same buffer to a final concentration of 0.1 U/ml. Incubation of the particles with the enzymes was carried out at 37°C on a waving platform shaker (Heidolph Polymax 1040, Heidolph Instruments GmbH, Schwabach, Germany) at 10 rpm. Samples were drawn after 1, 6, 24, 48, 72 and 96 hours and analyzed by RP-HPLC.

2.3. Analytical Methods

2.3.1. Endotoxin testing

The endotoxin values of eADF4(C16) hybrid protein solutions and particles used for the *in vitro* studies were determined as described in chapter 2.

2.3.2. Dynamic light scattering (DLS)

Particle size and size distribution of submicroparticles were measured as described in chapter 2.

2.3.3. Zeta potential

The zeta potential of eADF(C16) particles was measured as described in chapter 2.

2.3.4. Scanning electron microscopy (SEM)

SEM measurements of eADF4(C16) particle suspensions were conducted as described in chapter 2.

2.3.5. SIINFEKL release - analysis of the supernatant by RP-HPLC

The cleaved SIINFEKL peptide fragments were analyzed by RP-HPLC. The supernatant of each sample was removed from the particles by centrifugation (two times at 12,000 rpm for 30 minutes). The pellets were discarded and 180 µl of the supernatant was filled into HPLC glass inserts and analyzed by RP-HPLC (detection by UV-Vis at 220 nm). Volumes of 50 µl of the corresponding supernatants were separated at 30°C by a reversed phase YMC-Triart C18 column (YMC Europe GmbH, Dinslaken, Germany) using a Waters 2695 separations module (Waters Corporation, Milford, MA, USA). A gradient with two mobile phases was applied, using water + 0.1% [m/m] TFA (mobile phase A) and 100% acetonitrile + 0.1% [m/m] TFA (mobile phase B). Each run started with two minutes of 95% mobile phase A and was followed by a linear increase of mobile phase B from 5% to 100% over 28 minutes. A five-minute washing step with 100% mobile phase B was used to wash residual peptide/protein from the column. The separation run stopped with a five minute equilibration of the column at 95% mobile phase A. The detection was carried out on a Waters UV-Vis detector 2487 (Waters Corporation, Milford, MA, USA) at a wavelength of 220 nm to detect the SIINFEKL peptides. The amount of released SIINFEKL was calculated using a standard curve. The cleavage sites of the linkers had been described in literature earlier [3, 5, 23, 25]. Using the described cleavage sites, a SIINFEKL peptide with the sequence IGSIINFEKLG was cleaved from the hybrid protein with the cathepsin B cleavable linker. Cleaving the SIINFEKL peptide of the hybrid protein with the cathepsin S cleavable linker resulted in a peptide with the sequence LPGSIINFEKLG. These two peptides were used for the standard curve at concentrations of 10, 20, 30, 50 and 100 µg/ml dissolved in 50% DMSO / 50% water. The area of each of the peptides in the chromatogram was integrated and used for calculation of calibration curves after injection and analysis. Data analysis was performed using Chromeleon® 6.80 software (Dionex GmbH, Germering, Germany).

3. Results and Discussion

Two linker sequences were selected on the basis of the most promising data for cathepsin cleavable linkers [3, 5, 23, 24]. This process led to the selection of a cathepsin B cleavable sequence (GFLG) and a cathepsin S cleavable sequence (PMGLP). The intention to select two target enzymes (cathepsin S and B) was to reduce the dependency of one specific enzyme for antigen cleavage. The $OVA_{257-264}$ epitope SIINFEKL has been already used for the first generation eADF4(C16) hybrid protein particles. While no antigen presentation of the first generation eADF4(C16) hybrid protein

particles was identified, a successful uptake into antigen presenting cells (APCs) like macrophages and bone marrow derived dendritic cells (BMDC) was demonstrated (see chapter 5). To promote intracellular antigen cleavage, the two selected linker sequences were fused between the native eADF4(C16) framework and the SIINFEKL antigen at the C-terminal end (see Figure VI-1). The addition of the cleavable linker sequence resulted in a molecular weight of 49,415 Da for the cathepsin B cleavable eADF4(C16) hybrid protein (eADF4(C16)-CatB hybrid protein) and 49,253 Da for the cathepsin S cleavable eADF4(C16) hybrid protein (eADF4(C16)-CatS hybrid protein).

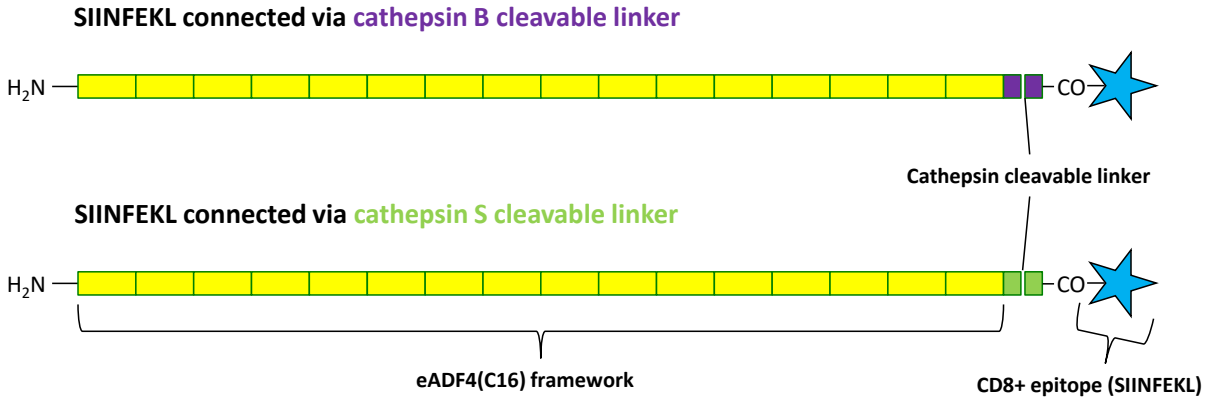

Figure VI-1:Schematic illustration of the newly designed second generation eADF4(C16) hybrid proteins. The difference to the first generation eADF4(C16) hybrid proteins is the addition of a cathepsin cleavable linker sequence between the native eADF4(C16) framework and the SIINFEKL antigen.

As a first step, the influence of the linker sequence of the newly designed, second generation eADF4(C16) hybrid proteins on the resulting particle size was evaluated. The particle size of the newly designed cathepsin cleavable hybrid protein particles is compared to the particle size of the native eADF4(C16) protein particles and the results are illustrated in Figure VI-2. While the eADF4(C16)-CatB hybrid protein particles with a Z-average particle size of 386 nm were in the same size range compared to the native eADF4(C16) particles (Z-average value of 369 nm), the particles prepared with the eADF4(C16)-CatS hybrid protein were notably larger and had a Z-average particle size of 510 nm. All particles were prepared using a micromixing device [26] and a protein concentration of 1 mg/ml at a temperature of 80°C.

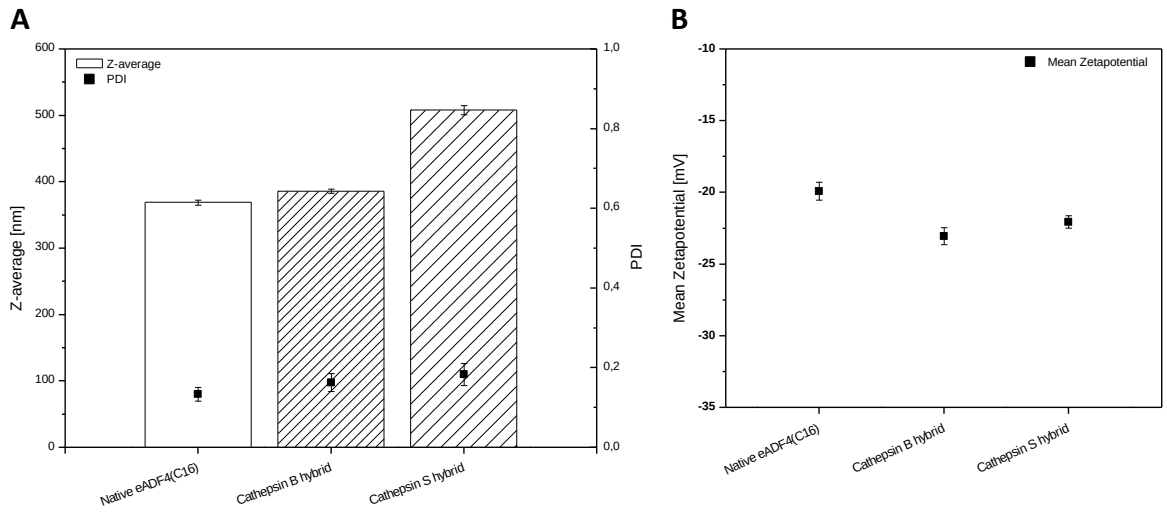

Figure VI-2: Properties of the second generation eADF4(C16) hybrid protein particles compared to native eADF4(C16) protein particles. A) Particle size given as the Z-average and the particle dispersity index (PDI) of eADF4(C16) particles prepared and 80°C and a protein concentration of 1.0 mg/ml.
B) Zeta potential of the second generation eADF4(C16) hybrid protein particles compared to native eADF4(C16) protein particles.

Particle size itself has a huge impact on the resulting antigen presentation [28]. Joshi et al. compared 17 µm, 7 µm, 1 µm, and 300 nm PLGA particles loaded with the model antigen Ovalbumin on the antigen-specific cytotoxic T cell response. The authors concluded, that 300 nm particles were more effective for a vaccination approach than the larger particles [29]. Foged et al. also emphasized, that particles in the size range below 500 nm are superior for an uptake into APCs [30]. These reports in combination with the eADF4(C16)-CatS hybrid protein particle size of 510 nm initiated size optimization studies for the preparation of the second generation eADF4(C16) hybrid protein particles using the micromixing device. The preparation of the eADF4(C16) protein particles is based on a salting out with kosmotropic ions according to the Hofmeister series (see Table VI-1). Two characteristics of the used salt solution affect the final particle size. The first one is the kosmotropic strength of the used ions of the salts and the second one is the ionic strength of the salt solutions [31]. A 2 M potassium phosphate solution was used for protein precipitation in previous studies [26] and for the preparation of the eADF4(C16) hybrid protein particles of the first generation. Due to the limit of solubility of the potassium phosphate used for the preparation of the precipitation buffer, another kosmotropic salt with a higher solubility was screened.

Table VI-1: The Hofmeister series of salts, separated in anions and cations. The ions used for eADF4(C16) protein precipitation are highlighted in bold.

Kosmotropic, salting-out ←									
	F^-	**PO_4^-**	**SO_4^{2-}**	CH_3COO^-	Cl^-	Br^-	I-		
$(CH_3)_4N^+$	$(CH_3)_2NH^+$	**NH_4^+**	**K^+**	Na^+	Cs^+	Li^+	Mg^{2+}	Ca^{2+}	Ba^{2+}
→ Chaotropic, salting-in									

The precipitating properties of ammonium sulfate have already been known since the early 70s and it has been commonly used for protein purification [32]. The preparation of ammonium sulfate solutions up to 4 M was possible at room temperature. In a small scale optimization study, the effect of an increasing ammonium sulfate strength with molarities ranging from 2 M to 4 M on the final eADF4(C16) protein particle size was evaluated and compared to a 2 M potassium phosphate solution. Due to the limited amount of the eADF4(C16)-CatS and eADF4(C16)-CatB hybrid proteins, the particle size optimization studies were performed with the native eADF4(C16) protein. The optimized particle preparation procedure was then transferred to the second generation eADF4(C16)-CatS and eADF4(C16)-CatB hybrid proteins in a second step. Further parameters like the protein concentration or the flowrate of the eADF4(C16) protein solution were evaluated for the 4 M ammonium sulfate concentration. The results of the particle optimization study are visualized in Figure VI-3. The influence of the used salt was negligible, as both salts already contain strong kosmotropic ions. However, the trend towards smaller particles with increasing the ionic strength of the salt solution is evident. The particle size decreased from 496 nm for the 2 M ammonium sulfate solution to 302 nm using the 4 M ammonium sulfate solution. Decreasing the protein concentration from 1 mg/ml to 0.5 mg/ml additionally lowered the final particle size to 274 nm. Finally, the influence of the flowrate on the particle size was studied. While keeping a high flowrate of 50 ml/min for the ammonium sulfate solution, the flowrate of the eADF4(C16) protein solution was lowered to only 25 ml/min. By that, the salt to protein ratio decreased again, similar to the reduced protein concentration of 0.5 mg/ml. Other than the reduced protein concentration, the decreased flowrate had no effect on the final particle size.

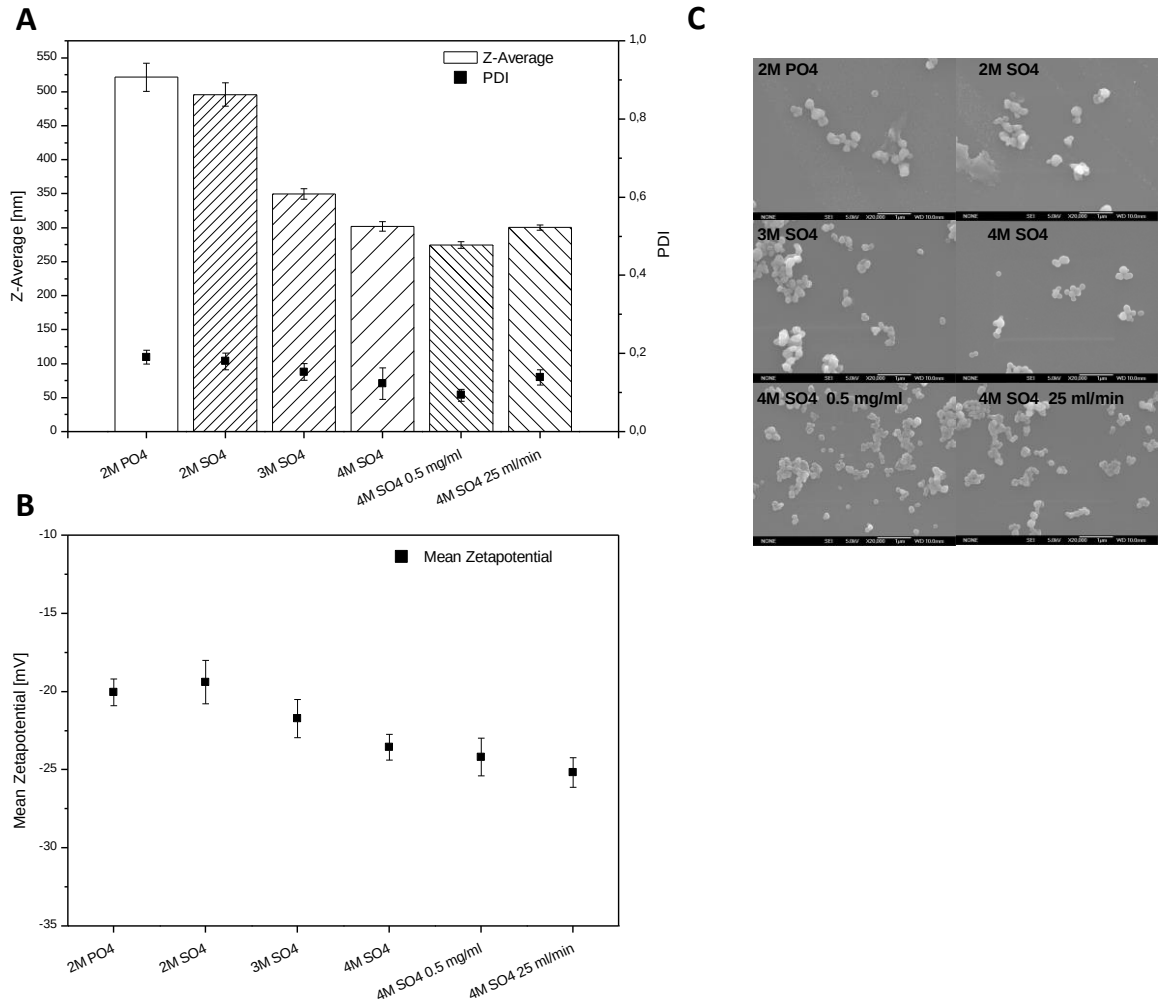

Figure VI-3: Properties of native eADF4(C16) protein particles after precipitation with different salt solutions and different ionic strengths (2M PO4: particle preparation using 2 M potassium phosphate. 2M to 4M SO4: particle preparation using 2 M to 4 M ammonium sulfate. 0.5 mg/ml: reduced protein concentration. 25 ml/min: decreased flowrate.)
A) Particle size given as the Z-average and the particle dispersity index (PDI).
B) Zeta potential of native eADF4(C16) protein particles after precipitation with different salt solutions.
C) SEM micrographs of native eADF4(C16) protein particles at a magnification of 20,000x. The particles were dried under vacuum and carbon sputtered before measurement.

As illustrated in Figure VI-3 B, particles prepared with the higher molar ammonium sulfate solutions showed a clear trend towards increasing negative zeta potentials. The increase of the negative zeta potential could consequently increase the colloidal stability of the particle suspension. The SEM micrographs in Figure VI-3 C show particles at a magnification of 20,000x. The particles were observably round shaped with a smooth and unimpaired surface.

The results from the particle size optimization screening suggested the use of a 4 M ammonium sulfate solution and a protein concentration of 0.5 mg/ml. However, due to the minor effect of the protein concentration on the final particle size and the higher yield using a 1 mg/ml protein solution, the transfer experiments to the second generation eADF4(C16)-CatS and eADF4(C16)-CatB hybrid proteins was performed at a protein concentration of 1 mg/ml.

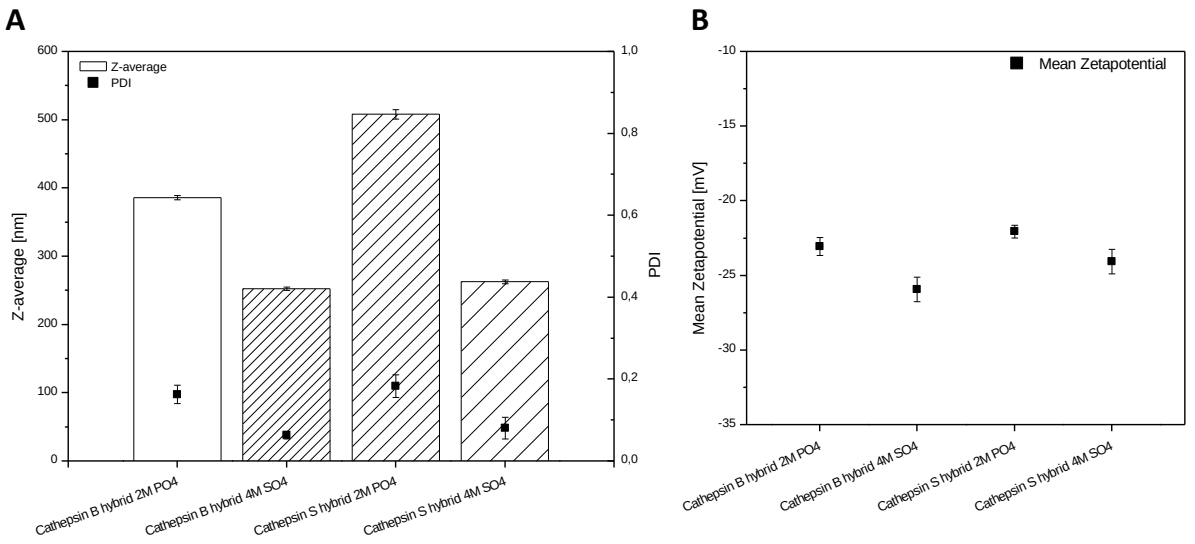

Figure VI-4: Properties of the eADF4(C16) cathepsin B and S hybrid protein particles using the optimized particle preparation process compared to the old process.
A) Particle size given as the Z-average and the particle dispersity index (PDI) prepared at a protein concentration of 1.0 mg/ml and using either a 2 M potassium phosphate solution (2M PO4) or a 4 M ammonium sulfate solution (4M SO4).
B) Zeta potential of the same particles described in A).

Figure VI-4 shows the particle size and zeta potential of the eADF4(C16)-CatS and eADF4(C16)-CatB hybrid protein particles using the optimized particle preparation method in comparison to the previously prepared particles. Using the 4 M ammonium sulfate salt solution for the protein precipitation resulted in clearly smaller particles with a lower PDI. The particle size is approximately 260 nm, independent of the used eADF4(C16) hybrid protein. As already observed for the native eADF4(C16) protein particles, the smaller eADF4(C16) hybrid protein particles exhibited a lower zeta potential compared to the larger ones (Figure VI-4 B). By using the optimized particle preparation process, the preparation of eADF4(C16)-CatS and eADF4(C16)-CatB hybrid protein particles with a size below 300 nm was possible, which allows a direct comparison to the eADF4(C16) hybrid protein particles of the first generation.

Because no antigen presentation was detected during the previous *in vitro* tests with the first generation eADF4(C16) hybrid protein particles, an enzymatic release test of the model antigen SIINFEKL was conducted. Because the two introduced linkers were designed for the cleavage of cathepsin S and cathepsin B, these two enzymes were used for the release experiments. Although the cathepsin S linker sequence (PMGLP) was designed for a cleavage by the cathepsin S enzyme and the cathepsin B linker sequence (GFLG) was designed to be cleaved by the cathepsin B enzyme, both eADF4(C16) hybrid protein particles were tested with both cathepsin enzymes. The predicted cleavage sites within the linker sequences were already published earlier [5, 22, 23, 25]. The published cleavage sites were used to identify the SIINFEKL peptide sequence that will be

cleaved from the eADF4(C16) hybrid protein particles. These peptides were purchased and used for the analysis of the cleavage experiments. For the cathepsin B linker, a cleavage site after the GFLG linker sequence was postulated (C16-GAVGFLG / IGSIINFEKLG) and the IGSIINFEKLG sequence was used for the quantification of the released antigen from the eADF4(C16)-CatB hybrid protein. Similarly, for the cathepsin S linker, a cleavage site within the PMGLP linker sequence was postulated (C16-PMG / LPGSIINFEKLG) and the LPGSIINFEKLG sequence was used for the quantification of the released antigen from the eADF4(C16)-CatS hybrid protein.

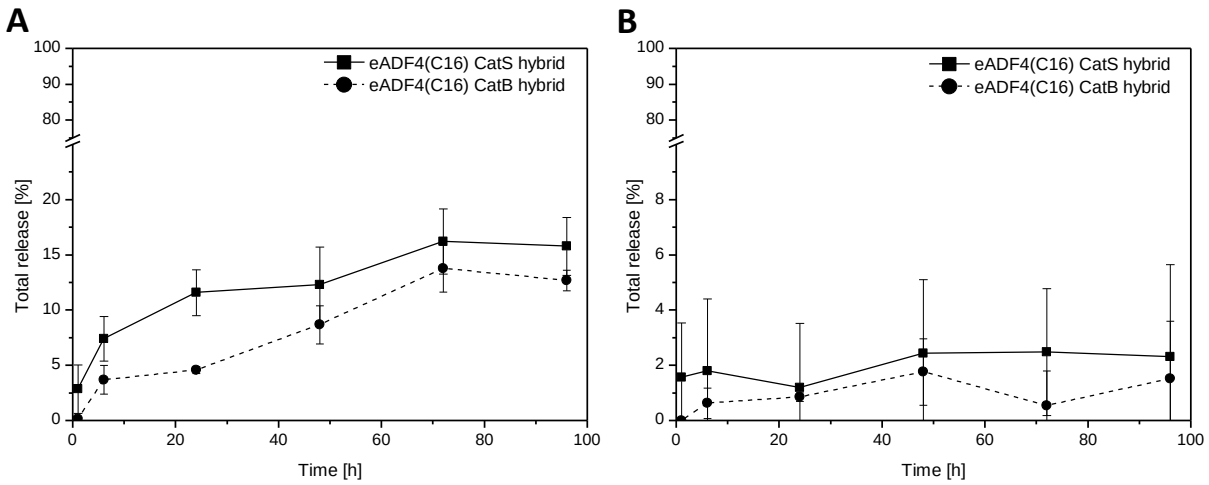

Figure VI-5: Differential release of the antigen with different cathepsin enzymes. The sequence LPGSIINFEKLG was used for the release from eADF4(C16)-CatS hybrid protein particles, while the sequence IGSIINFEKLG was used for the release from eADF4(C16)-CatB hybrid protein particles. Data are the mean and SD of 3 independent replicates.
A) eADF4(C16) hybrid protein particles were incubated with cathepsin S enzyme for 96 hours.
B) eADF4(C16) hybrid protein particles were incubated with cathepsin B enzyme for 96 hours.

Figure VI-5 shows the results of the release experiments performed with the enzymes cathepsin S (Figure VI-5 A) and cathepsin B (Figure VI-5 B). eADF4(C16) hybrid protein particles were incubated for 96 hours and the amount of released SIINFEKL peptide was evaluated using RP-HPLC analysis. Three conclusions can be drawn from the enzymatic release experiments. The cathepsin S enzyme was capable of cleaving both linker sequences (Figure VI-5 A). Although the linker which was assigned for the cleavage by the cathepsin S enzyme (PMGLP) was cleaved more effectively than the cathepsin B linker sequence (GFLG), total SIINFEKL amounts over 10% were released from both eADF4(C16) hybrid protein particles. The additional cleavage may result from a non-specific linker design in the eADF4(C16)-CatB hybrid protein. Peterson et al. investigated cathepsin B linker sequences, which were designed to be cleaved by the cathepsin B enzyme, but not by the cathepsin D enzyme [17]. The authors identified, that one of their linker sequences was finally cleaved by both enzymes. This finding emphasizes the broad proteolytic activity of the cathepsin enzyme class. At the same time, we already expected cleavage of the specific cathepsin S linker

PMGLP not to be cleaved by the cathepsin B enzyme [23]. This hypothesis was confirmed by results illustrated in Figure VI-5 B. Moreover, none of the linkers used for the second generation eADF4(C16) hybrid proteins was cleaved effectively by the cathepsin B enzyme (Figure VI-5 B). This result was surprising at the beginning, because the GFLG sequence was often reported as successful linker for a cathepsin B cleavage [18, 21]. However, the GFLG linker has never been used in combination with the eADF4(C16) spider silk protein. Due to the forced protein folding during the particle preparation process, the local surrounding of the linker was different to the unfolded protein in solution. Therefore, the cathepsin cleavage site of the cathepsin B linker sequence could be sterically hindered. Nevertheless, it might be possible to include a cathepsin B cleavage site in a different eADF4(C16) hybrid protein, because several different linker sequences have been already used for a cleavage with the cathepsin B enzyme. Instead of using the sequence GFLG, the dipeptide sequence Val-Cit [33] or the tetra peptides ALAL [34] and GGGF [20] may possibly be more effective in combination with the eADF4(C16) spider silk protein. Finally, the enzymatic cleavage activity was fast at the beginning of the incubation and slowed down over time. Especially the eADF4(C16)-CatS linker was effectively cleaved by the cathepsin S enzyme, where over 10% LPGSIINFEKLG were already released within the first 24 hours. After 74 hours of incubation, no increase of the released SIINFEKL could be observed, which was most probably due to the decrease of the enzymatic activity of both cathepsin enzymes. Putman et al. reported a slower release of the coupled 5-fluorouracil over time in their experiments as well [35]. However, APCs like macrophages display a higher cathepsin S and cathepsin B activity than other cells [25], which would result in a higher rate of SIINFEKL cleavage in cell based *in vitro* and *in vivo* mouse model experiments.

In order to evaluate the *in vitro* and *in vivo* properties of the newly designed eADF4(C16)-CatS and eADF4(C16)-CatBH protein particles, several batches of these particles were prepared. Exemplary for these batches, results of one eADF4(C16) protein particle batch are illustrated in Figure VI-6. The particles from this batch were finally used for the *in vivo* experiments performed by Inès Mottas at the group of Prof. Dr. Carole Bourquin at the University of Fribourg, Switzerland.

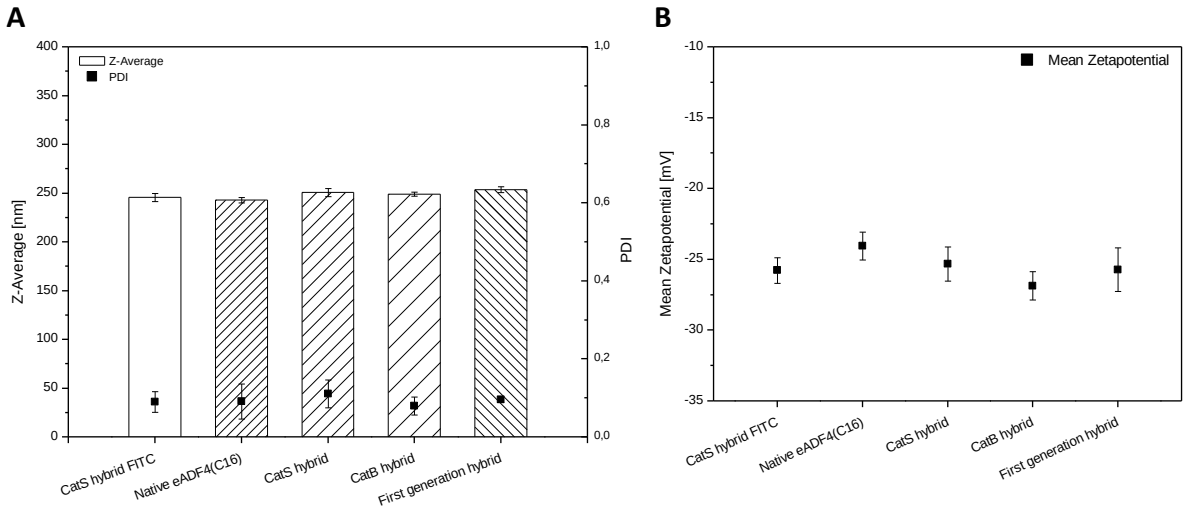

Figure VI-6: Properties of one exemplary eADF4(C16) protein particle batch used for the *in vitro* and *in vivo* experiments. The eADF4(C16)-CatS hybrid protein (CatS hybrid), the eADF4(C16)-CatB hybrid protein (CatB hybrid) and the native eADF4(C16) protein (Native eADF4(C16)) were compared to the N-terminal hybrid protein without linker sequence (first generation hybrid protein). The eADF4(C16)-CatS hybrid protein was additionally FITC labelled (CatS hybrid FITC) for flow cytometry and confocal microscopy analysis.
A) Particle size given as the Z-average and the particle dispersity index (PDI) prepared at a protein concentration of 1.0 mg/ml and a temperature of 80°C.
B) Zeta potential of the same particles described in A).

The optimized particle preparation method using a 4 M ammonium sulfate solution worked well for the eADF4(C16) protein particle batches used for the *in vitro* and *in vivo* studies. All different particle groups shown in Figure VI-6 are in a narrow size range between 242 nm and 254 nm. Also, the mean zeta potential is within a range of -27 mV to -24 mV very consistent among the different particle groups. Endotoxin content was analyzed after applying the endotoxin depletion process described earlier and the results are summarized in Table VI-2. The detected endotoxin values were all below 0.200 EU/mg protein, which was the limit of the assay after the necessary dilution before the measurements.

Table VI-2: Endotoxin values of one exemplary eADF4(C16) protein batch used for the *in vitro* and *in vivo* experiments in solution after applying the endotoxin depletion process. The LAL based Endosafe®-PTS reader was used to determine the endotoxin values. The eADF4(C16) proteins in solution were diluted 20-50-fold with HPW before measurement.

Type	Endotoxin values of eADF4(C16) solutions after endotoxin filtration
eADF4(C16)-CatS hybrid FITC labeled	<0.200 EU/mg
eADF4(C16) native	<0.200 EU/mg
eADF4(C16)-CatS hybrid	<0.200 EU/mg
eADF4(C16)-CatB hybrid	<0.200 EU/mg
eADF4(C16) first generation hybrid	<0.200 EU/mg

Particles were also examined by SEM microscopy. Figure VI-7 shows the micrographs of the non-FITC coupled particles used for the final *in vivo* experiments. In the micrographs roundly shaped particles are visible without damages or particle fragments. The actual particle size might appear smaller than the results from DLS measurements, because residual solvent had to be evaporated to dryness for the SEM images, whereas the DLS measurements were conducted in the suspended state.

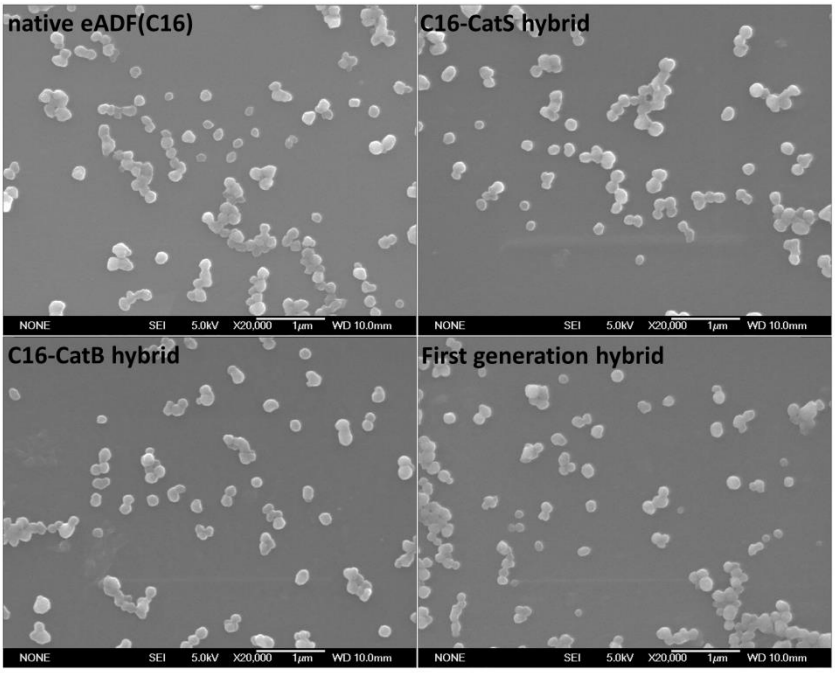

Figure VI-7: SEM micrographs of eADF4(C16) protein particles at a magnification 20,000x. The eADF4(C16) protein particles were dried under vacuum and carbon sputtered before measurement.

The different batches prepared for *in vitro* and *in vivo* testing were sent to our cooperation partner Prof. Dr. Carole Bourquin at the University of Fribourg, Switzerland for the *in vitro* and *in vivo* tests.

All the following results and graphs were compiled by Inès Mottas from October 2014 to November 2015 using the eADF4(C16) protein particles described before amongst other *in vitro* batches. I did not participate in the investigation of the following experiments and use the shared results just for illustration and discussion of the performance of the second generation eADF4(C16) hybrid protein particles containing the cathepsin cleavable linker sequences.

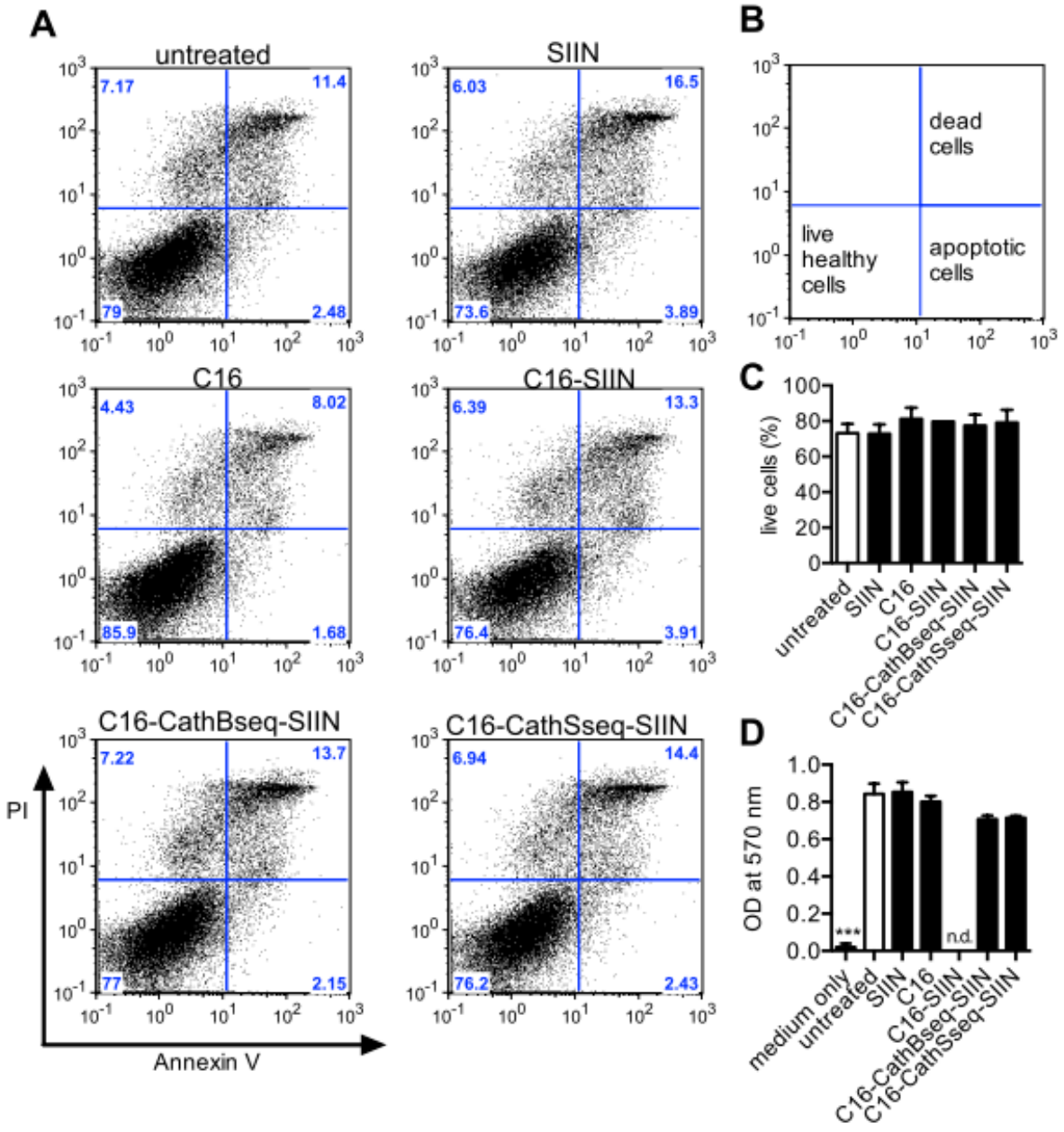

Figure VI-8: None of the spider silk particles induce BMDC cytotoxicity *in vitro*. BMDC (5x10 ^{4} cells/well) were cultured with spider silk particles at 505 µg NP/mL (=10 µg SIINFEKL/mL). After 24 hours of incubation, BMDC viability was assessed by flow cytometry and MTT assay.
(A) Representative dot plot from flow cytometry with propidium iodide (PI) and Annexin V.
(B) Scheme of the gating strategy to quantify live healthy cells (annexin V-/PI-).
(C) Percentage of live healthy cells (annexin V-/PI-).
(D) Optical density (OD) at 570nm correlating with formazan production from the MTT assay.
Condition without cells (medium only) was used as control. n.d.: not done. Asterisks (*, P<0.0001) indicate significant differences with untreated control group using one-way ANOVA followed by Dunnett's multiple comparison test.**
C and D) Each bar represents mean ± SEM of 3 independent experiments performed in duplicate. (Except for Panel C, C16-SIIN tested once in duplicate). SIIN: SIINFEKL peptide alone; C16: native eADF4(C16) particles; eADF4(C16)-SIIN: First generation hybrid particles; C16-CathBseq-SIIN: eADF4(C16)-CatB hybrid protein particles, C16-CathSseq-SIIN: eADF4(C16)-CatS hybrid protein particles.

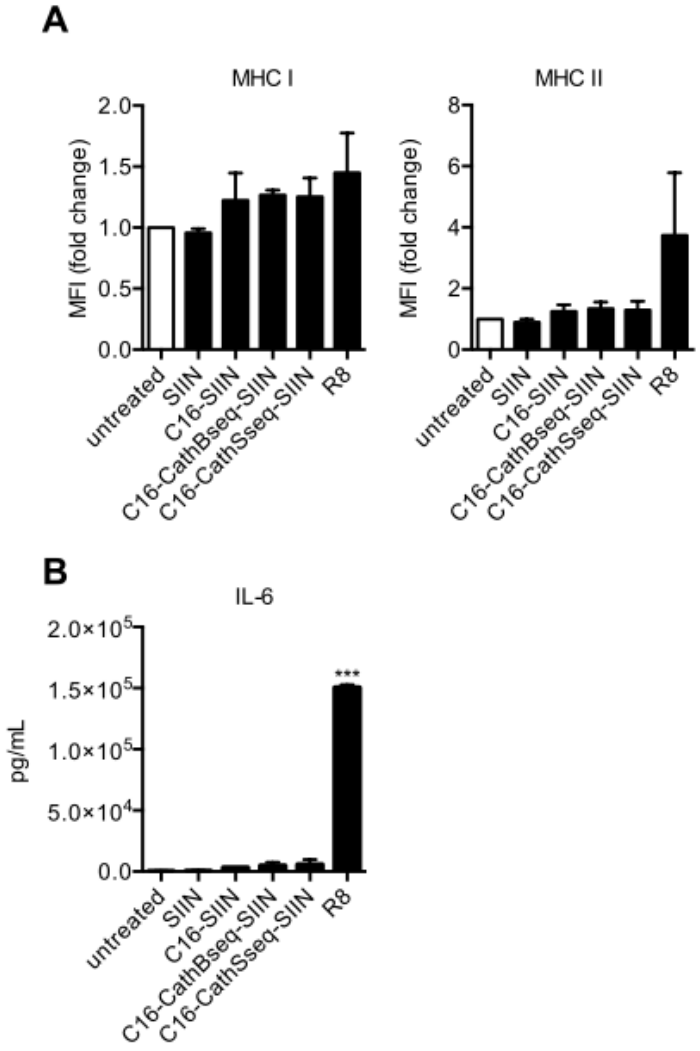

Figure VI-9: The spider silk particles do not induce BMDC immunological activation *in vitro*. BMDC (5x10 ^{4} cells/well) were cultured with spider silk particles at 50 µg NP/mL. After 24 hours of incubation, BMDC were analyzed by flow cytometry, whereas supernatant was collected for cytokine quantification. (A) Median fluorescent intensity (MFI) of BMDC surface activation markers: fold change compared to untreated sample.
(B) Cytokine quantification with ELISA.
R848 (R8), a TLR7 agonist, was used as positive control (0.25ug/mL). Asterisks (*, P<0.001) indicate significant differences with untreated control group using one-way ANOVA followed by Dunnett's multiple comparison test. Each bar represents mean ± SEM of 4 independent experiments performed in duplicate.**

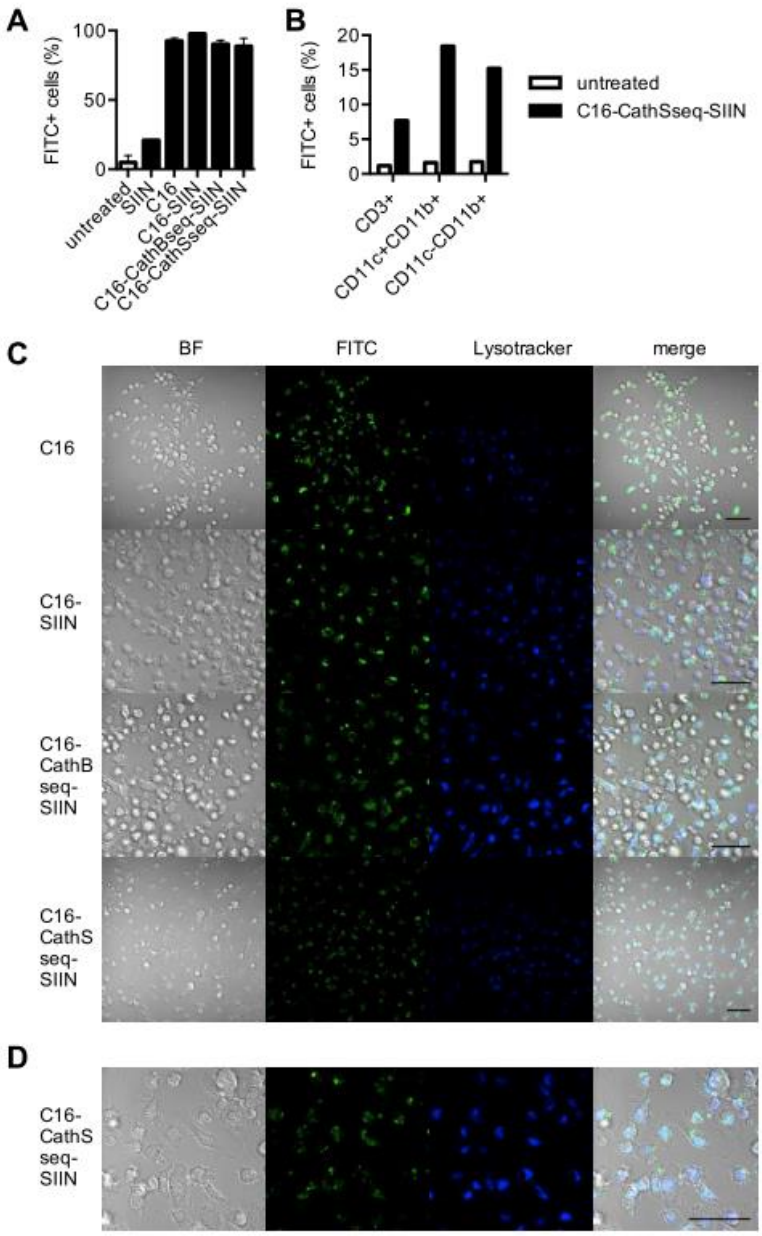

Figure VI-10: Spider silk particles are efficiently taken up by antigen-presenting cells.
(A) BMDC (5x10 ^{4} cells/well) were cultured with FITC-labelled spider silk particles at 50 µg NP/mL. After 24 hours of incubation, BMDC were isolated for flow cytometry analysis. Percentage of FITC-positive cells within BMDC (CD11c+) population was determined. Each bar represents mean ± SEM of 2 independent experiments performed in duplicate. (Except for C16-SIIN: tested once in duplicate).
(B) Freshly isolated splenocytes (5x10 ^{4} cells/well) were cultured 6 hours with FITC-labelled spider silk particles. After 6 hours of incubation, cells were analyzed by flow cytometry. Percentage of FITC-positive cells was determined in defined immune cell populations: T cells (CD3+), dendritic cells (CD11c+CD11b+) and monocytes/macrophages (CD11c-CD11b+). Graph depicts one representative experiment of 3. Each experiment was performed in duplicate.
C and D) BMDC (1.5x10 ^{5} cells/well) were incubated with Lysotracker for 1 hour and FITC-positive particles for an additional 4 hours before imaging with confocal microscopy. (C) Live cell imaging at 20x magnification and (D) 60x magnification.
Black bar: 50µm. BF: Bright field. Similar results were obtained for the other particles (data not shown).

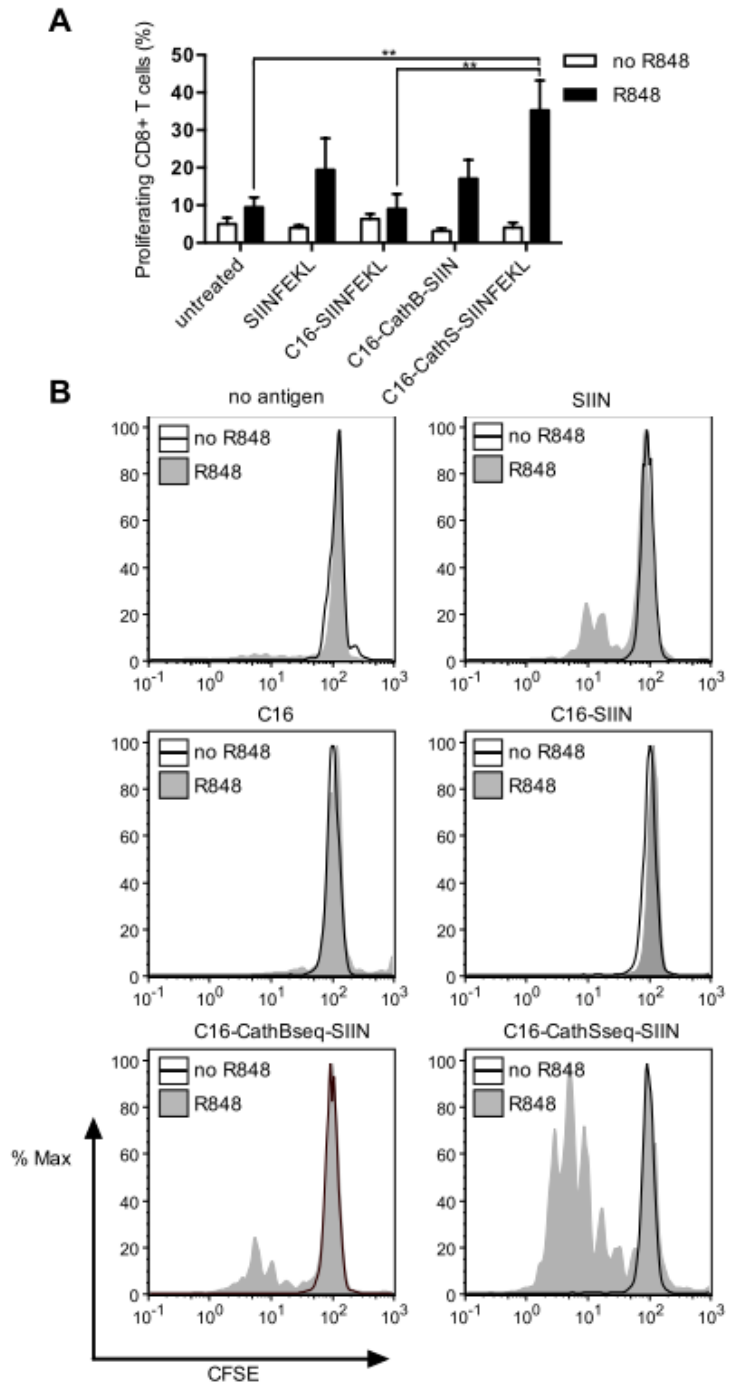

Figure VI-11: The Cathepsin S sequence is the most effective to induce SIINFEKL-dependent *in vitro* T-cell proliferation. BMDC (5x10 ^{4} ells /well) were cultured with spider silk particles at 50 µg NP/mL. R848 (0.25ug/mL) was used as adjuvant for BMDC activation. After 24 hours of incubation, CFSE-labelled CD3+CD8+ OT-I cells (10^5 cells /well) were added. After 3 days of co-culture, the cells were analyzed by flow cytometry.
(A) Percentage of proliferating cells within the T cell population (CD3+CD8+). Each bar represents mean ± SEM of 2 independent experiments performed in quadruplicate. Asterisks (, P<0.01) indicate significant differences between R848-treated groups using two-way ANOVA followed by Tukey's multiple comparison test.**
(B) Histogram of CFSE dilution from one representative experiment.

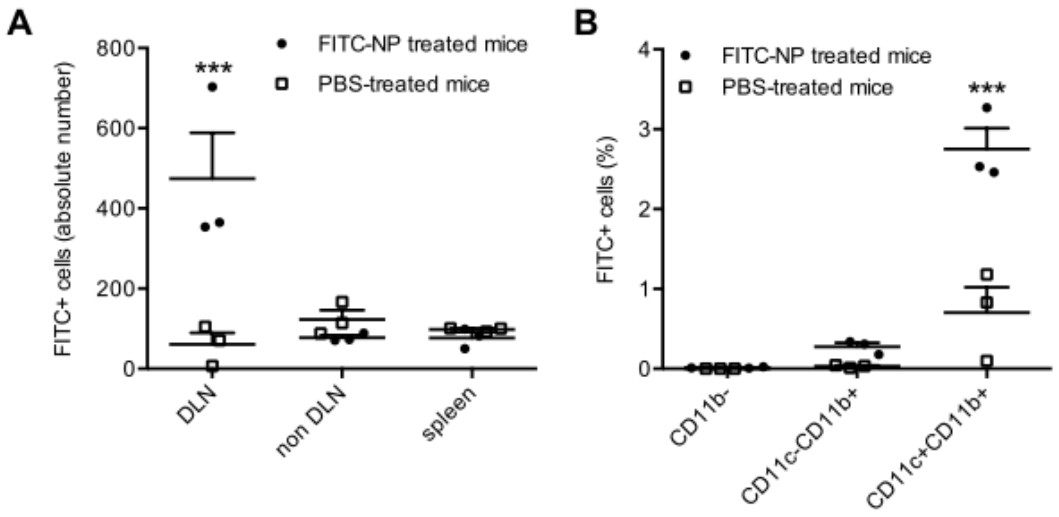

Figure VI-12: Spider silk particles accumulate in the draining lymph node *in vivo*. FITC-labelled C16-CathSseq-SIINFEKL particles were injected subcutaneously into the right flank of 3 mice (505 µg NP in 100 µL PBS per mouse). PBS was used as negative control. After 24 hours, the ipsilateral draining lymph nodes (DLN), the contralateral lymph nodes (non DLN) and the spleen were isolated for flow cytometry analysis.
(A) Number of FITC-positive cells in the different lymphatic organs.
(B) Percentage of FITC-positive cells within defined immune cell populations.
Each dot represents one mouse. Bars represent mean ± SEM. Asterisks (*, P<0.001) indicate significant differences when comparing FITC-NP treated mice with PBS-treated mice using two-way ANOVA followed by Bonferroni's multiple comparison test.**

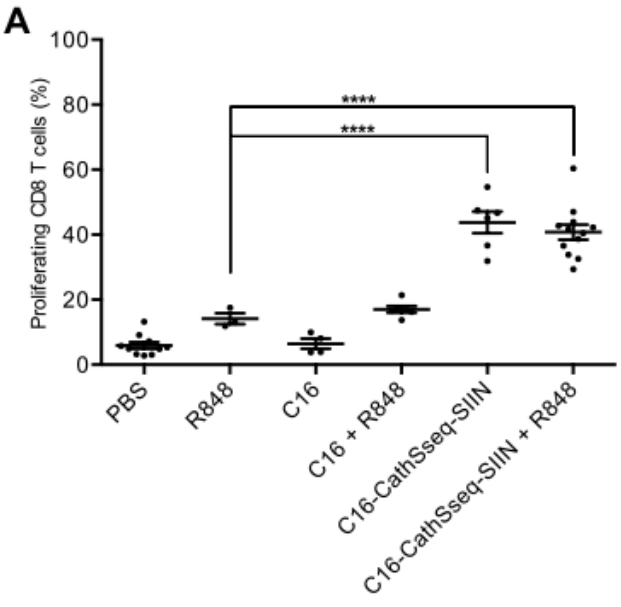

Figure VI-13: SIINFEKL-containing spider silk particles induce antigen-dependent T-cell proliferation *in vivo*. 10^6 CFSE-labelled CD3+CD8+ OT-I cells in 100 µL of PBS were injected intravenously into mice (each dot represents one mouse). 18 hours later, mice were vaccinated with spider silk NPs (505 µg NP in 100 µL PBS per mouse). R848 (25 µg) was used as adjuvant. 3 days after vaccination, the DLN were isolated for flow cytometry analysis to determine the proliferation of CD3+CD8+ CFSE-labelled OT-I cells. Each dot represents one mouse. Bars represent mean ± SEM. Asterisks (**, P<0.0001) indicate significant differences with R848-treated control using one-way ANOVA followed by Dunnett's multiple comparison test.**

The results presented in Figure VI-8 to Figure VI-13 summarize the experiments performed by Inès Mottas at the University of Fribourg. The cytotoxicity test readout by a Propidium iodide (PI) assay used in conjunction with Annexin V demonstrated once more, that eADF4(C16) protein particles are well tolerated by BMDCs (Figure VI-8). The flow cytometry results in Figure VI-8 C clearly show, that the percentage of living cells did not differ between untreated and eADF4(C16) protein particle incubated cells. In addition, the MTT test results proved our previously published results [36] and confirmed the statement, that native eADF4(C16) as well as eADF4(C16) hybrid protein particles were well tolerated by cells [36]. The fact, that eADF4(C16) protein particles did not induce BMDC immunogenicity (Figure VI-9) was important for a vaccine delivery system. In our approach, the eADF4(C16) protein particles served as a delivery system for the epitope SIINFEKL. According to the review of Singh et al. particulate vaccine carrier systems could be used for a co-administration of immunostimulatory adjuvants together with antigens if required [37]. The approach of combining an antigen, a delivery system and/or an immunostimulatory adjuvant, allows an individual design for various vaccines. In our case, the lack of immunogenicity of the eADF4(C16) protein particles is an important prerequisite. Particles with an intrinsic immunogenicity could most likely alter the effect of the SIINFEKL loaded eADF4(C16) protein particles versus the control SIINFEKL antigen. The presence of immunostimulatory contaminations (like endotoxins) could also lead to false results in the experiments [38].

Figure VI-10 illustrates the uptake of eADF4(C16) hybrid protein particles containing the cathepsin cleavable linker sequence. The cellular uptake of native eADF4(C16) protein particles and the uptake of eADF4(C16) hybrid protein particles of the first generation (containing no cathepsin cleavable linker) has been already shown in chapter 5 of this thesis. The merged images in Figure VI-10 C & D clearly show, that the second generation eADF4(C16) hybrid protein particles were processed in the lysosomal compartment within the cell after uptake. That means, that the newly designed second generation eADF4(C16) hybrid protein particles were in contact with the cathepsin enzymes, which were required for the cleavage and further processing of the SIINFEKL epitope [11]. The missing activation of T cells using the first generation eADF4(C16) hybrid protein particles was the reason for the introduction of the cleavable linker sequences. Figure VI-11 demonstrates that the introduction of the cathepsin S and cathepsin B cleavable linker sequences enabled the release of SIINFEKL, which led to an induction of the T cell proliferation *in vitro*. However, the eADF4(C16)-CatS hybrid protein particles were more effective in inducing a T cell proliferation compared to the eADF4(C16)-CatB hybrid protein particles. This result can be explained by the *in vitro* release experiments performed with cathepsin S and B enzymes (Figure

VI-5). Within the first 24 hours, the release of SIINFEKL from the eADF4(C16)-CatS hybrid protein particles using the cathepsin S enzyme was more than twice as effective compared to the eADF4(C16)-CatB hybrid protein particles, but leveled out to the end of the incubation time. The same trend, even more pronounced than in Figure VI-5, was also observable for the *in vitro* experiments using BMDCs (Figure VI-11 A). The eADF4(C16)-CatS hybrid protein particles were even more effective than the to the soluble SIINFEKL which served as control. Although an induction of T cell proliferation was observable, the co-administration of the immunostimulatory adjuvant R848 was indispensable for the *in vitro* BMDC assay. The level of proliferating T cells without the administration of R848 is at the same level, irrespective of the applied sample (Figure VI-11).

Figure VI-12 and Figure VI-13 show the results of the *in vivo* experiments performed in mice (performed by Inès Mottas). Figure VI-12 shows that eADF4(C16) protein particles accumulated in the draining lymph node (DLN) after administration. We have already shown, that eADF4(C16) protein particles are taken up by macrophages and BMDCs in *in vitro* experiments. The results illustrated in Figure VI-12 B point towards an uptake by dendritic cells (CD11c+CD11b+) rather than by macrophages (CD11c-CD11b+) or leukocytes (CD11b-). To understand these uptake characteristics, the size of the administered eADF4(C16) protein particles used for the *in vivo* experiments has to be taken into account. The tested eADF4(C16) particles were in the size range between 242 nm and 254 nm with a net negative surface charge of -27 mV to -24 mV (Figure VI-6). Slütter et al. summarized in their article, that different cellular uptake mechanisms are known for particles [28]. While particles of different sizes can be taken up by receptor-mediated endocytosis and phagocytosis, the uptake mechanism of macropinocytosis is limited to submicroparticles [39]. At the same time, immature dendritic cells exhibit a larger capacity for macropinocytosis than macrophages [28, 40]. Taking these two facts together, the preferred eADF4(C16) protein particle uptake by dendritic cells as shown in Figure VI-12 B is plausible for this particle size.

After cellular uptake by dendritic cells, the lysosomal compartment within the dendritic cells provides an optimal processing environment for the cathepsin cleavable eADF4(C16) hybrid protein particles. Compared to macrophages, the higher lysosomal pH and the reduced proteolytic activity are described as advantageous properties of dendritic cells [41]. These attributes allow an endosomal escape of the linked antigen for further processing to T cells. Similarly, the lower pH and the increase of lysosomal and phagosomal proteolysis lead to an activation of CD4 cells [41]. The epitope SIINFEKL, which was used for the eADF4(C16) hybrid protein particle studies, interacted with CD8+ cells and should be presented via the MHC-I pathway. As the results in Figure

VI-13 demonstrate, the eADF4(C16)-CatS hybrid protein particles were able to induce a CD8+ T cell proliferation in the *in vivo* mouse model. Since the eADF4(C16) hybrid protein particles were used for the first time *in vivo*, the overall good tolerability of these particles, which has been already shown in various *in vitro* experiments, was confirmed by this experiment.

Much more important is the fact, that the eADF4(C16)-CatS hybrid protein particles were able to induce the same level of proliferating CD8+ T cells either with, but also without the use of the immunostimulatory adjuvant R848. This was not expected, because the immune response is usually higher after the co-administration of an immunostimulatory adjuvant [42]. In our case, we can hypothesize the reasons for that. We already know that the cathepsin S enzyme is most likely cleaving the linker sequences used in both eADF4(C16) hybrid protein particles. Trombetta et al. reviewed the mechanisms of antigen processing and reported about the strong participation of the cathepsin S enzyme in the epitope presentation process [40]. Although several cathepsin enzymes are expressed in APCs, especially the cathepsin S enzyme seems to play an important role in the antigen presentation by both, the MHC class II and MHC class I pathway [11]. This strong involvement may serve as an internal cell booster similar to the effect of an extra immunostimulatory adjuvant.

Our studies on the second generation eADF4(C16) hybrid protein particles showed that the selection of the cathepsin cleavable linker has a huge impact on the final outcome. While both linker sequences were already used in several studies, the cathepsin S cleavable linker performed much better in the studies described here. Furthermore, the cathepsin B cleavable linker was not cleaved by the cathepsin B enzyme, which was the initial intention. The final *in vivo* results showed that the results from the enzymatic release experiments were useful as predictive method for the eADF4(C16) hybrid protein particle performance. Since cloning and production of a new eADF4(C16) hybrid protein is time consuming, initial enzymatic release experiments could serve as predictive method in future. Because the analytical methods for the detection of the model antigen Ovalbumin are well established [43], we used the CD8 epitope SIINFEKL for the characterization of the eADF4(C16) hybrid protein particles.

The next important step would be the further development of the hybrid concept to include a disease relevant antigen to the eADF4(C16) hybrid model and verify the findings from this study. Although we focused on the delivery of antigen to dendritic cells by the particle in the submicron size range, the preparation of eADF4(C16) hybrid protein particles in the micrometer range could be an additional idea for the targeting of macrophages [28]. Several methods for the fabrication

of eADF4(C16) microparticles have already been published, however not all of them are applicable for an up-scalable and endotoxin free preparation [31, 36, 44].

4. Conclusion

In conclusion, this study shows the ability of genetically engineered eADF4(C16) hybrid particles as peptide delivery system to induce CD8 T cell proliferation in an *in vivo* mouse model. Moreover, the quantity of proliferating T cells is on the same level after co-administering an immunostimulatory adjuvant or after administration without an immunostimulatory adjuvant. Importantly, this observation is not connected to an increased cytotoxicity or pro-inflammatory effect of the eADF4(C16) hybrid particles themselves. These findings also demonstrate the ability of the all-aqueous particle preparation method to produce uniformly sized particles in the submicrometer range. The optimization of the salting out process led to a robust preparation of uniformly sized submicroparticles with an endotoxin level below the detection limit of the assay. The fact that particles from two fully independent eADF4(C16) hybrid protein particle batches led to comparable *in vivo* results indicates a high robustness of these constructs and the pertaining manufacturing process.

The effect of the linker sequence, which was essential for the presentation of the antigen, was shown by the comparison between the incubation by cathepsin B and cathepsin S enzymes. While the cathepsin B enzyme was not able to cleave any linker, the cathepsin S enzyme was capable of cleaving both linker sequences. Therefore, the eADF4(C16)-CatS hybrid protein particles were also more effective inducing an immune response *in vivo* than the eADF4(C16)-CatB hybrid protein particles in the present study. These findings should be the basis for future studies to screen more cathepsin cleavable linker sequences and incorporate other epitopes. The resulting modified eADF4(C16) hybrid particles could be used for other therapeutic fields where DC cell targeting and T cell activation are of special interest. With the present study, a sound basis for a new peptide based all-in-one particular vaccination system is set.

5. References

[1] M. C. Garnett, “Targeted drug conjugates: principles and progress,” *Adv. Drug Deliv. Rev.*, vol. 53, no. 2, pp. 171–216, 2001.

[2] J. Khandare and T. Minko, “Polymer–drug conjugates: Progress in polymeric prodrugs,” *Prog. Polym. Sci.*, vol. 31, no. 4, pp. 359–397, 2006.

[3] R. Duncan, L. W. Seymour, K. B. O'Hare, P. A. Flanagan, S. Wedge, I. C. Hume, K. Ulbrich, J. Strohalm, V. Subr, F. Spreafico, M. Grandi, M. Ripamonti, M. Farao, and A. Suarato, "Preclinical evaluation of polymer-bound doxorubicin," *J. Control. Release*, vol. 19, no. 1–3, pp. 331–346, 1992.

[4] K. Kunath, P. Kopečková, T. Minko, and J. Kopeček, "HPMA copolymer–anticancer drug–OV-TL16 antibody conjugates. 3. The effect of free and polymer-bound Adriamycin on the expression of some genes in the OVCAR-3 human ovarian carcinoma cell line," *Eur. J. Pharm. Biopharm.*, vol. 49, no. 1, pp. 11–15, 2000.

[5] H. Soyez, E. Schacht, and S. Vanderkerken, "The crucial role of spacer groups in macromolecular prodrug design," *Adv. Drug Deliv. Rev.*, vol. 21, no. 2, pp. 81–106, 1996.

[6] G. Cavallaro, M. Campisi, M. Licciardi, M. Ogris, and G. Giammona, "Reversibly stable thiopolyplexes for intracellular delivery of genes," *J. Control. Release*, vol. 115, no. 3, pp. 322–334, 2006.

[7] G. F. Walker, C. Fella, J. Pelisek, J. Fahrmeir, S. Boeckle, M. Ogris, and E. Wagner, "Toward Synthetic Viruses: Endosomal pH-Triggered Deshielding of Targeted Polyplexes Greatly Enhances Gene Transfer in vitro and in vivo," *Mol. Ther.*, vol. 11, no. 3, pp. 418–425, 2005.

[8] C. M. Dawidczyk, C. Kim, J. H. Park, L. M. Russell, K. H. Lee, M. G. Pomper, and P. C. Searson, "State-of-the-art in design rules for drug delivery platforms: Lessons learned from FDA-approved nanomedicines," *J. Control. Release*, vol. 187, pp. 133–144, 2014.

[9] B. Turk, D. Turk, and V. Turk, "Lysosomal cysteine proteases: more than scavengers," *Biochim. Biophys. Acta - Protein Struct. Mol. Enzymol.*, vol. 1477, no. 1–2, pp. 98–111, 2000.

[10] V. Turk, "Lysosomal cysteine proteases: facts and opportunities," *EMBO J.*, vol. 20, no. 17, pp. 4629–4633, 2001.

[11] K. Honey and A. Y. Rudensky, "Lysosomal cysteine proteases regulate antigen presentation," *Nat. Rev. Immunol.*, vol. 3, no. 6, pp. 472–482, 2003.

[12] M. M. Mohamed and B. F. Sloane, "Cysteine cathepsins: multifunctional enzymes in cancer," *Nat. Rev. Cancer*, vol. 6, no. 10, pp. 764–775, 2006.

[13] J. J. Peterson and C. F. Meares, "Cathepsin Substrates as Cleavable Peptide Linkers in Bioconjugates, Selected from a Fluorescence Quench Combinatorial Library," *Bioconjug. Chem.*, vol. 9, no. 5, pp. 618–626, 1998.

[14] R. Ménard, E. Carmona, C. Plouffe, D. Brömme, Y. Konishi, J. Lefebvre, and A. C. Storer, "The specificity of the S1' subsite of cysteine proteases," *FEBS Lett.*, vol. 328, no. 1–2, pp. 107–110, 1993.

[15] G. Lalmanach, C. Serveau, M. Brillard-Bourdet, J. R. Chagas, R. Mayer, L. Juliano, and F. Gauthier, "Conserved cystatin segments as models for designing specific substrates and inhibitors of cysteine proteinases," *J. Protein Chem.*, vol. 14, no. 8, pp. 645–653, 1995.

[16] M. L. Biniossek, D. K. Nägler, C. Becker-Pauly, and O. Schilling, "Proteomic Identification of Protease Cleavage Sites Characterizes Prime and Non-prime Specificity of Cysteine Cathepsins B, L, and S," *J. Proteome Res.*, vol. 10, no. 12, pp. 5363–5373, 2011.

[17] J. J. Peterson and C. F. Meares, "Enzymatic Cleavage of Peptide-Linked Radiolabels from Immunoconjugates," *Bioconjug. Chem.*, vol. 10, no. 4, pp. 553–557, 1999.

[18] Y. Li, "Cathepsin B-cleavable doxorubicin prodrugs for targeted cancer therapy (Review)," *Int. J. Oncol.*, vol. 42, no. 2, pp. 373–383, 2012.

[19] C. C. Fraser, D. H. Altreuter, P. Ilyinskii, L. Pittet, R. A. LaMothe, M. Keegan, L. Johnston, and T. K. Kishimoto, "Generation of a universal CD4 memory T cell recall peptide effective in humans, mice and non-human primates," *Vaccine*, vol. 32, no. 24, pp. 2896–2903, 2014.

[20] G. L. DeNardo and S. J. DeNardo, "Evaluation of a Cathepsin-Cleavable Peptide Linked Radioimmunoconjugate of a Panadenocarcinoma MAb, m170, in Mice and Patients," *Cancer Biother. Radiopharm.*, vol. 19, no. 1, pp. 85–92, 2004.

[21] T. Kwon, J. Park, J. Yang, D. S. Yoon, S. Na, C.-W. Kim, J.-S. Suh, Y.-M. Huh, S. Haam, and K. Eom, "Nanomechanical In Situ Monitoring of Proteolysis of Peptide by Cathepsin B," *PLoS One*, vol. 4, no. 7, p. e6248, 2009.

[22] Y. E. Kurtoglu, M. K. Mishra, S. Kannan, and R. M. Kannan, "Drug release characteristics of PAMAM dendrimer-drug conjugates with different linkers," *Int J Pharm*, vol. 384, no. 1–2, pp. 189–194, 2010.

[23] N. Lutzner and H. Kalbacher, "Quantifying cathepsin S activity in antigen presenting cells using a novel specific substrate," *J Biol Chem*, vol. 283, no. 52, pp. 36185–36194, 2008.

[24] W. Shi, S. M. Ogbomo, N. K. Wagh, Z. Zhou, Y. Jia, S. K. Brusnahan, and J. C. Garrison, "The influence of linker length on the properties of cathepsin S cleavable 177Lu-labeled HPMA copolymers for pancreatic cancer imaging," *Biomaterials*, vol. 35, no. 22, pp. 5760–5770, 2014.

[25] S. M. Ogbomo, W. Shi, N. K. Wagh, Z. Zhou, S. K. Brusnahan, and J. C. Garrison, "177Lu-labeled HPMA copolymers utilizing cathepsin B and S cleavable linkers: synthesis, characterization and preliminary in vivo investigation in a pancreatic cancer model," *Nucl Med Biol*, vol. 40, no. 5, pp. 606–617, 2013.

[26] M. Hofer, G. Winter, and J. Myschik, "Recombinant spider silk particles for controlled delivery of protein drugs," *Biomaterials*, vol. 33, no. 5, pp. 1554–1562, 2012.

[27] K. Spieß, S. Wohlrab, and T. Scheibel, "Structural characterization and functionalization of engineered spider silk films," *Soft Matter*, vol. 6, no. 17, pp. 4168–4174, 2010.

[28] B. Slütter and W. Jiskoot, "Sizing the optimal dimensions of a vaccine delivery system: a particulate matter," *Expert Opin. Drug Deliv.*, vol. 13, no. 2, pp. 167–170, 2016.

[29] V. B. Joshi, S. M. Geary, and A. K. Salem, "Biodegradable Particles as Vaccine Delivery Systems: Size Matters," *AAPS J.*, vol. 15, no. 1, pp. 85–94, 2013.

[30] C. Foged, B. Brodin, S. Frokjaer, and A. Sundblad, "Particle size and surface charge affect particle uptake by human dendritic cells in an in vitro model," *Int J Pharm*, vol. 298, no. 2, pp. 315–322, 2005.

[31] U. K. Slotta, S. Rammensee, S. Gorb, and T. Scheibel, "An Engineered Spider Silk Protein Forms Microspheres," *Angew. Chemie Int. Ed.*, vol. 47, no. 24, pp. 4592–4594, 2008.

[32] T. P. King, "Separation of proteins by ammonium sulfate gradient solubilization," *Biochemistry*, vol. 11, no. 3, pp. 367–371, 1972.

[33] Y. Yoneda, S. C. J. Steiniger, K. Čapková, J. M. Mee, Y. Liu, G. F. Kaufmann, and K. D. Janda, "A cell-penetrating peptidic GRP78 ligand for tumor cell-specific prodrug therapy," *Bioorg. Med. Chem. Lett.*, vol. 18, no. 5, pp. 1632–1636, 2008.

[34] B. Schmid, D.-E. Chung, A. Warnecke, I. Fichtner, and F. Kratz, "Albumin-Binding Prodrugs of Camptothecin and Doxorubicin with an Ala-Leu-Ala-Leu-Linker That Are Cleaved by Cathepsin B: Synthesis and Antitumor Efficacy," *Bioconjug. Chem.*, vol. 18, no. 3, pp. 702–716, 2007.

[35] D. A. Putnam, J.-G. Shiah, and J. Kopeček, "Intracellularly biorecognizable derivatives of 5-fluorouracil," *Biochem. Pharmacol.*, vol. 52, no. 6, pp. 957–962, 1996.

[36] M. Lucke, G. Winter, and J. Engert, "The effect of steam sterilization on recombinant spider silk particles," *Int. J. Pharm.*, vol. 481, no. 1–2, pp. 125–131, 2015.

[37] M. Singh, A. Chakrapani, and D. O'Hagan, "Nanoparticles and microparticles as vaccine-delivery systems," *Expert Rev. Vaccines*, vol. 6, no. 5, pp. 797–808, 2007.

[38] M. R. Geier, H. Stanbro, and C. R. Merril, "Endotoxins in commercial vaccines," *Appl. Envir. Microbiol.*, vol. 36, no. 3, pp. 445–449, 1978.

[39] F. Sallusto, "Dendritic cells use macropinocytosis and the mannose receptor to concentrate macromolecules in the major histocompatibility complex class II compartment: downregulation by cytokines and bacterial products," *J. Exp. Med.*, vol. 182, no. 2, pp. 389–400, 1995.

[40] E. S. Trombetta and I. Mellman, "Cell biology of antigen processing in vitro and in vivo," *Annu Rev Immunol*, vol. 23, pp. 975–1028, 2005.

[41] M. Samie and P. Cresswell, “The transcription factor TFEB acts as a molecular switch that regulates exogenous antigen-presentation pathways.,” *Nat. Immunol.*, vol. 16, no. 7, pp. 729–736, 2015.

[42] D. T. O’Hagan and M. Singh, “Microparticles as vaccine adjuvants and delivery systems,” *Expert Rev. Vaccines*, vol. 2, no. 2, pp. 269–283, 2003.

[43] F. G. Gao, V. Khammanivong, W. J. Liu, G. R. Leggatt, I. H. Frazer, and G. J. P. Fernando, “Antigen-specific CD4+ T-Cell Help Is Required to Activate a Memory CD8+ T Cell to a Fully Functional Tumor Killer Cell,” *Cancer Res.*, vol. 62, no. 22, pp. 6438–6441, 2002.

[44] A. Lammel, M. Schwab, U. Slotta, G. Winter, and T. Scheibel, “Processing conditions for the formation of spider silk microspheres,” *ChemSusChem*, vol. 1, no. 5, pp. 413–416, 2008.

VII. NEBULIZATION OF EADF4(C16) PROTEIN PARTICLES

1. Introduction

Pulmonary drug delivery of active pharmaceutical ingredients (API) is used for two fields of application. The first one is the common strategy to locally treat respiratory diseases in the lung. The direct application of the drug to the target area allows higher local API concentrations while at the same time adverse side effects of a systemic application are minimized [1, 2]. The local drug delivery of steroids or bronchodilators is frequently used for the treatment of respiratory diseases like asthma, chronic obstructive pulmonary disease (COPD) and cystic fibrosis (CF) [3, 4]. Moreover, inhalative antibiotics like aztreonam, ciprofloxacin or gentamicin are used against lower airway infections or as treatment of airway infections of CF patients [5, 6]. The only approved and available inhalative biopharmaceutical for local therapy is Dornase alfa (DNase, trade name Pulmozyme®) for the hydrolysis of DNA in the mucus of CF patients [7].

Systemic drug delivery by pulmonary drug deposition is the second field of application. The advantage to an intravenous delivery is the non-invasive route of drug administration. The lower respiratory airways offer a large surface area interfacing with the blood circulating system [8, 9]. The thin epithelial barrier of approx. 0.1-1 µm of the lower airways' alveolar system facilitates high drug absorption into the blood stream [10, 11]. Moreover, the lower enzymatic activity compared to the gastro-intestinal (GI) tract and the avoidance of a first pass effect by the liver are beneficial for a systemic drug delivery [12, 13]. Although the success of inhaled nicotine by cigarettes or the inhalative administration of anesthetics clearly demonstrate the efficacy of systemic API application, no approved product for the pulmonary administration for systemic activity is yet on the market [14, 15]. Research mainly focused on the administration of inhalable insulin as alternative to the approved subcutaneous insulin for the treatment of diabetes.

However, both marketed inhalable insulin formulations (Exubera® and Afrezza®) were already withdrawn. A major challenge of systemic drug application by pulmonary administration is the achievement of adequate and reproducible plasma concentrations [16]. To overcome the bad efficiency or reproducibility, particulate drug delivery systems may serve as API depot for controlled drug release. The use of nebulized submicroparticles can improve API deposition in the lower airways [17].

While new developments in device design can further promote pulmonary drug delivery, pulmonary vaccination can be used to systemically induce immune response. Following the natural route of many pathogens, a lot of immune cells are located in the mucosa of oral, nasal or pulmonary tissue [18]. As a result of this, several reviews underline the enhanced antigenicity of pulmonary administered vaccines [19, 20]. The ease of handling of stabilized pulmonary vaccines and the lower costs due to the elimination of a cold chain could provide a huge benefit to the entire health system [18]. A first large scale study using pulmonary vaccination against measles was realized in Mexcio [21]. The results showed that the vaccination of children was more effective using pulmonary instead of subcutaneous vaccination [22]. The current *Measles Aerosol Vaccine Project* of the WHO is based on such results and is currently collecting data for a licensed pulmonary measles vaccine system [23]. The knowledge of the specific amino acid sequence of the pathogenic antigen and improvements in the field of recombinant DNA technology led to the development of peptide and plasmid DNA vaccination. Using solely the peptide or plasmid DNA and not the full pathogen has the advantage to instruct the immune system strictly to the disease-specific epitope thus limiting autoimmune toxicity. However, DNA plasmids are weakly immunogenic [20] and peptide vaccination has shown limited success due to rapid protease degradation [24].

Peptide incorporation into particulate delivery systems is one solution to overcome the fast degradation. Spider silk particles have already demonstrated their ability as carrier system for sensitive molecules like peptides or proteins [25–27]. By recombinant engineering of the eADF4(C16) spider silk protein, attachment of the $OVA_{257-264}$ epitope (SIINFEKL) was possible (see chapter 5 and chapter 6). Therefore, an administration of eADF4(C16) protein particles to the lung seems to be an attractive delivery attempt for pulmonary vaccination, because the peptide is protected by the particles and will be released once the particles have been taken up by antigen presenting cells. Thus, we performed a nebulization study comparing a pneumatic jet nebulizer (PARI TurboBOY) with an active VM nebulizer (PARI eFlow®). Three differently sized eADF4(C16) protein particles were prepared by different fabrication methods to evaluate the optimal particle size for the deposition to the lower airways.

2. Materials and methods

2.1. Materials

2.1.1. Recombinantly produced spider silk protein eADF4(C16)

The spray dried eADF4(C16) protein was provided by AMSilk GmbH (Martinsried, Germany). This bioengineered spider silk protein is based on the natural amino acid sequence of the ADF4 spidroin from *A. diadematus*. The design resulted in a molecular mass of 47.7 kDa, which is a result of one T7 Tag and sixteen repeats of the amino acid sequence GSSAAAAAAAASGPGGYGPENQGPSGPGGYGPGGP. The theoretical isoelectric point of the eADF4(C16) protein is 3.48, resulting in a net negative charge at a physiological pH of 7.4 An extinction coefficient of 46,400 $M^{-1}*cm^{-1}$ at 276 nm was used for the concentration determination by UV-Vis-spectroscopy.

2.1.2. Chemicals and reagents

Highly purified water (HPW) used in this study was generated by a purelab® device (ELGA LabWater, Celle, Germany). Sodium hydroxide solution (1 mol/L, EMPROVE® bio), di-potassium hydrogen phosphate (EMPROVE bio, European Pharmacopoeia (Ph. Eur.), British Pharmacopoeia (BP)), potassium dihydrogen phosphate (EMPROVE bio, Ph. Eur., BP, United States National Formulary (NF)) and the fuming hydrochloric acid 37% (EMPROVE bio, Ph. Eur, BP, Japanese Pharmacopoeia (JP)) were purchased from Merck KGaA, Darmstadt, Germany. Sodium chloride (NaCl, AnalaR NORMAPUR) was obtained from VWR Chemicals, Darmstadt, Germany. Tris(hydroxymethyl)aminomethane (Tris, Trizma® base, purity ≥99.9%) was purchased from Sigma Aldrich GmbH, Steinheim, Germany. Guanidinium thiocyanate (for molecular biology) was purchased from AppliChem GmbH, Darmstadt, Germany.

2.2. Methods

2.2.1. Particle preparation

The eADF4(C16) particles used for the nebulization study were prepared by two different preparation methods. The first one was particle preparation by a micromixing system [26], the second one was particle preparation by dialysis [28]. Both systems have been described earlier and were slightly modified to meet our requirements. The eADF4(C16) protein powder was dissolved in a 6 M guanidinium thiocyanate solution and subsequently dialyzed against a 10 mM

Tris(hydroxymethyl)aminomethane(Tris)/HCl solution at 2-8°C. A dialysis membrane with a molecular weight cut-off of 8,000 Da (Spectrum Laboratories, Rancho Dominguez, USA) was used. After dialysis, the solution was centrifuged and filtered through a 0.2 µm polyethersulfone (PES) filter (VWR International, Radnor, USA). The concentration of eADF4(C16) protein in solution was determined by an Agilent 8453 UV-Vis spectrophotometer (Agilent, Waldbronn, Germany) using a molar extinction coefficient of eADF4(C16) at 276 nm (ε = 46,400 $M^{-1}*cm^{-1}$). This solution was further adjusted to the desired concentrations for particle preparation with a filtered 10 mM Tris/HCl solution.

2.2.1.1. Submicroparticle preparation using a micromixing system

Processing of the spider silk solution into submicroparticles was carried out by micromixing using a high pressure syringe pump system. Both cylinders of the syringe pump system (Model 100 DX and Series D pump controller, Teledyne Isco, Lincoln, USA) were filled with pre-tempered eADF4(C16) solution (c=1.0 mg/ml) and pre-tempered 4 M ammonium sulfate solution of 80°C. The solutions were pumped at a high flow rate of 50 ml/min to a T-shape mixing element (inner diameter 0.5 mm, P-727 PEEK tee, Upchurch Scientific, Oak Harbor, USA) leading to an outlet tubing (inner diameter 0.5 mm, 1532 PEEK Tubing, Upchurch Scientific, Oak Harbor, USA) for suspension collection.

2.2.1.2. Microparticle preparation using a micromixing system

Processing of the spider silk solution into microparticles was carried out by micromixing using the same high pressure syringe pump system described before. Both cylinders of the syringe pump system (Model 100 DX and Series D pump controller, Teledyne Isco, Lincoln, USA) were filled with eADF4(C16) solution (c=10.0 mg/ml) and 2 M potassium phosphate solution (pH 8) at room temperature. The solutions were pumped at a low flow rate of 2.0 ml/min to a T-shape mixing element (inner diameter 0.5 mm, P-727 PEEK tee, Upchurch Scientific, Oak Harbor, USA) leading to an outlet tubing (inner diameter 1.0 mm, 1538 PEEK Tubing, Upchurch Scientific, Oak Harbor, USA) for suspension collection.

2.2.1.3. Microparticle preparation using dialysis

Simple dialysis was used to fabricate larger eADF4(C16) microparticles. The eADF4(C16) solution (c=10 mg/ml) was filled into a dialysis membrane with a molecular weight cut-off of 8,000 Da (Spectrum Laboratories, Rancho Dominguez, USA) and dialyzed against a 2 M potassium phosphate solution (pH 8) for 16 hours at room temperature.

Finally, eADF4(C16) particle suspensions from all three preparation methods were subsequently centrifuged at 14,000 rpm (SIGMA 4K15, Sigma Laborzentrifugen, Osterode am Harz, Germany) and washed with highly purified water (HPW) three times. A two minute ultrasonication (Sonopuls HD 3200, Bandelin electronic, Berlin, Germany) step completed the particle preparation procedure. The particle concentrations in mg/ml were determined gravimetrically after drying the particles under vacuum (13 mbar) overnight.

2.2.2. eADF4(C16) particle aerosolization

For aerosolization of eADF4(C16) particles, two different nebulization systems were evaluated. Pari LC Plus® nebulizer and Pari TurboBoy® compressor (PARI GmbH, Starnberg, Germany) were selected as nebulization system. Additionally, Pari eFlow® (PARI GmbH, Starnberg, Germany) was chosen as representative vibrating mesh nebulizer. Both nebulizers were filled with 2.5 ml of eADF4(C16) particle suspensions at concentrations of 1.0 mg/ml and 2.0 mg/ml. eADF4(C16) particles were diluted with highly purified water (HPW) to the desired concentration immediately prior to nebulization.

2.2.3. Nebulization efficiency (NE)

Nebulization efficiency (NE) was determined for both systems by weighing the nebulization device (ND) on a lab balance before nebulization and after end of operation. The latter was defined as time point where no more vapor was emitted from the nebulization device. The NE was calculated using equations (1) and (2).

(1) $$\text{Nebulization efficiency}\ (\%) = \frac{\text{Aerosolized eADF4(C16) suspension mass}}{\text{eADF4(C16) suspension mass loaded in nebulizer}} \text{x}100$$

(2) $$\text{Aerosolized drug mass}\ (\text{mg}) = \text{eADF4(C16) suspension mass loaded in ND} - \text{eADF4(C16)suspension mass remaining in ND post nebulization}$$

To determine the post nebulization weight, the whole instrument including the mouth piece was put on a lab balance after end of operation. This procedure ensured that only those portions of the eADF4(C16) particle suspensions that completely left the nebulization device were considered relevant for the NE calculation, whereas leftover material in the device reservoir was evaluated with respect to particle size and possible particle aggregation.

2.2.4. Deposition study

For the assessment of the deposition of eADF4(C16) particles from the nebulizer devices a twin-stage glass impinger (TSI) apparatus type A (Copley Scientific Ltd., Nottingham, UK) according to Ph. Eur chapter 2.9.18 was used. Highly purified water was used as suspension medium for the collection stages. 7 ml and 30 ml were filled in the upper and lower collection stages, respectively. The TSI was assembled and connected to a GLAX.SING.STA. pump (Erweka GmbH, Heussenstamm, Germany). The airflow through the TSI was adjusted to 60 l/min to simulate physiologic breathing air flow. The nebulization devices were connected with a rubber mouth piece adapter. The pump was started first to establish the airflow through the TSI and after 10 seconds the nebulization device was switched on. The airflow was stopped 30 seconds after end of operation and the total nebulization time was documented. The TSI was disassembled and volumes of stage 1 and 2 were collected in two graduated cylinders. Both stages were washed with additional HPW (stage1: 3 ml, stage 2: 5 ml) to recover residual eADF4(C16) particles. The wash solutions were united with the volumes of stages 1 and 2, respectively. Three TSI replicates were performed for each sample and concentration. The concentration of eADF4(C16) particles in the volume of the nebulization device reservoir as well as the concentration of stage 1 and 2 were analyzed photometrically at 546 nm. The concentration of the eADF4(C16) particles was calculated relative to calibration curves.

For the calibration of the photometric assay, each particle batch was diluted with HPW to the desired particle concentrations (concentrations of the submicroparticle batch: 0, 10, 20, 50, 100, 250 and 500 µg/ml. Concentrations of both microparticle batches: 0, 1, 5, 10, 20, 50, 100 and 200 µg/ml). The turbidity of the measurements was used for the calculation of calibration curves.

The eADF4(C16) particle fraction in stage 2 was considered as the respirable fraction (RF) as part of the total nebulized particle fraction and was calculated using equation (3).

(3) $$\text{Respirable fraction } (\%) = \frac{\text{eADF4(C16) particle fraction deposited in stage 2}}{\text{Nebulized eADF4(C16) particle fraction}} \text{x} 100$$

2.3. Analytical methods

2.3.1. eADF4(C16) particle size

Particle size was analyzed before and after nebulization to detect possible aggregation or fragmentation by the nebulization devices. Particles below 1 µm were analyzed by dynamic light

scattering, particles larger than 1 µm were analyzed by laser diffraction spectrometry.

2.3.1.1. Dynamic light scattering (DLS)

Particle size and size distribution of submicroparticles were measured as described in chapter 2.

2.3.1.2. Laser Diffraction Spectrometry (LDS)

Particle size and size distribution of microparticles were measured as described in chapter 3. If required, samples were diluted with water directly before each measurement to obtain transmittance values of 74.0-98.8%.

2.3.2. Scanning electron microscopy (SEM)

SEM measurements of eADF4(C16) particle suspensions were conducted as described in chapter 2.

3. Results and Discussion

The well characterized native eADF4(C16) protein was used to fabricate particles of three different sizes to evaluate a possible nebulization application for eADF4(C16) protein particles. The fabrication of particles in the submicron range was realized by the micromixing method described by Hofer et al. [26]. The conditions used for this process resulted in a particle size of 255.95 nm. These particles were labeled as the 250 nm particle group for the upcoming nebulization studies. The micromixing method was adopted for the preparation of particles in the low micrometer range. Therefore, the preparation temperature was lowered to room temperature, the eADF4(C16) protein concentration was 10-fold increased to 10 mg/ml and the flow rate of the pumps was adjusted to 2 ml/min, which corresponds to a 25-fold reduced mixing speed. Additionally, the inner diameter of the T-shape mixing outlet tubing was increased to 1.0 mm to allow particle forming to a larger size. The resulting particles were 2.52 µm in size. This particle group was titled as 2.5 µm particles for the nebulization experiments. The last particle preparation method used simple dialysis of the eADF4(C16) protein solution against a 2 M potassium phosphate solution for 16 hours at room temperature [28]. The particles prepared by dialysis were the largest of the studied particles with a mean diameter of 4.67 µm. These particles were labeled as 4.7 µm group for the eADF4(C16) protein particle nebulization studies. Figure VII-1 shows SEM micrographs of the fabricated particles prior to nebulization at different magnifications.

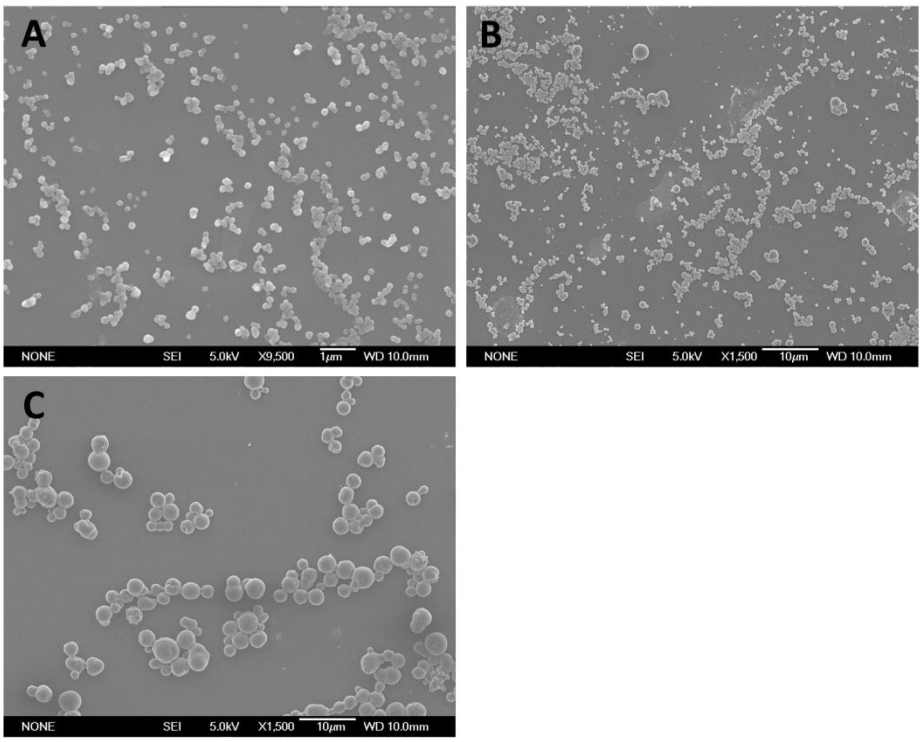

Figure VII-1: SEM micrographs of eADF4(C16) protein particles at a magnification of 9,500x (A) and 1,500x (B and C).
A) Particles prepared with the micromixing device, resulting in a mean particle size of 255.95 nm.
B) Particles prepared with the adopted micromixing device, resulting in a mean particle size of 2.52 µm.
C) Particles prepared by dialysis against 2 M potassium phosphate, resulting in a mean particle size of 4.67 µm.

All three particle batches are below the particle size limit of 5 µm, which is necessary for a pulmonary delivery into the lower airways [29]. The three differently sized eADF4(C16) protein particles were suspended in highly purified water (HPW) at concentrations of 1 mg/ml and 2 mg/ml.

The final nebulization efficiency is highly influenced by the type of nebulizer, which is used for the pulmonary administration of the particles [29]. For this reason, a direct comparison of a jet nebulizer, which has been in use already since decades, and an active vibrating mesh (VM) nebulizer, which was established in the early 2000s, was performed.

First, the deposition of the differently sized eADF4(C16) protein particles was evaluated using a twin-stage glass impinger (TSI) apparatus. The amount of eADF4(C16) protein particles in the lower stage was used for the calculation of the respirable fraction RF. The results of this calculation are illustrated in Figure VII-2.

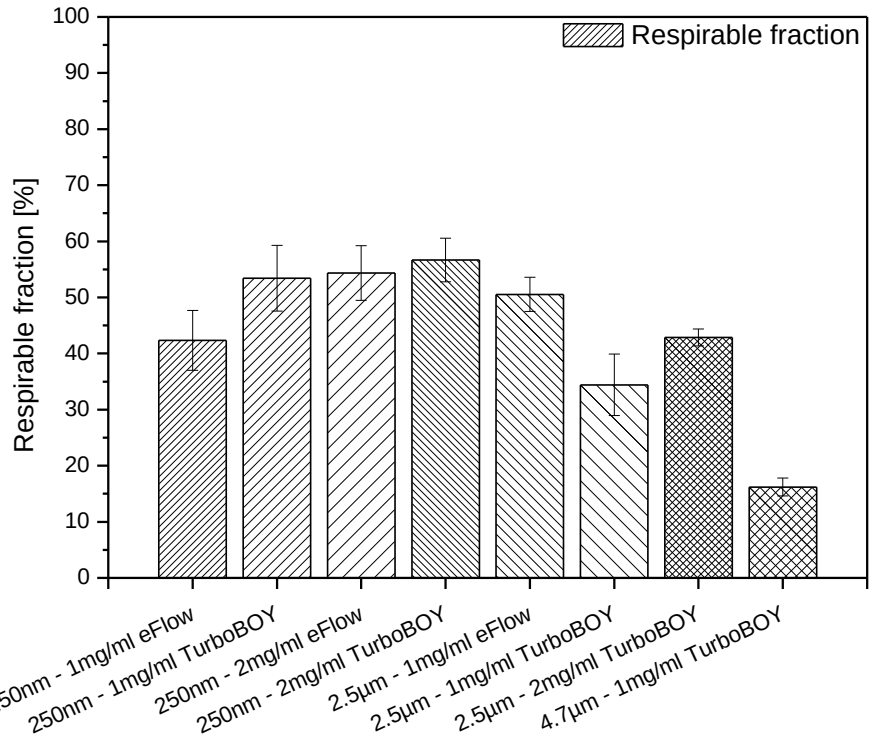

Figure VII-2: Impact of the particle size, particle concentration and nebulizer device on the respirable fraction (RF). The first term of the figure caption defines the size of the used particle suspension (250nm, 2.5 µm or 4 µm), the second term shows the concentration of the particles in the suspension (either 1 or 2 mg/ml) and the last term displays the used type of nebulizer (PARI eFlow or PARI TurboBOY).

The eADF4(C16) protein particles used for the nebulization studies showed a good deposition to the lower airways, resulting in a respirable fraction of up to 56.7% for the 250 nm eADF4(C16) protein particles aerosolized by the TurboBOY at a concentration of 2 mg/ml. However, only the eADF4(C16) protein particles smaller than 4.7 µm feature high RF values, whereas the 4.7 µm particles were mostly not able to reach the lower airways, which results in a RF of only 16.2%. The aerosolized 2.5 µm particle group showed RF values between 34.4% and 50.5% (Figure VII-2). With regards to values reported in the literature, the following conclusions can be drawn: similar values were reported by Fuchs et al. for the nebulization of 150 nm gelatin nanoparticles by a passive VM device, while the use of an active VM device resulted in slightly increased RF values [30]. In addition, the authors studied the performance of the particle nebulization by a metered dose inhaler (MDI). However, the MDI device was identified to be not be suitable for a nanoparticle delivery to the therapeutically relevant lower airways [30]. Liu et al. showed in their study using solid lipid nanoparticles with a size of approx. 110 nm that further optimization can significantly increase the RF [31]. The initial RF of around 40% was increased after the formulation was optimized to a final RF of 82.1% using an air-jet nebulizer. The type of nebulizer used also highly influenced the lung deposition of the 2.5 µm group in our study, as the deposition to the related

lower airways by the eFlow device was 1.5-fold more effective than by the TurboBOY. However, this was only true for the 1 mg/ml group. The eFlow was not able to nebulize both the higher concentrated 2.5 µm eADF4(C16) protein particles and the 4.7 µm eADF4(C16) protein particles, which were studied only at the lower concentration of 1 mg/ml. Although we never determined the viscosity of the eADF4(C16) protein particle suspension, the viscosity could be one reason for the nebulization problems with the eFlow device. Ghazanfari et al. proved that the viscosity is a critical factor affecting the aerosolization of suspensions [17]. The authors observed a prolonged nebulization time with increasing viscosity of a formulation. While the overall duration of nebulization, which was defined as the time from the start of the device until end of operation, was well below 10 minutes for the 250 nm particle group, the nebulization time of the eFlow device increased to 20 minutes for the 2.5 µm particle group at a concentration of 1 mg/ml.

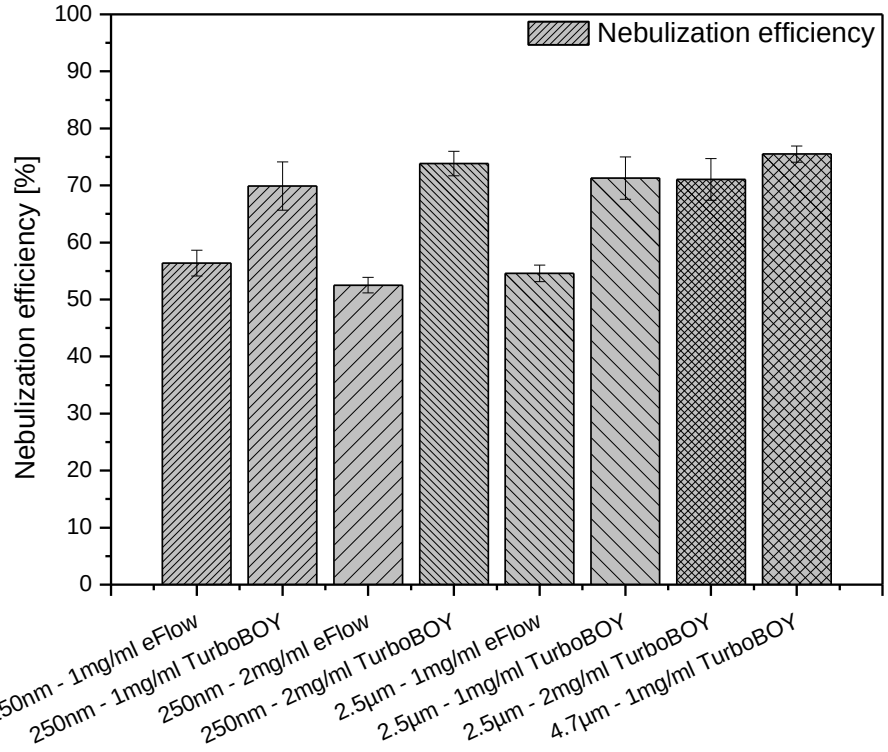

Figure VII-3: Dependence of the particle size, particle concentration and nebulizer device on the nebulization efficiency (NE). The first term of the figure caption defines the size of the used particle suspension (250nm, 2.5 µm or 4 µm), the second term shows the concentration of the particles in the suspension (either 1 or 2 mg/ml) and the last term displays the used type of nebulizer (PARI eFlow or PARI TurboBOY).

The good RF values of the eFlow device were somehow surprising after knowing the nebulization efficiency (NE) values illustrated in Figure VII-3. While the NE was around 70% for the TurboBOY, the NE values of the eFlow device were only between 52.5% and 56.4%. These results demonstrate, that a large amount of eADF4(C16) protein particles remained in the nebulization

device after end of operation, where no more vapor was emitted from the nebulization device. Neither the particle size nor the particle concentration had an effect on the NE, which remained constant within the repeated measurements for both devices. The relatively low NE values of the used devices could potentially be increased by the change to a different nebulizer. Fuchs et al. demonstrated with gelatin nanoparticles that NE values up to 97.8% are possible with an appropriate nebulization device [30]. While two of their three studied nebulizers showed NE values above 94%, the NE of their third device was only around 50%, which is comparable to the NE of the here studied eFlow device.

Second, the impact of the nebulization on the eADF4(C16) protein particle size was assessed. Therefore, fractions of the two impinger stages as well as a fraction of the residual volume in the nebulization device reservoir were analyzed by dynamic light scattering (particle size <1 µm) or by laser diffraction spectrometry (particles >1 µm). The results of the submicroparticles showed no clear trend towards a size separation between the first and second stage of the glass impinger (Figure VII-4 A). In addition, the residual particles in the device reservoir were in the same size range as the nebulized particles and did not show any aggregation. The aerosolization process did not alter the particle size of the submicroparticles compared to the control particles, which were analyzed along with the nebulized particles. On the contrary, the results of the microparticles displayed a separation between the first and second stage of the impinger and an accumulation of larger particles in the remaining volume of the device reservoir (Figure VII-4 B). The particle size of the microparticles on both stages of the glass impinger was smaller than the size of the control particles. This finding lead to the assumption that smaller microparticles were preferably aerosolized by the nebulization devices, whereas the larger particles accumulated in the remaining volume of the reservoir.

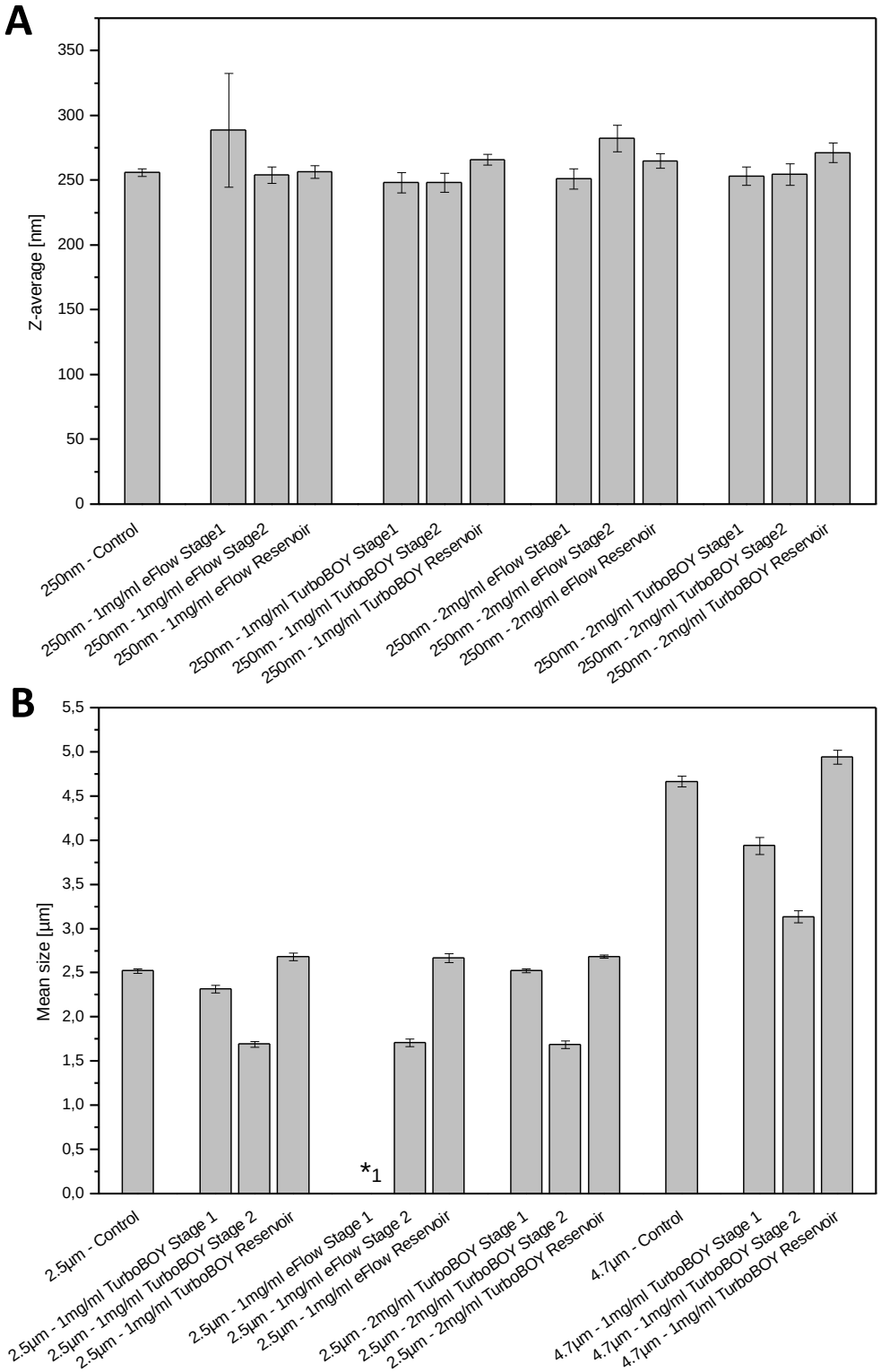

Figure VII-4: A) Particle size of eADF4(C16) protein submicroparticles determined by dynamic light scattering after nebulization in dependence of the particle concentration and nebulizer device. The size analysis was performed with fractions of the two impinger stages and a fraction of the remaining reservoir volume. Particles without nebulization were analyzed as control.
B) Particle size of eADF4(C16) protein microparticles determined by laser diffraction spectrometry after nebulization in dependence of the particle concentration and nebulizer device. The size analysis was performed with fractions of the two impinger stages and a fraction of the remaining reservoir volume. Particles without nebulization were analyzed as control.
$*_1$: The particle concentration of the fraction in the upper stage was too low to determine a reliable particle size.

The non-uniform distribution of the microparticles could result from sedimentation of these particles in water. The speed of sedimentation depends on the size or mass of the particles, which means that the smaller submicroparticles were more stable during the aerosolization time [32]. The high amount of the RF together with the uniform particle size distribution after nebulization leads to the conclusion to use of eADF4(C16) protein submicroparticles instead of microparticles for nebulization.

4. Conclusion

In this study, eADF4(C16) spider silk protein particles were used for a nebulization approach for the first time. We assessed the basic feasibility of eADF4(C16) protein particle aerosolization by the analysis of three different particle sizes at two different concentrations with two different nebulization devices. The results of the experiments demonstrated that pulmonary application of eADF4(C16) protein particles is generally feasible. Although we did no optimization of the eADF4(C16) protein particle formulation, high RF values were achieved for the 250 nm and 2.5 µm particles (Figure VII-2). The colloidal stability of the particles after nebulization was verified by the analysis of the particle size at the lower impinger stage. The present study focused on the feasibility of nebulization using unloaded eADF4(C16) protein particles. In a next step, the nebulization of drug loaded eADF4(C16) protein particles should be performed. As there is always a risk to lose loaded drug during the aerosolization process, the eADF4(C16) hybrid protein particles presented in chapter 6 could be a promising alternative. Due to the integration of the active pharmaceutical part into the amino acid sequence of the drug carrier molecule, the risk of drug loss during nebulization is very low. However, the possibility of particle aggregation of the eADF4(C16) protein particle suspension is still given. Therefore, the development of a dry powder inhaler (DPI) could provide a smart alternative to provide a long-term stable application form of eADF4(C16) protein particles. Hofer et al. already demonstrated the possibility to produce a dried eADF4(C16) protein particle powder by freeze drying [26]. The freeze-dried product could be used as an inhalative powder formulation. Claus et al. developed a dry powder inhalation system based on the disintegration and aerosolization of lyophilizates by an air impact [33]. Finally, the effect of aerosolized eADF4(C16) protein particles on living cells by an *in vitro* assay has to be demonstrated.

5. References

[1] A. Maillet, L. Guilleminault, E. Lemarié, S. Lerondel, N. Azzopardi, J. Montharu, N. Congy-Jolivet, P. Reverdiau, B. Legrain, C. Parent, D.-H. Douvin, J. Hureaux, Y. Courty, M. De Monte, P. Diot, G. Paintaud, A. Le Pape, H. Watier, and N. Heuzé-Vourc'h, "The Airways, a Novel Route for Delivering Monoclonal Antibodies to Treat Lung Tumors," *Pharm. Res.*, vol. 28, no. 9, pp. 2147–2156, 2011.

[2] G. Pilcer and K. Amighi, "Formulation strategy and use of excipients in pulmonary drug delivery," *Int. J. Pharm.*, vol. 392, no. 1–2, pp. 1–19, 2010.

[3] I. A. Yang, K. Fong, E. H. A. Sim, P. N. Black, and T. J. Lasserson, "Inhaled corticosteroids for stable chronic obstructive pulmonary disease," *Cochrane Database Syst. Rev.*, no. 2, p. CD002991, 2007.

[4] M. R. Littner, J. S. Ilowite, D. P. Tashkin, M. Friedman, C. W. Serby, S. S. Menjoge, and T. J. Witek, "Long-acting bronchodilation with once-daily dosing of tiotropium (Spiriva) in stable chronic obstructive pulmonary disease," *Am. J. Respir. Crit. Care Med.*, vol. 161, no. 4 Pt 1, pp. 1136–1142, 2000.

[5] D. Banerjee and D. Stableforth, "The Treatment of Respiratory Pseudomonas Infection in Cystic Fibrosis," *Drugs*, vol. 60, no. 5, pp. 1053–1064, 2000.

[6] B. K. Rubin and R. W. Williams, "Aerosolized Antibiotics for Non-Cystic Fibrosis Bronchiectasis," *Respiration*, vol. 88, no. 3, pp. 177–184, 2014.

[7] H. J. Fuchs, D. S. Borowitz, D. H. Christiansen, E. M. Morris, M. L. Nash, B. W. Ramsey, B. J. Rosenstein, A. L. Smith, and M. E. Wohl, "Effect of Aerosolized Recombinant Human DNase on Exacerbations of Respiratory Symptoms and on Pulmonary Function in Patients with Cystic Fibrosis," *N. Engl. J. Med.*, vol. 331, no. 10, pp. 637–642, 1994.

[8] J. S. Patton, "Mechanisms of macromolecule absorption by the lungs," *Adv. Drug Deliv. Rev.*, vol. 19, no. 1, pp. 3–36, 1996.

[9] J. S. Patton and P. R. Byron, "Inhaling medicines: delivering drugs to the body through the lungs," *Nat. Rev. Drug Discov.*, vol. 6, no. 1, pp. 67–74, 2007.

[10] N. Butz, C. Porté, H. Courrier, M. . Krafft, and T. . Vandamme, "Reverse water-in-fluorocarbon emulsions for use in pressurized metered-dose inhalers containing hydrofluoroalkane propellants," *Int. J. Pharm.*, vol. 238, no. 1–2, pp. 257–269, 2002.

[11] E. Rytting, J. Nguyen, X. Wang, and T. Kissel, "Biodegradable polymeric nanocarriers for pulmonary drug delivery," *Expert Opin. Drug Deliv.*, vol. 5, no. 6, pp. 629–639, 2008.

[12] A. Adjei, *Inhalation delivery of therapeutic peptides and proteins*. Informa Health Care, 1997.

[13] A. Tronde, B. Nordén, H. Marchner, A.-K. Wendel, H. Lennernäs, and U. H. Bengtsson, "Pulmonary Absorption Rate and Bioavailability of Drugs in Vivo in Rats: Structure–Absorption Relationships and Physicochemical Profiling of Inhaled Drugs," *J. Pharm. Sci.*, vol. 92, no. 6, pp. 1216–1233, 2003.

[14] I. Gonda, "Systemic Delivery of Drugs to Humans via Inhalation," *J. Aerosol Med.*, vol. 19, no. 1, pp. 47–53, 2006.

[15] C. A. Ruge, J. Kirch, and C.-M. Lehr, "Pulmonary drug delivery: from generating aerosols to overcoming biological barriers-therapeutic possibilities and technological challenges.," *Lancet. Respir. Med.*, vol. 1, no. 5, pp. 402–13, 2013.

[16] D. A. Edwards, A. Ben-Jebria, and R. Langer, "Recent advances in pulmonary drug delivery using large, porous inhaled particles.," *J. Appl. Physiol.*, vol. 85, no. 2, pp. 379–85, 1998.

[17] T. Ghazanfari, A. M. A. Elhissi, Z. Ding, and K. M. G. Taylor, "The influence of fluid physicochemical properties on vibrating-mesh nebulization," *Int. J. Pharm.*, vol. 339, no. 1–2, pp. 103–111, 2007.

[18] D. Lu and A. J. Hickey, "Pulmonary vaccine delivery," *Expert Rev. Vaccines*, vol. 6, no. 2, pp. 213–226, 2007.

[19] P. Sahdev, L. J. Ochyl, and J. J. Moon, "Biomaterials for Nanoparticle Vaccine Delivery Systems," *Pharm. Res.*, vol. 31, no. 10, pp. 2563–2582, 2014.

[20] M. Singh, A. Chakrapani, and D. O'Hagan, "Nanoparticles and microparticles as vaccine-delivery systems," *Expert Rev. Vaccines*, vol. 6, no. 5, pp. 797–808, 2007.

[21] F. T. Cutts, C. J. Clements, and J. V. Bennett, "Altenative Routes of Measles Immunization: a Review," *Biologicals*, vol. 25, no. 3, pp. 323–338, 1997.

[22] J. V Bennett, J. Fernandez de Castro, J. L. Valdespino-Gomez, M. de L. Garcia-Garcia, R. Islas-Romero, G. Echaniz-Aviles, A. Jimenez-Corona, and J. Sepulveda-Amor, "Aerosolized measles and measles-rubella vaccines induce better measles antibody booster responses than injected vaccines: randomized trials in Mexican schoolchildren," *Bull. World Health Organ.*, vol. 80, no. 10, pp. 806–812, 2002.

[23] A. M. Henao-Restrepo, M. Greco, X. Laurie, O. John, and T. Aguado, "Measles Aerosol Vaccine Project," *Procedia Vaccinol.*, vol. 2, no. 2, pp. 147–150, 2010.

[24] C. L. Slingluff, "The Present and Future of Peptide Vaccines for Cancer," *Cancer J.*, vol. 17, no. 5, pp. 343–350, 2011.

[25] A. Florczak, A. Mackiewicz, and H. Dams-Kozlowska, "Functionalized Spider Silk Spheres As Drug Carriers for Targeted Cancer Therapy," *Biomacromolecules*, vol. 15, no. 8, pp. 2971–2981, 2014.

[26] M. Hofer, G. Winter, and J. Myschik, "Recombinant spider silk particles for controlled delivery of protein drugs," *Biomaterials*, vol. 33, no. 5, pp. 1554–1562, 2012.

[27] C. Blüm and T. Scheibel, "Control of Drug Loading and Release Properties of Spider Silk Sub-Microparticles," *Bionanoscience*, vol. 2, no. 2, pp. 67–74, 2012.

[28] A. Lammel, M. Schwab, U. Slotta, G. Winter, and T. Scheibel, "Processing conditions for the formation of spider silk microspheres," *ChemSusChem*, vol. 1, no. 5, pp. 413–416, 2008.

[29] C. O'Callaghan and P. W. Barry, "The science of nebulised drug delivery," *Thorax*, vol. 52 Suppl 2, pp. S31–S44, 1997.

[30] S. Fuchs, J. Klier, A. May, G. Winter, C. Coester, and H. Gehlen, "Towards an inhalative in vivo application of immunomodulating gelatin nanoparticles in horse-related preformulation studies," *J. Microencapsul.*, vol. 29, no. 7, pp. 615–625, 2012.

[31] J. Liu, T. Gong, H. Fu, C. Wang, X. Wang, Q. Chen, Q. Zhang, Q. He, and Z. Zhang, "Solid lipid nanoparticles for pulmonary delivery of insulin," *Int. J. Pharm.*, vol. 356, no. 1–2, pp. 333–344, 2008.

[32] A. N. Martin, "Physical Chemical Approach to the Formulation of Pharmaceutical Suspensions," *J. Pharm. Sci.*, vol. 50, no. 6, pp. 513–517, 1961.

[33] S. Claus, T. Schoenbrodt, C. Weiler, and W. Friess, "Novel dry powder inhalation system based on dispersion of lyophilisates," *Eur. J. Pharm. Sci.*, vol. 43, no. 1–2, pp. 32–40, 2011.

VIII. POLYCATIONIC SPIDER SILK PROTEIN PARTICLES FOR DRUG DELIVERY

1. Introduction

Polymeric drug delivery systems for controlled delivery of different pharmaceutical molecules including proteins and peptides have been investigated over the last decades [1]. A protective delivery system is of special interest for protein and peptide based drugs, as these molecules are sensitive to chemical modifications and denaturation during storage or fast proteolysis after application [2]. For this purpose, particulate delivery systems like microspheres or nanoparticles made of biodegradable polymers have been studied due to their good biocompatibility [3]. However, particulate carrier systems are not only used to protect the loaded drug molecule, but are designed to control the drug release for a sustained or targeted drug delivery [4]. The polymer as basis for the particulate drug delivery system affects the overall performance of the whole system, with regards to toxicity, biocompatibility and cheap and easy processability [5]. The most common polymers used for the preparation of drug carriers are either synthetic or naturally occurring materials. The most extensively studied polymers are the synthetic poly(ethylene glycol) (PEG), poly(methyl methacrylate) (PMMA) and polylactic-co-glycolic acid (PLGA) [6, 7]. The latter one has the advantage of being biodegradable after application [8]. In the field of natural polymers used for particle preparation, chitosan, human serum albumin (HAS) and gelatin were of special interest amongst others [9]. Nevertheless, most polymers are not suitable for the drug delivery of pharmaceutical relevant proteins due to the required organic solvents, usage of toxic cross-linking agents, unfavorable pH extremes or mechanical stress during particle fabrication [10–12]. In order to overcome these drawbacks, new biomaterials have been evaluated for drug delivery applications. Silk proteins including silk fibroin from the silkworm *Bombyx mori* as well as spider silk proteins have the advantage of being considered non-toxic and are processable by an all-aqueous preparation method [5].

Particulate carrier systems cannot be loaded with every drug due to the either positive or negative surface charge at a given pH. The charge of a polymer or protein particle at a defined pH is defined by the isoelectric point (pI) [13]. Thus, molecules with a pI < 7 exhibit a negative surface charge during studies at neutral pH, while molecules with a pI > 7 will have a positive surface charge. The previously studied eADF4(C16) spider silk protein has a pI of 3.48, which results in negatively

charged protein particles at neutral pH [14]. Besides the eADF4(C16) protein, also albumin [15], PLGA [16], chitosan [17] and gelatin type B [18] particles are negatively charged at neutral pH. In this context, gelatin represents a material, that offers the possibility to be used either as negatively or positively charged at neutral pH, depending on the processing of the raw material. Due to the negative net charge of these molecules at neutral pH, drugs for loading have to be neutral or positively charged in order to be adsorbed to the particle matrix. The current options for a drug delivery of positively charged molecules are cationic liposomes or cationic polymers. Although liposomes typically show a good safety profile, studies have demonstrated an inflammatory response and liver accumulation without liver-specific targeting after administration [19, 20]. Polyethylenimine (PEI), chitosan and gelatin type B are cationic polymers used for gene and drug delivery. Due to the mucoadhesive properties of chitosan, nasal, peroral and pulmonary drug delivery are possible [17]. However, high transfection efficiency seems to be related to a significant toxicity [21]. The drawback of chitosan and gelatin particles is moreover the necessity of cross-linking after preparation [18]. On the other hand, gelatin offers the possibility to fabricate particles with a negative or positive surface charge, due to the commercial availability of type A and type B gelatin with different pIs [18].

The newly developed eADF4(κ16) protein was designed to maintain most properties of the standard eADF4(C16) protein in combination with a positive surface charge at neutral pH [22]. The positive surface charge allows the loading of negatively charged molecules and comparative studies to the standard eADF4(C16) protein. Doblhofer at al. already showed the possibility of loading negatively charged low molecular weight drugs and nucleic acids onto eADF4(κ16) protein microparticles. Furthermore, coating of the eADF4(κ16) protein microparticles with negatively charged eADF4(C16) protein in a layer-by-layer approach has been demonstrated [22].

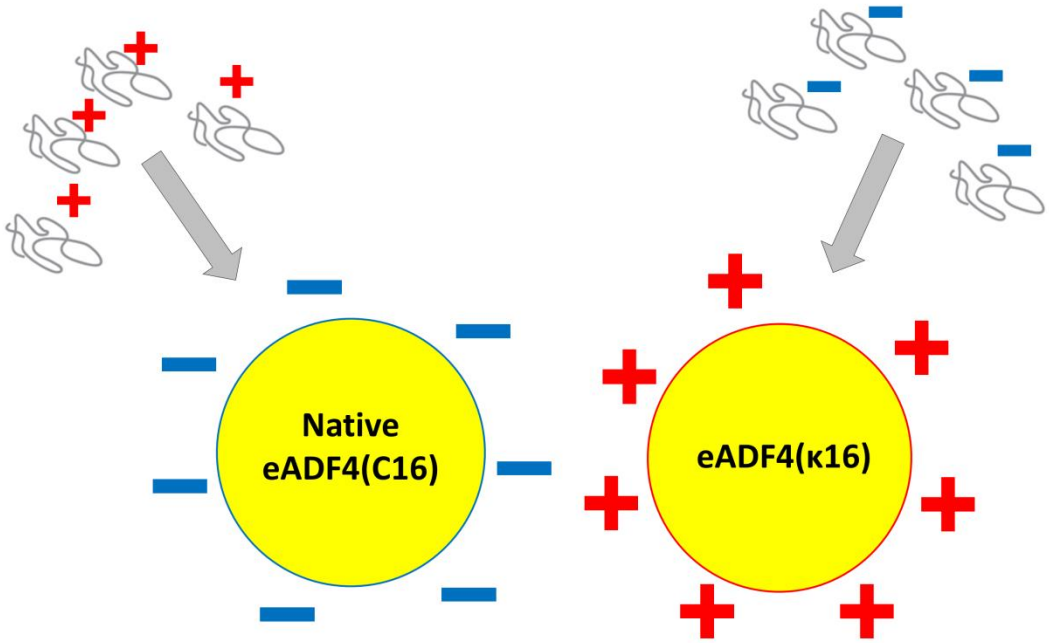

Figure VIII-1: Schematic charge differences between the standard eADF4(C16) protein particles and the newly developed eADF4(κ16) protein particles at neutral pH. Loading of negatively charged proteins is now possible with the positively charged eADF4(κ16) protein particles.

The aim of this study was to investigate the possibility of loading protein molecules on the eADF4(κ16) particles and to compare the results to the previously published results for the negatively charged eADF4(C16) protein particles [14]. The surface charge differences of the two spider silk protein particles at neutral pH are schematically illustrated in Figure VIII-1. In accordance to the study by Hofer et al. using the standard eADF4(C16) protein particles, remote loading of positively charged proteins was performed after particle preparation. In order to evaluate the influence of the molecular weight on the loading mechanism, three proteins with different molecular weights were chosen for the loading experiments.

Secondly, the colloidal stability of the newly developed eADF4(κ16) protein particles was evaluated at different pH and ionic strengths, because previously published studies reported a rapid aggregation of positively charged molecules after i.v. administration [23]. The colloidal stability was evaluated by analysis of the particle size and zeta potential measurements.

2. Materials and methods

2.1. Materials

2.1.1. Engineered polycationic spider silk protein eADF4(κ16)

The standard eADF4(C16) spider silk proteins used so far displays negative net charges at physiological pH. This is the result of 16 glutamic acid residues in the proteins amino acid sequence. Doblhofer et al. [22] designed a new spider silk protein with a net positive charge, based on the eADF4(C16) framework. The exchange of the glutamic acid residues by lysine residues resulted in the generation of the new eADF4(κ16) protein. The eADF4(κ16) protein consists of a T7-TAG followed by 16 repetitions of the following amino acid sequence: GSSAAAAAAAASGPGGYGPKNQGPSGPGGYGPGGPG.

The eADF4(κ16) protein has a molecular weight of 47.68 kDa and a theoretical isoelectric point of 9.7. In comparison, the eADF4(C16) protein has a similar molecular weight of 47.7 kDa but a theoretical isoelectric point of 3.48. The whole design and cloning of the eADF4(κ16) spider silk protein was realized in the group of Prof. Dr. Thomas Scheibel in Bayreuth. The production in *E. coli* and downstream processing was also performed in the group of Prof. Dr. Thomas Scheibel. The final protein was freeze dried to a free-flowing powder of a white color. An extinction coefficient of 47,680 $M^{-1}*cm^{-1}$ at 280 nm was used for the concentration determination by UV-Vis-spectroscopy.

2.1.2. Ovalbumin

Ovalbumin form chicken egg white was purchased from Sigma Aldrich GmbH (Steinheim, Germany). Ovalbumin is a glycoprotein from the serpin family with 386 amino acids and a molecular weight of 45 kDa [24]. The isoelectric point of ovalbumin is 4.5 [25] resulting in a negative charge at neutral pH. Ovalbumin is extensively used as model antigen in vaccine studies [26] and was also considered as antigen in the eADF4(C16) hybrid approach described in chapter 5 and chapter 6.

2.1.3. Anakinra

Anakinra (trade name Kineret®) was obtained from Swedish Orphan Biovitrum AB (Stockholm, Sweden). It is a recombinant human interleukin 1 receptor antagonist with a molecular weight of 17.3 kDa [27]. Anakinra is approved for the treatment of rheumatic arthritis for adult persons and has a theoretical isoelectric point of 5.46. Due to the short half-life of the protein, daily

administration is needed and therefore loading on particles to form a depot is beneficial. For concentration determination by UV-Vis spectroscopy an extinction coefficient of 13,392M^{-1}*cm^{-1} at 280 nm [27] was used.

2.1.4. Insulin lispro

Insulin lispro (trade name Humalog®) was obtained from Lilly Deutschland GmbH (Bad Homburg, Germany). Insulin lispro is a fast acting insulin analogon based on the reversed arrangement of the amino acids lysine and proline. Due to the rearrangement of the original amino acid sequence of human insulin, insulin lispro has the same molecular weight as human insulin with 5.8 kDa [28]. Due to this low molecular weight, the insulin lispro was selected as small protein molecule for the loading experiments. The isoelectric point of the insulin lispro protein is 5.4 [29], which results also to a negative charge at neutral pH. An extinction coefficient of 0.9521 ml/mg^{-1}/cm^{-1} at 277.5 nm [30] was used for the concentration determination by UV-Vis spectroscopy.

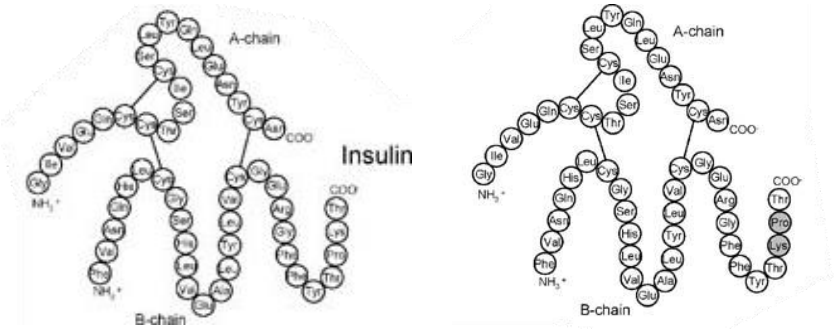

Figure VIII-2: Human insulin (left) and insulin lispro (right) taken from Thevis et al. [28].

2.1.5. Chemicals and reagents

Highly purified water (HPW) used for this study was generated by a purelab® device (ELGA LabWater, Celle, Germany). Sodium hydroxide solution (1 mol/L, EMPROVE® bio), di-potassium hydrogen phosphate (EMPROVE bio, European Pharmacopoeia (Ph. Eur.), British Pharmacopoeia (BP)), potassium dihydrogen phosphate (EMPROVE bio, Ph. Eur., BP, United States National Formulary (NF)) and the fuming hydrochloric acid 37% (EMPROVE bio, Ph. Eur, BP, Japanese Pharmacopoeia (JP)) were purchased from Merck KGaA, Darmstadt, Germany. Sodium chloride (NaCl, AnalaR NORMAPUR) was obtained from VWR Chemicals, Darmstadt, Germany. Tris(hydroxymethyl)aminomethane (Tris, Trizma® base, purity ≥99.9%) was purchased from Sigma Aldrich GmbH, Steinheim, Germany. Guanidinium thiocyanate (for molecular biology) and 4-(2-Hydroxyethyl)-1-piperazine-1-ethanesulfonic acid (HEPES, for molecular biology) were purchased from AppliChem GmbH, Darmstadt, Germany.

2.2. Methods

2.2.1. Preparation of eADF4(κ16) protein particles

The same particle preparation technique using a micromixing system as described in chapter 3 was used for the preparation of eADF4(κ16) protein particles. A molar extinction coefficient of eADF4(κ16) protein at 280 nm (ε = 47,680 $M^{-1}*cm^{-1}$) was used for concentration determination by UV-Vis spectroscopy.

2.2.2. Colloidal stability

The colloidal stability studies of eADF4(κ16) particles were performed at three different pH values of 7.0, 8.5 and 12.0. Although the environment at the pH of 12.0 might be a harsh condition for protein particles, this pH was chosen to change the surface charge of the eADF4(κ16) protein with a theoretical isoelectric point of 9.7 from positive to negative. Each pH value was studied at three different ionic strengths of 30 mM, 60 mM and 100 mM. At the pH of 7, a phosphate buffer and a HEPES buffer were used. At pH of 8.5, a Tris buffer was chosen and at the pH of 12.0, a phosphate buffer was used. The eADF4(κ16) particles in purified water were centrifuged (15,000 rpm, 30 minutes), the supernatant discarded and the particles redispersed to a final particle concentration of 0.25 mg/ml in the desired buffer medium. The particles in the respective buffer were stored at room temperature without agitation. Samples were analyzed right after redispersion, after 1 hour of storage and after 24 hours of storage. The particle size, the size distribution and the zeta potential were analyzed using a Zetasizer Nano ZS (Malvern Instruments, Worcestershire, UK).

2.2.3. eADF4(κ16) particle loading

Loading of eADF4(κ16) particles was carried out with three different proteins on the basis of previous studies with eADF4(C16) particles [14]. The eADF4(κ16) particles were loaded via diffusion with the proteins ovalbumin, Anakinra and insulin lispro. The loading process was performed in a 30 mM Tris buffer at pH 8.0 (loading buffer). A stock solution of the corresponding protein to be tested was prepared by dissolving the protein in the loading buffer (ovalbumin) or by dialysis against the loading buffer (Anakinra and insulin lispro). The eADF4(κ16) particles in HPW were diluted to a stock dispersion with a 100 mM Tris buffer pH 8.0 resulting in a final ionic strength of 30 mM Tris (identical to the loading buffer). For particle loading, appropriate volumes of the protein stock solution, the eADF4(κ16) stock dispersion and the loading buffer were mixed to achieve a final particle concentration of 0.5 mg/ml and the desired w/w-ratio [%] of protein to

eADF4(κ16) particles (see equation (1)).

$$(1)\quad \text{w/w-ratio}\,[\%] = \frac{\text{Amount of model protein used for loading [µg]}}{\text{Amount of eADF4(κ16)particles used for loading [µg]}} * 100$$

The mixture was incubated for 30 minutes at room temperature under mild agitation at 40 rpm (Polymax 1040, Heidolph Instruments GmbH, Schwabach, Germany). After incubation, 75 µL of the eADF4(κ16) particle dispersion were used for DLS measurements. At the same time, the remaining volume of 925 µl was centrifuged at 15,000 rpm for 30 minutes. The supernatant was then analyzed for residual protein content by UV-Vis spectroscopy. The residual amount of ovalbumin (molecular weight 45 kDa) was calculated by a calibration curve at 280 nm. The native ovalbumin was measured at concentrations of 0.00195-1.0 mg/ml and absorption at 280 nm was used for the calculation of the ovalbumin calibration curve. Residual amount of Anakinra (molecular weight 17.3 kDa) was calculated using the extinction coefficient of 13,392M^{-1}*cm^{-1} at 280 nm [27]. Residual amount of insulin lispro (molecular weight 5.8 kDa) was calculated using the extinction coefficient of 0.9521 ml/mg^{-1}/cm^{-1} at 277.5 nm [30]. The loading [%, w/w] and loading efficiency [%, w/w] were determined using equations (2) and (3).

$$(2)\quad \text{Loading}\,[\%] = \frac{\text{Amount of model protein loaded on eADF4(κ16) particles [µg]}}{\text{Amount of eADF4(κ16) particles [µg]}} * 100$$

$$(3)\quad \text{Loading efficiency}\,[\%] = \frac{\text{Amount of model protein loaded on eADF4(κ16) particles [µg]}}{\text{Amount of model protein initially added [µg]}} * 100$$

2.2.4. Analytical Methods

2.2.4.1. Dynamic light scattering (DLS)

Particle size and size distribution of submicroparticles were measured as described in chapter 2.

2.2.4.2. Zeta potential

The zeta potential of eADF(C16) particles was measured as described in chapter 2.

2.2.4.3. Scanning electron microscopy (SEM)

SEM measurements of eADF4(C16) particle suspensions were conducted as described in chapter 2.

3. Results and Discussion

The recently developed eADF4(κ16) protein was processed using the same procedure as described by Hofer et al. for the standard eADF4(C16) protein to identify possible differences between the two contrarily charged proteins [14]. Dialysis against a 10 mM Tris/HCl buffer (pH 8) at 2-8°C had to be performed at a lower concentration (approx. 2 mg/ml) after dissolution of the eADF4(κ16) protein powder in a 6 M guanidinium thiocyanate solution. Already at the used protein concentration of 2 mg/ml protein precipitation during the dialysis process was observable, irrespective of using a 20 mM sodium acetate-acetic acid buffer at pH 5.0 or a 10 mM Tris/HCl buffer at pH 8.0. Therefore, the 10 mM Tris/HCl buffer was used for dialysis of the eADF4(κ16) protein in order to keep the whole particle preparation process as consistent as possible. The precipitation of the dialyzed eADF4(κ16) protein solution into submicroparticles using the micromixing system was the most critical part of the particle preparation process. During studies with the second generation eADF4(C16) hybrid protein (chapter 6), we had already seen that the protein itself has a huge impact on the final particle size. At this time, the charge of the spider silk protein has changed due to a replacement of glutamic acid residues of the eADF4(C16) by lysine residues at the eADF4(κ16) protein. Therefore, we studied different precipitating solutions on the final eADF4(κ16) particle size and compared the eADF4(κ16) particles with standard eADF4(C16) protein particles as shown in Figure VIII-3.

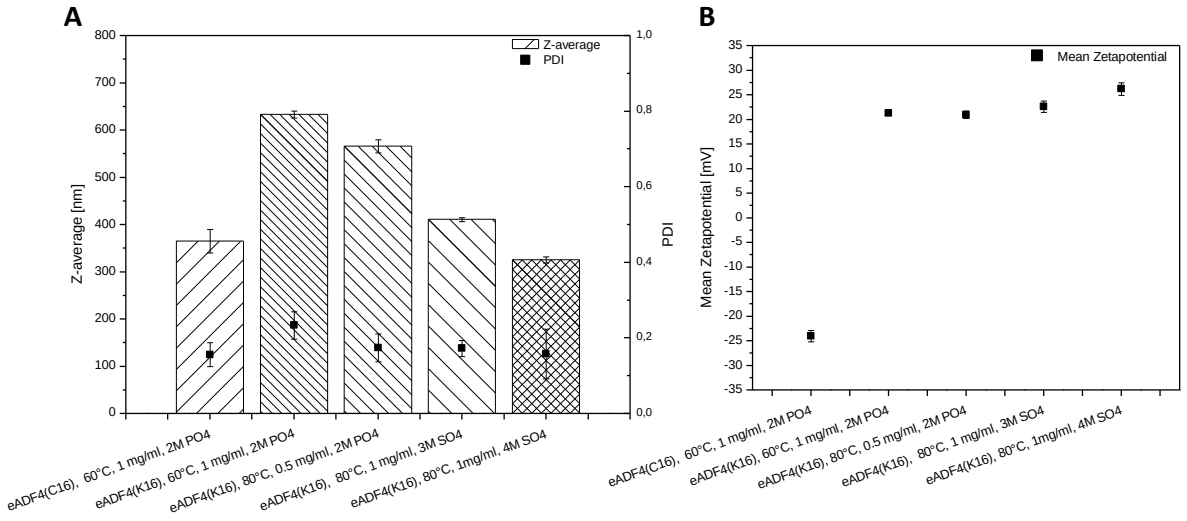

Figure VIII-3: Properties of the eADF4(κ16) protein particles compared to the standard eADF4(C16) protein particles.
A) Particle size given as the Z-average and the particle dispersity index (PDI) of eADF4(κ16) and eADF4(C16) particles prepared at different conditions. Standard eADF4(C16) particles were prepared at 60°C at a protein concentration of 1 mg/ml with a 2 M potassium phosphate solution. The different eADF4(κ16) protein particles were prepared at 60-80°C at protein concentrations of 0.5-1 mg/ml with either a 2 M potassium phosphate or 3-4 M ammonium sulfate solutions.
B) Zeta potential of particles described in A).

The final particle size of the eADF4(κ16) particles is much larger compared to the standard eADF4(C16) particle even though the particles were prepared using the same conditions. While the standard eADF4(C16) protein particles displayed a particle size of 365 nm, the particle size of the eADF4(κ16) protein particles was 633 nm. By modification of the particle forming process using a 4 M ammonium sulfate solution, the final particle size of the eADF4(κ16) protein particles could be decreased to 325 nm. The influence of the kosmotropic salts used for protein precipitation has already been described in chapter 6 for the preparation of the second generation eADF4(C16) hybrid protein particles. More important for the evaluation of the eADF4(κ16) protein particles were the measurements of the surface charge in neutral solutions. Figure VIII-3 B shows the results of the zeta potential measurements. As expected, the standard eADF4(C16) protein particles displayed a negative surface charge, whereas the eADF4(κ16) protein particles exhibited a positive surface charge. The measured values of the eADF4(κ16) protein submicroparticles were between 21 and 26 mV (Figure VIII-3 B). These values of the eADF4(κ16) protein particles zeta potential should guarantee a stable aqueous dispersion. Doblhofer et al. reported already a positive zeta potential of around 8 mV after fabrication of eADF4(κ16) protein microparticles [22]. The difference of the reported zeta potential values of the eADF4(κ16) protein microparticles used by Doblhofer et al. and the eADF4(κ16) submicroparticles used in this study might be caused by the ionic strength and pH of the used dilution medium for the measurements.

Like the eADF4(C16) protein particle suspensions, the eADF4(κ16) protein particles were stored in highly purified water (HPW) at 2-8°C. A short term stability study of the eADF4(κ16) protein submicroparticle suspension stored at a concentration of 1.8 mg/ml at 2-8°C showed a moderate increase of the particle size of 4.1% over a period of 4 weeks. The PDI increased in the same time from 0.174 at the start to 0.253 after 4 weeks storage. The results indicate that the eADF4(κ16) protein submicroparticle suspension is stable in HPW.

In order to evaluate the impact of pH and ionic strength on the eADF4(κ16) protein particles, a colloidal stability study was performed based on the report of Hofer et al. [14]. Due to the different pI of the eADF4(κ16) protein, different buffer systems were selected for the colloidal stability study. The eADF4(κ16) protein submicroparticle suspensions were studied at 30 mM, 60 mM and 100 mM ionic strength and at pH 7.0, pH 8.5 and pH 12.0. The phosphate buffer at pH 12 was chosen to evaluate the particle behavior after a change of the zeta potential to negative values above the pI of 9.7. Figure VIII-4 illustrates the results of the colloidal stability study over time.

The absolute value of the zeta potential decreased with increasing ionic strength at pH 7.0 and pH 8.5 while it increased with increasing ionic strength at pH 12.0. The latter increase of the zeta

potential is due to the predicted switch of the zeta potential from positive to negative values at the pH of 12. Furthermore, the zeta potential values stayed almost at the same level after incubation over 24 hours. That means that the storage time does not affect the zeta potential of the eADF4(κ16) protein particles. On the contrary, the particle size is highly affected by all studied parameters. While the increasing particle size with increasing ionic strength within one buffer group was expected before and is explicable with the zeta potential of the particles (see Figure VIII-4 B, D and E), the large particle size increase at pH 7.0 was surprising (see Figure VIII-4 A & B). As mentioned above, best colloidal stability is given when eADF4(κ16) particles are stored in HPW.

The effect of decreasing the pH below the pI of 9.7 resulted in a progressive particle agglomeration. Usually, particle aggregation and stabilization can be explained by the DLVO theory, whereupon particles are stabilized by an electrostatic repulsive barrier [31]. With an increasing zeta potential, the repulsive forces are rising and the whole system becomes more stable [32]. According to this, the chosen pH of 7.0 should result in the most stable formulation for the eADF4(κ16) protein particles.

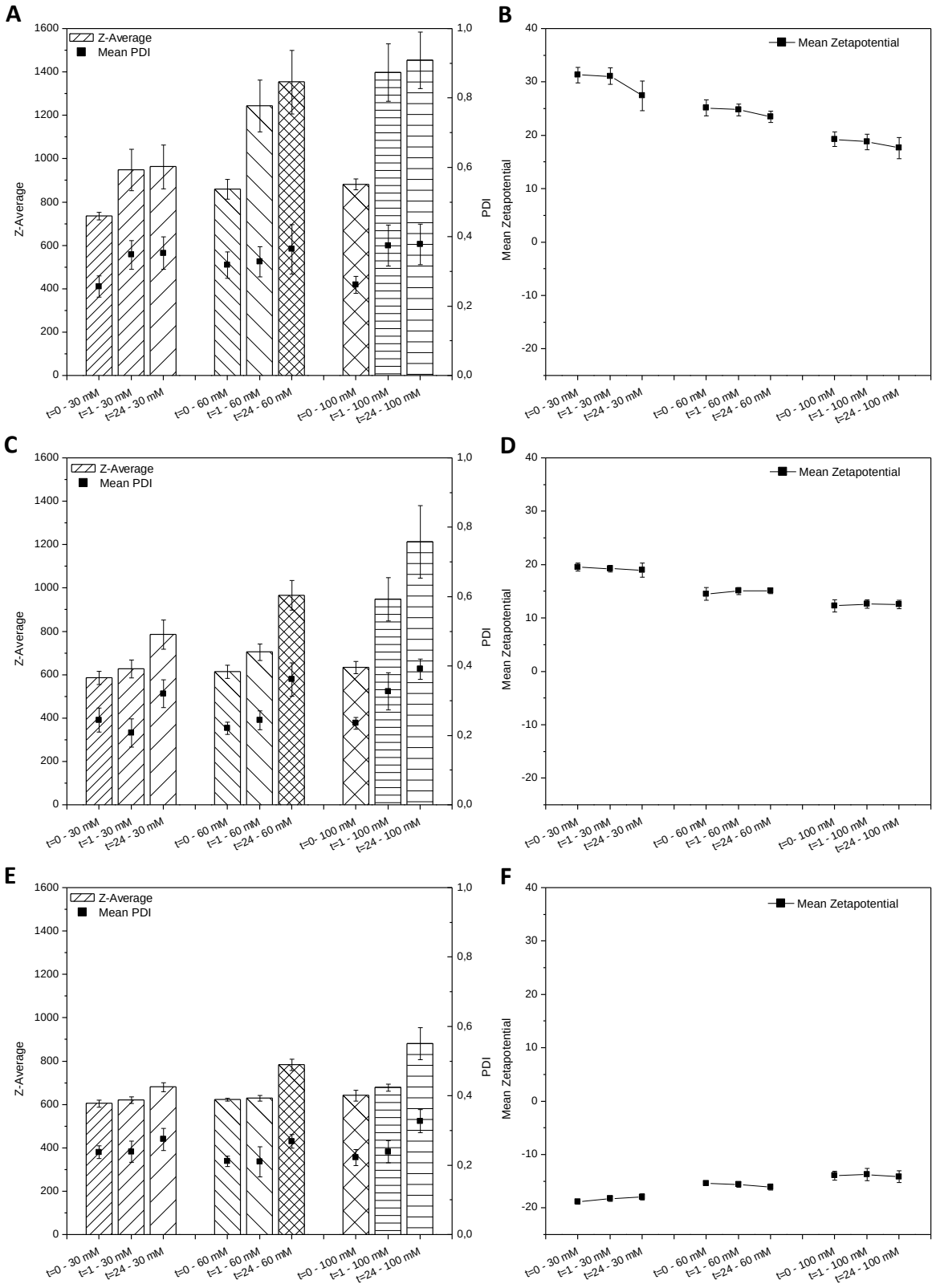

Figure VIII-4: Results of the colloidal stability study performed with eADF4(κ16) protein particles at pH 7.0 (HEPES buffer), pH 8.5 (Tris buffer) and pH 12.0 (phosphate buffer) at 30 mM, 60 mM and 100 mM ionic strength.
A) Particle size and PDI as well as B) the zeta potential of eADF4(κ16) particles incubated at p 7.0.
C) Particle size and PDI as well as D) the zeta potential of eADF4(κ16) particles incubated at p 8.5.
E) Particle size and PDI as well as F) the zeta potential of eADF4(κ16) particles incubated at p 12.0.

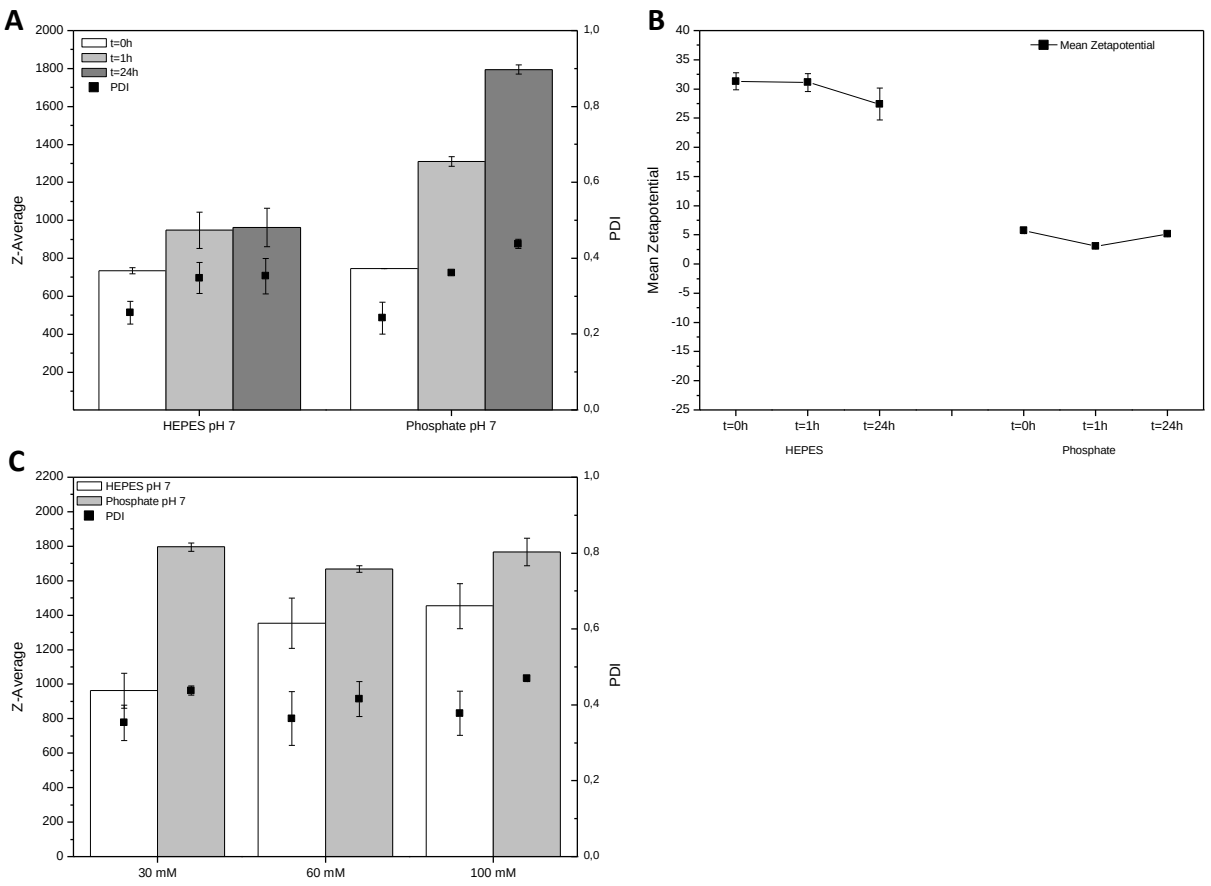

Figure VIII-5: A) Particle size and PDI of eADF4(κ16) protein particles incubated at pH 7 (either with a HEPES or a phosphate buffer) and an ionic strength of 30 mM over a period of 24 hours.
B) Zeta potential of eADF4(κ16) protein particles incubated at pH 7 (either with a HEPES or a phosphate buffer) and an ionic strength of 30 mM over a period of 24 hours.
C) Particle size and PDI of eADF4(κ16) protein particles incubated at pH 7 (either with a HEPES or a phosphate buffer) and ionic strength of 30 mM, 60 mM and 100 mM at the 24 hour time point.

To exclude buffer salt effects on the eADF4(κ16) protein particle stability at pH 7.0, a second study was conducted to compare particles suspended in HEPES buffer to particles suspended in phosphate buffer at pH 7.0 (see Figure VIII-5). Interestingly, the use of the phosphate buffer at pH 7.0 was even worse than the HEPES buffer. The particle size of the eADF4(κ16) protein particles increased rapidly over the incubation time resulting to over twice the size compared to the start (Figure VIII-5 A & C). The incubation with the phosphate buffer led to a drop of the zeta potential to values below 10 mV (Figure VIII-5 B), which could be the reason for particle aggregation.

In conclusion, the results of the colloidal stability suggest the use of HPW or a low ionic strength buffer for the storage of the eADF4(κ16) protein particle suspensions. Additionally, storage at negative zeta potential is preferable, although a buffer system above pH 10.0 is not favorable for most of the pharmaceutically used proteins or peptides. The instability of the eADF4(κ16) protein particles in solution is not yet fully understood. Although zeta potential measurements indicated

towards a stable suspension, non-DLVO forces might play a role for particle aggregation of positively charged spider silk proteins [33]. Interestingly, the native eADF4(C16) protein particles showed the highest particle size increase at pH 3, where the eADF4(C16) protein is positively charged.

Drug delivery by spider silk protein particles has already been investigated by Lammel et al. and Hofer et al. using the standard eADF4(C16) protein [14, 34] and by Doblhofer et al. using the eADF4(κ16) protein to fabricate microparticles, which were loaded with low molecular weight drugs [22]. Here, we were using proteins for loading eADF4(κ16) protein submicroparticles. Proteins are much larger in size causing possible steric interactions with the carrier system, while the charge is defined by the amino acid sequence of the protein molecule [35]. We selected three pharmaceutically relevant proteins with different molecular weights for the remote loading experiments. All three proteins display a pI below 6.0 resulting in a net negative charge at neutral pH, allowing a remote loading of the pre-fabricated eADF4(κ16) protein particles.

In order to ensure the colloidal stability of the eADF4(κ16) protein particles during the incubation time and to guarantee the net negative charge of the proteins, a 30 mM Tris buffer, pH 8.0 was used. The incubation time was defined to be 30 minutes and the final particle concentration was adjusted to 0.5 mg/ml. The same ionic strength, particle concentration and incubation time were also used by Hofer et al. for the remote loading studies with the eADF4(C16) protein particles [14].

Ovalbumin with a molecular weight of 45 kDa [24] was the largest of the three tested proteins. Using a 20% w/w-ratio (a 1:5 ratio given in percent) of ovalbumin to eADF4(κ16) protein particles, a maximum loading of 7.8% [w/w] ovalbumin could be achieved by incubation. The associated loading efficiencies decreased with increasing ratios of ovalbumin to eADF4(κ16) protein particles from 92.4% to 39.2%. The eADF4(κ16) protein particle size increased from 791 nm to 2,661 nm, while the zeta potential decreased from 18.3 mV to -2.3 mV at the same time (illustration see Figure VIII-6).

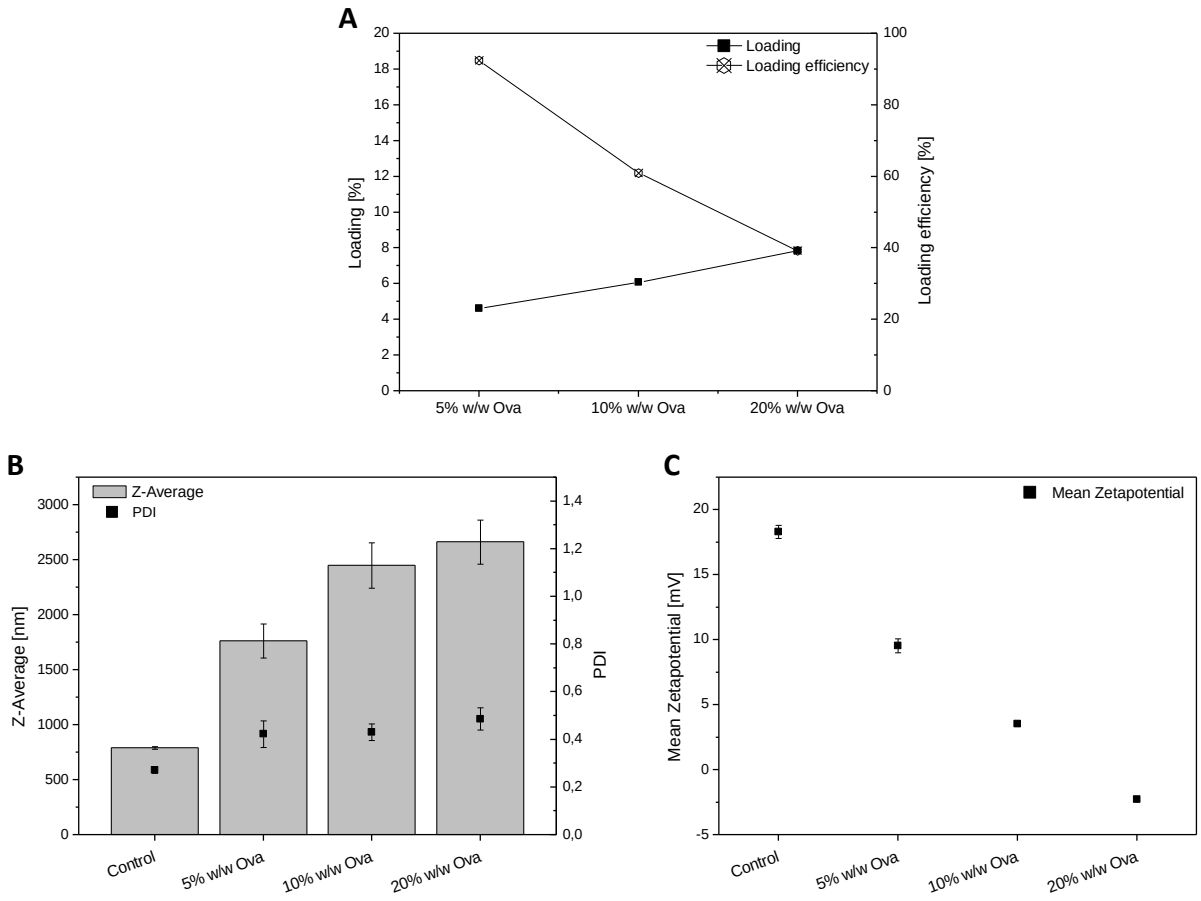

Figure VIII-6: Remote loading of eADF4(κ16) protein particles with ovalbumin.
A) Loading and loading efficiencies as a result of an increasing w/w-ratio of ovalbumin to eADF4(κ16) protein particles during incubation for 30 minutes using a 30 mM Tris buffer at pH 8.0.
B) Particle size, PDI and C) zeta potential of the ovalbumin loaded eADF4(κ16) protein particles after 30 minutes incubation time using a 30 mM Tris buffer at pH 8.0.

The drop of the zeta potential to negative values at the 20% w/w-ratio of ovalbumin to eADF4(κ16) protein particles and the increasing particle size for higher ovalbumin to eADF4(κ16) protein particle ratio indicates surface loading. The eADF4(κ16) protein particle surface charge alters to negative values due to the adsorption of negatively charged ovalbumin. If we assume that the pore size of the eADF4(κ16) protein particle matrix is smaller than the hydrodynamic radius of the ovalbumin molecules, the negative zeta potential is a logical consequence. This is in good accordance with previously published results of the eADF4(C16) protein, where a molecular weight cutoff of 27 kDa for a matrix loading using dextran was determined [36]. In addition, comparative studies with fluorescently labeled lysozyme and fluorescently labeled bovine serum albumin (BSA) confirmed these findings. While the smaller lysozyme molecules (14.3 kDa) were able to freely diffuse into the eADF4(C16) protein particles matrix, the larger BSA molecules (66 kDa) only adsorbed to the eADF4(C16) protein particles surface [14].

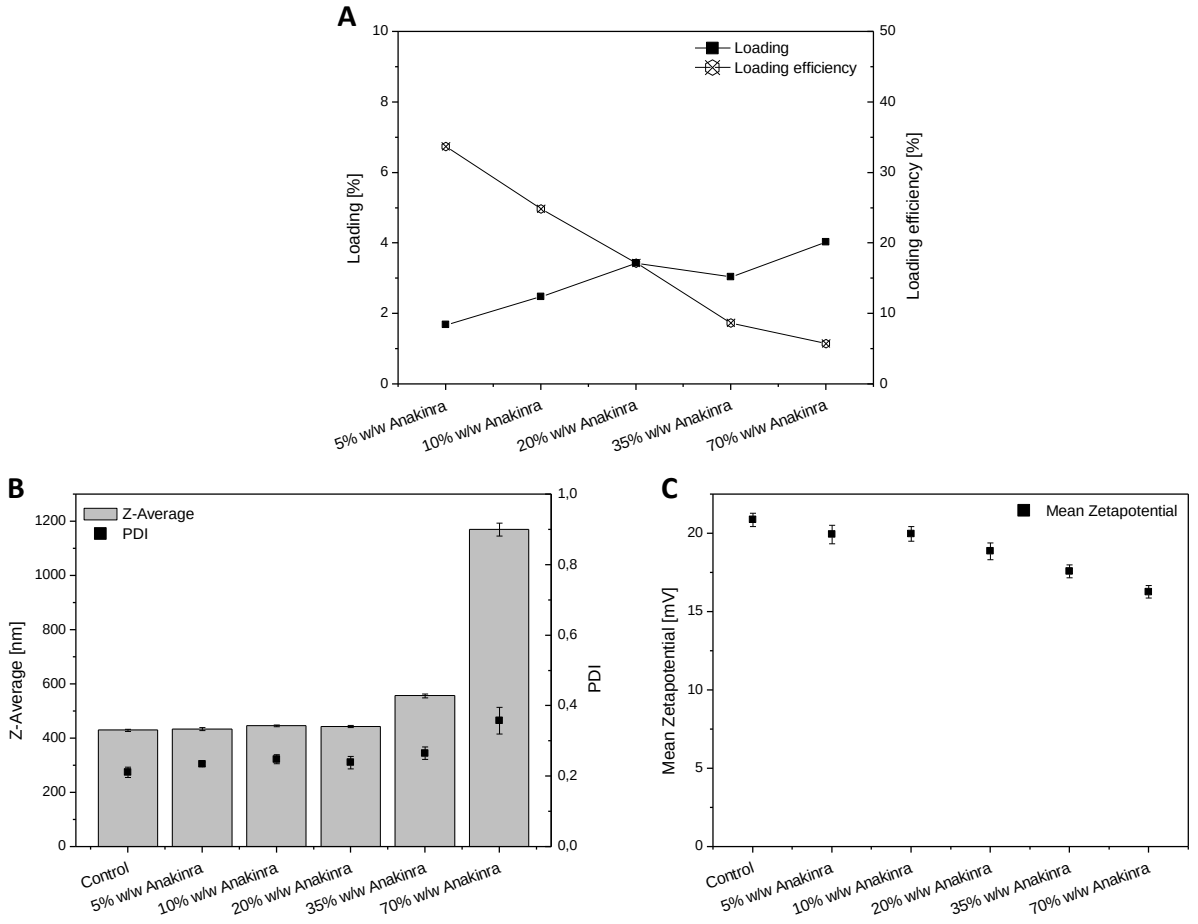

Figure VIII-7: Remote loading of eADF4(κ16) protein particles with Anakinra.
A) Loading and loading efficiencies as a result of an increasing w/w-ratio of Anakinra to eADF4(κ16) protein particles during incubation for 30 minutes using a 30 mM Tris buffer at pH 8.0.
B) Particle size, PDI and C) zeta potential of the Anakinra loaded eADF4(κ16) protein particles after 30 minutes incubation time using a 30 mM Tris buffer at pH 8.0.

Next, the loading behavior of Anakinra, a smaller molecule with a molecular weight of 17.3 kDa [27], was investigated. However, total loading values for Anakinra were only at 4% [w/w] using a 70% w/w-ratio of Anakinra to eADF4(κ16) protein particles (Figure VIII-7 A). Besides this low loading, also the loading efficiency at all tested ratios was below 35% ranging to a minimum of only 5.8% at the 70% w/w-ratio. This results made eADF4(κ16) protein particles unfavorable for the drug delivery application of Anakinra. By contrast, the zeta potential was only slightly affected during the Anakinra loading experiments (Figure VIII-7 C). Nevertheless, a particle aggregation with an increasing particle size was clearly detectable at the highest w/w-ratios of 35% and 70% (Figure VIII-7 B).

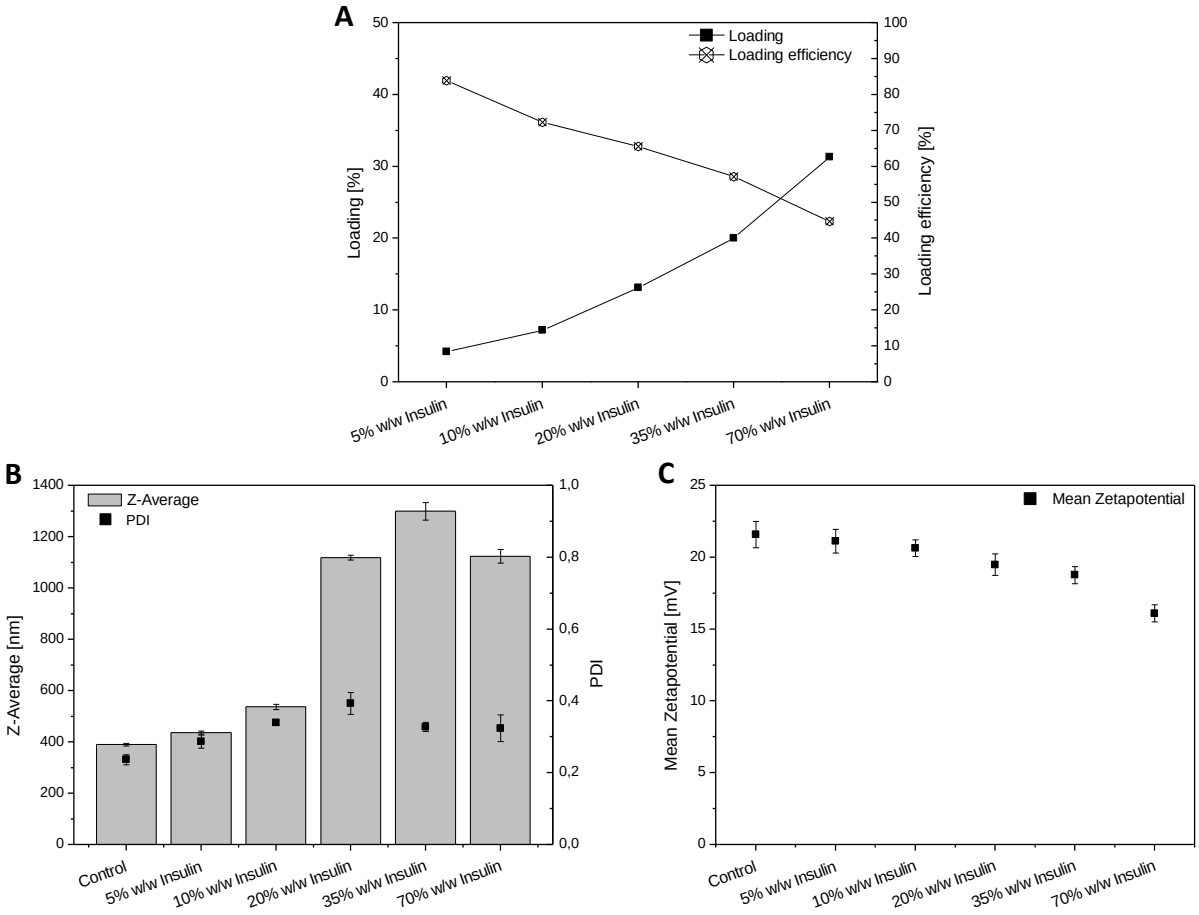

Figure VIII-8: Remote loading of eADF4(κ16) protein particles with insulin lispro.
A) Loading and loading efficiencies as a result of an increasing w/w-ratio of insulin lispro to eADF4(κ16) protein particles during incubation for 30 minutes using a 30 mM Tris buffer at pH 8.0.
B) Particle size and C) zeta potential of the insulin lispro loaded eADF4(κ16) protein particles after 30 minutes incubation time using a 30 mM Tris buffer at pH 8.0.

Insulin lispro was finally used as very small protein to further evaluate the remote loading behavior of eADF4(κ16) protein particles. Insulin lispro is one of the smallest proteins with a molecular weight of 5.8 kDa [28]. With a pI of 5.4, insulin lispro is negatively charged at neutral pH like both previously investigated proteins. In contrast to poor Anakinra loading values below 4% [w/w], insulin lispro remote loading was within a range of 4.2% to 31.3% [w/w] at corresponding w/w-ratios of insulin lispro to eADF4(κ16) protein particles of 5% to 70% (Figure VIII-8 A). The loading efficiencies between 89.9% and 44.7% were quite high, although the loading efficiency decreased already between the 5% and 10% insulin lispro w/w-ratios and did not form a plateau like described for the lysozyme and nerve growth factor loading experiments with the eADF4(C16) protein particles [14]. In addition, a particle size increase was observed beginning between the 10% and 20% w/w-ratios of insulin lispro to eADF4(κ16) protein particles, which was not related to the particles zeta potential.

In order to evaluate the results of the three loading experiments, the grand average of hydropathy (GRAVY) value for the proteins was calculated by addition of the hydropathy values of the proteins amino acid residues divided by the number of residues in the sequence [37]. The GRAVY value provides information on the hydrophilic-hydrophobic character of a protein or peptide. While a negative score indicates a hydrophilic character, a positive score points towards hydrophobic proteins. The scores were calculated using the ProtParam tool [38] and the results are shown in Table VIII-1.

Table VIII-1: Calculated GRAVY scores of the three proteins used for the remote loading experiments with eADF4(κ16) protein particles. The score was calculated using the ProtParam tool [38].

	Ovalbumin	Anakinra	Insulin lispro
GRAVY score	-0.001	-0.412	0.218

The GRAVY scores for ovalbumin and especially insulin lispro indicate towards a hydrophobic character of these two proteins. On the contrary, Anakinra appears to be a more hydrophilic protein based on the negative GRAVY score. If the GRAVY score is then associated to the results of the loading experiments, loading of the eADF4(κ16) protein particles is most likely influenced by hydrophobic van der Waals forces. The hydrophilic Anakinra protein showed the worst loading on the eADF4(κ16) protein particles, whereas the hydrophobic insulin lispro displayed the highest w/w-loading values over 30%.

Nevertheless, we observed a particle size increase already at the lowest insulin lispro ratio (Figure VIII-8 B). Particle size increased slowly from 390 nm (control) to 537 nm (10% w/w-ratio) at the lower ratios, followed by severe particle aggregation observed at w/w-ratios higher than 20% insulin lispro to eADF4(κ16) protein particles (Figure VIII-8 B). While the particle size increase observed during the ovalbumin loading experiments was caused by a drop of the zeta potential, the zeta potential changed only slightly during the insulin lispro loading from 21.6 mV (control) to 16.1 mV (70% w/w-ratio). We attribute the particle size increase to the general instability of the particles at neutral pH, which was demonstrated by the colloidal stability experiments (Figure VIII-4). In principle, the colloidal stability of the particles could be improved by choosing a basic pH. However, the surface charge of the eADF4(κ16) protein particles would then change to negative values, which allows loading of only positively charged protein molecules again. In addition, protein stability at basic pH is poor.

4. Conclusion

Our results add more information about the eADF4(κ16) protein particles to the previously published data of eADF4(κ16) protein microparticles and allow a comparison to the eADF4(C16) protein particles. Our approach focused on the potential use of the eADF4(κ16) protein particles in the submicron range for drug delivery. The modified particle preparation process developed for the second generation eADF4(C16) hybrid protein particles could be applied also to the eADF4(κ16) protein to form smaller submicroparticles. The colloidal stability of the smaller submicroparticles was analyzed at different pH and ionic strength and the influence of the used buffer salts at pH 7 was illustrated. The best stability was achieved for suspending eADF4(κ16) protein particles in HPW. With increasing ionic strength, particle aggregation of the eADF4(κ16) protein particles occurred. The best colloidal stability of the eADF4(κ16) protein particles was identified at basic pH, where the particles exhibited a negative surface charge.

Remote loading was most efficient with smaller and hydrophobic protein molecules. Proteins with a molecular weight > 45 kDa most likely only adsorbed to the particle surface and did not permeate into the particle matrix. Compared to the loading and loading efficiencies of the previously studied eADF4(C16) protein particles, remote loading of eADF4(κ16) protein particles was less successful. The loading mechanism was however influenced more by hydrophobic van der Waals forces.

5. References

[1] G. Luckachan and C. Pillai, “Biodegradable Polymers-A Review on Recent Trends and Emerging Perspectives,” *J. Polym. Environ.*, vol. 19, no. 3, pp. 637–676, 2011.

[2] W. R. Gombotz and D. K. Pettit, “Biodegradable Polymers for Protein and Peptide Drug Delivery,” *Bioconjug. Chem.*, vol. 6, no. 4, pp. 332–351, 1995.

[3] R. H. Müller, K. Mäder, and S. Gohla, “Solid lipid nanoparticles (SLN) for controlled drug delivery – a review of the state of the art,” *Eur. J. Pharm. Biopharm.*, vol. 50, no. 1, pp. 161–177, 2000.

[4] M. . Hans and A. . Lowman, “Biodegradable nanoparticles for drug delivery and targeting,” *Curr. Opin. Solid State Mater. Sci.*, vol. 6, no. 4, pp. 319–327, 2002.

[5] E. Wenk, H. P. Merkle, and L. Meinel, “Silk fibroin as a vehicle for drug delivery applications,” *J. Control. Release*, vol. 150, no. 2, pp. 128–141, 2011.

[6] J. Khandare and T. Minko, “Polymer–drug conjugates: Progress in polymeric prodrugs,” *Prog. Polym. Sci.*, vol. 31, no. 4, pp. 359–397, 2006.

[7] J. Panyam and V. Labhasetwar, “Biodegradable nanoparticles for drug and gene delivery to cells and tissue,” *Adv. Drug Deliv. Rev.*, vol. 55, no. 3, pp. 329–347, 2003.

[8] T. G. Park, “Degradation of poly(lactic-co-glycolic acid) microspheres: effect of copolymer composition,” *Biomaterials*, vol. 16, no. 15, pp. 1123–1130, 1995.

[9] A. Kumari, S. K. Yadav, and S. C. Yadav, “Biodegradable polymeric nanoparticles based drug delivery systems,” *Colloids Surfaces B Biointerfaces*, vol. 75, no. 1, pp. 1–18, 2010.

[10] V. R. Sinha and A. Trehan, “Biodegradable microspheres for protein delivery,” *J. Control. Release*, vol. 90, no. 3, pp. 261–280, 2003.

[11] K. E. Uhrich, S. M. Cannizzaro, R. S. Langer, and K. M. Shakesheff, “Polymeric Systems for Controlled Drug Release,” *Chem. Rev.*, vol. 99, no. 11, pp. 3181–3198, 1999.

[12] A. Prokop, E. Kozlov, G. W. Newman, and M. J. Newman, “Water-based nanoparticulate polymeric system for protein delivery: permeability control and vaccine application,” *Biotechnol. Bioeng.*, vol. 78, no. 4, pp. 459–466, 2002.

[13] E. J. Cohn, “The isoelectric points of the proteins in certain vegetable juices,” *J. Gen. Physiol.*, vol. 2, no. 2, pp. 145–160, 1919.

[14] M. Hofer, G. Winter, and J. Myschik, “Recombinant spider silk particles for controlled delivery of protein drugs,” *Biomaterials*, vol. 33, no. 5, pp. 1554–1562, 2012.

[15] M. Roser, D. Fischer, and T. Kissel, “Surface-modified biodegradable albumin nano- and microspheres. II: effect of surface charges on in vitro phagocytosis and biodistribution in rats,” *Eur. J. Pharm. Biopharm.*, vol. 46, no. 3, pp. 255–263, 1998.

[16] R. Rietscher, J. A. Czaplewska, T. C. Majdanski, M. Gottschaldt, U. S. Schubert, M. Schneider, and C.-M. Lehr, “Impact of PEG and PEG-b-PAGE modified PLGA on nanoparticle formation, protein loading and release,” *Int. J. Pharm.*, vol. 500, no. 1–2, pp. 187–195, 2016.

[17] S. A. Agnihotri, N. N. Mallikarjuna, and T. M. Aminabhavi, “Recent advances on chitosan-based micro- and nanoparticles in drug delivery,” *J. Control. Release*, vol. 100, no. 1, pp. 5–28, 2004.

[18] A. O. Elzoghby, “Gelatin-based nanoparticles as drug and gene delivery systems: Reviewing three decades of research,” *J. Control. Release*, vol. 172, no. 3, pp. 1075–1091, 2013.

[19] J.-M. Williford, J. Wu, Y. Ren, M. M. Archang, K. W. Leong, and H.-Q. Mao, “Recent Advances in Nanoparticle-Mediated siRNA Delivery,” *Annu. Rev. Biomed. Eng.*, vol. 16, no. 1, pp. 347–370, 2014.

[20] H. Sakurai, K. Kawabata, F. Sakurai, S. Nakagawa, and H. Mizuguchi, “Innate immune response induced by gene delivery vectors,” *Int. J. Pharm.*, vol. 354, no. 1–2, pp. 9–15, 2008.

[21] R. Arote, T.-H. Kim, Y.-K. Kim, S.-K. Hwang, H.-L. Jiang, H.-H. Song, J.-W. Nah, M.-H. Cho, and C.-S. Cho, “A biodegradable poly(ester amine) based on polycaprolactone and polyethylenimine as a gene carrier,” *Biomaterials*, vol. 28, no. 4, pp. 735–744, 2007.

[22] E. Doblhofer and T. Scheibel, “Engineering of Recombinant Spider Silk Proteins Allows Defined Uptake and Release of Substances,” *J. Pharm. Sci.*, vol. 104, no. 3, pp. 988–994, 2015.

[23] T. Nomoto, Y. Matsumoto, K. Miyata, M. Oba, S. Fukushima, N. Nishiyama, T. Yamasoba, and K. Kataoka, “In situ quantitative monitoring of polyplexes and polyplex micelles in the blood circulation using intravital real-time confocal laser scanning microscopy,” *J. Control. Release*, vol. 151, no. 2, pp. 104–109, 2011.

[24] J. A. Huntington and P. E. Stein, “Structure and properties of ovalbumin,” *J. Chromatogr. B Biomed. Sci. Appl.*, vol. 756, no. 1–2, pp. 189–198, 2001.

[25] L. Stevens, “Egg white proteins,” *Comp. Biochem. Physiol. Part B Comp. Biochem.*, vol. 100, no. 1, pp. 1–9, 1991.

[26] A. P. Basto, M. Badenes, S. C. P. Almeida, C. Martins, A. Duarte, D. M. Santos, and A. Leitão, “Immune response profile elicited by the model antigen ovalbumin expressed in fusion with the bacterial OprI lipoprotein,” *Mol. Immunol.*, vol. 64, no. 1, pp. 36–45, 2015.

[27] R. Liebner, R. Mathaes, M. Meyer, T. Hey, G. Winter, and A. Besheer, “Protein HESylation for half-life extension: Synthesis, characterization and pharmacokinetics of HESylated anakinra,” *Eur. J. Pharm. Biopharm.*, vol. 87, no. 2, pp. 378–385, 2014.

[28] M. Thevis, A. Thomas, and W. Schänzer, “Mass spectrometric determination of insulins and their degradation products in sports drug testing,” *Mass Spectrom. Rev.*, vol. 27, no. 1, pp. 35–50, 2008.

[29] C. Munsick, R. Murray, T. Dziubla, A. M. Lowman, J. I. Joseph, and M. C. Torjman, “Quantitation of humalog insulin by reversed-phase high-performance liquid chromatography,” *J. Diabetes Sci. Technol.*, vol. 1, no. 4, pp. 603–607, 2007.

[30] R. J. Woods, J. Alarcón, E. McVey, and R. J. Pettis, “Intrinsic fibrillation of fast-acting insulin analogs,” *J. Diabetes Sci. Technol.*, vol. 6, no. 2, pp. 265–276, 2012.

[31] B. A. Matthews and C. T. Rhodes, “Use of the Derjaguin, Landau, Verwey, and Overbeek Theory to Interpret Pharmaceutical Suspension Stability,” *J. Pharm. Sci.*, vol. 59, no. 4, pp. 521–525, 1970.

[32] J. Liu and E. Luijten, “Stabilization of Colloidal Suspensions by Means of Highly Charged Nanoparticles,” *Phys. Rev. Lett.*, vol. 93, no. 24, p. 247802, 2004.

[33] M. Elimelech, J. Gregory, and J. Xiadong, *Particle deposition and aggregation: measurement, modelling and simulation*. Oxford: Butterworth-Heinemann, 1995.

[34] A. Lammel, M. Schwab, M. Hofer, G. Winter, and T. Scheibel, “Recombinant spider silk particles as drug delivery vehicles,” *Biomaterials*, vol. 32, no. 8, pp. 2233–2240, 2011.

[35] C. Lehermayr, H.-C. Mahler, K. Mäder, and S. Fischer, “Assessment of Net Charge and Protein–Protein Interactions of Different Monoclonal Antibodies,” *J. Pharm. Sci.*, vol. 100, no. 7, pp. 2551–2562, 2011.

[36] K. D. Hermanson, M. B. Harasim, T. Scheibel, and A. R. Bausch, “Permeability of silk microcapsules made by the interfacial adsorption of protein,” *Phys. Chem. Chem. Phys.*, vol. 9, no. 48, p. 6442, 2007.

[37] J. Kyte and R. F. Doolittle, “A simple method for displaying the hydropathic character of a protein,” *J. Mol. Biol.*, vol. 157, no. 1, pp. 105–132, 1982.

[38] “ExPASy ProtParam tool.” [Online]. Available: http://web.expasy.org/protparam/.

IX. FINAL SUMMARY AND CONCLUSION

Particulate drug delivery systems are considered to offer considerable advantages compared to simple solutions when it comes to drug and vaccine delivery. Among other things, superiority of particulate drug delivery systems was shown in terms of protection of sensitive drugs against degradation or controlled release of encapsulated drugs after administration. Factors like biocompatibility and biodegradability of the carrier material has led to an intensive research in the field of new materials with improved properties. With the possibility to produce recombinant spider silk proteins on large scale, this material has gained more and more interest in the scientific community. Previous studies in the field of particulate drug delivery systems based on the recombinant spider silk protein eADF4(C16) were conducted by Andreas Lammel and Martin Schwab. In their experiments, they demonstrated that eADF4(C16) particles can be fabricated by an all-aqueous salting out process [1]. Subsequent loading experiments using small molecules showed the fundamental possibility to use eADF4(C16) particles as particulate drug delivery system [2]. Based on the work of Andreas Lammel and Martin Schwab, Markus Hofer was able to further improve the particle preparation technique resulting in excellent reproducibility and the possibility for a later scale up of the production [3]. Using the improved particle preparation technique, loading of eADF4(C16) submicroparticles with protein drugs was demonstrated. High loading efficiencies up to 95% by simple remote loading were achieved using lysozyme and nerve growth factor as model drugs. Protein drugs will benefit most from a protective drug delivery system, because proteins usually degrade rapidly after administration. However, release of the loaded drugs was challenging throughout all experiments. Any changes of pH, ionic strength or addition of other plasma proteins significantly accelerated the release.

Based on these results, the overall aim of this thesis was the design of a recombinant eADF4(C16) hybrid protein, which already incorporates an epitope in the amino acid sequence, and the subsequent preparation of submicroparticles for subcutaneous vaccination. The hybrid approach prevents the unwanted release of the loaded drug by changes of the particle environment. In addition, peptide vaccination is still lacking in success due to fast protease degradation and the possibility of the epitope to directly bind to receptors of non-antigen-presenting cells (APCs). Here, particulate drug delivery systems can protect the sensitive epitope and act as a carrier for enhanced APC uptake. Since vaccination studies can be influenced by unwanted cytotoxicity or

immunogenicity, important prerequisites like sterility and low endotoxin content of the eADF4(C16) particles had to be fulfilled.

In chapter 1 a general introduction into the topic of spider silk proteins and the application of particulate drug delivery systems for vaccination is given. There is still a clear need for a delivery system, which can be prepared in a non-toxic environment with as few preparation steps as possible resulting in reproducible properties. Reviewing current literature, the need for a particulate delivery system in the area of vaccination becomes apparent. However, strict safety regulations for the approval of new adjuvants exist.

Different endotoxin depletion methods of eADF4(C16) protein, subsequent endotoxin free particle preparation and characterization and a cell based cytotoxicity test of endotoxin depleted eADF4(C16) particles are presented in chapter 2. Endotoxin depletion was studied using several different methods, including heat inactivation, endotoxin filtration and chemical treatment. While moist heat during an autoclave process at 121°C for 15 minutes did not impair the eADF4(C16) protein, dry heat of 180°C for 3 hours visibly degraded the protein. The screening of several filters resulted in the selection of one filter, which effectively removed endotoxins from an eADF4(C16) solution with high recovery of the spider silk protein. Chemical treatment by alkali showed a significant reduction of the endotoxin load. However, the remaining endotoxin level after treatment was still too high for routine use. Particle properties after endotoxin depletion using autoclave treatment, filtration or a combination of both were studied. Both, autoclave treatment and filtration influenced the final particle size and zeta potential. In the end, a combination of autoclave treatment and filtration was determined as final setup, which generated eADF4(C16) particles with comparable size to untreated particles. The cytotoxicity experiments using a MTT test confirmed the good performance of endotoxin depleted particles by a combination of autoclave treatment and filtration.

Sterility as important prerequisite for parenteral administration was addressed in chapter 3. Commonly used biodegradable polymers are not able to withstand the conditions during steam sterilization, however eADF4(C16) protein is. Therefore, we performed steam sterilization of eADF4(C16) particles prepared in a non-sterile environment and assessed the influence of extended autoclave treatment on the final particle properties. Neither the particle size nor the protein secondary structure was altered after extended steam sterilization conditions. A change of the thermal stability at elevated temperature was observed for eADF4(C16) microparticles, surprisingly resulting in an increased thermal stability of the microparticles after steam sterilization. The good cellular compatibility of steam sterilized eADF4(C16) particles was

demonstrated in a final cytotoxicity test. No cytotoxic effects were observed for particle concentrations up to final concentrations of 5 mg/ml.

In chapter 4, chemical coupling of eADF4(C16) with the the model antigen $OVA_{257-264}$ (SIINFEKL) was evaluated. Chemical coupling using cleavable linkers for SIINFEKL administration was assessed as current state-of-the-art method to compare the results of the eADF4(C16) hybrid proteins presented in chapter 5 and 6. One of the used linkers was cleavable in acidic pH (hydrazone linker), while the other one was a disulfide cleavable linker. Two routes of linking, in particular linking in solution or linking to pre-produced particles, were evaluated. It turned out, that the pH sensitive linkage showed better results for linking dissolved eADF4(C16) protein, the disulfide linkage performance was better when linking SIINFEKL to pre-produced particles. In addition, the hydrazone linkage of SIINFEKL to the eADF4(C16) protein led to an increase of particle size after particle preparation. Finally, the chemically linked eADF4(C16)-SIINFEKL particles showed a poorer outcome in the *in vitro* studies compared to the second generation eADF4(C16) hybrid protein particles. However, chemical linkage of peptides to the eADF4(C16) protein is generally possible and was demonstrated in chapter 4.

In chapter 5, the development of eADF4(C16) hybrid protein particles and their performance is described. The straightforward system of an eADF4(C16) hybrid protein by addition of the $OVA_{257-264}$ epitope (SIINFEKL) to the eADF4(C16) amino acid sequence was investigated in chapter 5. Three eADF4(C16) hybrid proteins were studied, differing at the position of the SIINFEKL epitope, which was attached either at the N-terminal, the C-terminal or at the N- and C-terminal (bi-terminal) end of the eADF4(C16) protein. The addition of the epitope to the eADF4(C16) protein sequence was investigated with regards to final particle size, particle size distribution, zeta potential, protein secondary structure and thermal stability. Compared to native eADF4(C16) particles, no changes were detected for all three eADF4(C16) hybrid protein particles. Fluorescence labelling using FITC was implemented for all eADF4(C16) proteins. The FITC labelling did not alter the particle properties, as shown by comparison to untreated eADF4(C16) particles. Cellular uptake studies using macrophages were conducted after successfully implementing the endotoxin depletion and fluorescence labelling steps into the particle preparation process. The *in vitro* uptake studies using macrophages showed that the native and all three eADF4(C16) hybrid protein particles were internalized by an active uptake mechanism. LysoTracker staining confirmed the successful uptake into the acidic organelles like endosomes or lysosomes of the macrophages. Although the eADF4(C16) hybrid particles were effectively internalized, no antigen presentation was detected in further *in vitro* experiments. It is possible, that the epitope on the

eADF4(C16) hybrid protein particles was either sterically hidden inside the particle matrix or the epitope was generally recognized, but cleavage of the epitope from the eADF4(C16) sequence was impossible.

Since no antigen presentation could be shown for the eADF4(C16) hybrid protein particles in chapter 5, a second generation of eADF4(C16) hybrid protein particles was designed and tested. The respective results are described in chapter 6. In order to release the epitope after cellular uptake, two different peptide based linkers were incorporated between the amino acid sequence of the eADF4(C16) protein and the SIINFEKL epitope resulting in two eADF4(C16) hybrid proteins. The first second generation eADF4(C16) hybrid protein contained a cathepsin B cleavable linker sequence, the second a cathepsin S cleavable linker sequence. After optimization of the particle preparation process to result in uniform particles, release of the SIINFEKL epitope from both second generation eADF4(C16) hybrid protein particles was tested. High levels of the epitope were detected in the supernatant after incubation with the cathepsin S enzyme, while only low levels of the epitope were identified in the supernatant after incubation with the cathepsin B enzyme. Based on the release test, further *in vitro* experiments proved that none of the eADF4(C16) particles was cytotoxic or immunogenic. Furthermore, effective SIINFEKL-dependent T cell proliferation was verified. Encouraged by these *in vitro* results, successful epitope delivery by the cathepsin S cleavable eADF4(C16) hybrid protein particles was shown in an *in vivo* mouse model. Particle uptake into dermal dendritic cells was observed after subcutaneous administration. Subcutaneous vaccination using the eADF4(C16)-CatS hybrid protein particles resulted in effective induction of T cell proliferation *in vivo*. Interestingly, eADF4(C16)-CatS hybrid protein particles induced the same level of proliferating T cells after administration with or without an additional immunostimulatory adjuvant.

A different application approach for the administration of eADF4(C16) particles was examined in chapter 7. The feasibility of eADF4(C16) particle aerosolization was studied, because pulmonary administration could enhance the antigenicity and simplify the handling of new vaccine formulations. A systematic evaluation of the influence of particle size, particle concentration and type the of nebulization device on the lung deposition was performed. It was found that the smallest particles with a diameter of 250 nm were mainly deposited in the simulated lower airways, while particles with a diameter of 4.7 µm were either trapped in the nebulization device or found in the simulated upper airways. The good colloidal stability of the eADF4(C16) particles after nebulization and nebulization efficiencies of up to 70% provides a good basis for further investigations, for example using the second generation eADF4(C16) hybrid protein particles.

In chapter 8, the recently developed eADF4(κ16) protein was used to assess the possibility of loading negatively charged molecules on spider silk particles. The exchange of the glutamic acid residues of the eADF4(C16) protein by lysine residues in the eADF4(κ16) protein resulted in a new spider silk protein with a positive surface charge at neutral pH [4]. While colloidal stability of the particles was sufficient at neutral pH, especially at low ionic strength, best results have been obtained at basic pH, where the eADF4(κ16) particles had a negative surface charge. Simple remote loading of three model proteins showed that smaller and hydrophobic proteins were loaded more effectively. Although simple remote loading was generally possible, loading and loading efficiencies of the previously studied eADF4(C16) particles were much better. Thus, it can be concluded that the hybrid approach presented in chapter 6 could lead to an improvement of eADF4(κ16) protein loading, if positively charged spider silk particles are of interest.

Taking together the results of all chapters, eADF4(C16) hybrid protein particles can serve as promising drug delivery system in the field of vaccination. Up-scaleable methods for endotoxin depletion and sterilization are available, which can be easily integrated into the robust, all-aqueous particle preparation method. Integrating a cathepsin cleavable linker between the antigen and the eADF4(C16) sequence was necessary for an intracellular antigen processing. The remarkable outcome of the *in vivo* mouse vaccination studies using the second generation eADF4(C16) hybrid protein particles should be the basis for future studies. Other types of linkers or epitopes may be incorporated into new eADF4(C16) hybrid proteins and used for therapeutic vaccination, where dendritic cell targeting and T cell activation are of special interest [5]. In addition, lung application of nebulized eADF4(C16) hybrid protein particles provides a further route of administration, which could potentially improve vaccination efficiency.

1. References

[1] A. Lammel, M. Schwab, U. Slotta, G. Winter, and T. Scheibel, “Processing conditions for the formation of spider silk microspheres,” *ChemSusChem*, vol. 1, no. 5, pp. 413–416, 2008.

[2] A. Lammel, M. Schwab, M. Hofer, G. Winter, and T. Scheibel, “Recombinant spider silk particles as drug delivery vehicles,” *Biomaterials*, vol. 32, no. 8, pp. 2233–2240, 2011.

[3] M. Hofer, G. Winter, and J. Myschik, “Recombinant spider silk particles for controlled delivery of protein drugs,” *Biomaterials*, vol. 33, no. 5, pp. 1554–1562, 2012.

[4] E. Doblhofer and T. Scheibel, “Engineering of Recombinant Spider Silk Proteins Allows Defined Uptake and Release of Substances,” *J. Pharm. Sci.*, vol. 104, no. 3, pp. 988–994, 2015.

[5] F. O. Nestle, A. Farkas, and C. Conrad, “Dendritic-cell-based therapeutic vaccination against cancer,” *Curr. Opin. Immunol.*, vol. 17, no. 2, pp. 163–169, 2005.

X. APPENDIX

1. List of Presentations and Publications

Lucke M, Winter G, Engert J. *The effect of steam sterilization on recombinant spider silk particles.* Int J Pharm 2015; 481:125–31. doi: 10.1016/j.ijpharm.2015.01.024.]

Lucke M, Elsner M, Blüm C, Engert J, Slotta U, Römer L, Winter G, Scheibel T. *Entwicklung und Charakterisierung von Partikeln aus Spinnenseidenproteinen.* Medizin Innovativ – MedTech Pharma 2014 incl. BMBF-Symposium Medi-WING, Nuremberg, July 2014

Lucke M, Winter G, Engert J. *Steam Sterilization of Spider Silk Protein Microparticles.* 9th World Meeting on Pharmaceutics, Biopharmaceutics and Pharmaceutical Technology, Lisbon, Portugal, March 2014

Lucke M, Hofer M, Winter G, Engert J. *Delivery of proteins using spider silk particles as carrier systems* - in Scientifically Speaking. Controlled Release Society (CRS) Newsletter 2013 August 30(4):13-15

2. Curriculum Vitae

MATTHIAS ANDREAS LUCKE

PERSONAL DETAILS

PROFESSIONAL EXPERIENCE

EDUCATION

2012 - 2015	PhD thesis Department of Pharmaceutical Technology and Biopharmaceutics Research group of Prof. Dr. Gerhard Winter, LMU Munich Supervisor: PD Dr. habil. Julia Engert
2011	Licensed Pharmacist
2011 (6 Months)	Internship at Boehringer Ingelheim RCV Department Discovery ADME, Vienna, Austria
2010 - 2011 (6 Months)	Internship at the St. Anna pharmacy, Munich, Germany
2006 - 2010	Undergraduate studies: Pharmacy at the Friedrich-Alexander-University Erlangen- Nuremberg, Germany